molecules

MDPI

Article

Expanding the Role of Sub-Exploited DOE-High Energy Extraction and Metabolomic Profiling towards Agro-Byproduct Valorization: The Case of Carotenoid-Rich Apricot Pulp

Thalia Tsiaka [1,2], Charalambos Fotakis [1], Dimitra Z. Lantzouraki [1,2], Konstantinos Tsiantas [2], Eleni Siapi [1], Vassilia J. Sinanoglou [2,*] and Panagiotis Zoumpoulakis [1,2,*]

1 Institute of Chemical Biology, National Hellenic Research Foundation, 48, Vas. Constantinou Ave., 11635 Athens, Greece; thtsiaka@eie.gr (T.T.); bfotakis@yahoo.com (C.F.); dlantzouraki@eie.gr (D.Z.L.); esiapi@eie.gr (E.S.)

2 Laboratory of Chemistry, Analysis & Design of Food Processes, Department of Food Science and Technology, University of West Attica, Ag. Spyridonos, 12243 Egaleo, Greece; kostastsiant@hotmail.gr

* Correspondence: vsina@uniwa.gr (V.J.S.); pzoump@eie.gr (P.Z.); Tel.: +30-210-5385553 (V.J.S.); +30-210-7273872 (P.Z.)

Academic Editor: Luca Rastrelli

Received: 10 April 2020; Accepted: 6 June 2020; Published: 11 June 2020

Abstract: Traditional extraction remains the method-of-choice for phytochemical analyses. However, the absence of an integrated analytical platform, focusing on customized, validated extraction steps, generates tendentious and non-reproducible data regarding the phytochemical profile. Such a platform would also support the exploration and exploitation of plant byproducts, which are a valuable source of bioactive metabolites. This study deals with the incorporation of (a) the currently sub-exploited high energy extraction methods (ultrasound (UAE)- and microwave-assisted extraction (MAE)), (b) experimental design (DOE), and (c) metabolomics, in an integrated analytical platform for the extensive study of plant metabolomics and phytochemical profiling. The recovery of carotenoids from apricot by-products (pulp) is examined as a case study. MAE, using ethanol as solvent, achieved higher carotenoid yields compared to UAE, where 1:1 chloroform-methanol was employed, and classic extraction. Nuclear magnetic resonance (NMR)-based metabolomic profiling classified extracts according to the variations in co-extractives in relation to the extraction conditions. Extracts with a lower carotenoid content contained branched-chain amino acids as co-extractives. Medium carotenoid content extracts contained choline, unsaturated fatty acids, and sugar alcohols, while the highest carotenoid extracts were also rich in sugars. Overall, the proposed pipeline can provide different the phytochemical fractions of bioactive compounds according to the needs of different industrial sectors (cosmetics, nutraceuticals, etc.).

Keywords: apricot byproduct; carotenoids; ultrasound-assisted extraction (UAE); microwave-assisted extraction (MAE); nuclear magnetic resonance (NMR) spectroscopy; multivariate chemometric analysis

1. Introduction

Plant metabolomics is the answer to traditional phytochemical approaches, which are focused on the analysis of specific targeted metabolites, usually a group of bioactive compounds (i.e., carotenoids, polyphenols, alkaloids, and amino acids), and not on the complete and detailed metabolic profile of the plant substrate or plant byproducts. However, the different composition of the plant matrix, any possible enzymatic degradation or chemical breakdown of plant metabolites, and the lack of a tailor-made validated extraction step crucially affect the final quality of the metabolomic study and

the number of identified metabolites [1]. Among these factors, the step of sample preparation is of the utmost importance, since the information provided by high throughput analytical techniques is highly dependent on the selected extraction method. Therefore, special attention should be paid to the development of a comprehensive extraction methodology that can investigate the plant metabolome as exhaustively as possible [1].

Classic extraction is the method-of-choice in the majority of analytical studies [2,3]. Most of the time, traditional extraction methods are based on the previous experience and knowledge of the researchers, who apply them without further optimization or validation. Meanwhile, high energy extraction methods (e.g., ultrasound-assisted extraction (UAE) or microwave-assisted extraction (MAE)) are gaining ground, but are still ignored or sub-exploited in plant metabolomics studies. Nevertheless, these techniques circumvent decisive bottlenecks of classic approaches related to the extraction cost, efficiency, fractionation ability, and time [4]. In addition, the optimization of high energy extraction through experimental design (DOE) models provides answers to questions such as (a) which parameters are crucial for the extraction?, (b) do the interactions between extraction parameters critically affect extraction yields?, and (c) is it possible to enrich the obtained extract with different co-extracting phytonutrients from the substrate by modifying and adjusting the extraction conditions?. The latter issue is of unique importance for the industry of natural products since, even when an extraction is selective, the final natural extract also contains other secondary metabolites in lower concentrations [5,6]. Therefore, the upgraded role of DOE-optimized-high energy extraction in plant metabolomics merits further investigation to generate a robust sample preparation step for further analytical studies [7].

Recently, European Union reports revealed that almost 70% of total food processing ends up as waste or byproducts and foresaw an increase of 30% in the disposal of food byproducts by 2020 [8]. This insight, along with the intensive use of plant-derived natural ingredients, the threat of wild crafting, unsustainable harvesting practices, undernourishment, and increased food prices [9], forged the concepts of 'food from food' and 'byproducts to co-products' through the use of low-waste agro-industry production and the development of modern pipelines for the extraction and valorization of therapeutic natural agent/extracts from plant byproducts [10–12].

Reports by the Food and Agriculture Organization Corporate Statistical Database (FAOSTAT) place Greece in the top twenty producer and exporting countries of apricots (*Prunus armeniaca*) worldwide. As a sequent, a large production size generates immense quantities of apricot byproducts with high contents of carotenoids and sugars, and then secondarily, phenolics (rutin, catechin, epicatechin, and chlorogenic acid) and amino acids [13]. Focusing on apricot pulp carotenoids, the orange color unveils the presence of carotenes (α-, β-, and γ- carotene, etc.) rather than xanthophylls (zeaxanthin, lutein, β-cryptoxanthin, etc.). Among α- and β-carotene, the β-isomer is the prevailing form in plant tissues, while zeaxanthin is the main xanthophyll, but its content can be 50-times lower than that of β-carotene [14]. Therefore, apricot byproducts may be a low-cost and sustainable natural source of potential bioactive compounds [13].

In particular, β-carotene acts as an antioxidant and major precursor of vitamin A (retinol), since it presents 100% provitamin A activity due to its two β-ionone rings [13]. It enhances the immune system by regulating intercellular signaling pathways, cell differentiation, growth factors, and cell apoptosis. Moreover, it offers protection against atherosclerosis and coronary diseases [15]. In addition, there is strong evidence for the significance of β-carotene metabolic pathways in the risk reduction for some types of cancer (lung, head, prostate, skin, liver, breast, and colorectum cancer). Nonetheless, in order to avoid negative effects, many clinical intervention studies recommend low-dosage dietary intake levels of β-carotene supplements [16]. Cases of multi-carotenoid supplementation indicated positive results for Alzheimer diseases and vision impairments by balancing the adverse effects of different kinds of degeneration, UV radiation, malfunctions, and oxidative stress [13].

Considering the importance of natural extracts as a novel and promising nutraceutical and cosmeceutical trend, the current work aims to provide an integrated platform for the fast and

reproducible delivery of extracts highly enriched in certain phytochemicals. The production and study of carotenoid-rich extracts from apricot's industrial by-products is selected as a case study. To fulfill this aim, the individual objectives of the study are (i) to access information not only for the targeted substances (carotenoids), but also for important untargeted secondary metabolites; (ii) to unveil the metabolite variations in carotenoid-rich high-energy extracts; and (iii) to classify extracts based on the extraction conditions.

2. Results and Discussion

2.1. Extraction Solvent

Selecting the ideal extraction solvent for a certain class of bioactive compounds is based on the (a) substrate nature, (b) target compound's physicochemical properties, (c) solvent's polarity/affinity to the extracted analytes, and (d) extraction technique principals/mechanisms [17].

Three *trans*-carotenoids—β-carotene, lutein, and zeaxanthin—were detected and quantified in apricot pulp. Carotenoids' peaks and mass transitions are shown in Figure 1a,b.

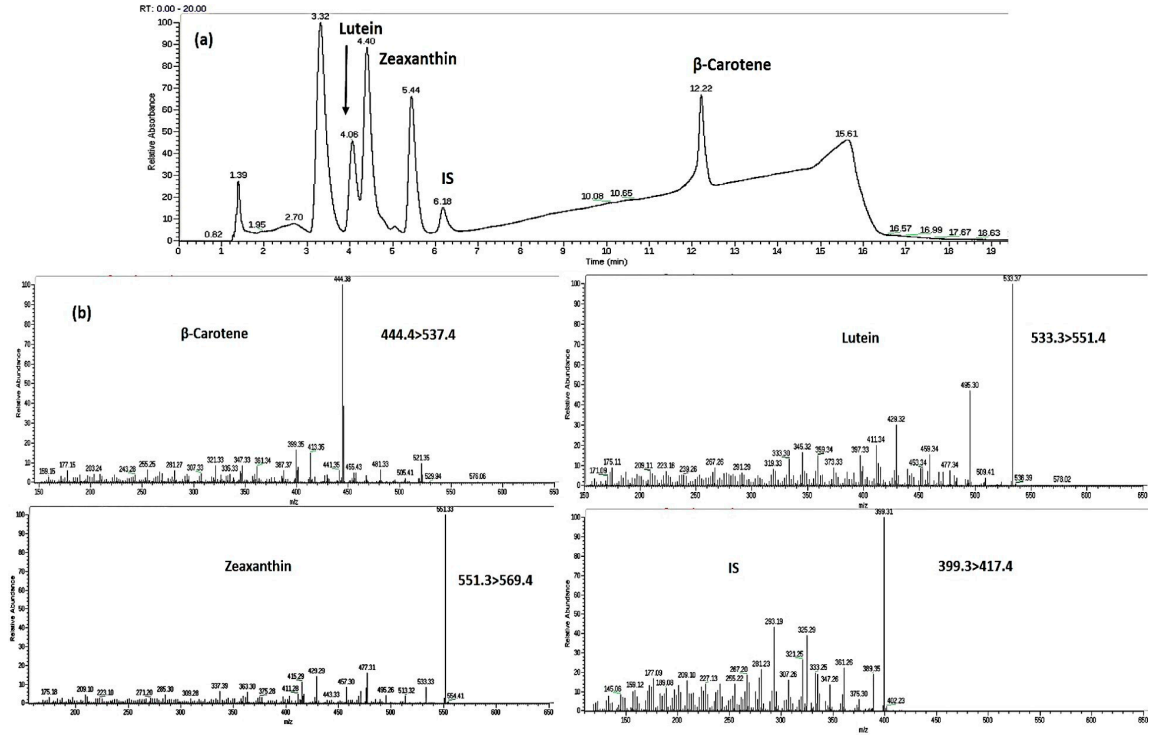

Figure 1. Carotenoids' (**a**) chromatographic peaks and (**b**) mass transitions.

Based on the lipophilic nature of carotenoids, eight different extraction systems were investigated (Table S1) and selected based on (i) the established knowledge regarding the solvents used for carotenoid extraction; (ii) the physicochemical properties of the solvents, which affect and differentiate their extracting ability with UAE or MAE; and (iii) the results of previous studies of our lab concerning the extraction of carotenoids from other substrates [14]. According to the results (Figure 2), alcohols and most of their mixtures provided higher extraction yields in both techniques.

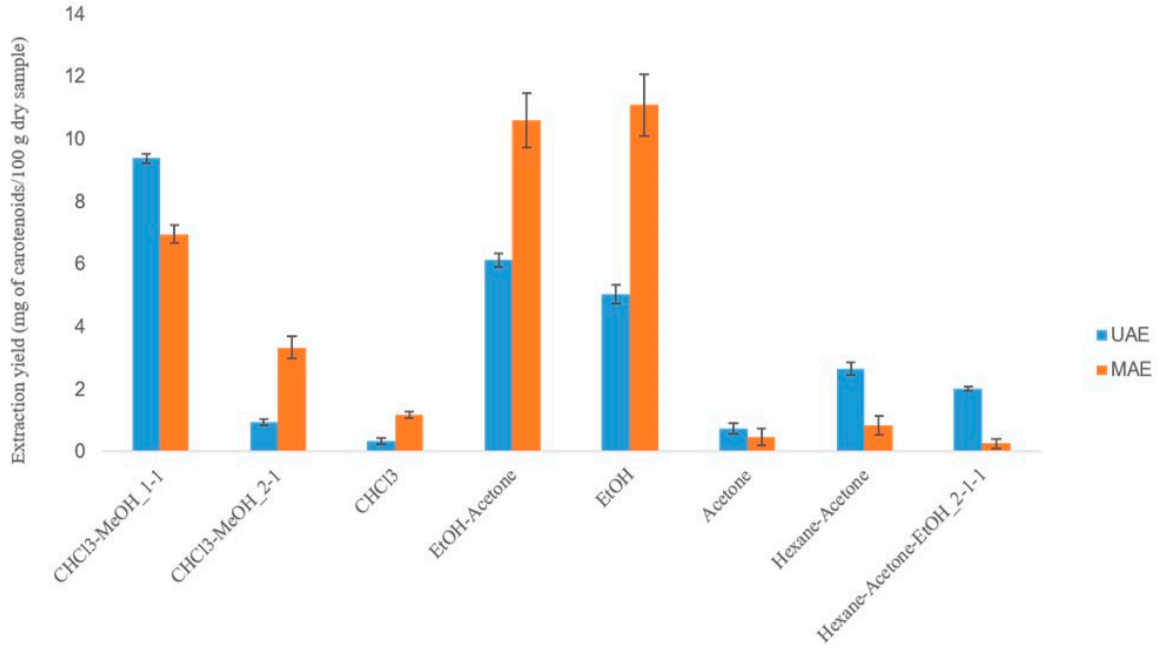

Figure 2. Selecting the optimal ultrasound-assisted extraction (UAE) and microwave-assisted extraction (MAE) solvent system for carotenoid extraction from apricot pulp.

The extracting ability of UAE relies on the acoustic cavitation phenomenon, which is induced by solvents with a high surface tension, low viscosity, and vapor pressure. All examined solvents exhibited similar values of surface tension, but methanol and ethanol had a significantly lower vapor pressure compared to the other extracting agents. In terms of the two alcohols, methanol has a lower viscosity than ethanol and therefore, its combination with a solvent which also has a low viscosity (chloroform) provided higher extraction yields [18]. The dielectric constant values and transparency to microwaves (MWs) determine the adequacy of an MAE solvent. Since the MAE mechanism is a result of dipole rotation and ionic conductivity, solvents with a high dielectric constant (usually more polar solvents) efficiently absorb MWs and become more suitable for MAE. Therefore, ethanol emerged as the optimal solvent for carotenoid MAE [19].

2.2. Extraction Temperature

The extraction process using microwaves and ultrasounds involves a complex interplay between different phenomena which contribute to solid matrix disruption and solvent diffusion into the substrate. The temperature requires special attention during the extraction process due to its binary effect on the extracted compounds. On the one hand, increased temperatures enhance cell disruption and the release of target compounds to the solvent medium, while at the same time, a rampant increase of temperature may result in the degradation of extracted constituents [18]. In our case, the UAE temperature was adjusted to 30–35 °C by inserting the extraction flask into an ice bath and monitoring the temperature throughout the extraction procedure. Low temperatures are recommended for UAE, in order to avoid an increase of the solvent's vapor pressure, which limits the collapse of cavitation bubbles and, by extension, the appearance of sonochemical effects [17]. In open vessel MAE, the extraction temperature is interrelated with the applied MW energy and extraction time. However, the MAE temperature never exceeds the boiling point of the extraction solvent. Increased temperatures enhance the extracting potency of MAE solvent due to the viscosity/surface tension decrease and cell component disruption [20]. As previously reported [21], β-carotene is stable until 60 °C, so the MAE temperature was set to this value.

2.3. UAE and MAE Optimization Using DOE Models

The effect of the extraction time (X_1, minutes), US/MW power (X_2, W), and solvent/material ratio (X_3, mL g^{-1}) on the carotenoid extraction yield was evaluated using 2^3 full factorial and Box–Behnken (BBD) design. All experimental runs were performed using a 1:1 *v*/*v* mixture of methanol-chloroform, for UAE and ethanol, for MAE.

2.3.1. Screening Design (2^3 Full Factorial Design)

A screening design was applied in order to (i) limit the wide values' range of the selected factors in a region where higher yields were achieved and (ii) direct the imminent optimization model (response surface model) to this region. The eight experiments of the 2^3 full factorial design were carried out in a random order to avoid systematic errors. The extraction yields of 2^3 design experiments are shown in Table S2a,b. The goodness-of-fit for the screening models was assessed using the determination coefficient (R^2) and the determination coefficient adjusted for the degrees of freedom (R^2_{adj}). The first index indicates how well the produced models fit the dataset and the second one determines which terms of the equation, proposed by the models, truly affect the response. A model where the values of the two coefficients are higher than 0.8 and their difference is around 0.2 describes the dataset well. Regarding our case, the 2^3 design could reliably direct the upcoming Box–Behnken model to the value range where higher carotenoid yields would be obtained, since $R^2 = 0.920$ and $R^2_{adj} = 0.814$ for UAE and $R^2 = 0.987$ and $R^2_{adj} = 0.954$ for MAE. Based on the *p*-values, special attention should be paid to the adjustment of the solvent/material ratio (*p*-values ≤ 0.05) in both extraction techniques (Table S3a). According to two-dimensional (2D) contour plots, UAE performed better at extraction times over 10 min when the ultrasound (US) power and solvent/material ratio were set at high values (≥600 W and ≥30 mL g^{-1}, respectively) (Figure S1a–c). An MAE optimization model should be focused on extraction times from 5 to 20 min, an MW power lower than 150 W, and a high solvent/material ratio (≥50 mL g^{-1}) (Figure S1d–f).

2.3.2. Response Surface Methodology Models (Box–Behnken Design)

Box–Behnken optimization models, driven by the trends revealed in the prior screening designs, were applied for accomplishing the optimal extraction values of high energy techniques. The model-proposed experimental runs and carotenoid content for each run are illustrated in Table S2a,b. The processing of the dataset resulted in two (one for each extraction method) predictive second-order polynomial equations. Terms with high *p*-values (*p*-value ≥ 0.05) were considered statistically insignificant and excluded from the equations. Therefore, the final model equations (Equations (1) and (2)), expressed in normalized values, consisted of the following terms:

$$\begin{gathered}\text{UAE yield (mg of total carotenoids 100 g}^{-1}\text{ dry sample)} = 8.706 - 1.80x_1 + 1.003{x_1}^2 + \\ 0.80{x_2}^2 + 1.021{x_3}^2 + 0.5280{x_1}^2x_2 + 0.4674\, x_1{x_2}^2 - 1.761x_1x_3 - 1.819{x_1}^2x_3 + 2.023x_2x_3,\end{gathered} \quad (1)$$

$$\begin{gathered}\text{MAE yield (mg of total carotenoids 100 g}^{-1}\text{ dry sample)} = 15.91 - 0.3208{x_1}^2 + \\ 2.767x_2 - 1.116{x_2}^2 + 1.372x_1x_2 + 1.554x_1{x_2}^2 - 2.332x_1x_3 - 3.784x_2x_3.\end{gathered} \quad (2)$$

The significance of all equation terms is illustrated in Pareto charts (Figure S2), where the important terms are the ones that outstrip the threshold of *p*-value ≤ 0.05 (red line). Taking into consideration the *p*-value ≤ 0.05 criterion presented in the ANOVA table (Table S3b), UAE was significantly affected by the linear term of the extraction time (x_1), the quadratic term of the solvent/material ratio ($x_3{}^2$), and the interaction between the solvent/material linear term and (a) the extraction time quadratic term ($x_1{}^2x_3$) and (b) the US power linear term (x_2x_3) (Figure S2a). UAE yields presented a directly proportional linear relationship with the extraction time and a directly proportional exponential relationship with the solvent/material ratio, explained by the positive sign of x_1 and $x_3{}^2$ terms in Equation (1). Furthermore, the linear (x_2) and quadratic term ($x_2{}^2$) of MW power, the interaction

between the extraction time linear term and MW power quadratic term ($x_1x_2^2$), and the interaction between the solvent/material linear term and the linear terms of the extraction time (x_1x_3) and MW power (x_2x_3) played the most important roles in MAE carotenoid yields. As illustrated in Figure S2b, the linear term of MW power affected the final result more than the quadratic term. Therefore, the positive sign of the x_2 term in Equation (2) revealed the directly proportional dependence of MAE yields and MW power.

The BBD models were considered reliable according to R^2 and R^2_{adj} values, which were relatively high and close to one another (R^2 = 0.886 and R^2_{adj} = 0.714 for UAE and R^2 = 0.876 and R^2_{adj} = 0.767 for MAE). Moreover, only a percentage of around 10% of the total variations was not interpreted by the produced models. The good fitness of the BBD models for the experimental data was also established by the *p*-values corresponding to the total model and not each term, which were ≥0.05 (*p*-value UAE = 0.941, *p*-value MAE = 0.979), confirming that there was no models' lack-of-fit (Table S3b). In addition, the robustness of our models was evaluated through the standard deviations (UAE stdev = 2.2, MAE stdev = 2.6) of the four repetitions at the center points (0,0,0). All previous results are presented in the ANOVA table (Table S3b).

2.3.3. Evaluate the Effects of Extraction Factors under Optimization

Three-dimensional (3D) response surface methodology (RSM) plots were generated for an evaluation of the effects of the DOE-optimized extraction factors on the carotenoid yield when UAE (Figure 3a–c) and MAE (Figure 4a–c) were employed. RSM plots depict the combinatorial effect, each time, of two of the investigated extraction factors on the carotenoid content, while the third parameter is kept constant at the medium value level (0).

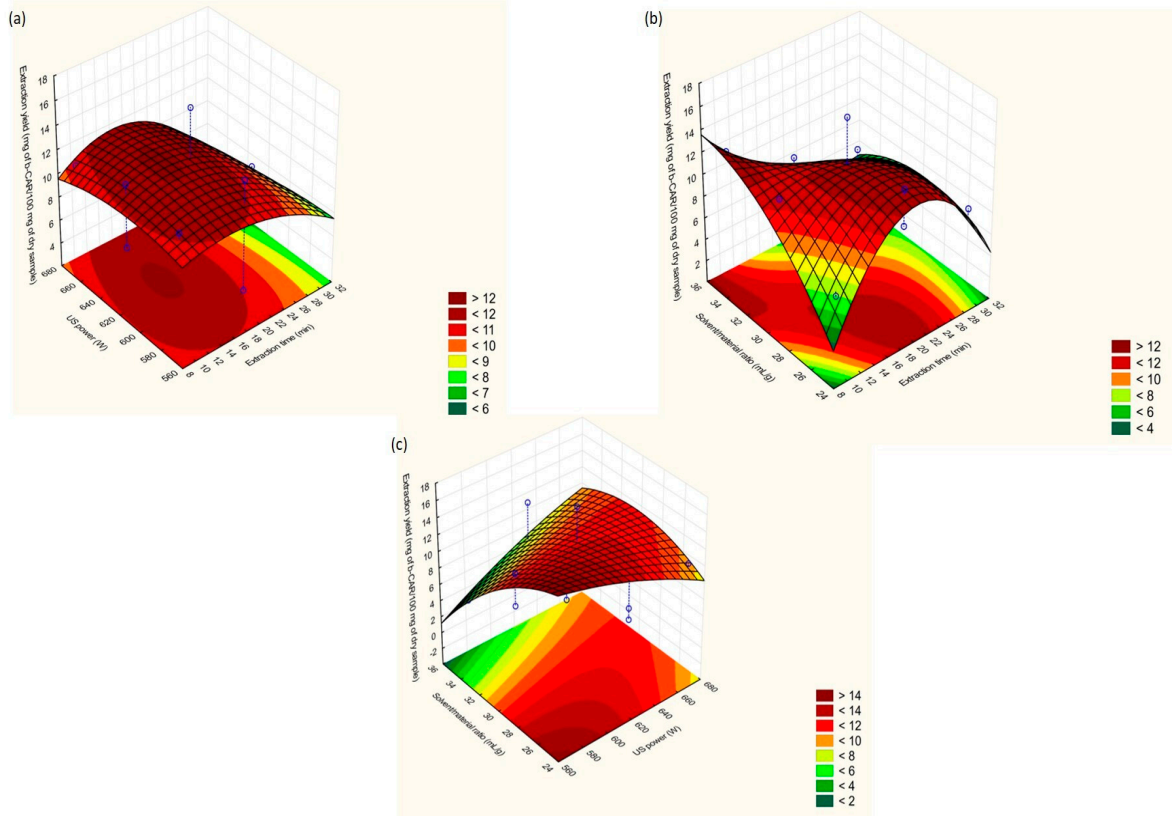

Figure 3. Response surface methodology (RSM) plots for UAE: (**a**) extraction time vs. US power; (**b**) US power vs. solvent/material ratio; (**c**) solvent/material ratio vs. extraction time.

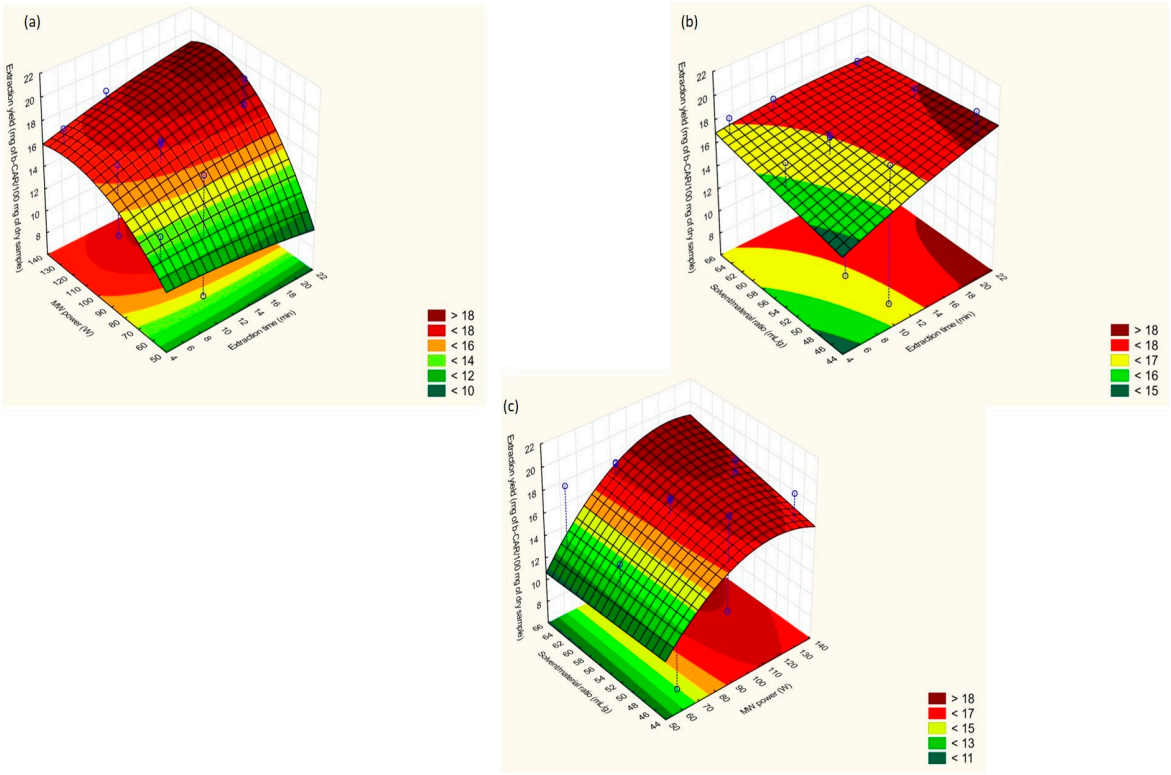

Figure 4. RSM plots for MAE: (**a**) extraction time vs. MW power; (**b**) MW power vs. solvent/material ratio; (**c**) solvent/material ratio vs. extraction time.

Extraction Time

As stated in Figure 3a,b, UAE was favored at extraction times between 10 and 20 min. A closer look at these figures showed that at even a 10 min extraction time, high extraction could be achieved when the US power and solvent/material ratio had values of 600–620 W and 30-35 mL g^{-1}, respectively. Studies regarding carotenoid UAE from plant tissues indicated that carotenoids may be degraded at a prolonged extraction time (over 15 min). Therefore, a 10 to 20-min period seems ideal for carotenoid recovery from agro-byproducts [22].

Compared to UAE, MAE is a more complex process due to the interrelation of the extraction time, temperature, and MW power. Other research groups [23] have examined the co-dependence of these three parameters and showed that extended extraction times of over 15 min resulted in high carotenoid yields when the MW power was adjusted to 100–140 W. This was also confirmed in the present work (Figure 4a). In addition, a higher extraction time and higher solvent/material ratio provided higher carotenoid yields (Figure 4b).

US/MW Power

In general, the positive impact of sonochemical effects is more pronounced at an increased US power, which improves cell wall disruption and solvent penetration. Recent research has asserted that a US power of over 250 W negatively affected the extraction efficiency, but US exposure lasted for long periods (40–100 min) [17]. However, a high US power (580–620 W) recovered high concentrations of carotenoids when applied for short periods (8–15 min) (Figure 3a,c).

An increasing trend for extraction yields was observed (Figure 4a,c) at 100–140 W of MW power. For this power range, the increase of the extraction temperature was slower and steady throughout the MAE process. Therefore, the release of target compounds from substrate tissues was more efficient due to more gradual solvent heating. A higher MW power may (i) deteriorate the extracted labile molecules or (ii) cause solvent losses from extreme solvent heating and lead to reduced extraction rates.

On the other hand, low irradiation values do not cause complete cell disruption and extraction yields are thus usually lower [23].

Solvent/Material Ratio

According to the UAE Pareto chart (Figure S2a), the solvent/material ratio was viewed as the most critical extraction factor. As showcased in Figure 3b,c, solvent volumes between 25 and 35 mL seem to be high enough to adequately diffuse and dissolve the extracted compounds. The addition of extra volume did not maximize carotenoid migration to the solvent due to the increase of the diffusion distance from the extracting medium and the examined matrix [24].

The MAE regression equation (Equation (2)) indicated, in quite significant terms, the interaction between the solvent/material ratio and MW power and extraction time (Figure S2b). When the extraction time varies from 15 to 20 min and MW power from 100 to 120 W, the solvent/material ratio should be adjusted to 44–56 (mL g^{-1}) for obtaining the maximum extraction yields (Figure 4b,c). Larger solvent volumes demanded longer periods (≥20 min) of MW irradiation at the mentioned values, in order to achieve uniform solvent heating and thus efficient carotenoid recovery. Nevertheless, extended extraction times of MW radiation could promote the degradation of thermosensitive compounds due to excessive heating of the extraction solvent, such as β-carotene or zeaxanthin [25].

Optimal Extraction Conditions

The third and final step of DOE optimization strategies refers to the conduction of experiments around the regions of the values where the response is maximized according to the equations produced by BBD (Equations (1) and (2)). Three experimental combinations were proposed and performed optimally. The lack of a significant difference (Student's t-test) between the predicted and experimental values proved the reliability of DOE-optimized extractions (Table S4).

The optimal values of UAE and MAE parameters for carotenoid recovery from apricot byproducts are presented in Table 1.

Table 1. Optimal values of UAE and MAE parameters for carotenoid recovery from apricot byproducts.

Extraction Parameters	Optimal Values	
	UAE	**MAE**
Extraction solvent (*v*/*v*)	Methanol:chloroform 1:1	Ethanol
Extraction time (min)	10	20
US/MW power (W)	600	120
Solvent/material ratio (mL g^{-1})	35	45
US pulse sequence (s)/MW ramping time (min)	15 ON 5 OFF	0
Extraction yield (mg of carotenoids 100 g^{-1} dry sample) (±stdev), n = 3 [1]	11.12 (±0.34)	19.28 (±0.27)

[1] n: number of sample replicates measured under repeatability conditions.

2.4. Comparison of Optimized UAE, MAE, and Conventional (Folch) Extractions

At this point, in order to prove the efficiency of MAE and UAE, it is critical to provide comparative data for MAE and UAE and Folch, which is a widely used conventional extraction methodology for the recovery of lipid components, such as carotenoids. According to the results delivered by LC-MS/MS analysis for the carotenoid content of apricot pulp, β-carotene, zeaxanthin, and lutein were quantified (Table S2).

MAE extracts almost 2.5-times more β-carotene than UAE. This outcome is probably related to (a) the high polarity of ethanol, which allows the absorbance of MW energy and the acceleration of the MAE process, and (b) the combinatorial effect of MW power and the increased (compared to UAE) extraction temperature, which causes looseness and disruption of the tight cell structure and the

enhanced diffusion of β-carotene in ethanol [21]. Additionally, the Folch method does not appear to be an apt choice for β-carotene recovery from fruit tissues, since the β-carotene content is 19-fold and 7.5-fold lower than in MAE and UAE, respectively.

The lower extraction yield of UAE compared to MAE may be attributed to the degradation of β-carotene to *cis*-isomers, oxygenated derivatives, and β-*apo*-carotenals (i.e., 15-*Z*-β-carotene, di-*Z*-β-carotene, and 9-*cis*-β-carotene) due to isomerization, oxidation, and cleavage reactions caused by US [26].

The same trend was also observed for apricot's xanthophylls. The Folch method recovered a minor amount of zeaxanthin and lutein, which was one order of magnitude lower than the xanthophylls' content of high energy techniques. Unlike the significant difference in the β-carotene concentration, UAE and MAE extracted equal amounts of zeaxanthin and lutein (Table 2). The ratio of *trans*-xanthophylls to *trans*-β-carotene in MAE and Folch is around 1:20–1:25, while in UAE, this ratio is 1:10, implying that the degradation of β-carotene in UAE was more severe (Table 2).

Table 2. Carotenoid content of apricot pulp determined by LC-MS/MS.

Carotenoids Content (mg 100 g^{-1} Dry Sample), v = 3 [1]	**Optimized UAE Extract**	**Optimized MAE Extract**	**Folch Extract**
β-Carotene	7.72 (±0.98)	19.7 (±1.6)	1.44 (±0.87)
Zeaxanthin	0.71 (±0.33)	0.66 (±0.25)	0.020 (±0.041)
Lutein	0.82 (±0.19)	0.82 (±0.12)	0.07 (±0.24)
Final carotenoid content expressed in mg kg^{-1} of raw apricot pulp sample (N = 3) [2]			
Average weight (g) of raw apricot pulp samples (±stdev), n = 10 [3]		17.1 (±2.1)	
Average weight (g) of lyophilized apricot pulp samples (±stdev), n = 10 [3]		3.23 (±0.39)	
Average moisture (%) of raw apricot pulp, n = 10 [3]		81.25	
	UAE Extracts	MAE Extracts	Folch Extract
β-Carotene content (mg kg^{-1} raw apricot pulp) (±stdev)	14.58 (±0.98)	37.2 (±1.6)	2.72 (±0.87)
Zeaxanthin content (mg kg^{-1} raw apricot pulp) (±stdev)	1.34 (±0.33)	1.25 (±0.25)	0.038 (±0.041)
Lutein content (mg kg^{-1} raw apricot pulp) (±stdev)	1.55 (±0.19)	1.55 (±0.12)	0.13 (±0.24)

[1] Number of LC-MS/MS replicates, [2] number of extraction replicates, and [3] number of samples.

The content of carotenoid-rich fruits and fruit byproducts, like apricots, varies markedly when the variety, cultivar and hybrids, geographical origin, climatic differences, genotype, ripening, and development stages alter. Hence, it is a quite intricate task to deliver an unbiased comparison of the different extraction techniques used to extract carotenoids from such substrates. Nevertheless, the current MAE process managed to extract four-times more β-carotene, but similar xanthophyll equivalents, when compared to accelerated solvent extraction (ASE), while UAE and ASE resulted in almost the same final carotenoid content [27]. Classic extraction, applied to different varieties of apricots cultivated in New Zealand and USA, achieved a β-carotene yield close to that of MAE. The higher yields of lutein obtained by Leong et al.'s (2012) classic method may support the hypothesis of xanthophyll's isomerization under certain conditions of high energy extractions [14,28]. To wrap up the results of the extraction of carotenoids using high energy techniques, it becomes clear that especially MAE's role should be revised and upgraded.

2.5. NMR-Based Metabolic Profiling for DOE Apricot Extracts to Elucidate Co-Extractives

Nuclear magnetic resonance (NMR) is one of the most implemented and efficient analytical platforms used for the elucidation of metabolites from complex mixtures, including natural extracts. Therefore, NMR spectroscopy was integrated as an additional complementary technique for the simultaneous elucidation of the high concentration co-extracted metabolites other than carotenoids

that shape the different metabolic profiles of each group [29] (Figure S3). The examined samples were (i) the extracts of all of the different UAE and MAE solvents; (ii) indicative DOE-high energy extracts with a lower, medium, and higher carotenoid content; (iii) the optimal UAE and MAE extracts; and (iv) Folch extracts. Table 3 presents the assignment of 15 major metabolites identified in the ^{1}H-NMR spectra of the different samples. For the assignment, previous literature findings and 2D NMR experiments (gCOSY, gHSQC, and gHMBC) were utilized (Figure S4).

Table 3. Characteristic ^{1}H-NMR peaks of apricot byproduct extracts identified in the principal component analysis (PCA) groups.

Compounds	^{1}H Chemical Shift	Peak Multiplicity [1]
Valine	0.99, 1.04, 2.28	(d), (d), (m)
Leucine	0.98, 0.96	(d, *J* = 7.5), (d, *J* = 7.5)
Isoleucine	0.94, 1.01, 1.25, 1.45, 1.96, 3.66	(t), (d), (m), (m), (m), (m)
Alanine	1.48	(d)
Lysine	1.61	(t)
Choline	3.10	(s)
Fatty acids	1.26	(m)
Myo-inositol	3.67, 3.78	(t), (t)
Malic acid	2.68, 2.78	(dd), (dd)
Lactic acid	1.34	(d)
Formic acid	8.40	(s)
Fructose	3.53, 4.04	(t), (t)
Sucrose	4.18, 5.39	(d), (d, *J* = 3.9)
Glucose	5.12	(d)
Xylose	5.07	(d)

[1] (s): single peak, (d): doublet, (dd): doublet of doublets, (t): triplet, (m): multiplet, and *J*: coupling constant.

In Figure 5, the superimposed spectra belong to the (a) optimal UAE (blue spectrum) (b) optimal MAE (red spectrum), and (c) Folch apricot pulp extracts (green spectrum). Folch extracts presented peaks in the amino acid region (Figure 5a). On the other hand, the optimal UAE and optimal MAE extracts contained, according to Figure 5b,c, fatty acids and myo-inositol or sugars, respectively.

Principal component analysis (PCA) provided an overview of the trends and possible outliers of high energy extracts [30]. This unsupervised analysis copes with how the extraction parameters shape the profile of co-extracted metabolites. The PCA model (Figure 6) framed three groups. Group 1 (green dots) contained extracts with a relatively low carotenoid content (under 5 mg 100 g^{-1} dry sample), Group 2 (blue dots) contained those with a medium carotenoid content (between 5–15 mg 100 g^{-1} dry sample), and Group 3 (red dots) consisted of extracts with a high carotenoid yield (over 15 mg 100 g^{-1} dry sample) (Figure 6 and Table S5).

The primary factor for sample classification was the polarity of the extraction solvent, rather than the extraction technique used, since Group 1 (green dot), which shows a different trend from Group 3 (red dots), mostly contains extracts of less polar solvents, regardless of the extraction technique used (Figure 6 and Table S5). The effect of the extraction method was outlined implicitly, since every solvent shows a different behavior when interacting with US or MW due to its different physical properties (polarity, viscosity, vapor pressure, diffusion coefficient, etc.).

In Figure 6, Folch samples are outliers, proving that the conventional technique exhibits a distinct metabolic profile compared to high energy approaches. This fact is in accordance with the LC-MS/MS results (Table 2), where classic methods also presented lower carotenoid yields. Folch samples

exhibited a high content of valine, isoleucine and leucine, fatty acids, lactic acid, alanine, and malic acid, as presented in the contribution plot in Figure S5.

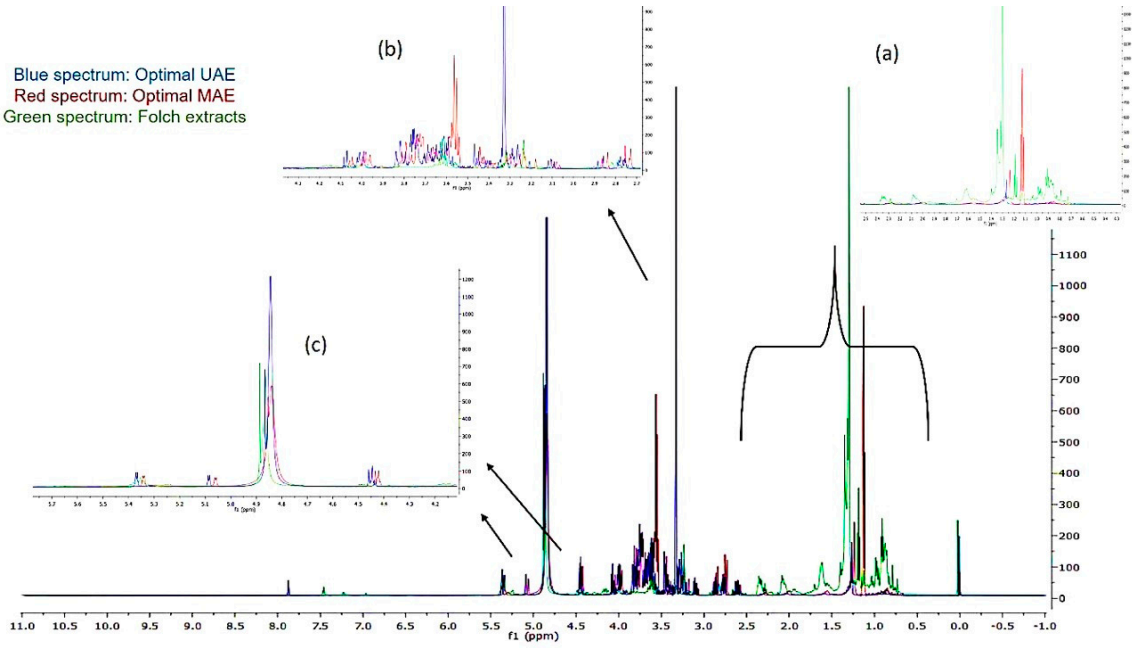

Figure 5. Regions of (**a**) amino acids, (**b**) fatty acids and myo-inositol, and (**c**) mono- and di-saccharides in superimposed ^{1}H-NMR spectra of optimal UAE, optimal MAE, and Folch extracts.

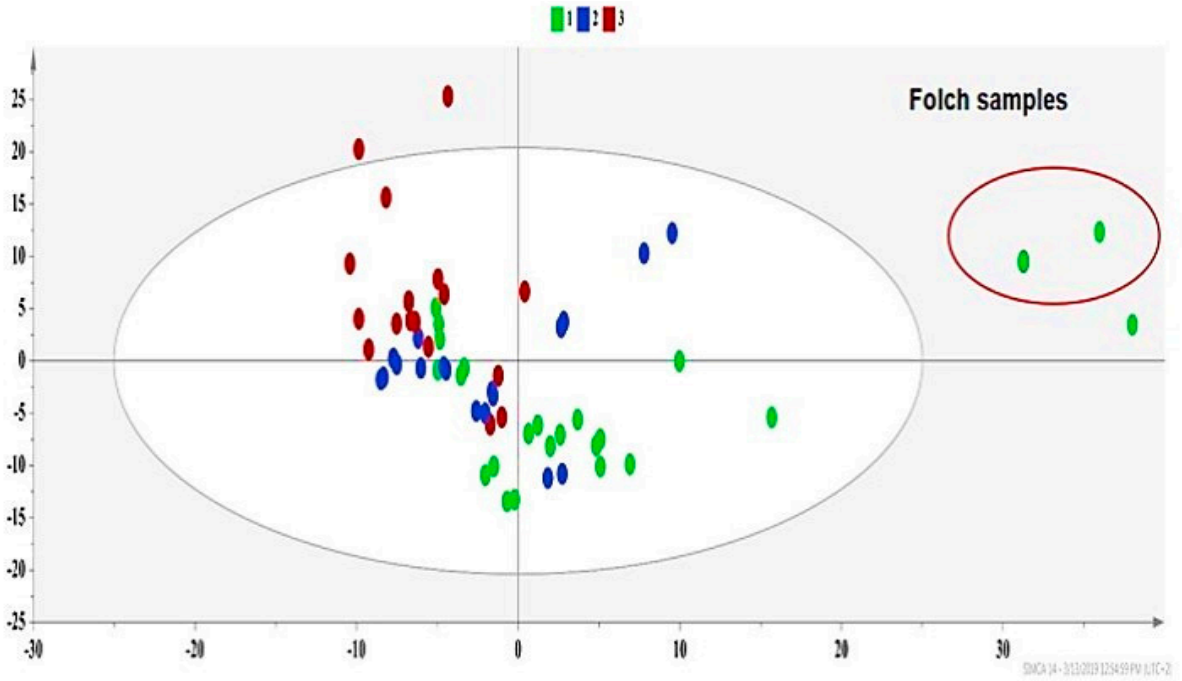

Figure 6. PCA of experimental design (DOE)-extracts PCA-X, where A = 2, N = 57, $R^2X(cum)$ = 0.73, $Q^2(cum)$ = 0.57, green dots = apricot pulp samples with a low extraction yield (≤5 mg carotenoids 100 g $^{-1}$ dry sample), blue dots = apricot pulp samples with a medium extraction yield (5–15 mg carotenoids 100 g^{-1} dry sample), and red dots = apricot pulp samples with a high extraction yield (≥15 mg carotenoids 100 g^{-1} dry sample).

We excluded the Folch samples and produced a second PCA model (Figure 7), where the trend for the formation of three groups is still evident. Besides the solvent polarity, the grouping of extracts (Figure 7) gave a hint regarding the effect of extraction parameters, highlighting the US/MW power and the solvent/material ratio as more critical variables. More explicitly, Group 2 mainly includes extracts of more polar solvents, such as methanol and ethanol, and UAE extracts with a higher US power and solvent/material ratio (Tables S2a and S5). Furthermore, the common factors between the extracts of Group 3, which are primarily MAE extracts, are a higher MW power and solvent/material ratio (Tables S2b and S5).

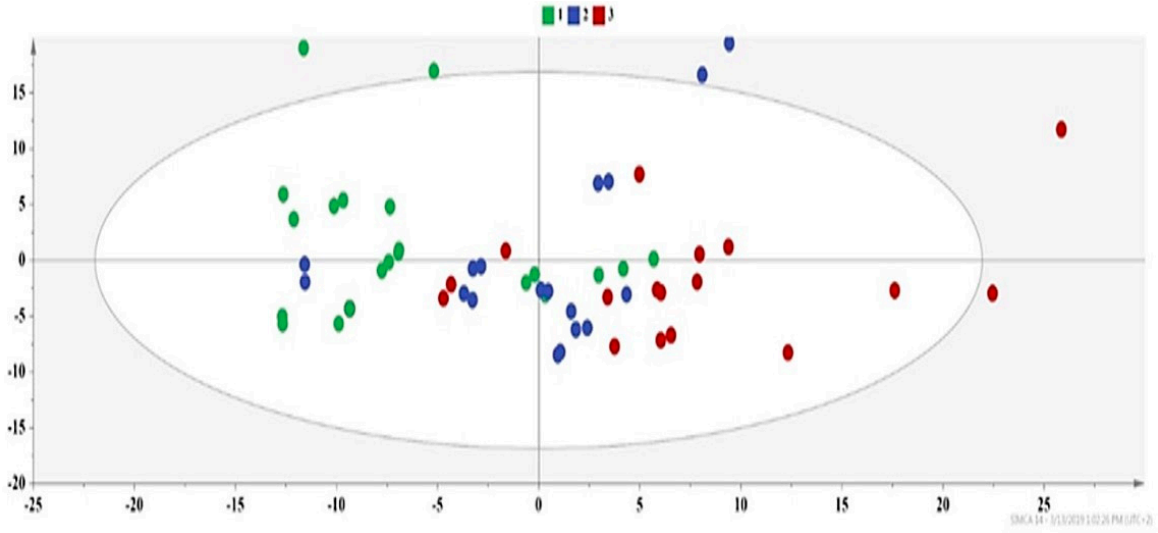

Figure 7. PCA of DOE-extracts excluding Folch samples PCA-X, where A = 2, N = 54, $R^2X(cum)$ = 0.87, $Q^2(cum)$ = 0.67, green dots = apricot pulp samples with a low extraction yield (≤5 mg carotenoids 100 g^{-1} dry sample), blue dots = apricot pulp samples with a medium extraction yield (5–15 mg carotenoids 100 g^{-1} dry sample), and red dots = apricot pulp samples with a high extraction yield (≥15 mg carotenoids 100 g^{-1} dry sample).

Subsequently, class information was embedded in supervised models of Orthogonal Projections to Latent Structures Discriminant Analysis (OPLS-DA) to identify the key metabolites responsible for extract differentiation [2]. The OPLS-DA models provided a valid separation of DOE-extracts according to their $R^2Y(cum)$ and $Q^2(cum)$ values. In each case, the discriminant co-extractives were highlighted by S-line plots (Figures 8b, 9b, 10b and 11b). The discriminant power of each metabolite is demonstrated with a color code and shows an increasing trend from green to red. Therefore, the important metabolites' peaks for cluster discrimination are depicted with an orange to red color. The respective contents of each metabolite responsible for the discrimination were framed in box-plots (Figures 9c, 10c and 11c), disclosing a pattern in line with the carotenoid yield and UAE/MAE parameters. Permutation testing and receiver operating characteristic (ROC) curves were employed and verified the OPLS-DA model's reliability (Figure S6a–d).

In particular, the class information enclosed in the first OPLS-DA (Figure 8a) model included the group with a low carotenoid content (Group 1 in green) and one new group comprised of Group 2 and Group 3 (Group 2,3 in yellow), due to the localization of most of Group's 2 samples together with Group 3 in the PCA model presented in Figure 7.

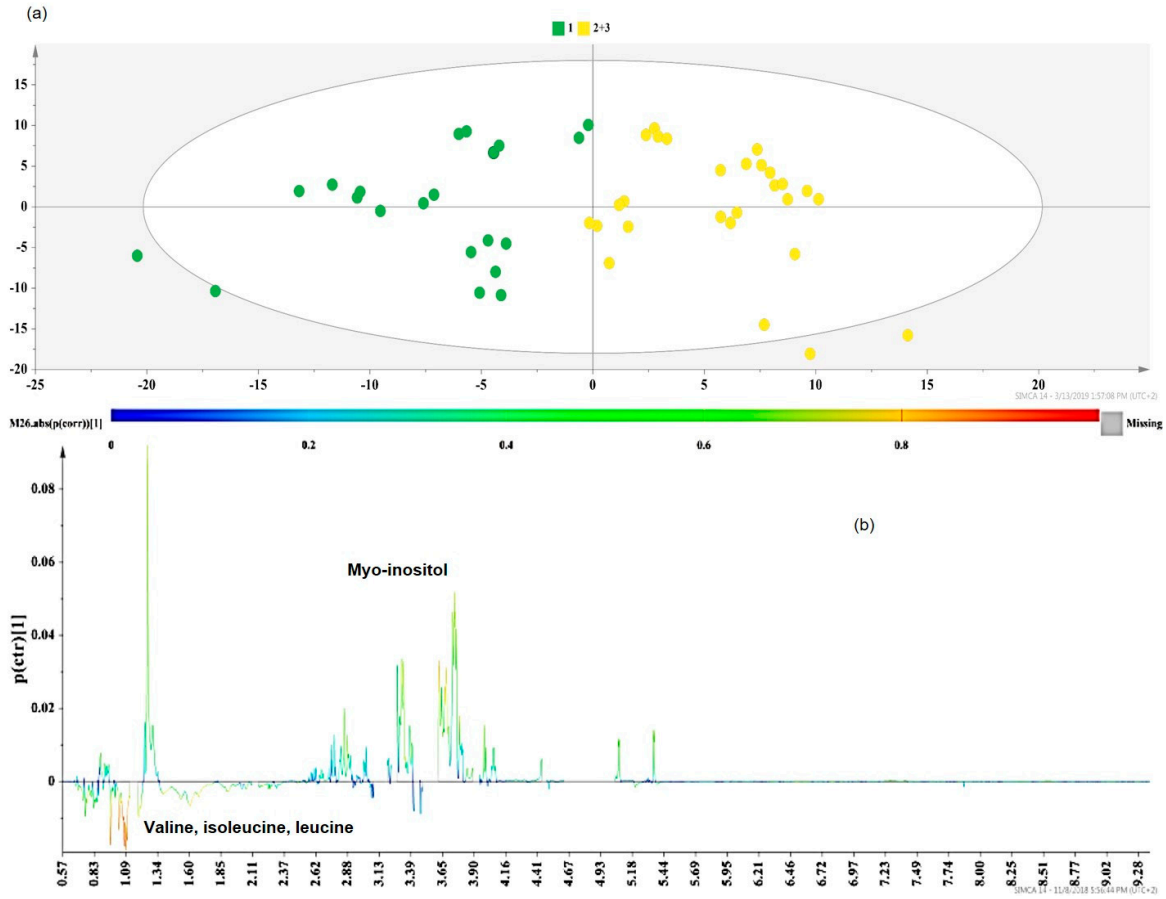

Figure 8. (**a**) Orthogonal Projections to Latent Structures Discriminant Analysis (OPLS-DA) model of Group 1 vs. Group 2+3 DOE apricot extracts, Pareto scaled, where A = 1 + 1 + 0 (N = 48, $R^2Y(cum) = 0.706$, $Q^2(cum) = 0.596$, $p < 0.05$), green dots = apricot pulp samples with a low extraction yield (≤5 mg carotenoids 100 g^{-1} dry sample), and yellow dots = apricot pulp samples with a higher extraction yield (between 5 and more than 20 mg carotenoids 100 g^{-1} dry sample); (**b**) S-line plot of the OPLS-DA model.

Extracts with low carotenoid yields (Group 1, green dots) were enriched in branched-chained hydrophobic amino acids (valine, leucine, and isoleucine) (Figure 8b). The above-mentioned amino acids are among apricots' beneficial secondary components due to their numerous biological activities [31]. The co-extraction of these metabolites was favored in more nonpolar solvents (acetone, chloroform, and *n*-hexane) or their mixtures with methanol. According to previous studies [32], the UAE conditions, especially the time and US power, can initiate amino acid degradation reactions in cases where highly polar solvents are used. Therefore, the combination of less polar solvents with a relatively low US power (575–625 W) (Tables S2a and S5) in Group 1 samples seems to provide apricot pulp extracts with important levels of certain amino acids [32].

Myo-inositol was highlighted as an additional marker discriminating Group 1 (low carotenoid content, green dots) from the cluster of Groups 2 and 3 (higher carotenoid yield, yellow dots) (Figure 8b). Myo-inositol is a sugar polyalcohol which participates in plant development by promoting the biosynthesis of molecules responsible for the cell wall structure [33]. Our results are in agreement with previous results, where cyclitols (myo-inositol, d-pinitol, etc.) were mostly extracted at higher UAE solvent volumes and extraction times [34] (Tables S2a and S5) (Groups 2,3 in yellow). As stated in other studies [35], MAE extracts containing inositol were obtained at short extraction times (≤20 min) and high solvent/material ratios, which is a finding that is in accordance with our study (Tables S2b and S5) (Groups 2,3 in yellow).

An in-pairs OPLS-DA investigation of the three carotenoid-dependent groups pinpointed additional differentiating metabolites. Other prevalent components in the separation of Group 1 (low carotenoid yields, green dots) and Group 2 (carotenoid yields between 5 and 15 mg 100 g^{-1} dry sample, blue dots) (Figure 9a) along the second principal component (PC2) were choline and fatty acids, which are key metabolites of Group 2 (Figure 9b). Box-plots of Figure 9c show that in Group 1 (red bars), where less polar solvents were used for extraction (Table S5), hydrophobic amino acids, valine, and leucine presented a higher content. The presence of these amino acids in Group 2 (red dots) was not significant, as the solvent of the samples, which were UAE extracts (Table S5), was more polar (a mixture of methanol and chloroform). However, the use of a unique common solvent in all samples of Group 2 provided more reproducible results regarding the recovery of valine and leucine, since all samples of Group 2 showed a small distribution around the median value (Figure 9c, green bars).

On the other hand, choline, fatty acids, and myo-inositol characterize the extracts of Group 2. According to box-plots, Group 1 (green dots) contained a very low content of fatty acids (Figure 9c, red bars), since UAE or MAE fatty acid extraction requires a longer extraction time than the one applied (15 min for both techniques) [36,37].

The dataset of Group 2 (blue dots) comprises UAE extracts obtained by applying a unique-for-each-sample combination of extraction conditions, since they correspond to different runs of 2^3 and BBD design (Table S2a). Therefore, the higher variability in the myo-inositol and choline range (Figure 9c, green bars) can be explained. It is worth mentioning that most of the samples of Group 2 were acquired at a higher US power (≥600 W) and solvent/material ratios (≥30 mL g^{-1}) (Tables S2a and S5).

Choline is acknowledged as an essential macronutrient, mainly present in lipid foods or plant oils (i.e., apricot kernel oil) as choline derivatives with lipid components (glycerophosphatidylcholine, phosphocholine, and sphingomyelin) [38]. Moreover, oleic (C18:1) and linoleic (C18:2) acids are two of the most predominant fatty acids in the lipid fraction of apricot byproducts, with a content of ~20% and ~10% of the total unsaturated fatty acids, respectively. As shown in Figure 9b, extracts of nonpolar solvents and UAE extracts with a relatively high solvent/material ratio (30–35 mL g^{-1}) and US power (625–675 W) belonging in Group 2 (blue dots) (Tables S2a and S5) presented increased levels of choline and fatty acids. Specifically, fatty acid concentration differences and variations between the groups were determined by using the characteristic peak at 1.30 ppm, which corresponds to the overlap of methylene groups (-CH_2-) (except for those in position α- and β- from the carboxyl group) of the fatty acids' chain. This outcome is consistent with the results of other studies [39] concerning the effect of UAE parameters on the fatty acid profile of the pumpkin lipid fraction, where less polar solvents and higher solvent volumes favor the recovery of lipid constituents, such as fatty acids and choline.

Following a similar pattern, the discrimination of Group 1 (in green) and Group 3 (in red) (Figure 10a) was attributed to the same metabolites (Figure 10b). Valine, isoleucine, and leucine did not significantly contribute to the discrimination in Group 3 (Figure 10b), but the distribution of the content values (especially in the case of valine) was small (Figure 10c, green bars) due to the use of ethanol (solvent with a higher polarity), as the only extraction solvent of these samples.

Although lactic acid, present in unripe apricots and fruit byproducts [40], is a discriminant metabolite of Group 1 (in green) (Figure 10b), the distinct extraction solvent systems used for the extracts of this group (while the rest of the extraction conditions were kept constant) (Table S1) resulted in a higher distribution of the samples around the median value (Figure 10c).

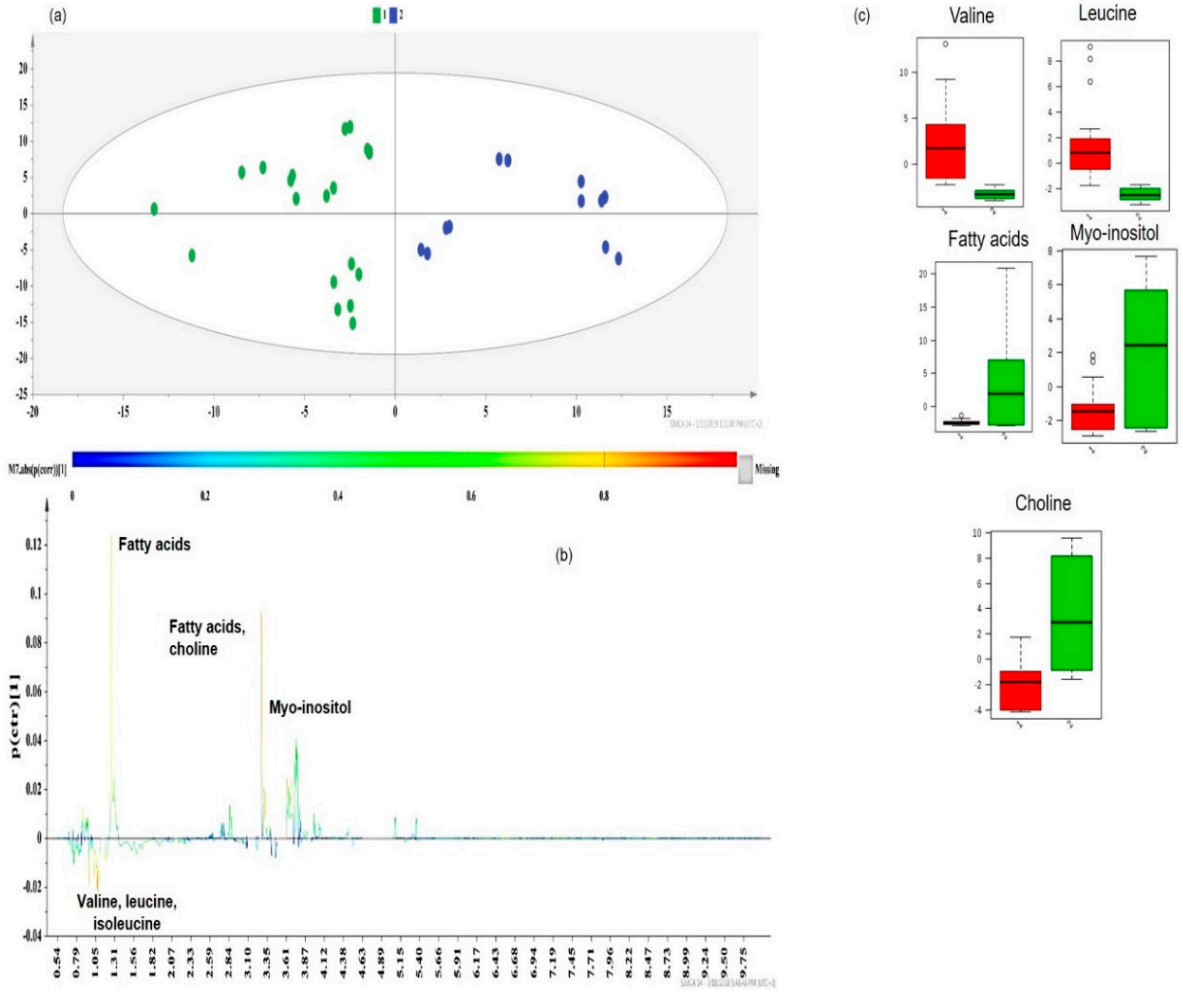

Figure 9. (**a**) OPLS-DA model of Group 1 vs. Group 2 DOE apricot extracts, Pareto scaled, where A = 1 + 1 + 0 (N = 31, $R^2Y(cum) = 0.725$, $Q^2(cum) = 0.630$, $p < 0.05$), green dots = apricot pulp samples with a low extraction yield (≤5 mg carotenoids 100 g^{-1} dry sample), and blue dots = apricot pulp samples with a medium extraction yield (5–15 mg carotenoids 100 g^{-1} dry sample); (**b**) S-line plot of the OPLS-DA model; (**c**) box-plots of the discriminant metabolites, where red box-plots correspond to Group 1 (green dots) and green box-plots correspond to Group 2 (blue dots).

Furthermore, it is interesting to note that the role of myo-inositol and fatty acids was equally significant for this classification when compared to the previous OPLS-DA model (i.e., Group 1 vs. Group 2). As reported by other research groups [36,37], the recovery of lipids and fatty acids, either extracted by UAE or MAE, is more efficient at higher extraction times than the ones applied (15 min) in the studied extracts of Group 1 (green dots) (Tables S2 and S5).

Additionally, it is more than expected that fructose plays a key role in Group 3 (red dots), which mainly contains MAE extracts, since the more polar solvents (ethanol), higher temperatures, and higher solvent/material ratios applied upheld sugar extraction [41–43]. However, due to the different extraction conditions for each run (Tables S2b and S5), a higher distribution of group samples was observed (Figure 10c, green bar).

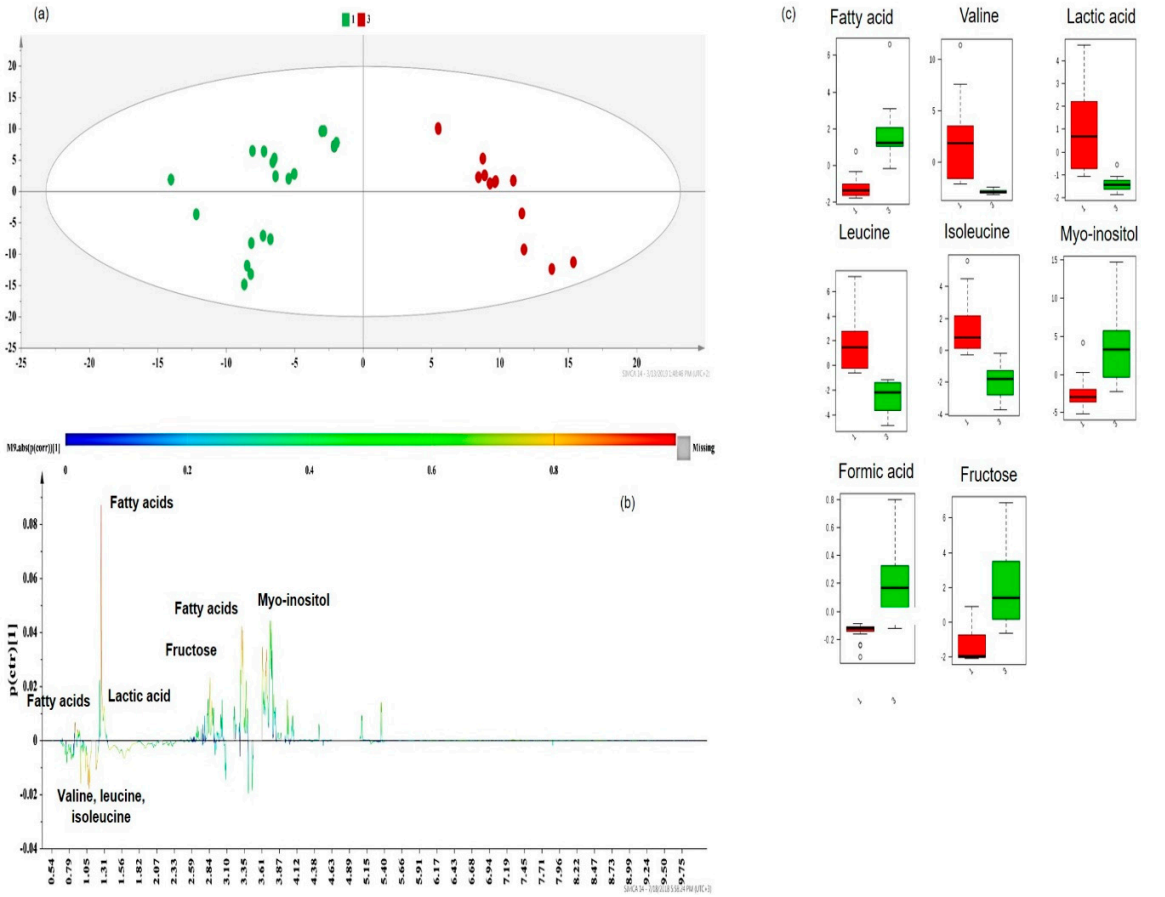

Figure 10. (**a**) OPLS-DA model of Group 1 vs. Group 3 DOE apricot extracts, Pareto scaled, where A = 1 + 1 + 0 (N = 32, $R^2Y(cum) = 0.889$, $Q^2(cum) = 0.836$, $p < 0.05$), green dots = apricot pulp samples with a low extraction yield (≤5 mg carotenoids 100 g^{-1} dry sample), and red dots = apricot pulp samples with a medium extraction yield (≥15 mg carotenoids 100 g^{-1} dry sample); (**b**) S-line plot of the OPLS-DA model; (**c**) box-plots of the discriminant metabolites, where red box-plots correspond to Group 1 (green dots) and green box-plots correspond to Group 3 (red dots).

Ultimately, the trend along the second principal component (PC2) resulted in the discrimination of DOE-extracts with medium (Group 2 in blue) and high (Group 3 in red) carotenoid contents (Figure 11a). Although, as stated before, Group 1 (low carotenoid content) presented a higher content of amino acids, valine, leucine, and lysine still play quite an important role in the discrimination of Group 2 (blue dots) and Group 3 (red dots) (Figure 11b). According to the box-plots in Figure 11c, valine, leucine, and lysine in Group 2 (red color bars) presented a higher content than in Group 3 (green bars). Group 2, comprised of UAE extracts whose extraction solvent mixture includes a less polar solvent (chloroform), shows a higher affinity to non-polar amino acids than ethanol, which is the solvent of Group 3 samples (Tables S2a and S5).

The higher distribution of values in amino acid box-plots (Figure 11c, red bars) concerning the extracts of Group 2 (blue dots), may be attributed to the great variation in the extraction time used in each of the samples, which ranged from 5 to 35 min, while the US power and solvent/material ratio were kept at high values (≥600 W and ≥30 mL g^{-1}, respectively).

Despite the contribution of amino acids in the discrimination of the two groups, the major metabolites playing a crucial role in their separation were apricots' mono- and di-saccharides [41,44] (Figure 11b). Group 3 (red dots) primarily includes MAE extracts. Higher extraction temperatures of MAE (~60 °C) and solvent/material ratios facilitate the extraction of mono-saccharides, such as glucose, xylose, and fructose, and di-saccharides, such as sucrose [42] (Tables S2b and S5). Moreover, the high US powers of UAE extracts in Group 2 (in blue) promote mono-saccharides' (glucose and xylose) than

di-saccharide recovery (Tables S2a and S5) [43]. The symmetrical distribution and the tight grouping of Group 2 and Group 3 samples in the relative box-plots of sugars (Figure 11c) are more likely a result of keeping the values of the MAE temperature (~60 °C) and UAE's US power (600–675 W) high, but quite constant, among the extracts (Tables S2 and S5).

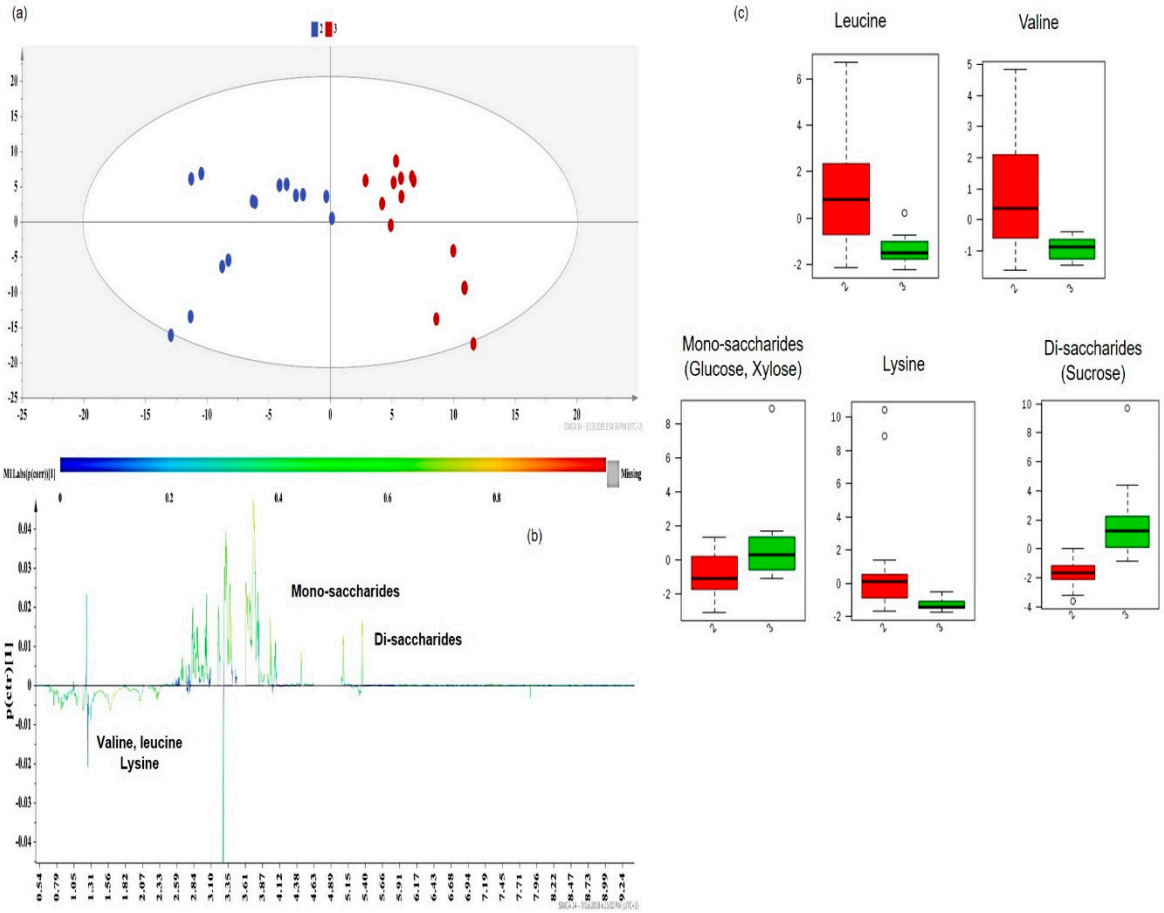

Figure 11. (**a**) OPLS-DA model of Group 2 vs. Group 3 DOE apricot extracts, Pareto scaled, where A = 1 + 1 (N = 27, $R^2Y(cum) = 0.780$, $Q^2(cum) = 0.642$, $p < 0.05$), blue dots = apricot pulp samples with a low extraction yield (5–15 mg carotenoids 100 g^{-1} dry sample), and red dots = apricot pulp samples with a medium extraction yield (≥15 mg carotenoids 100 g^{-1} dry sample); (**b**) S-line plot of the OPLS-DA model; (**c**) box-plots of the discriminant metabolites, where red box-plots correspond to Group 2 (blue dots) and green box-plots correspond to Group 3 (red dots).

To conclude, a final extract with a lower carotenoid content and branched-chain amino acids can be obtained by using non-polar solvents in UAE or MAE. A product containing choline, unsaturated fatty acids, sugar alcohols, and medium carotenoids content can be delivered at a high US power and solvent volumes. Finally, a sugar- and carotenoid-rich extract is provided when MAE at a high MW power, higher temperatures (compared to UAE), and higher solvent volumes is applied.

In conclusion, the NMR-based screening of extracts, which are delivered by different extraction methods at distinct extraction conditions, should be considered as a quite useful basic research tool for (a) enabling standardization and (b) directing a future large-scale extraction procedure towards the acquisition of extracts containing different bioactive components with 'tailor-made' biological activities.

3. Materials and Methods

3.1. Reagents and Standards

Beta-carotene and *trans*-β-apo-8′-carotenal were purchased from Sigma-Aldrich (St. Louis, MO, USA). *trans*-Lutein and *trans*-zeaxanthin were acquired from Extrasynthese (Genay, France). All solvents tested were of analytical grade. Acetone was purchased from ChemLab (Zedelgem, Belgium), while chloroform, methanol, ethanol, and *n*-hexane were obtained from Merck (Darmstadt, Germany). Scharlau (Barcelona, Spain). Fluka (Darmstadt, Germany) and Fischer Chemical (Pittsburgh, PA, USA) provided LC-MS grade methanol, acetonitrile, and methyl-tert-butyl ether (MTBE).

3.2. Plant Material and Sample Preparation

Apricot pulp was kindly provided by Danais S.A. Fruit Processing Industry & Export Company (www.danais-sa.com). Apricot fruits of the 'Bebekos' variety, which represents 70% of Greek production, were collected from the region of Argos, Peloponnese, Greece, during June 2017. Apricot byproducts, which were generated during the processing and compression of raw fruits, mainly included skin and also flesh with a particle size of over 0.5 mm.

Apricot pulp was freeze dried in a ModulyoD Freeze Dryer, equipped with a Thermo Savant ValuPump VLP200 (Thermo Electron Corporation, Thermo Fischer, Waltham, MA, USA). Freeze-drying was selected as the pulp drying method since it protects sensitive metabolites from degradation during long-term storage. This method removes sample moisture that may produce undesirable chemical reactions and promote microbial growth [45]. Lyophilization is a requisite step for carotenoid extraction, as the water content of byproducts hinders the recovery of non-hydrophilic compounds from plant substrates [15]. Dried material was homogenized and powdered in a laboratory mill (Type ZM1, Retsch GmbH, Haan, Germany). Dry material and all samples and extracts were kept in glass jars and vials at −20 °C.

3.3. Extraction Instrumentation and Processes

The ultrasound-assisted extraction (UAE) process was carried out by a Vibra-Cell VCX 750 (20 kHz, 750 W) ultrasonics processor (Sonics and Materials Inc., Newtown, USA), equipped with a piezoelectric converter and 13 mm diameter probe fabricated from titanium alloy Ti–6Al–4V. The microwave-assisted extraction (MAE) process was performed by a CEM Focused Microwave System, Model Discover (CEM Corporation, Matthews, NC, USA), in an open vessel or focused microwave (FMAE) mode with a reflux system placed above the open cell. A Centrifuge CL30 (Thermo Scientific, Waltham, MA, USA) was employed for the classical extraction. All extraction experiments were conducted according to our previous works [18] and their steps are described in the Supplementary Data.

3.4. Construction of DOE Models

A two-level full factorial design, 2^3, and a symmetrical 16-run three-level Box–Behnken design (BBD) were selected for screening and optimization purposes, respectively. DOE extraction factors were the (a) extraction time, X_1 (min); (b) US/MW power, X_2 (W); and (c) solvent/material ratio, X_3 (mL g^{-1}). The impact of the above extraction factors on the carotenoid content, measured by LC-MS/MS, was evaluated through an assessment of the factors' main effects and interactions [18]. The analysis of DOE models is unbiased when extraction variables take coded normalized dimensionless values (x_1, x_2, x_3) instead of their real values (X_1, X_2, X_3), which are expressed in different physical units. The two-level full factorial and BBD real and normalized values are shown in Table 4. Data and graphs were delivered using the Statistica package (Version 12, Stat Soft, Inc., Tulsa, OK, USA). Measurements' confidence level was set at 95% (p-values ≤ 0.05).

Table 4. Normalized and real values of UAE/MAE experimental factors for a two-level full factorial design (2^3) and Box–Behnken design (BBD) for apricot byproducts.

Coded Values	−1	0	+1
		2^3 design	
		UAE	
Extraction time (X_1, min)	5		35
US power (X_2, W)	375		675
Solvent/material ratio (X_3, mL g^{-1})	10		35
		MAE	
Extraction time (X_1, min)	5	-	30
MW power (X_2, W)	70	-	200
Solvent/material ratio (X_3, mL g^{-1})	20	-	60
		BBD	
		UAE	
Extraction time (X_1, min)	10	20	30
US power (X_2, W)	577	622	675
Solvent/material ratio (X_3, mL g^{-1})	25	30	35
		MAE	
Extraction time (X_1, min)	5	10	20
MW power (X_2, W)	60	90	130
Solvent/material ratio (X_3, mL g^{-1})	45	65	55

3.5. Identification and Quantitation of Apricot Pulp Carotenoids by Liquid Chromatography-Photodiode Array-Tandem Mass Spectrometry (LC-PDA-MS/MS)

Liquid chromatography (LC) instrumentation was a combination of (a) a quaternary pump, (b) an autosampler with a tray oven set at 10 °C (Accela, Thermo Scientific, Waltham, MA, USA), (c) an Acclaim C30 reversed-phase column (3 µm particle size, 150 × 2.1 mm i.d) thermostatted at 20 °C, and (d) a guard column. The injection volume was set at 5 µL and the mobile phase flow rate was set at 350 µL/min. Mobile phase solvents were (A) acetonitrile (ACN), (B) methanol (MeOH), and (C) methyl-tert-butyl ether (MTBE). The eluting gradient program was the following: 0–5 min (30% A, 70% B), 5.1–13 min (22.9% A, 65.8% B, and 11.3% C), 13.1–14 min (5% A, 75% B, and 20% C), 14–14.1 min (30% A, 70% B), and 14.10–20 min (30% A, 70% B). MeOH-MTBE 50:50 *v*/*v* was the injection solvent.

No modifiers were added to the mobile phase as acetic and formic acid reduced m/z intensities and ammonium acetate was not preferred for lipid compounds [46]. The photodiode array (PDA) detector was set at 424, 445, and 455 nm. The ion trap mode of the LTQ Orbitrap Velos mass spectrometer (Thermo Scientific, USA) was used for mass spectrometry (MS) identification. MS/MS measurements were performed in a positive mode using an atmospheric pressure chemical ionization (APCI) source at a mass scan width of 150–650 *m*/*z*.

Source parameters were optimized by applying a Plackett–Burman design (Table S6, Figure S7), as described in the supplementary data. Polyester filters (15 mm diameter, 0.45 µm pore size, Macherey-Nagel, Duren, Germany) was utilized for sample filtration. LC-MS/MS data were processed with Xcalibur software (version 2.1, Thermo Scientific, Waltham, MA, USA).

The development [47,48] and validation (Tables S7 and S8) of the LC-PDA-MS/MS [18,24,49–51] method are fully described in the supplementary data.

3.6. NMR Spectroscopy for the Elucidation of Non-Carotenoid Secondary Metabolites of Apricot Extracts

A Varian-600 MHz NMR spectrometer (Varian, Palo Alto, CA, USA) was used for acquiring NMR spectra. All spectra were obtained at an ambient temperature (25 °C) with a triple resonance {HCN} probe.

3.6.1. Sample Preparation and NMR Measurements

Twenty milligrams (20 mg) of apricot extract dry residue was dissolved in 550 μL of d_4-methanol, and 50 μL of TSP 5 mM (internal standard) was then added. Samples were transferred to 5 mm NMR tubes.

A one dimension-Nuclear Overhauser effect spectroscopy (1D-NOE) pulse sequence was applied for ^{1}H-NMR spectra. Spectra acquisition was performed at 128 transients collected with 128 K data points, a spectral width of 7163.9 Hz, a relaxation delay of 1 s, an acquisition time of 4.454 s, and a mixing time of 200 ms. The receiver gain was constant during all acquisitions.

Two dimensional (2D) experiments of gCOSY, gHMBCad, and gHSQCad, recorded at 25 °C, enabled the identification of extract metabolites. An analysis of 2D spectra was carried out using MestReNova v.14.1 software (Mestrelab Research, S.L., Santiago de Compostela, Spain). Metabolite elucidation was facilitated by 2D NMR spectra plus reported data and cross-referenced with the web-server metabolite database Metaboneer, which is an in-house fully automated metabolite identification platform [52].

3.6.2. Data Reduction and Spectral Alignment

All spectra were processed by MestReNova v.14.1 software for phasing, baseline correction, removal of the methanol peak, binning into spectral buckets of 0.001 ppm, and normalization to the reference compound standardized area. All spectra were converted to ASCII format and then imported into MATLAB (R2006a, Mathworks, Inc. 2006, Natick, MA, USA), where they were aligned using the Correlation Optimized Warping (COW) method.

3.7. Multivariate Data Analysis

The SIMCA-P version 14.0 (Umetrics, Umeå, Sweden) was used for the statistical processing of NMR data from apricot pulp analysis. The first step was the acquisition of a general overview and the visualization of trends and outliers among apricot extracts by applying the exploratory PCA analysis.

Further analysis of the NMR dataset occurred with supervised OPLS-DA models, in order to estimate the between-class and within-class variation. All models were derived at a 95% confidence level after being mean-centered with Pareto scaling, which only includes low/medium intensity metabolites in the model if they display systematic variation.

The extraction variables and conditions that were singled out for their class discriminating power were revealed from loading plots. Models' goodness-of-fit and predictive ability were evaluated by R^2 ($0 \leq R^2 \leq 1$) and Q^2 ($0 \leq Q^2 \leq 1$) values, respectively. R^2 refers to the data variance interpreted by the model, while cumulative Q^2 describes the variance of the data which are predictable by the model. In OPLS-DA models, the statistical importance of R^2 and Q^2 is evaluated through response permutation testing (999 permutations employed in our study) and a receiver operating characteristic (ROC) curve. In a permutation test plot, a model is valid when the intercept of the Q^2 regression line is lower than zero and the intercept of the R^2 regression line is crucially lower than that of the original [53]. A model is also considered significant when ROC values are ≥0.75. S-line plots highlighted the metabolites that contributed to DOE extract discrimination.

4. Conclusions

In recent years, coping with the problem of agro-byproduct accumulation and disposal has created new potential for the profitable and eco-friendly management of food and agro-waste through the use

of innovative analytical strategies. In the current project, the results of the implementation of UAE and MAE for the recovery of carotenoids and other bioactive co-extractives from apricot pulp are summarized below.

Carotenoids from apricot byproducts were obtained in higher amounts when MAE was applied. Compared to classic extraction (the Folch method), high energy extractions provided higher (19-times more in the case of MAE) carotenoid yields.

Reflecting on the concept of transforming a byproduct to high-added value products, the potential of NMR spectroscopy for apricot byproducts was explored.

Despite the fact that MAE provided higher carotenoid yields, the main co-extractives of these samples were sugars, whose removal and clean-up could be more challenging and laborious than for other co-extractives.

Furthermore, extracts of Group 2 (Table S5), mostly obtained by UAE at a high US power and solvent/material ratio, can result in an extract with combined biological activities due to their significant content of carotenoids (improving eye health, immune-modulating properties, anti-allergic, anti-aging, and sun-protective activity) [13,54], choline (enhancing brain health and cognitive function, affecting detoxification pathways and organs, such as the liver and kidneys) [55–57], myo-inositol (promoting female fertility, treating polycystic ovary syndrome, reducing anxiety, and restoring insulin resistance) [58–60], and unsaturated fatty acids (health-promoting agents against fat burning, affecting inflammation, steroid signaling, and membrane-bound protein functions, participating in glucose/lipid metabolism) [61–63].

Although MAE provided extracts with higher carotenoids yields, in the case of a prospective scaling-up of high energy extraction processes in the field of nutraceuticals or cosmetics, UAE will probably emerge as a more suitable approach, as it delivered extracts with a significant carotenoid content, rich in other bioactive constituents (choline, myo-inositol, and fatty acids), and with a lower sugar concentration, compared to MAE extracts.

Therefore, summarizing the results of this research, high energy extraction methods emerge as an attractive alternative for tackling any challenges or drawbacks of the current large-scale extraction methods from an industrial point of view, as they provide high quality extracts. These results should be considered as an elementary index or starting point for the development of nutraceutical supplements.

This study is the first to integrate high energy extraction techniques, DOE models, LC-MS/MS, and NMR spectroscopy, in order to correlate extracts of different carotenoid yields with particular secondary metabolites by adjusting UAE or MAE parameters and to allow imminent standardization of the extraction procedure to obtain multi-targeted and multi-functional natural extracts. In that way, high energy extractions can be re-evaluated and upgraded to reliable sample preparation steps in the field of plant metabolomics.

Supplementary Materials: The following are available online at http://www.mdpi.com/1420-3049/25/11/2702/s1, Figure S1: Contour plots of (**a**) UAE extraction time vs. US power; (b) UAE US power vs. solvent/material ratio; (c) UAE solvent/material ratio vs. extraction time; (d) MAE extraction time vs. MW power; (e) MAE MW power vs. solvent/material ratio; and (f) MAE solvent/material ratio vs. extraction time; Figure S2: Pareto charts of (a) UAE and (b) MAE, where 1 = extraction time, 2 = US or MW power, 3 = solvent/material ratio, L = linear terms, and Q = quadratic terms; Figure S3: 1D-NMR spectrum of a characteristic apricot extract (i.e., UAE ethanol-acetone extract): (a) ^{1}H-NOESY spectrum; (b) chemical shifts region of amino acids, lactic acid, and fatty acids; (c) chemical shifts region of myo-inositol, choline, and malic acid; (d) chemical shifts region of sugars; Figure S4: 2D spectra of a characteristic extract of (a) Group 1 gCOSY; (b) Group 1 gHSQCad; (c) Group 2 gCOSY; (d) Group 2 gHSQCad; (e) Group 3 gCOSY; and (f) Group 3 gHSQCad; Figure S5: Contribution plot of Folch samples; Figure S6: Permutation testing and ROC curves of OPLS-DA models: (a) Group 1 vs. 2+3; (b) Group 1 vs. 2; (c) Group 1 vs. 3; and (d) Group 2 vs. 3; Figure S7: Plackett–Burman design: Normal probability plot of the effect of APCI parameters on the β-carotene intensity; Table S1: UAE and MAE extraction yields of different solvent systems; Table S2: Randomized experimental runs and carotenoid extraction yield of 23 and BBD models of (a) UAE and (b) MAE; Table S3: ANOVA table of (a) 2^3 design and (b) BBD model for UAE and MAE of apricot pulp carotenoids; Table S4: Predicted and observed extraction yields of apricot pulp at optimal experimental combinations proposed by the BBD model; Table S5: Apricot pulp sample classification produced by PCA models; Table S6: Plackett–Burman design: Coded and real values of APCI parameters; Table S7. Analytical

figures of merit of LC-MS/MS for apricot pulp carotenoid determination; Table S8. Precision, accuracy, and process recovery of the LC-MS/MS method for apricot pulp carotenoid determination.

Author Contributions: Conceptualization, T.T., P.Z., and V.J.S.; methodology, T.T., C.F., D.Z.L., and E.S.; software, T.T. and C.F.; validation, T.T.; formal analysis, T.T., D.Z.L., K.T., and E.S.; investigation, T.T.; resources, P.Z., and V.J.S.; data curation, T.T.; writing—original draft preparation, K.T. and T.T.; writing—review and editing, C.F., E.S., C.F., D.Z.L., P.Z., and V.J.S.; supervision, P.Z. and V.J.S.; project administration, P.Z. and V.J.S.; funding: P.Z. and V.J.S. All authors have read and agreed to the published version of the manuscript.

Funding: This research received no external funding. It was financially supported by internal resources.

Acknowledgments: Samples of this study were provided by Danais S.A Fruit Processing Industry & Export Company (www.danais-sa.com) (Argos, Peloponnese, Greece). Special thanks to Evangelia Kapiri, Martha Hatziriga, and Nikolaos Giannopoulos, pre-graduate students from the Department of Food Science and Technology, University of West Attica, for their contribution to the extraction experiments.

Conflicts of Interest: The authors declare no conflict of interest.

References

1. Bijttebier, S.; Van der Auwera, A.; Foubert, K.; Voorspoels, S.; Pieters, L.; Apers, S. Bridging the gap between comprehensive extraction protocols in plant metabolomics studies and method validation. *Anal. Chim. Acta* **2016**, *935*, 136–150. [CrossRef] [PubMed]
2. Fotakis, C.; Tsigrimani, D.; Tsiaka, T.; Lantzouraki, D.Z.; Strati, I.F.; Makris, C.; Tagkouli, D.; Proestos, C.; Sinanoglou, V.J.; Zoumpoulakis, P. Metabolic and antioxidant profiles of herbal infusions and decoctions. *Food Chem.* **2016**, *211*, 963–971. [CrossRef] [PubMed]
3. De Falco, B.; Lanzotti, V. NMR spectroscopy and mass spectrometry in metabolomics analysis of Salvia. *Phytochem. Rev.* **2018**, *17*, 951–972. [CrossRef]
4. Tsiaka, T.; Sinanoglou, V.J.; Zoumpoulakis, P. Extracting Bioactive Compounds From Natural Sources Using Green High-Energy Approaches: Trends and Opportunities in Lab- and Large-Scale Applications. In *Ingredients Extraction by Physicochemical Methods in Food*; Grumezescu, A.M., Holban, A.M., Eds.; Handbook of Food Bioengineering; Academic Press: Cambridge, MA, USA, 2017; Volume 4, pp. 307–365, ISBN 978-0-12-811521-3.
5. Acquadro, S.; Appleton, S.; Marengo, A.; Bicchi, C.; Sgorbini, B.; Mandrone, M.; Gai, F.; Peiretti, P.G.; Cagliero, C.; Rubiolo, P. Grapevine Green Pruning Residues as a Promising and Sustainable Source of Bioactive Phenolic Compounds. *Molecules* **2020**, *25*, 464. [CrossRef] [PubMed]
6. Žlabur, J.Š.; Žutić, I.; Radman, S.; Pleša, M.; Brnčić, M.; Barba, F.J.; Rocchetti, G.; Lucini, L.; Lorenzo, J.M.; Domínguez, R.; et al. Effect of Different Green Extraction Methods and Solvents on Bioactive Components of Chamomile (*Matricaria chamomilla L.*) Flowers. *Molecules* **2020**, *25*, 810. [CrossRef]
7. Luque de Castro, M.D.; Delgado-Povedano, M.M. Ultrasound: A subexploited tool for sample preparation in metabolomics. *Anal. Chim. Acta* **2014**, *806*, 74–84. [CrossRef]
8. Saini, R.K.; Moon, S.H.; Keum, Y.S. An updated review on use of tomato pomace and crustacean processing waste to recover commercially vital carotenoids. *Food Res. Int.* **2018**, *108*, 516–529. [CrossRef] [PubMed]
9. Atanasov, A.G.; Waltenberger, B.; Pferschy-Wenzig, E.M.; Linder, T.; Wawrosch, C.; Uhrin, P.; Temml, V.; Wang, L.; Schwaiger, S.; Heiss, E.H.; et al. Discovery and resupply of pharmacologically active plant-derived natural products: A review. *Biotechnol. Adv.* **2015**, *33*, 1582–1614. [CrossRef]
10. Pimentel-Moral, S.; de la Luz Cádiz-Gurrea, M.; Rodríguez-Pérez, C.; Segura-Carretero, A. Recent advances in extraction technologies of phytochemicals applied for the revaluation of agri-food by-products. In *Functional and Preservative Properties of Phytochemicals*; Prakash, B., Ed.; Academic Press: Cambridge, MA, USA, 2020; pp. 209–239. ISBN 978-0-12-818593-3.
11. Lai, W.T.; Khong, N.M.H.; Lim, S.S.; Hee, Y.Y.; Sim, B.I.; Lau, K.Y.; Lai, O.M. A review: Modified agricultural by-products for the development and fortification of food products and nutraceuticals. *Trends Food Sci. Tech.* **2017**, *59*, 148–160. [CrossRef]
12. Chemat, F.; Vian, M.A.; Cravotto, G. Green extraction of natural products: Concept and principles. *Int. J. Mol. Sci.* **2012**, *13*, 8615–8627. [CrossRef]
13. Saini, R.K.; Nile, S.H.; Park, S.W. Carotenoids from fruits and vegetables: Chemistry, analysis, occurrence, bioavailability and biological activities. *Food Res. Int.* **2015**, *76*, 735–750. [CrossRef] [PubMed]

14. Campbell, O.E.; Padilla-Zakour, O.I. Phenolic and carotenoid composition of canned peaches (*Prunus persica*) and apricots (*Prunus armeniaca*) as affected by variety and peeling. *Food Res. Int.* **2013**, *54*, 448–455. [CrossRef]
15. Saini, R.K.; Keum, Y.S. Carotenoid extraction methods: A review of recent developments. *Food Chem.* **2018**, *240*, 90–103. [CrossRef] [PubMed]
16. Tanaka, T.; Shnimizu, M.; Moriwaki, H. Cancer chemoprevention by carotenoids. *Molecules* **2012**, *17*, 3202–3242. [CrossRef] [PubMed]
17. Chemat, F.; Rombaut, N.; Sicaire, A.G.; Meullemiestre, A.; Fabiano-Tixier, A.S.; Abert-Vian, M. Ultrasound assisted extraction of food and natural products. Mechanisms, techniques, combinations, protocols and applications. A review. *Ultrason. Sonochem.* **2017**, *34*, 540–560. [CrossRef] [PubMed]
18. Tsiaka, T.; Lantzouraki, D.Z.; Siapi, E.; Sinanoglou, V.J.; Heropoulos, G.A.; Calokerinos, A.C.; Zoumpoulakis, P. Macular carotenoids in lipid food matrices: DOE-based high energy extraction of egg yolk xanthophylls and quantification through a validated APCI(+) LC-MS/MS method. *J. Chromatogr. B* **2018**, *1096*, 160–171. [CrossRef]
19. Belwal, T.; Ezzat, S.M.; Rastrelli, L.; Bhatt, I.D.; Daglia, M.; Baldi, A.; Devkota, H.P.; Orhan, I.E.; Patra, J.K.; Das, G.; et al. A critical analysis of extraction techniques used for botanicals: Trends, priorities, industrial uses and optimization strategies. *TrAC Trends Anal. Chem.* **2018**, *100*, 82–102. [CrossRef]
20. Chan, C.H.; Yusoff, R.; Ngoh, G.-C.; Kung, F.W.-L. Microwave-assisted extractions of active ingredients from plants. *J. Chromatogr. A* **2011**, *1218*, 6213–6225. [CrossRef]
21. Hiranvarachat, B.; Devahastin, S.; Chiewchan, N.; Vijaya Raghavan, G.S. Structural modification by different pretreatment methods to enhance microwave-assisted extraction of β-carotene from carrots. *J. Food Eng.* **2013**, *115*, 190–197. [CrossRef]
22. Mercado-Mercado, G.; Montalvo-González, E.; González-Aguilar, G.A.; Alvarez-Parrilla, E.; Sáyago-Ayerdi, S.G. Ultrasound-assisted extraction of carotenoids from mango (*Mangifera indica* L. 'Ataulfo') by-products on *in vitro* bioaccessibility. *Food Biosci.* **2018**, *21*, 125–131. [CrossRef]
23. Chuyen, H.V.; Nguyen, M.H.; Roach, P.D.; Golding, J.B.; Parks, S.E. Microwave-assisted extraction and ultrasound-assisted extraction for recovering carotenoids from Gac peel and their effects on antioxidant capacity of the extracts. *Food Sci. Nutr.* **2018**, *6*, 189–196. [CrossRef] [PubMed]
24. Song, J.; Yang, Q.; Huang, W.; Xiao, Y.; Li, D.; Liu, C. Optimization of *trans* lutein from pumpkin (*Cucurbita moschata*) peel by ultrasound-assisted extraction. *Food Bioprod. Proc.* **2018**, *107*, 104–112. [CrossRef]
25. Nayak, B.; Dahmoune, F.; Moussi, K.; Remini, H.; Dairi, S.; Aoun, O.; Khodir, M. Comparison of microwave, ultrasound and accelerated-assisted solvent extraction for recovery of polyphenols from *Citrus sinensis* peels. *Food Chem.* **2015**, *187*, 507–516. [CrossRef]
26. Carail, M.; Fabiano-Tixier, A.-S.; Meullemiestre, A.; Chemat, F.; Caris-Veyrat, C. Effects of high power ultrasound on all-E-β-carotene, newly formed compounds analysis by ultra-high-performance liquid chromatography-tandem mass spectrometry. *Ultrason. Sonochem.* **2015**, *26*, 200–209. [CrossRef]
27. Zaghdoudi, K.; Pontvianne, S.; Framboisier, X.; Achard, M.; Kudaibergenova, R.; Ayadi-Trabelsi, M.; Kalthoum-Cherif, J.; Vanderesse, R.; Frochot, C.; Guiavarc'h, Y. Accelerated solvent extraction of carotenoids from: Tunisian Kaki (*Diospyros kaki* L.), peach (*Prunus persica* L.) and apricot (*Prunus armeniaca* L.). *Food Chem.* **2015**, *184*, 131–139. [CrossRef] [PubMed]
28. Leong, S.Y.; Oey, I. Effects of processing on anthocyanins, carotenoids and vitamin C in summer fruits and vegetables. *Food Chem.* **2012**, *133*, 1577–1587. [CrossRef]
29. Botoran, O.R.; Ionete, R.E.; Miricioiu, M.G.; Costinel, D.; Radu, G.L.; Popescu, R. Amino Acid Profile of Fruits as Potential Fingerprints of Varietal Origin. *Molecules* **2019**, *24*, 4500. [CrossRef]
30. Andreou, V.; Strati, I.F.; Fotakis, C.; Liouni, M.; Zoumpoulakis, P.; Sinanoglou, V.J. Herbal distillates: A new era of grape marc distillates with enriched antioxidant profile. *Food Chem.* **2018**, *253*, 171–178. [CrossRef]
31. Sochor, J.; Skutkova, H.; Babula, P.; Zitka, O.; Cernei, N.; Rop, O.; Krska, B.; Adam, V.; Provazník, I.; Kizek, R. Mathematical evaluation of the amino acid and polyphenol content and antioxidant activities of fruits from different apricot cultivars. *Molecules* **2011**, *16*, 7428–7457. [CrossRef]
32. Carrera, C.; Ruiz-Rodríguez, A.; Palma, M.; Barroso, C.G. Ultrasound-assisted extraction of amino acids from grapes. *Ultrason. Sonochem.* **2015**, *22*, 499–505. [CrossRef]
33. Rebecca, O.P.S.; Boyce, A.N.; Somasundram, C. Isolation and identification of myo-inositol crystals from dragon fruit (*Hylocereus polyrhizus*). *Molecules* **2012**, *17*, 4583–4594. [CrossRef] [PubMed]

34. Tetik, N.; Yüksel, E. Ultrasound-assisted extraction of d-pinitol from carob pods using Response Surface Methodology. *Ultrason. Sonochem.* **2014**, *21*, 860–865. [CrossRef] [PubMed]
35. Ruiz-Aceituno, L.; García-Sarrió, M.J.; Alonso-Rodriguez, B.; Ramos, L.; Sanz, M.L. Extraction of bioactive carbohydrates from artichoke (*Cynara scolymus* L.) external bracts using microwave assisted extraction and pressurized liquid extraction. *Food Chem.* **2016**, *196*, 1156–1162. [CrossRef] [PubMed]
36. Ramandi, N.F.; Ghassempour, A.; Najafi, N.M.; Ghasemi, E. Optimization of ultrasonic assisted extraction of fatty acids from *Borago Officinalis* L. flower by central composite design. *Arab. J. Chem.* **2017**, *10*, S23–S27. [CrossRef]
37. Esquivel-Hernández, D.A.; Rodríguez-Rodríguez, J.; Rostro-Alanis, M.; Cuéllar-Bermúdez, S.P.; Mancera-Andrade, E.I.; Núñez-Echevarría, J.E.; García-Pérez, J.S.; Chandra, R.; Parra-Saldívar, R. Advancement of green process through microwave-assisted extraction of bioactive metabolites from *Arthrospira Platensis* and bioactivity evaluation. *Bioresour. Technol.* **2017**, *224*, 618–629. [CrossRef]
38. Yonemori, K.M.; Lim, U.; Koga, K.R.; Wilkens, L.R.; Au, D.; Boushey, C.J.; Le Marchand, L.; Kolonel, L.N.; Murphy, S.P. Dietary choline and betaine intakes vary in an adult multiethnic population. *J. Nutr.* **2013**, *143*, 894–899. [CrossRef]
39. Hernández-Santos, B.; Rodríguez-Miranda, J.; Herman-Lara, E.; Torruco-Uco, J.G.; Carmona-García, R.; Juárez-Barrientos, J.M.; Chávez-Zamudio, R.; Martínez-Sánchez, C.E. Effect of oil extraction assisted by ultrasound on the physicochemical properties and fatty acid profile of pumpkin seed oil (*Cucurbita pepo*). *Ultrason. Sonochem.* **2016**, *31*, 429–436. [CrossRef]
40. Kim, H.-R.; Kim, I.-D.; Dhungana, S.K.; Kim, M.-O.; Shin, D.-H. Comparative assessment of physicochemical properties of unripe peach (*Prunus persica*) and Japanese apricot (*Prunus mume*). *Asian Pac. J. Trop. Biomed.* **2014**, *4*, 97–103. [CrossRef]
41. Bae, H.; Yun, S.K.; Yoon, I.K.; Nam, E.Y.; Kwon, J.H.; Jun, J.H. Assessment of organic acid and sugar composition in apricot, plumcot, plum, and peach during fruit development. *J. Appl. Bot. Food Qual.* **2014**, *87*.
42. Ren, B.; Chen, C.; Li, C.; Fu, X.; You, L.; Liu, R.H. Optimization of microwave-assisted extraction of *Sargassum thunbergii* polysaccharides and its antioxidant and hypoglycemic activities. *Carbohydr. Polym.* **2017**, *173*, 192–201. [CrossRef]
43. Wang, K.; Li, M.; Wen, X.; Chen, X.; He, Z.; Ni, Y. Optimization of ultrasound-assisted extraction of okra (*Abelmoschus esculentus* (L.) Moench) polysaccharides based on response surface methodology and antioxidant activity. *Int. J. Biol. Macromol.* **2018**, *114*, 1056–1063. [CrossRef] [PubMed]
44. Lahaye, M.; Falourd, X.; Quemener, B.; Devaux, M.-F.; Audergon, J.-M. Histological and cell wall polysaccharide chemical variability among apricot varieties. *LWT Food Sci.Technol.* **2014**, *58*, 486–496. [CrossRef]
45. Mushtaq, M.Y.; Choi, Y.H.; Verpoorte, R.; Wilson, E.G. Extraction for metabolomics: Access to the metabolome. *Phytochem. Anal.* **2014**, *25*, 291–306. [CrossRef] [PubMed]
46. Cajka, T.; Fiehn, O. Comprehensive analysis of lipids in biological systems by liquid chromatography-mass spectrometry. *TrAC-Trend Anal. Chem.* **2014**, *61*, 192–206. [CrossRef]
47. Rivera, S.M.; Christou, P.; Canela-Garayoa, R. Identification of carotenoids using mass spectrometry. *Mass Spectrom. Rev.* **2014**, *33*, 353–372. [CrossRef]
48. Van Breemen, R.B.; Dong, L.; Pajkovic, N.D. Atmospheric Pressure Chemical Ionization Tandem Mass Spectrometry of Carotenoids. *Int. J. Mass. Spectrom.* **2012**, *312*, 163–172. [CrossRef]
49. Abraham, J. International Conference On Harmonisation Of Technical Requirements For Registration Of Pharmaceuticals For Human Use. In *Handbook of Transnational Economic Governance Regimes*; Tietje, C., Brouder, A., Eds.; Brill|Nijhoff: Leiden, The Netherlands, 2010; ISBN 978-90-04-18156-4.
50. Nimalaratne, C.; Wu, J.; Schieber, A. Egg Yolk Carotenoids: Composition, Analysis, and Effects of Processing on Their Stability. In *Carotenoid Cleavage Products*; American Chemical Society: Washington, DC, USA, 2013; Volume 1134, pp. 219–225. ISBN 978-0-8412-2778-1.
51. Gupta, P.; Sreelakshmi, Y.; Sharma, R. A rapid and sensitive method for determination of carotenoids in plant tissues by high performance liquid chromatography. *Plant Methods* **2015**, *11*, 5. [CrossRef]
52. Filntisi, A.; Fotakis, C.; Asvestas, P.; Matsopoulos, G.K.; Zoumpoulakis, P.; Cavouras, D. Automated metabolite identification from biological fluid 1H NMR spectra. *Metabolomics* **2017**, *13*, 146. [CrossRef]

53. Marincola, F.C.; Dessì, A.; Pattumelli, M.G.; Corbu, S.; Ossicini, C.; Ciccarelli, S.; Agostino, R.; Mussap, M.; Fanos, V. (1)H NMR-based urine metabolic profile of IUGR, LGA, and AGA newborns in the first week of life. *Clin. Chim. Acta* **2015**, *451*, 28–34. [CrossRef]
54. Rodriguez-Amaya, D.B. Update on natural food pigments-A mini-review on carotenoids, anthocyanins, and betalains. *Food Res. Int.* **2019**, *124*, 200–205. [CrossRef]
55. Jacobson, S.W.; Carter, R.C.; Molteno, C.D.; Stanton, M.E.; Herbert, J.S.; Lindinger, N.M.; Lewis, C.E.; Dodge, N.C.; Hoyme, H.E.; Zeisel, S.H.; et al. Efficacy of Maternal Choline Supplementation During Pregnancy in Mitigating Adverse Effects of Prenatal Alcohol Exposure on Growth and Cognitive Function: A Randomized, Double-Blind, Placebo-Controlled Clinical Trial. *Alcohol Clin. Exp. Res.* **2018**, *42*, 1327–1341. [CrossRef] [PubMed]
56. Pera, B.; Krumsiek, J.; Assouline, S.E.; Marullo, R.; Patel, J.; Phillip, J.M.; Román, L.; Mann, K.K.; Cerchietti, L. Metabolomic Profiling Reveals Cellular Reprogramming of B-Cell Lymphoma by a Lysine Deacetylase Inhibitor through the Choline Pathway. *EBioMedicine* **2018**, *28*, 80–89. [CrossRef] [PubMed]
57. Zeisel, S.H.; da Costa, K.-A. Choline: An essential nutrient for public health. *Nutr. Rev.* **2009**, *67*, 615–623. [CrossRef] [PubMed]
58. Monastra, G.; Unfer, V.; Harrath, A.H.; Bizzarri, M. Combining treatment with myo-inositol and D-chiro-inositol (40:1) is effective in restoring ovary function and metabolic balance in PCOS patients. *Gynecol. Endocrinol.* **2017**, *33*, 1–9. [CrossRef] [PubMed]
59. Laganà, A.S.; Garzon, S.; Casarin, J.; Franchi, M.; Ghezzi, F. Inositol in Polycystic Ovary Syndrome: Restoring Fertility through a Pathophysiology-Based Approach. *Trends Endocrinol. Metab.* **2018**, *29*, 768–780. [CrossRef] [PubMed]
60. Brunst, K.J.; Ryan, P.H.; Altaye, M.; Yolton, K.; Maloney, T.; Beckwith, T.; LeMasters, G.; Cecil, K.M. Myo-inositol mediates the effects of traffic-related air pollution on generalized anxiety symptoms at age 12 years. *Environ. Res.* **2019**, *175*, 71–78. [CrossRef]
61. Garcia-Cervera, E.; Figueroa-Valverde, L.; Pool Gomez, E.; Rosas-Nexticapa, M.; Lenin, H.-H.; Virginia, M.-A.; Perla, P.-G.; Regina, C.-C. Biological activity exerted by omega-3 fatty acids on body mass index, glucose, total cholesterol and blood pressure in obese children. *Integr. Obesity Diabetes* **2018**, *4*. [CrossRef]
62. Innes, J.K.; Calder, P.C. Omega-6 fatty acids and inflammation. *Prostaglandins Leukot. Ess. Fat. Acids* **2018**, *132*, 41–48. [CrossRef]
63. Rogero, M.; Calder, P. Obesity, Inflammation, Toll-Like Receptor 4 and Fatty Acids. *Nutrients* **2018**, *10*, 432. [CrossRef]

Sample Availability: Not available.

molecules

MDPI

Article

On the Identification and Quantification of Ergothioneine and Lovastatin in Various Mushroom Species: Assets and Challenges of Different Analytical Approaches

Konstantinos Tsiantas [1,2], Thalia Tsiaka [1], Georgios Koutrotsios [3], Eleni Siapi [1], Georgios I. Zervakis [3], Nick Kalogeropoulos [4] and Panagiotis Zoumpoulakis [1,2,*]

1 Institute of Chemical Biology, National Hellenic Research Foundation 48, Vas. Constantinou Ave., 11635 Athens, Greece; ktsiantas@uniwa.gr (K.T.); thtsiaka@eie.gr (T.T.); esiapi@eie.gr (E.S.)
2 Department of Food Science and Technology, University of West Attica, Ag. Spyridonos, 12243 Egaleo, Greece
3 Laboratory of General and Agricultural Microbiology, Department of Crop Science, Agricultural University of Athens, 11855 Athens, Greece; georgioskoutrotsios@gmail.com (G.K.); zervakis@aua.gr (G.I.Z.)
4 Laboratory of Chemistry, Biochemistry, Physical Chemistry of Foods, Department of Nutrition and Dietetics, School of Health Science and Education, Harokopio University, 70 El. Venizelou Str., 17661 Athens, Greece; nickal@hua.gr
* Correspondence: pzoump@uniwa.gr; Tel.: +30-210-53855522

Abstract: In recent years, mushrooms have drawn the attention of agro-industries and food-industries as they were considered to be valuable natural sources of health promoting compounds such as β-glucans, ergothioneine, and lovastatin. The detection and quantification of such compounds by implementing reliable analytical approaches is of the utmost importance in order to adjust mushrooms' cultivation conditions and maximize the production in different species. Toward this direction, the current study focuses on the comparison of ultraviolet–visible (UV–Vis) spectrometry and liquid chromatography–mass spectrometry (LC–MS) methods (a) by evaluating the content of ergothioneine and lovastatin in mushrooms and (b) by highlighting any possible substrate-based interferences that hinder the accurate determination of these two compounds in order to propose the technique-of-choice for a standardized bioactive compounds monitoring. For this purpose, mushrooms produced by three species (i.e., *Agaricus bisporus*, *Pleurotus ostreatus*, and *P. citrinopileatus*) on various cultivation substrates, namely wheat straw (WS), winery (grape marc (GM)), and olive oil (OL) by-products, were examined. Among the two applied techniques, the developed and validated LC–MS methods, exhibiting relatively short analysis time and higher resolution, emerge as the methods-of-choice for detecting ergothioneine and lovastatin in mushrooms. On the contrary, UV–Vis methods were hindered due to co-absorbance of different constituents, resulting in invalid results. Among the studied mushrooms, *P. citrinopileatus* contained the highest amount of ergothioneine (822.1 ± 20.6 mg kg^{-1} dry sample), whereas *A. bisporus* contained the highest amounts of lovastatin (1.39 ± 0.014 mg kg^{-1} dry sample). Regarding the effect of different cultivation substrates, mushrooms produced on OL and WS contained the highest amount of ergothioneine, while mushrooms deriving from GM-based substrates contained the highest amount of lovastatin.

Keywords: mushrooms; ergothioneine; lovastatin; ultraviolet–visible spectroscopy (UV–Vis); liquid chromatography–mass spectrometry (LC–MS)

Citation: Tsiantas, K.; Tsiaka, T.; Koutrotsios, G.; Siapi, E.; Zervakis, G.I.; Kalogeropoulos, N.; Zoumpoulakis, P. On the Identification and Quantification of Ergothioneine and Lovastatin in Various Mushroom Species: Assets and Challenges of Different Analytical Approaches. *Molecules* **2021**, *26*, 1832. https://doi.org/10.3390/molecules26071832

Academic Editor: Hiroyuki Kataoka

Received: 2 February 2021
Accepted: 18 March 2021
Published: 24 March 2021

1. Introduction

From the ancient years, mushrooms have been an integral part of many different culture diets such as the Asian, the European, and the American. Besides that, mushrooms were the basic ingredients of ethno-pharmacology and folklore medicine [1], since they exert several health-promoting properties, such as antioxidant, anti-inflammatory, anti-cancer, antimicrobial, anti-cholesterol, prebiotic, geno-protective, and immunomodulating activities, which are associated with specific compounds present in mushrooms, like

ergothioneine, polysaccharides (chitosan, β-glucan), terpenes, lectins, and lovastatin [2–8]. Although the beneficial effects of mushroom consumption are well-established, their biological activities and mechanism of action varies among species [9].

Currently, the advances on agricultural practices and the introduction of modern non-conventional approaches have improved the efficiency of mushroom cultivation. As a result, more than thirty mushroom species are commercially cultivated, and the production of more than twenty are currently on the scaling-up stage [10]. According to Food and Agriculture Organization (FAO) statistics, mushroom production shows an increasing trend of about one million tons per year, disclosing a huge socioeconomical and commercial impact at a global level [11]. Species of the genera *Agaricus* (white button mushroom) and *Pleurotus* (oyster mushroom) are among the top-five in the world mushroom supply [12].

Focusing on mushrooms' secondary metabolites, ergothioneine and lovastatin are important metabolites of fungal growth with well-established bioactive properties. Therefore, optimization of the cultivation conditions and practices is of the utmost importance [13]. Ergothioneine (ESH) is a water-soluble thiol compound, whose composition involves the amino acids histidine, cysteine, and methionine [14]. In recent years, ergothioneine held researcher's attention because of its beneficial effects against autoimmune disorders, such as rheumatoid arthritis and Chron's disease, that are strongly related to ergothioneine's antioxidant properties [15]. According to current in vitro studies, decreased blood and tissue levels of ergothioneine have been observed in some diseases, such as chronic inflammatory conditions, cardiovascular disorders, and ischemia, suggesting that ergothioneine can play a pivotal protective role in various pathological conditions [16].

Lovastatin (LOV) is a natural statin, mainly produced by *Aspergillus terreus* strains [17]. It is widely known, over years, that statins can lower total and low-density lipoprotein (LDL) cholesterol levels and reduce the risk of coronary heart disease by competitively inhibiting 3-hydroxy-3-methylglutaryl coenzyme A (HMG CoA) reductase, which is a critical rate-limiting enzyme in the production of cholesterol [18,19]. In addition to the previously mentioned main action of statins, lovastatin has revolutionized the treatment of hypercholesterolemia and it is proven to be therapeutically and preventatively effective in the treatment of major types of diseases, like atherosclerosis, sepsis, peripheral arterial and vascular disease, cerebral vascular disease, ischemic disease, and bone fracture [20]. Lovastatin in mushrooms can be present in its lactone form or in its hydroxyl metabolite. This bioconversion is bidirectional and significantly affected by the prevailing pH conditions [21]. At a low pH, most of the acidic form is converted to the lactone-quantifiable lovastatin even though the equilibrium is still present [22]. Therefore, cultivation conditions, special pre-treatments, or pH adjustments during analysis can affect the identified form of lovastatin.

The development and validation of robust, fast, accurate, and reliable analytical methodologies to determine the actual concentration of ergothioneine and lovastatin by sidestepping any possible interferences or errors generated by other co-existing mushroom constituents is of major importance. According to already published works, both ergothioneine and lovastatin absorb light at 238 and 254 nm, respectively. Until now, there have been no published studies where ultraviolet-visible (UV–Vis) spectroscopy was implemented for detecting ergothioneine and lovastatin as a stand-alone technique.

Spectrophotometric detectors, like a diode array detector (DAD), coupled with liquid chromatography (LC), have been extensively used for the identification and quantification of the two analytes in mushrooms [23]. In most cases, the applied liquid-chromatography ultraviolet (LC–UV) approaches are time consuming (analysis time >20 min), not fully validated methods, that may lead to an under-estimation or over-estimation of the relatively low (compared to other mushrooms metabolites) ergothioneine and lovastatin content [24,25]. Accordingly, the hyphenation of faster LC technologies of improved resolution ability with mass spectrometry (MS) promotes enhanced sensitivity, higher selectivity, and higher sample throughput of the LC–MS technique, compared to high-pressure liquid chromatography with ultra-violet detector (HPLC–UV) methods. Up to date, the assets

of LC–MS methods are reflected particularly in ergothioneine and lovastatin analyses in dietary supplements, blood, and different human body tissues [26,27]. Nonetheless, this methodology has not been broadly applied to determine ergothioneine and lovastatin content in mushrooms where the presence of other co-extracted molecules may hinder the export of unbiased results.

One of the benchmarks of the present study was to assess the good performance of a simple, fast, low-cost, easily portable, in-the-field measurements-technique, like UV-Vis spectrophotometry, by (i) juxtaposing it with LC-MS outcomes and (ii) evaluating if the spectrophotometric approach could provide equally reliable and valid results since there are no reports that examine if UV-Vis is suitable or not for determining ergothioneine and lovastatin. Thus, two different analytical methodologies based on UV–Vis and LC–MS techniques were developed and compared in order to (a) appoint the method/technique-of-choice for the analysis of bioactive compounds present in low concentrations, such as ergothioneine and lovastatin in mushrooms of three species (i.e., *Agaricus bisporus*, *Pleurotus ostreatus*, and *P. citrinopileatus*) and reveal any possible interferences that impede their determination including the use of various cultivation substrates (in the case of *P. citrinopileatus*), and (b) compare and identify mushroom species with higher content of ergothioneine and lovastatin. Overall, results of this study contribute to the appropriate selection of mushroom species along with the methodical choice of optimal cultivation conditions, which shape the final content of mushrooms in different bioactive compounds.

2. Results and Discussion

2.1. Results of Validation of LC-MS Methods

Analytical figures of merit of LC-MS analysis for ergothioneine and lovastatin are presented in Table 1.

Table 1. Analytical figures of the merit of liquid chromatography–mass spectrometry (LC-MS) for ergothioneine (ESH) and lovastatin (LOV) determination.

Analytical Figures of Merit	ESH	LOV
Concentration range (μg mL^{-1})	0.05–45 (n = 14) [1]	0.001–1 (n = 10) [1]
Slope (a) (± standard error-sa)	0.0307 (±0.00023)	35.47 (±0.18)
Intercept (b) (± standard error-sb)	0.0012 (±0.0051)	0.090 (±0.065)
R^2 (Correlation coefficient)	0.9993	0.9998
Limit of Detection-LoD (μg mL^{-1})	0.02	0.00039
Limit of Quantification LoQ (μg mL^{-1})	0.06	0.0012

[1] n = the number of the standard solutions of different concentrations tested.

The results for repeatability, reproducibility, accuracy, and a matrix effect at three levels of concentration (quality control-QC samples) for both methods are summarized in Table 2. Since the present study does not address the analysis of biological samples or drugs, relative standard deviation (RSD%) values for repeatability and intermediate precision were satisfactory for both methods, not exceeding the maximum acceptable value of 15% [28]. Process recoveries for ergothioneine, regarding all mushroom species and substrates, ranged from 75.0% to 85.0%. Accordingly, extraction recovery for lovastatin varied from 63.0% to 79.2%.

2.2. Determination of Ergothioneine and Lovastatin Content of Mushrooms Produced in Conventional Substrates

Ergothioneine and lovastatin contents of different mushrooms, produced in conventional substrates (wheat straw and manure for *A. bisporus*, wheat straw for *Pleurotus* spp.), by using UV–Vis and LC–MS, is presented in Table 3.

Table 2. Precision, accuracy, and matrix effect of LC–MS method of ergothioneine and lovastatin.

Analyte	Quality Control Levels		
Ergothioneine	5.0 μg mL^{-1} (n = 3) [2]	25.0 μg mL^{-1} (n = 3) [2]	40 μg mL^{-1} (n = 3) [2]
Intra–Day Precision (%RSD)	4.0	2.0	0.2
Inter–Day Precision (%RSD) N = 3 [1]	7.5	1.9	2.5
Accuracy	102.95	100.95	99.67
Matrix Effect (%)	68.4	83.5	75.0
Lovastatin	0.005 μg mL^{-1} (n = 3) [2]	0.05 μg mL^{-1} (n = 3) [2]	0.5 μg mL^{-1} (n = 3) [2]
Intra–Day Precision (%RSD)	13.6	4.91	4.04
Inter–Day Precision (%RSD) N = 3 [1]	0.7	3.21	1.73
Accuracy	81.56	105.17	96.8
Matrix Effect (%)	42.08	15.9	8.3

[1] N: The number of consecutive days for inter–day precision determination. [2] n: the number of QC replicates. RSD%: relative standard deviation.

Table 3. Ergothioneine–Lovastatin content in mushrooms of three species cultivated in conventional substrates by using ultraviolet-visible (UV–Vis) spectroscopy and LC–MS.

Method	Ergothioneine Content (mg kg^{-1} Dry Sample) [a]		
	A. bisporus	***P. ostreatus***	***P. citrinopileatus***
UV–Vis	7100 (±300) [c]	9200 (± 800) [b]	8300 (±1100) [b]
LC–MS	521.2 (±14.7) [d]	607.3 (±11.2) [c]	822.1 (±20.6) [b]
Method	**Lovastatin Content (mg kg^{-1} Dry Sample) [a]**		
UV–Vis	1050 (±80) [b]	930 (±100) [b]	840 (±250) [b]
LC-MS	1.39 (±0.014) [b]	1.11 (±0.042) [c]	0.158 (±0.005) [d]

[a] Each value is expressed as mean ± standard error (n = 3), [b–d] Different letters within a row, indicate statistically significant differences at $p < 0.05$.

According to LC–MS results, p-values indicated that ergothioneine contents differed significantly among all three species, offering a clear discrimination of the studied mushrooms based on their identity. In contrast, UV–Vis analysis sorted the investigated samples into two different groups based on ergothioneine concentration. Furthermore, it can be noted that ergothioneine concentration was an order of magnitude higher when UV–Vis method was applied, implying the existence of a possible positive error in spectrophotometric measurements.

Comparisons among the three mushrooms examined, which are demonstrated in both methods, *P. citrinopileatus* contained the highest amounts of ergothioneine, indicating that this particular species is more suitable for an ergothioneine-oriented mushroom production (Table 3). Several comparative studies report that *Pleurotus* species and *P. ostreatus* contain higher concentrations of ergothioneine compared to other edible mushrooms [23,29]. This is possibly associated with differences or changes in the biosynthetic pathways, which are responsible for the formation of ergothioneine, among mushroom species. Moreover, another important factor appears to be the bioavailability of compounds that can activate ergothioneine biosynthesis. For instance, the higher ergothioneine content of *P. ostreatus* may be ascribed to the higher levels of the precursor molecules histidine, cysteine, and methionine, that *P. ostreatus* contain, when compared to *A. bisporus* [30].

Similarly, based on lovastatin content measured by LC–MS, the samples were classified into three different groups, whereas, according to UV–Vis results, no statistically significant difference was observed among the mushrooms examined (p-values > 0.05) (Table 3). As in the case of ergothioneine's spectrometric determination, lovastatin content using UV–Vis was over-estimated. *Agaricus bisporus* showed a higher amount of lovastatin than both *Pleurotus* species. However, *A. bisporus* and *P. ostreatus* lovastatin concentrations did not deviate much (Table 3). Nonetheless, the *P. citrinopileatus* strain used, which produced fruit

bodies with a high content in ergothioneine, would not be proposed for the cultivation of lovastatin-rich mushrooms. These differentiations can be affected by many factors, such as the fungal strain and/or the substrate, since lovastatin production is crucially affected by the content of carbon and nitrogen [31], differences in gene adjustment, and bioavailability of compounds that can activate lovastatin biosynthesis, such as methionine, glutamate, glycine, and histidine [32].

2.3. Determination of Ergothioneine and Lovastatin Content of P. citrinopileatus Mushrooms from Different Substrates

Since *P. citrinopileatus* is a species that has not been thoroughly investigated, it was the one selected to be cultivated not only in the commonly used wheat straw (WS) substrate, but also in two "non-conventional" cultivation substrates, namely grape marc (GM) and olive by-products (OL). Ergothioneine and lovastatin content in the derived mushrooms were measured by using UV–Vis and LC–MS (Table 4).

Table 4. Ergothioneine and lovastatin content of *P. citrinopileatus* mushrooms cultivated in three substrates, wheat straw (WS), grape marc (GM), and olive by-products (OL) by using UV–Vis and LC–MS.

Method	Ergothioneine Content (mg kg^{-1} Dry Sample) [a]		
	WS	**GM**	**OL**
UV–Vis	8300 (±1100) [b]	11800 (±1400) [b]	6700 (±1100) [b]
LC–MS	822.1 (±20.6) [b]	637.2 (±24.5) [c]	884.5 (±20.0) [b]
Method	**Lovastatin Content (mg kg^{-1} Dry Sample) [a]**		
UV–Vis	840 (±250) [b]	860 (±180) [b]	904 (±0.241) [b]
LC-MS	0.158 (±0.005) [c]	0.218 (±0.014) [b]	0.161 (±0.009) [c]

[a] Each value is expressed as mean ± standard error (n = 3), [b, c] Different letters within a row, indicate statistically significant differences at $p < 0.05$

It's interesting to mention that UV–Vis results showed no statistically significant differences (p-value > 0.05) in both ergothioneine and lovastatin contents among mushrooms from three substrates. On the other hand, LC–MS methods indicated that *P. citrinopileatus* produced in OL contained the highest amount of ergothioneine (although differences were not significant versus those of mushrooms deriving from WS), while *P. citrinopileatus* cultivated in GM exhibited the highest concentration of lovastatin (Table 4). These results revealed that the nature of growth substrate can play an important role in ergothioneine and lovastatin biosynthesis of *P. citrinopileatus*. It was observed that ergothioneine and lovastatin levels detected in GM substrates in a polyphenol-rich matrix differed significantly from those determined in WS and OL (Table 4). This is likely due to suppression (ergothioneine) or overexpression (lovastatin) mechanisms involved in the pertinent biosynthetic pathways, resulting in low ergothioneine and high lovastatin content in GM-cultivated mushrooms, respectively.

However, it is possible that these mechanisms may also be associated with various bioactive compounds present in the substrates examined. These compounds can act either as precursors, inducers, or inhibitors of the examined analytes biosynthesis affecting ergothioneine and lovastatin final content in mushrooms [33]. The differences in the type and nature of phenolic compounds and amino acids contained in each one of the studied agricultural by-products may be considered as the key factor for the under-production or over-production of the investigated compounds. However, this is not underlined evidently in existing literature, and further research is required in order to shed light on the effect of substrates' bioactive compounds in the production of ergothioneine and lovastatin. Apart from that, these additional bioactive compounds (i.e., polyphenols, amino acids, etc.) of the growth medium can be absorbed by the mushrooms, increasing not only their nutritional but also their added value [34].

2.4. Comparing Analytical Approaches for the Identification and Quantification of Ergothioneine and Lovastatin in Mushrooms

2.4.1. Ultraviolet-visibleSpectroscopy (UV–Vis)

As already mentioned, several bioactive compounds absorb in the wavelengths analyzed for ergothioneine and lovastatin, increasing the possibility of providing false positive errors in the final measurements. More specifically, ergothioneine was analyzed at 260 nm (Figure 1), which is a region of the spectrum in which some nucleic acids and aromatic amino acids (present in mushrooms) absorb light [35,36]. It is known that nucleic acids represent large amounts of nonprotein nitrogen in fungi [30]. In addition, *Pleurotus* mushrooms and grape marc by-products contain a higher amount of the aromatic amino acid phenylalanine, which may absorb at the same wavelength used for ergothioneine's spectrophotometric determination, leading to an erroneously increased ergothioneine's peak area (Tables 3 and 4).

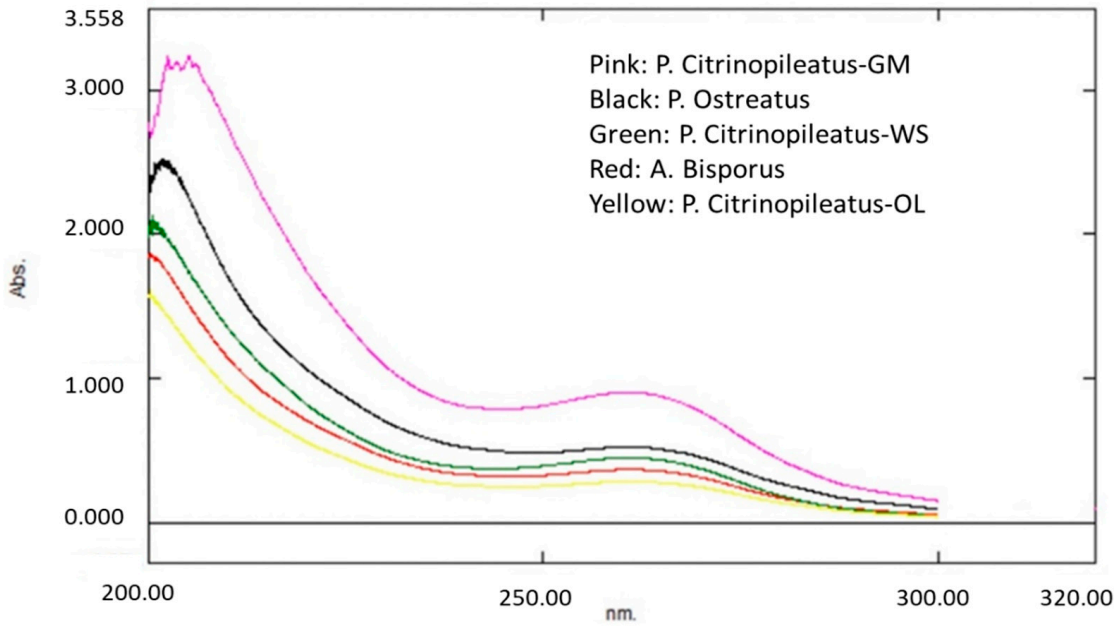

Figure 1. Ergothioneine ultra-violet spectroscopy (UV–Vis) spectra of mushrooms of three species, i.e., *A. bisporus*, *P. ostreatus*, and *P. citrinopileatus*. The latter was cultivated in three substrates (wheat straw (WS), grape marc (GM), and olive by-products (OL)).

In contrast, *Agaricus* mushrooms and olive by-products do not contain equally high concentrations of such amino acids [37,38]. This may be related to the lower ergothioneine content measured in *A. bisporus* and *P. citrinopileatus*-OL mushrooms by UV–Vis spectroscopy (Tables 3 and 4). In addition, phenolic content in mushrooms or in their cultivation substrates can affect UV–Vis quantification. These positive errors may affect more *P. citrinopileatus* samples rather than other mushrooms produced on WS-based substrates, since *P. citrinopileatus* samples are also derived from agricultural by-products that contain significant amounts of phenolic compounds [39,40]. Especially, wines and wineries residues, like grape marc, contain quercetin rhamnoside, kaempferol, hydroxybenzoic acid derivatives, and myricetin 3-O-glucoside that can absorb in similar wavelengths to that of ergothioneine's UV–Vis determination, explaining the excessively higher concentrations of ergothioneine presented in Table 5 [41,42].

Regarding the levels of lovastatin detected, it should be noted that there are some intermediates of the lovastatin biosynthesis pathway and some structural analogues of lovastatin that can absorb light at 232–238 nm, i.e., the wavelengths selected for lovastatin's UV–Vis analysis [43]. These intermediates are mostly degraded compounds, such as methyl esters, anhydro, methoxy, and acetate ester forms of lovastatin, that can absorb in those

wavelengths due to the diene groups they include [44]. Similarly, olive by-products (olive leaves and olive mill waste) contain tyrosol, hydroxytyrosol, apigenin, and *p*-coumaric acid hexoside that can absorb in similar wavelengths to lovastatin [45].

These hypotheses could be supported by the results of the present work (Tables 3 and 4). Moreover, by comparing the UV–Vis spectra of pure lovastatin from literature [46] with the corresponding UV–Vis spectra of the mushroom samples examined (Figure 2), it was noticed that the hydroxyl metabolite of lovastatin likely coexists with the lactone form. This can be assumed by the presence of one broad peak instead of two separate sharp peaks, with one for lovastatin and one for lovastatin acid, which is a highly unstable metabolite that can easily be converted to the lactone form. As proven by the interpretation of the results of UV–Vis analysis, a more selective technique, like LC–MS, may be more suitable for the quantification of ergothioneine and lovastatin in order to avoid a possible interference.

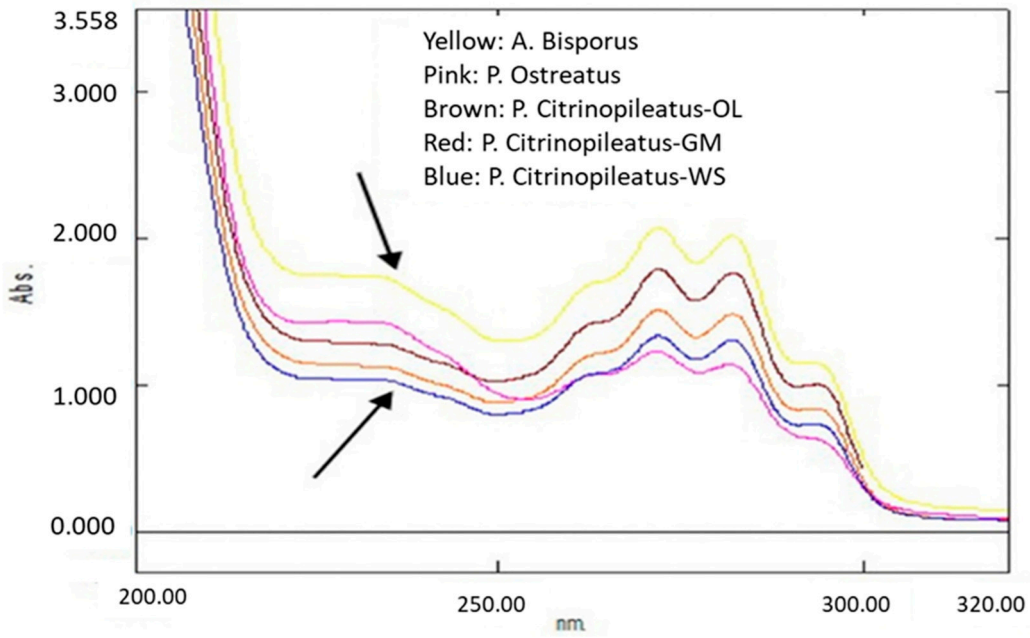

Figure 2. Lovastatin UV–Vis spectra of three species, i.e., *A. bisporus*, *P. ostreatus*, and *P. citrinopileatus*. The latter was cultivated in three substrates (WS, GM, and OL).

2.4.2. Liquid Chromatography–Mass Spectrometry (LC–MS)

Ergothioneine contents determined in *P. ostreatus* and *P. citrinopileatus*-WS (Table 3), by the developed LC–MS method, were similar to those reported in other studies, such as Lin et al. [47], who found a 997 mg ergothioneine kg^{-1}dry sample by using a high-pressure liquid chromatography with a diode array detector (HPLC–DAD) method. Additionally, the LC–MS results of our study were in accordance with results provided by Weigand-Heller et al. [48], who also implemented an LC–MS methodology to evaluate ergothioneine's content in *Agaricus* mushrooms.

P. citrinopileatus samples, which were produced in OL, demonstrated the highest ergothioneine content than any other mushroom sample, irrespectively of species or a cultivation substrate, while *P. citrinopileatus*-GM along with *A. bisporus* mushrooms contained the lowest content (Tables 3 and 4). As already stated, this finding is possibly related to the different compounds that non-conventional growth substrates contain including phenolic compounds and amino acids. Both amino acids and polyphenols hindered the UV–Vis determination of the two analytes due to their co-absorbance at specific wavelengths.

Lovastatin contents of the studied mushrooms were considerably lower than that reported in other studies [23,24]. The present outcome seems to be related to the greater sensitivity of the Orbitrap MS instrumentation used for lovastatin determination compared to the mass detectors used in the other studies. Relying on the higher resolution and

sensitivity of our validated LC–MS methodology, we can assume that it can quantify or even detect lovastatin in samples of extremely low content.

The need to apply a more sensitive and accurate technique for the evaluation of lovastatin content is also underscored by reviewing the presently published literature. Although, in the current study, lovastatin was detected in all mushroom samples, there are conflicting reports concerning the content of lovastatin in *P. ostreatus and P. citrinopileatus*. For example, Lam & Okello [25], Lin et al. [47], and Cohen et al. [49] did not detect lovastatin in *P. ostreatus* and *P. citrinopileatus* mushrooms, while Lo et al. [24] determined high concentrations of the same analyte. Along with the applied detection methodology, different cultivation practices (strain type, pH, aeration, temperature, and incubation period) as well as methods of extraction and measurement could also affect lovastatin production and determination.

To sum up, LC–MS platforms emerge as the method-of-choice for the accurate determination of both ergothioneine and lovastatin since they circumvent the interferences and drawbacks of UV–Vis protocols. Taking into consideration the results of the developed LC–MS methods, *P. citrinopileatus* could be considered an efficient alternative to the most common commercial species (i.e., *A. bisporus* and *P. ostreatus*) for the production of ergothioneine-rich mushrooms. Even though *P. citrinopileatus* would not be selected as the most appropriate species (on the basis of the outcome provided by the single strain examined) for producing mushrooms rich in lovastatin, its cultivation in novel non-conventional substrates, e.g., based on grape marc, can raise the final lovastatin content, highlighting the exploitation potential of such by-products in mushroom cultivation.

3. Materials and Methods

3.1. Reagents and Standards

Standards of lovastatin and simvastatin (SIMV, Internal Standard, IS) were purchased from European Pharmacopoeia (purity >98%, Strasbourg, France). Ergothioneine was purchased from Sigma Aldrich (purity >99%, St. Louis, MO, USA), while methimidazole (METH, IS) was purchased from Thermo Fisher (purity >99%, Erlenbachweg, Germany).

All standard stock solutions of lovastatin, simvastatin, and methimidazole were prepared in acetonitrile, while acetonitrile-water 7:3 (% *v*/*v*) was used to dissolve the water-soluble ergothioneine. The prepared stock solutions were stored at −18 °C. All solvents were of an LC–MS grade. Acetonitrile was purchased from Sigma Aldrich (St. Louis, MO, USA) and water was from Sharlau (Barcelona, Spain). Methanol was provided by ChemLab (Zadeglem, Belgium), while formic acid was obtained from Fisher Scientific (Hampton, VA, USA).

3.2. Biological Material–Mushroom Cultivation

Mushrooms of three species (Fungi and Basidiomycota) were examined in this study. Those of *Pleurotus ostreatus* and *Agaricus bisporus* were purchased from a local market, while *P. citrinopileatus* was cultivated at the Laboratory of General and Agricultural Microbiology, Agricultural University of Athens. Three substrates were used for this purpose, i.e., wheat straw (WS), grape marc plus wheat straw (GM; 1:1, *w*/*w*), and two-phase olive mill waste plus olive leaves (OL; 1:1, *w*/*w*). Their preparation process, the inoculation of the fungal strain (LGAM 158), and the conditions for mushroom production were previously described [50]. Grape marc was obtained by a winery located in Nemea (Peloponnese). Olive leaves and two-phase olive mill waste were obtained from an olive mill located in Kalamata (Peloponnese), and wheat-straw was kindly provided by Dirfis Mushrooms SA (Euboea).

3.3. Sample Preparation

After cultivation, whole mushrooms were collected and frozen to −20 °C for one day and freeze dried in a ModulyoD Freeze Dryer, equipped with a Thermo Savant ValuPump VLP200 (Thermo Electron Corporation, Thermo Fischer, Waltham, MA, USA).

Freeze drying was selected as the optimum drying method since it protects sensitive metabolites and bioactive compounds from degradation during long-term storage. This method removes samples' moisture that may produce undesirable chemical reactions and promote microbial growth [51]. Prior to analyses, dried material was homogenized and powdered in a laboratory mill (Type ZM1, Retch GmbH, Haan, Germany). Dry material and all samples and extracts were kept in airtight packaging bags and vials at −20 °C.

3.4. Extraction Procedure

The extraction process applied for the ergothioneine recovery was based on an already published protocol [29], slightly modified with regard to the centrifugation conditions. Ergothioneine was extracted from 100 mg of dried mushroom powder with 10 mL of 1:4 (% *v*/*v*) aqueous methanol by vigorous shaking for 20 min in a vortex (Falc Instruments, Bergamo, Italy), which is followed by centrifugation (Centrifuge Z32 HK, Hermle, Wehingen, Germany) at 3650 rcf for 20 min. After centrifugation, 8 mL of the supernatant were placed in the freeze dryer in order to acquire the dry residue of the extracts.

The lovastatin extraction procedure was based on a previously developed extraction process with slight modifications [23]. Lovastatin was extracted from 400 mg dried mushroom powder with 4 mL of acetonitrile followed by vigorous shaking (Falc Instruments, Italy). This was followed for 2 h at 250 rpm. The extract was then centrifuged for 20 min at 3650 rcf. Three mL of the supernatant were evaporated using a nitrogen pump to remove the extraction solvent.

3.5. Ergothioneine–Lovastatin Analysis

3.5.1. Ultraviolet–Visible Spectroscopy (UV–Vis)

Ultraviolet–Visible (UV-Vis) analysis was conducted by using a dual beam spectrophotometer (UV- 1900, Shimadzu Corporation, Kyoto Japan), while scanning from 200 to 400 nm was performed to determine maximum wavelengths. After reviewing the spectra of the two investigated compounds, ergothioneine analysis was performed at 260 nm, while lovastatin analysis took place at 232 nm instead of 238 nm in order to minimize possible interferences (Figure 3).

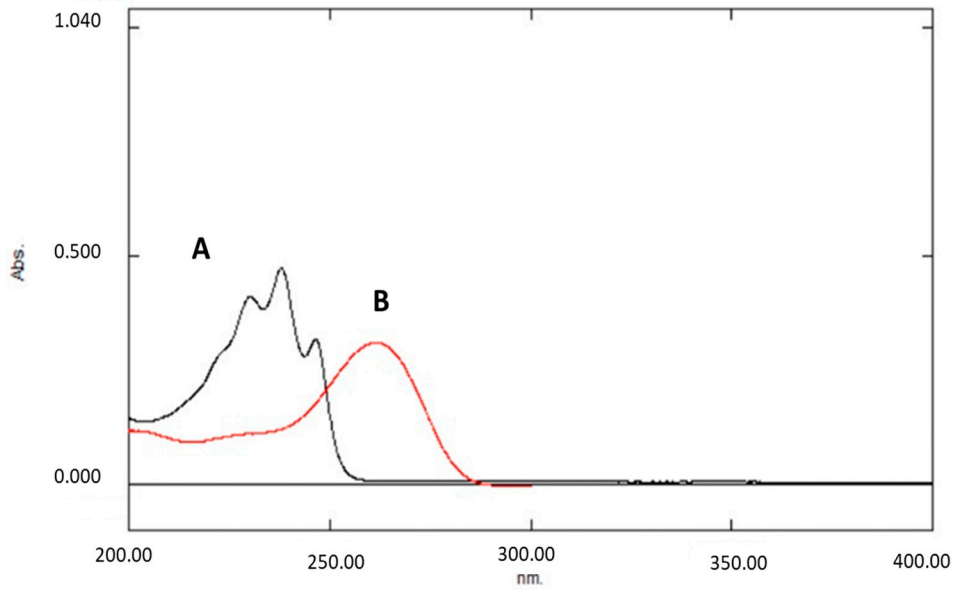

Figure 3. Lovastatin absorption peaks at 232, 238, and 247 nm (A) and ergothioneine absorption peak at 260 nm (B).

The linearity of calibration curves was determined by using standard solutions of the two compounds with concentrations ranging from 1 to 20 μg mL^{-1} for both ergothioneine

and lovastatin. Coefficient factors (R^2) were 0.9979 for ergothioneine and 0.9988 for lovastatin, verifying the method's linearity. Two to five (2–5) milligrams of each mushroom extract's dry residue were dissolved in 10 mL of 3:7 (v/v) methanol–water for ergothioneine and in 5 mL of acetonitrile for lovastatin. All spectra were processed by UV Probe software (2.7 version, Shimadzu Corporation, Kyoto, Japan).

3.5.2. Liquid Chromatography–Mass Spectrometry (LC–MS)

Liquid chromatography mass spectrometry (LC–MS) analysis was used for the identification and quantification of ergothioneine and lovastatin in mushroom species. The instrumentation of liquid chromatography for both methods included a quaternary pump, an autosampler with a tray oven set at 25 °C (Accela, Thermo Scientific, Waltham, USA), and a guard column. For ergothioneine analysis, a Kromacil C18 column (3.5 μm particle size, 100 × 2.1 mm i.d.) was used at 25 °C, while lovastatin separation was performed by an Acquity C18 column (1.7 particle size, 100 × 2.1 mm i.d.) at 25 °C. Finally, injection volume for both analyses was set at 10 μL.

Ergothioneine and methimazole (I.S) were separated using a 15-min gradient elution program, which consisted of water with 0.1% formic acid (Solvent A) and acetonitrile (Solvent B) at a steady flow rate of 0.2 mL min^{-1}. The gradient started with 30% of solvent A, increased to 50% over 10 min of analysis, and, in 15 min, the percentage of solvent A ramped to initial conditions (30%). On the other hand, lovastatin and simvastatin (I.S) were separated using a 10-min isocratic elution program, which consisted of water with 0.1% formic acid (Solvent A, 40%) and acetonitrile (Solvent B, 60%).

For ergothioneine analysis, a 3D quadrupole ion trap LCQ FLEET (Thermo Scientific, USA) mass spectrometer was used, while for lovastatin–where a detector of higher resolution was required– an LTQ Orbitrap Velos mass spectrometer (Thermo Scientific, USA) was utilized. Tandem mass spectrometry MS/MS measurements were performed in a positive mode using an electrospray chemical ionization (ESI) source at mass scan width of 100–350 m/z for ergothioneine and 250–550 m/z for lovastatin, respectively. The mass tolerance window for mass identification of product ions was set at ±5 ppm. Source parameters are fully described in Table 5. All spectra were processed by Xcalibur software (Version 3.0, Thermo Scientific, USA).

Table 5. Optimized values of electrospray chemical ionization (ESI) parameters for the examined compounds.

Source Parameters	Lovastatin-Simvastatin	Ergothioneine-Methimidazole
S-LENS RF Amplitude (V)	60	120
Sheath gas flow rate (arbitrary units, a.u)	8	7
Auxiliary gas flow rate (arbitrary units, a.u)	0	0
Sweep gas flow rate (arbitrary units, a.u)	0	0
Vaporizer temperature (°C)	320	300
Capillary temperature (°C)	220	200
Cone voltage (kV)	4	4.5
Isolation mass width	2	1.5
Collision energy (eV)	33 (lovastatin) 35 (simvastatin)	15 for ESH

The identification and quantification of the two analytes under determination was based on the fragmentation of the precursor ions into the respective product ions using a single reaction monitoring (SRM) technique. More specifically, product fragments of ergothioneine with m/z = 186.1 (C8H15N3S) were observed (Figure 4a) at a retention time (RT) of 1.10 min. Based on the MS results and previous published data, these fragments are characteristic of the fragmentation of the precursor ion called ergothioneine [16]. An

exception was the identification of methimazole for which only the precursor ion with m/z = 114.9, observed at a retention time of 1.38 min, was used for the analysis (Figure 4b).

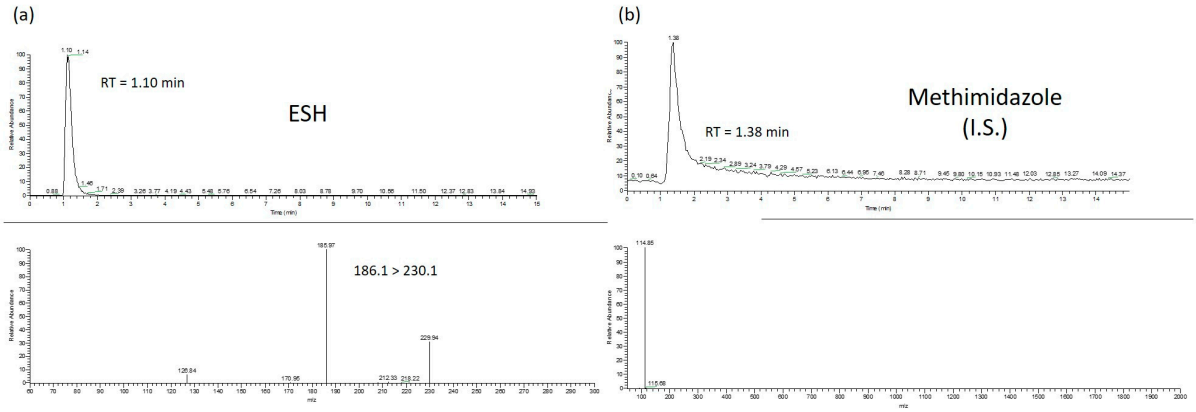

Figure 4. Representative chromatographs and mass spectra of Ergothioneine (**a**) and Methimidazole (internal standard) (**b**).

Similarly, during the identification and quantification of lovastatin, a product ion of m/z = 325.1772 ($C_{17}H_{21}ON_6$) was observed at a retention time of 5.19 min. Even though lovastatin and simvastatin were fragmented to the same product ion, a sufficient separation was achieved because the second compound was eluted at a different retention time of 7.12 min (Figure 5a). Taking into consideration the standard solutions analyzed and previous published results [52], this ion is characteristic of the fragmentation of the precursor ion of lovastatin and simvastatin (Figure 5b).

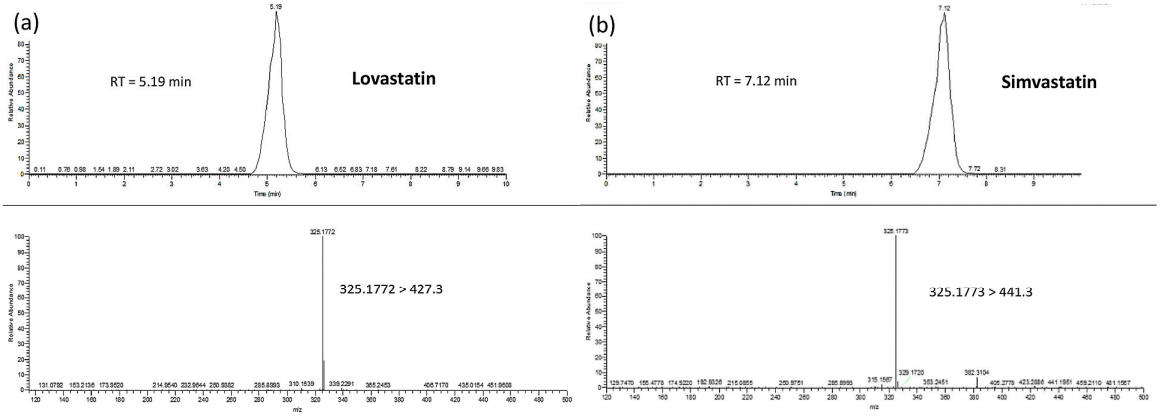

Figure 5. Representative chromatographs and mass spectra of Lovastatin (**a**) and Simvastatin (internal standard) (**b**).

3.6. Liquid Chromatography–Mass Spectrometry Methods' Validation

Liquid chromatography–mass spectrometry (LC-MS) methods' validation was performed in terms of linearity, accuracy, intra-day (repeatability) and inter-day (reproducibility) precision, extraction recovery, and a matrix effect (ME). Validation runs were conducted on three consecutive days. The linearity was determined using fourteen ergothioneine standards with concentrations ranging from 0.05 to 45 μg mL^{-1} and ten lovastatin standards with concentrations ranging from 0.001 to 1 μg mL^{-1}. The concentrations of ergothioneine, recorded in mushrooms, present higher variability and a wider concentration range than lovastatin. Thus, a calibration curve including a more extended range of concentrations were constructed in the case of ergothioneine (n = 14 instead of n = 10, in the case of lovastatin). Due to the wider selected concentration range, more concentration levels (n = 14) of the standard solutions were required to assure the linearity of ergothioneine's calibration curve. Finally, in order to determine the detection (LoD) and quantification limits (LoQ) of the two developed methods, the guidelines of the Official Journal of the European Communities

was adopted [53]. For that purpose, 0.01 μg mL^{-1} of ergothioneine and 0.001 μg mL^{-1} of the lovastatin standard were used, respectively.

For the estimation of intra-day precision and accuracy, three replicates (n = 3) of low, medium, and high concentrations of quality control (QC) samples were analyzed. More specifically for ergothioneine, QC samples of 5, 25, and 40 μg mL^{-1} were used, while, for lovastatin, QC samples of 0.005, 0.05, and 0.5 μg mL^{-1} were determined. The inter-day precision (or intermediate precision) was assessed by analysis of three batches of QC on three different days (n = 3 replicates per day, N = 3 different days for each concentration level). The precision was defined as the relative standard deviation (RSD%) and the accuracy was expressed as a relative error (RE%).

For the determination of the extraction recovery for ergothioneine and lovastatin, three different samples were analyzed: un-spiked mushroom samples (A), spiked mushroom samples with 10 μg mL^{-1} of ergothioneine, or 0.05 μg mL^{-1} of lovastatin (B) and standard solutions of these corresponding concentrations (C). The equation below (Equation (1)) was used to define the extraction recoveries.

$$\text{Recovery} = \frac{(B - A)}{C} \times 100 \quad (1)$$

The matrix effect (ME) estimation was conducted at low, medium, and high concentration levels by comparing the peak areas of each analyte spiked in mushroom samples with those of standard solutions at the same concentration. For that purpose, *A. bisporus* and *P. ostreatus* mushroom samples were pooled together while *P. citrinopileatus* mushroom samples, produced in three substrates, were examined separately. Peak areas of standard solutions were defined as A, whereas the peak areas of samples spiked with analyte were defined as B. The ratio below (Equation (2)) was used to evaluate the matrix effect.

$$\text{Matrix Effect} = \frac{B}{A} \times 100 \quad (2)$$

3.7. Statistical Analysis

The statistical analysis of the results of the different analytical techniques was performed by one-way analysis of variance (ANOVA). In this study, the basic criterion for statistical significance, at a 95% confidence level, was p-value ≤ 0.05. For the calculation of the p-value, three measurements of the samples were included (n = 3).

4. Conclusions

Despite the fact that UV–Vis is a relatively inexpensive and rapid method, the outcome of the present work suggests that it should not be acknowledged as the most suitable technique for the identification and quantification of ergothioneine and lovastatin in mushrooms due to numerous restrictions imposed by the different co-existing mushroom constituents absorbing at the same wavelength or close wavelengths. Specifically, the phenolic profile and amino acids of mushrooms and cultivation substrates are considered to be the major factors affecting the accurate quantification of these compounds by spectrometric methods. The impact of these bioactive compounds on UV–Vis-determined ergothioneine and lovastatin content is more pronounced in the comparison of mushrooms from different cultivation substrates (GM and OL) rather than among mushroom species. Therefore, the possible application of this technique, could potentially provide misleading results regarding the selection of the most suitable substrate(s) for an ergothioneine-rich or lovastatin-rich mushroom production. Perhaps, the optimization of the implemented extraction methodologies or the replacement of the existing extraction techniques with more selective procedures resulting at higher product yields, could be an area of future investigation.

In contrast, the LC–MS methods implemented, which combined precision and higher sensitivity, showed significant differences in ergothioneine and lovastatin content (Tables 3 and 4) in comparisons among species and substrates that were not observed during UV–Vis determination. Ergothioneine, although detected in all samples, was sig-

nificantly higher in *P. citrinopileatus* mushrooms (822.1 (±20.6) mg kg^{-1} dry sample). In contrast, the lovastatin content in *A. bisporus* (1.39 (±0.014 mg kg^{-1} dry samples) was higher than in *Pleurotus* mushrooms. Nonetheless, lovastatin levels could be increased by using suitable/alternative cultivation substrates. In addition, *P. citrinopileatus* mushrooms produced on OL showed the highest levels of ergothioneine, (884.5 (±20.0) mg kg^{-1} dry sample), while fruitbodies from GM-based substrates contained the highest amounts of lovastatin (0.218 (±0.014) mg kg^{-1} dry sample).

Since non-conventional substrates seem to have an impact on the biosynthetic pathways and the final content of the examined compounds, the elucidation of the relationship between substrates' content in other bioactive compounds (e.g., phenolics, amino acids) and ergothioneine or lovastatin yields would be an area of investigation. However, more mushroom strains/species and a wider range of substrates need to be studied to provide solid evidence confirming these assumptions.

Author Contributions: Conceptualization, G.I.Z., P.Z., and N.K. Methodology, K.T., T.T., E.S., and G.K. Validation, K.T. and T.T. Formal analysis, K.T., T.T., and G.K. Data curation, T.T and G.K. Writing original draft preparation, K.T, T.T., and P.Z. Writing review and editing, K.T., T.T., N.K., P.Z., and G.I.Z. Supervision, G.I.Z. and P.Z. Project administration, G.I.Z. and P.Z. All authors have read and agreed to the published version of the manuscript.

Funding: This research has been co-financed by the European Union and Greek national founds (European Social Fund-ESF) through the Operation Program Competiveness, Entrepreneurship, and Innovation, under the call RESEARCH-CREATE-INNOVATE (project code: T1EDK-02560).

Institutional Review Board Statement: Not applicable.

Informed Consent Statement: Not applicable.

Data Availability Statement: The data presented in this study are available on request from the corresponding author.

Conflicts of Interest: The authors declare no conflict of interest. The funders had no role in the design of the study, in the collection, analyses, or interpretation of data, in the writing of the manuscript, or in the decision to publish the results.

Sample Availability: Not available.

References

1. Rathore, H.; Prasad, S.; Sharma, S. Mushroom Nutraceuticals for Improved Nutrition and Better Human Health: A Review. *Pharma Nutr.* **2017**, *5*, 35–46. [CrossRef]
2. Gargano, M.L.; van Griensven, L.J.; Isikhuemhen, O.S.; Lindequist, U.; Venturella, G.; Wasser, S.P.; Zervakis, G.I. Meidicinal mushrooms: Valuable biological resources of high exploitation potential. *Plant Biosyst.* **2017**, *151*, 548–565. [CrossRef]
3. Patel, S.; Goyal, A. Recent Developments in Mushrooms as Anti-Cancer Therapeutics: A Review. *3 Biotech* **2012**, *2*, 1–15. [CrossRef] [PubMed]
4. Koutrotsios, G.; Patsou, M.; Mitsou, E.K.; Bekiaris, G.; Kotsou, M.; Tarantilis, P.; Pletsa, V.; Kyriakou, A.; Zervakis, G.I. Valorization of olive by-products as substrates for the cultivation of *Ganoderma lucidum* and *Pleurotus ostreatus* mushrooms with enhanced functional and prebiotic properties. *Catalysts* **2019**, *9*, 537. [CrossRef]
5. El Enshasy, H.A.; Hatti-Kaul, R. Mushroom Immunomodulators: Unique Molecules with Unlimited Applications. *Trends Biotechnol.* **2013**, *31*, 668–677. [CrossRef]
6. Boulaka, A.; Christodoulou, P.; Vlassopoulou, M.; Koutrotsios, G.; Bekiaris, G.; Zervakis, G.I.; Kyriacou, A.; Zervou, M.; Georgiadis, P.; Pletsa, V. Genoprotective properties and metabolites of β-glucan-rich edible mushrooms following in vitro human faecal fermentation. *Molecules* **2020**, *25*, 3554. [CrossRef]
7. Muszyńska, B.; Grzywacz-Kisielewska, A.; Kała, K.; Gdula-Argasińska, J. Anti-Inflammatory Properties of Edible Mushrooms: A Review. *Food Chem.* **2018**, *243*, 373–381. [CrossRef]
8. Kała, K.; Kryczyk-Poprawa, A.; Rzewińska, A.; Muszyńska, B. Fruiting Bodies of Selected Edible Mushrooms as a Potential Source of Lovastatin. *Eur. Food Res. Technol.* **2020**, *246*, 246–722. [CrossRef]
9. Reis, F.S.; Barros, L.; Martins, A.; Ferreira, I.C.F.R. Chemical Composition and Nutritional Value of the Most Widely Appreciated Cultivated Mushrooms: An Inter-Species Comparative Study. *Food Chem. Toxicol.* **2012**, *50*, 191–197. [CrossRef]
10. Atila, F.; Owaid, M.N.; Shariati, M.A. The Nutritional and Medical Benefits of *Agaricus bisporus*: A Review. *J. Microbiol. Biotechnol. Food Sci.* **2017**, *7*, 281–286. [CrossRef]
11. FAOSTAT. Available online: http://www.fao.org/faostat/en/#data/TP/visualize (accessed on 25 November 2020).

12. Royse, D.J.; Baars, J.; Tan, Q. *Edible and Medicinal Mushrooms: Technology and Applications*; Wiley-Blackwell: Hoboken, NJ, USA, 2017; pp. 5–13.
13. Kim, M.Y.; Lee, S.J.; Ahn, J.K.; Kim, E.H.; Kim, M.J.; Kim, S.L.; Moon, H.I.; Ro, H.M.; Kang, E.Y.; Seo, S.H.; et al. Comparison of Free Amino Acid, Carbohydrates Concentrations in Korean Edible and Medicinal Mushrooms. *Food Chem.* **2009**, *113*, 386–393. [CrossRef]
14. Stampfli, A.R.; Blankenfeldt, W.; Seebeck, F.P. Structural Basis of Ergothioneine Biosynthesis. *Curr. Opin. Struct. Biol.* **2020**, *65*, 1–8. [CrossRef] [PubMed]
15. Halliwell, B.; Cheah, I.K.; Tang, R.M.Y. Ergothioneine–a Diet-Derived Antioxidant with Therapeutic Potential. *FEBS Lett.* **2018**, *592*, 3357–3366. [CrossRef]
16. Ey, J.; Schömig, E.; Taubert, D. Dietary Sources and Antioxidant Effects of Ergothioneine. *J. Agric. Food Chem.* **2007**, *55*, 6466–6474. [CrossRef] [PubMed]
17. Lingappa, K.; Babu, C.V.; Siddalingeshwar, K.G.; Pramod, T. Isolation, Screening and Rapid Confirmation of Lovastatin Producing Strains of Aspergillus Terreus. *Indian J. Microbiol.* **2004**, *44*, 133–136.
18. Seenivasan, A.; Subhagar, S.; Aravindan, R.; Viruthagiri, T. Microbial Production and Biomedical Applications of Lovastatin. *Indian J. Pharm. Sci.* **2008**, *70*, 701–709. [PubMed]
19. Patel, Y. Medicinal Properties of *Pleurotus* Species (Oyster Mushroom): A Review. *World J. Fun. Plant. Biol.* **2012**, *3*, 01–12.
20. Goswami, S.; Vidyarthi, A.S.; Bhunia, B.; Mandal, T. A Review on Lovastatin and Its Production. *J. Biochem. Technol.* **2013**, *4*, 581–587.
21. Mulder, K.C.L.; Mulinari, F.; Franco, O.L.; Soares, M.S.F.; Magalhães, B.S.; Parachin, N.S. Lovastatin Production: From Molecular Basis to Industrial Process Optimization. *Biotechnol. Adv.* **2015**, *33*, 648–665. [CrossRef]
22. Lisec, B.; Radež, I.; Žilnik, L.F. Solvent Extraction of Lovastatin from a Fermentation Broth. *Sep. Purif. Technol.* **2012**, *96*, 187–193. [CrossRef]
23. Chen, S.-Y.; Ho, K.-J.; Hsieh, Y.-J.; Wang, L.-T.; Mau, J.-L. Contents of Lovastatin, γ-Aminobutyric Acid and Ergothioneine in Mushroom Fruiting Bodies and Mycelia. *LWT* **2012**, *47*, 274–278. [CrossRef]
24. Lo, Y.-C.; Lin, S.-Y.; Ulziijargal, E.; Chen, S.-Y.; Chien, R.-C.; Tzou, Y.-J.; Mau, J.-L. Comparative Study of Contents of Several Bioactive Components in Fruiting Bodies and Mycelia of Culinary-Medicinal Mushrooms. *Int. J. Med. Mushrooms* **2012**, *14*, 357–363. [CrossRef]
25. Lam, Y.S.; Okello, E.J. Determination of Lovastatin, β-Glucan, Total Polyphenols, and Antioxidant Activity in Raw and Processed Oyster Culinary-Medicinal Mushroom, *Pleurotus ostreatus* (Higher Basidiomycetes). *Int. J. Med. Mushrooms* **2015**, *17*, 117–128. [CrossRef] [PubMed]
26. Yuan, H.; Wang, F.; Tu, J.; Peng, W.; Li, H. Determination of Lovastatin in Human Plasma by Ultra-Performance Liquid Chromatography–Electrospray Ionization Tandem Mass Spectrometry and Its Application in a Pharmacokinetic Study. *J. Pharm. Biomed.* **2008**, *46*, 808–813. [CrossRef]
27. Cheah, I.K.; Tang, R.M.Y.; Yew, T.S.Z.; Lim, K.H.C.; Halliwell, B. Administration of Pure Ergothioneine to Healthy Human Subjects: Uptake, Metabolism, and Effects on Biomarkers of Oxidative Damage and Inflammation. *Antioxid. Redox. Sign.* **2017**, *26*, 193–206. [CrossRef] [PubMed]
28. González, A.G.; Herrador, M.Á.; Asuero, A.G. Intra-Laboratory Assessment of Method Accuracy (Trueness and Precision) by Using Validation Standards. *Talanta* **2010**, *82*, 1995–1998. [CrossRef] [PubMed]
29. Sapozhnikova, Y.; Brydwell, W.C.; Lobato, A.; Roming, B. Effect of UV-B radiation levels on concentrations of phytosterols, ergothioneine and polyphenolic compounds in mushroom powders used as dietary supplements. *J. Agric. Food Chem.* **2014**, *62*, 3034–3042. [CrossRef]
30. Maftoun, P.; Johari, H.; Soltani, M.; Malik, R.; Othman, N.Z.; El Enshasy, H.A. The Edible Mushroom *Pleurotus* Spp.: I. Biodiversity and Nutritional Values. *Int. J. Biotechnol. Well. Indus.* **2015**, *4*, 67–83.
31. Alarcón, J.; Águila, S. Lovastatin Production by Pleurotus Ostreatus: Effects of the C: N Ratio. *Z. für Nat. C* **2006**, *61*, 95–98. [CrossRef]
32. Hajjaj, H.; Niederberger, P.; Duboc, P. Lovastatin Biosynthesis by Aspergillus Terreus in a Chemically Defined Medium. *Appl. Environ. Microbiol.* **2001**, *67*, 2596–2602. [CrossRef] [PubMed]
33. Zhang, Y.; Chen, Z.; Wen, Q.; Xiong, Z.; Cao, X.; Zheng, Z.; Zhang, Y.; Huang, Z. An Overview on the Biosynthesis and Metabolic Regulation of Monacolin K/Lovastatin. *Food Funct.* **2020**, *11*, 5738–5748. [CrossRef]
34. Koutrotsios, G.; Kalogeropoulos, N.; Kaliora, A.; Zervakis, G.I. Toward an increased functionality in oyster (*Pleurotus*) mushrooms produced on grape marc or olive mill wastes serving as sources of bioactive compounds. *J. Agric. Food Chem.* **2018**, *66*, 5971–5983. [CrossRef]
35. Porterfield, J.Z.; Zlotnick, A. A Simple and General Method for Determining the Protein and Nucleic Acid Content of Viruses by UV Absorbance. *Virology* **2010**, *407*, 281–288. [CrossRef]
36. Hazra, C.; Samanta, T.; Mahalingam, V. A Resonance Energy Transfer Approach for the Selective Detection of Aromatic Amino Acids. *J. Mater. Chem. C* **2014**, *2*, 10157–10163. [CrossRef]
37. Mattila, P.; Salo-Väänänen, P.; Könkö, K.; Aro, H.; Jalava, T. Basic Composition and Amino Acid Contents of Mushrooms Cultivated in Finland. *J. Agric. Food Chem.* **2002**, *50*, 6419–6422. [CrossRef] [PubMed]

38. Chirinang, P.; Intarapichet, K.-O. Amino Acids and Antioxidant Properties of the Oyster Mushrooms, *Pleurotus ostreatus* and *Pleurotus sajor-caju*. *Sci. Asia* **2009**, *35*, 326–331. [CrossRef]
39. Lafka, T.-I.; Sinanoglou, V.; Lazos, E.S. On the Extraction and Antioxidant Activity of Phenolic Compounds from Winery Wastes. *Food Chem.* **2007**, *104*, 1206–1214. [CrossRef]
40. Leouifoudi, I.; Harnafi, H.; Zyad, A. Olive Mill Waste Extracts: Polyphenols Content, Antioxidant, and Antimicrobial Activities. *Adv. Phar. Sci.* **2015**, *2015*, 1–11. [CrossRef]
41. Rubilar, M.; Pinelo, M.; Shene, C.; Sineiro, J.; Nuñez, M.J. Separation and HPLC-MS Identification of Phenolic Antioxidants from Agricultural Residues: Almond Hulls and Grape Pomace. *J. Agric. Food Chem.* **2007**, *55*, 10101–10109. [CrossRef]
42. Fotakis, C.; Kokkotou, K.; Zoumpoulakis, P.; Zervou, M. NMR Metabolite Fingerprinting in Grape Derived Products: An Overview. *Food. Res. Int.* **2013**, *54*, 1184–1194. [CrossRef]
43. Xie, X.; Watanabe, K.; Wojcicki, W.A.; Wang, C.C.C.; Tang, Y. Biosynthesis of Lovastatin Analogs with a Broadly Specific Acyltransferase. *Chem. Biol.* **2006**, *13*, 1161–1169. [CrossRef]
44. Li, Y.; Zhang, F.; Wang, Z.; Hu, Z. Identification and Chemical Profiling of Monacolins in Red Yeast Rice Using High-Performance Liquid Chromatography with Photodiode Array Detector and Mass Spectrometry. *J. Pharm. Biomed.* **2004**, *35*, 1101–1112. [CrossRef] [PubMed]
45. Kontogianni, V.G.; Gerothanassis, I.P. Phenolic Compounds and Antioxidant Activity of Olive Leaf Extracts. *Nat. Prod. Res.* **2012**, *26*, 186–189. [CrossRef]
46. Seenivasan, A.; Gummadi, S.N.; Panda, T.; Théodore, T. Quantification of Lovastatin Produced by *Monascus purpureus*. *Open Biotechnol. J.* **2015**, *9*, 6–13. [CrossRef]
47. Lin, S.-Y.; Chen, Y.-K.; Yu, H.-T.; Barseghyan, G.S.; Asatiani, M.D.; Wasser, S.P.; Mau, J.-L. Comparative Study of Contents of Several Bioactive Components in Fruiting Bodies and Mycelia of Culinary-Medicinal Mushrooms. *Int. J. Med. Mushrooms* **2013**, *15*, 315–323. [CrossRef]
48. Weigand-Heller, A.J.; Kris-Etherton, P.M.; Beelman, R.B. The Bioavailability of Ergothioneine from Mushrooms (*Agaricus bisporus*) and the Acute Effects on Antioxidant Capacity and Biomarkers of Inflammation. *Prev. Med.* **2012**, *54*, S75–S78. [CrossRef]
49. Cohen, N.; Cohen, J.; Asatiani, M.D.; Varshney, V.K.; Yang, Y.-C.; Li, Y.-H.; Mau, J.-H.; Wasser, S.P. Chemical composition and nutritional and medicinal value of fruit bodies and submerged cultured mycelia of culinary-medicinal higher basidiomycetes mushrooms. *Int. J. Med. Mushrooms* **2014**, *16*, 273–291. [CrossRef] [PubMed]
50. Koutrotsios, G.; Mountzouris, K.C.; Chatzipavlidis, I.; Zervakis, G.I. Bioconversion of Lignocellulosic Residues by *Agrocybe cylindracea* and *Pleurotus ostreatus* Mushroom Fungi–Assessment of Their Effect on the Final Product and Spent Substrate Properties. *Food Chem.* **2014**, *161*, 127–135. [CrossRef]
51. Ma, L.; Chen, H.; Zhu, W.; Wang, Z. Effect of Different Drying Methods on Physicochemical Properties and Antioxidant Activities of Polysaccharides Extracted from Mushroom *Inonotus obliquus*. *Food. Res. Int.* **2013**, *50*, 633–640. [CrossRef]
52. Wujian, J.; Kuan-Wei, P.; Sihyung, Y.; Huijing, S.; Mario, S.; Zhuo, W.M. A Simple Protein Precipitation-Based Simultaneous Quantification of Lovastatin and Its Active Metabolite Lovastatin Acid in Human Plasma by Ultra-Performance Liquid Chromatography-Tandem Mass Spectrometry Using Polarity Switching. *J. Chromatogr. Sep. Tech.* **2015**, *6*, 268–287. [PubMed]
53. Union, P.O. of the E. CELEX1, 2002/657/EC: Commission Decision of 12 August 2002 implementing Council Directive 96/23/EC concerning the performance of analytical methods and the interpretation of results (Text with EEA relevance) (notified under document number C(2002) 3044). Available online: https://op.europa.eu/el/publication-detail/-/publication/ed928116-a955-4a84-b10a-cf7a82bad858/language-en (accessed on 15 November 2020).

Food Chemistry 370 (2022) 131022

Contents lists available at ScienceDirect

Food Chemistry

journal homepage: www.elsevier.com/locate/foodchem

Enhancing the nutritional and functional properties of *Pleurotus citrinopileatus* mushrooms through the exploitation of winery and olive mill wastes

Georgios Koutrotsios [a], Dimitra Tagkouli [b], Georgios Bekiaris [a], Andriana Kaliora [b], Thalia Tsiaka [c], Konstantinos Tsiantas [c,d], Iordanis Chatzipavlidis [a], Panagiotis Zoumpoulakis [c,d], Nick Kalogeropoulos [b,*], Georgios I. Zervakis [a,*]

[a] *Agricultural University of Athens, Laboratory of General and Agricultural Microbiology, Iera Odos 75, 11855 Athens, Greece*
[b] *Harokopio University, Department of Nutrition and Dietetics, Laboratory of Chemistry, Biochemistry and Physical Chemistry of Foods, El. Venizelou 70, 17671 Kallithea, Greece*
[c] *Institute of Chemical Biology, National Hellenic Research Foundation 48, Vas. Constantinou Ave., 11635 Athens, Greece*
[d] *Department of Food Science and Technology, University of West Attica, Ag. Spyridonos, 12243 Egaleo, Greece*

ARTICLE INFO

Keyword:
Golden oyster mushroom
Bioactive compound
Antioxidant activity
Amino acid
Lovastatin
Functionality

ABSTRACT

Treatment and disposal of wineries and olive-oil mills waste is usually associated with complex processes, which are often of limited wide-scale applicability. Olive-leaves plus two-phase olive mill waste (OLW) or grape marc plus wheat straw (GMW) were assessed as substrates for the cultivation of the choice edible mushroom *Pleurotus citrinopileatus*. GMW led to increased mushroom biological efficiency and shorter production cycles. Antioxidant activities, triterpenic acids, free amino acids, lovastatin and ergosterol were significantly higher in fruitbodies from GMW; the latter compound was positively correlated with squalene concentrations in substrates. Glucans, resveratrol and fatty acids content showed minor differences among mushrooms from the three substrates examined, whereas ergothioneine was significantly higher in fruitbodies grown on OLW. High correlations were noted for oleanolic, ursolic and amino acid content in mushrooms and their respective substrates. Moreover, FTIR spectra revealed variations in fruitbodies content in bioactive compounds which were associated with the substrates used.

1. Introduction

Current commercial edible mushroom production amounts to approximately 34 million metric tons, representing a 30-fold increase over the last three decades, in parallel with a rise in per capita consumption (presently 4.7 kg/person/year compared to about 1 kg/person/year in 1997) (Royse, Baars, & Tan, 2017). *P. citrinopileatus* Singer (or "golden oyster mushroom") is indigenous to East and Southeast Asia, and grows on fallen trees and stumps of broad-leaf species. It was initially cultivated in China, but soon became popular because of the fruitbodies bright yellow color, unique flavor and texture. This species is one of the best candidates for the much-sought after diversification of the global mushroom market since its cultivation is associated with large yields of high-quality end-product.

Olive mill and winery by-products are two of the main agro-industrial wastes in the wider Mediterranean region; yet, their integrated management and safe disposal is particularly challenging due to the huge volume, seasonality in production and high organic load. Although the use of such waste streams has been previously examined in the cultivation of *Pleurotus* mushrooms (Koutrotsios, Mountzouris, Chatzipavlidis, & Zervakis, 2014; Zervakis, Koutrotsios, & Katsaris, 2013), it was not until recently that their content in bioactive compounds was associated with enhanced properties of the end-product (Koutrotsios, Kalogeropoulos, Kaliora, & Zervakis, 2018; Tagkouli et al., 2020).

As regards *P. citrinopileatus*, pertinent studies have focused at evaluating the potential of various lignocellulocic by-products (e.g., cereal grasses, sugarcane bagasse, coffee residues, coir waste and cardboard industrial waste) to support satisfactory mushroom yields (Freitas et al., 2018; Kulshreshtha, Mathur, Bhatnagar, & Kulshreshtha, 2013; Liang,

* Corresponding authors.
E-mail addresses: nickal@hua.gr (N. Kalogeropoulos), zervakis@aua.gr (G.I. Zervakis).

https://doi.org/10.1016/j.foodchem.2021.131022
Received 21 March 2021; Received in revised form 25 August 2021; Accepted 29 August 2021
Available online 2 September 2021

Wu, Shieh, & Cheng, 2009). However, little information is available about the composition of fruitbodies cultivated on various agro-wastes, and no data exist on the effect of substrates on the mushroom content in bioactive compounds and their functional properties. Hence, the main objectives of the present work were (a) to investigate the suitability of olive mill and winery by-products as novel substrates in *P. citrinopileatus* production by examining key cultivation parameters, and (b) to assess the substrates impact on mushrooms antioxidant activity and on the concentration of several bioactive compounds, i.e., free amino acids, individual phenolics and triterpenic acids, glucans, ergosterol, lovastatin and ergothioneine. Particular emphasis was placed at detecting/evaluating associations between the content of selected functional components in substrates and fruitbodies in order to determine their production and exploitation potential.

2. Materials and methods

2.1. Chemicals and reagents

Ergosterol, squalene, *p*-hydroxybenzoic acid, gallic acid, *p*-coumaric acid, *p*-hydroxyphenylacetic acid, resveratrol, ursolic acid and 2,4,6-tris (2- pyridyl)-s-triazine (TPTZ) were obtained from Sigma (Steinheim, Germany). Folin-Ciocalteu reagent, bis(trimethylsilyl)-trifluoroacetamide (BSTFA), 1,1-diphenyl-2-picrylhydrazyl radical (DPPH), 6-hydroxy-2,5,7,8-tetramethylchroman-2-carboxylic acid (Trolox), oleanolic acid, and 3-(4-hydroxyphenyl)-1-propanol were purchased from Aldrich (Steinheim, Germany). Cholesterol and vanillic acid were obtained from Serva (Heidelberg, Germany). Lovastatin and simvastatin (used as internal standard) were acquired from European Pharmacopoeia (Strasbourg, France). Ergothioneine and methimidazole (internal standard) were purchased by Sigma (Steinheim, Germany) and Thermo Fischer (Erlenbachweg, Germany), respectively.

2.2. Fungal strain and mushroom cultivation process

For the purposes of this study, a commercial strain of *Pleurotus citrinopileatus* (Basidiomycota, Agaricales) was used; the fungus is routinely maintained in potato dextrose agar and preserved in the culture collection of the Laboratory of General and Agricultural Microbiology, Agricultural University of Athens, under the accession code 'LGAM 158′. To prepare the mushroom cultivation substrates, two-phase olive mill waste and olive leaves were obtained from an olive mill located in the area of Kalamata (southwest Peloponnese, Greece), grape marc derived from a winery located in Nemea (northeast Peloponnese, Greece), while wheat straw was kindly provided by Dirfis Mushrooms SA (Evvoia, Greece). These raw materials were used to prepare the following three substrates: (a) GMW: grape marc plus wheat straw 1:1 w/w; (b) OLW: olive mill by-products (olive leaves and two-phase olive mill waste 1:1 w/w) and (c) WHS: wheat straw (control). Polypropylene autoclavable bags were filled with 1 kg of substrate and sterilized twice (1 h, 121 °C, 1.1 atm). Cereal grain spawn of *P. citrinopileatus* was prepared as previously described (Koutrotsios et al., 2014) and was used for inoculating the sterilized substrates at a ratio of 4% w/w. Incubation took place at 27 °C in the dark. When substrates were fully colonized, four holes of 2 cm diameter were opened in each bag and environmental conditions were regulated as follows: relative air humidity at 95 ± 2 %, temperature at 16 °C, and illumination at 700 lx/m^2 (16 h/day with fluorescent lamps). After mushroom primordia formation, CO_2 levels were maintained at <1200 ppm, relative humidity at 80 ± 2%, and illumination at 1000 lx/m^2 (12 h/day) until the end of the cultivation process.

To assess the impact of each substrate on mushroom production and cultivation performance, the following parameters were examined (Koutrotsios et al., 2014): (a) the time length of each stage of the mushrooms crop cycle (incubation, formation of mushroom primordia and total cultivation period including harvest of three production flushes); (b) earliness (i.e., time elapsed from the day of substrate inoculation until the day of primordia appearance); (c) mushroom yield (fresh weight of the mushrooms obtained); (d) average mushroom weight measured as the ratio of total yield over the total number of individual fruitbodies harvested; (e) biological efficiency (BE) calculated as the percentage ratio of fresh mushroom weight over the dry weight of the respective substrate and (f) productivity, expressed as the ratio of the BE value over the time length (in days) of the respective cultivation period.

2.3. Preparation of substrate and mushroom samples for analyses

Four different samples from each substrate (obtained just after preparation and prior to inoculation with the fungus) were processed for analysis of selected compounds or elements (Supplementary Material, Table S1). In addition, five mushroom samples (replicates; all obtained from the first production flush) from each substrate were analyzed. Samples were freeze-dried in a Telstar Cryodos apparatus (Telstar Industrial, S.L., Terrassa, Spain) and the resulting material was ground to a fine powder, wrapped in sealed plastic bags and stored in the dark at −20 °C prior to analysis.

2.4. Extraction of phenolics and determination of total phenolic content

Extraction of phenolics was performed as previously described with minor modifications (Kalogeropoulos, Yanni, Koutrotsios, & Aloupi, 2013). In brief, freeze-dried mushroom samples (0.5 g) were extracted with 10 mL methanol at room temperature by shaking for 48 h in the dark. Separation of extracts was performed by centrifugation at 2500 rpm for 10 min, and residues were re-extracted with 2.5 mL methanol for 2 h. Then extracts were combined, methanol volume was reduced to 2 mL under a rotary evaporator (Rotavapor -R, Büchi Labortechnic AG, Flawil, Switzerland), and samples were sealed in GC vials and kept at −20 °C.

Total phenolic content (TPC) was determined in mushrooms methanolic extracts by the Folin-Ciocalteu assay, adapted to micro-scale by Arnous, Makris, and Kefalas (2002). Absorbance was measured at 750 nm with a U-2001 spectrophotometer (Hitachi Instruments Inc., Tokyo, Japan); gallic acid was used for the calibration curve, and the results are presented as mg gallic acid equivalents (mg GAE) per 100 g of dried mushrooms.

2.5. Determination of individual phenolic compounds and triterpenic acids

A selective ion monitoring (SIM) GC–MS method was applied for the detection of four target phenolic compounds, one stilbene and two triterpenic acids as previously described (Kalogeropoulos et al., 2013), based on the comparison of the retention times and ratios of two to three fragments ions of each compound with those of commercial pure standards (Koutrotsios, Kalogeropoulos, Stathopoulos, Kaliora, & Zervakis, 2017). Briefly, 2 g of freeze-dried samples were extracted with 40 mL methanol for 48 h in the dark, at room temperature. After centrifugation, the residues were re-extracted for 2 h with 10 mL methanol. After solvent removal, the extract was re-dissolved in 1 mL methanol, the phenolic compounds and triterpenic acids were derivatised to their trimethylsilylethers (TMS) and were quantitated by using target and qualifier ions of commercial standards at predetermined ratios and by employing 3-(4-hydroxyphenyl)-1-propanol as internal standard (Supplementary Material, Table S2).

2.6. Assessment of antioxidant activity of mushroom extracts

The antioxidant activity of mushrooms methanolic extracts was assessed by measuring the radical scavenging activity and the reducing antioxidant potential through the use of the DPPH (AAR) and the ferric

ion reducing power (FRAP) oxidation assays, respectively (Arnous et al., 2002). For both assays, Trolox was used as calibration standard and the results were expressed as mmol Trolox equivalents (TEs) per 100 g of mushroom dry weight.

In addition, inhibition of copper-induced lipid oxidation in total serum solubilized in phosphate buffer saline (PBS), by using lag time as a criterion for antioxidative potency, was evaluated as a more biologically relevant assay to assess the antioxidant activity of mushrooms methanolic extracts. Venous blood was collected under sterile conditions from healthy humans, and serum was obtained after centrifugation at 3000 rpm, in 14 °C for 10 min, directly after collection. The study of the kinetics of copper-induced oxidation in 12-fold diluted serum was performed by monitoring the absorbance of lipid oxidation products at 245 nm using an ELISA reader (PowerWaveXS2, Microplate Spectrophotometer, BioTek, Vermont, USA). At time point 0, $CuSO_4$ was added in serum (20 μL) to a final concentration of 10^{-5} M in PBS. Different doses of tested extracts were added to mixture in 1 μL of PBS. Copper-induced oxidation of lipids in serum leads to conjugated dienic hydroperoxides that absorb at 245 nm. The kinetics of oxidation was analyzed in terms of the lag-time prior to oxidation, and was expressed in seconds.

2.7. Determination of fatty acids and ergosterol

Fatty acids were determined by GC–MS in the form of their methyl esters (FAME), after hot saponification of freeze-dried samples (100–200 mg) with 0.5 M KOH in methanol (2 mL) for 15 min at 90 °C, followed by reaction with 14% BF_3 in methanol (1.5 mL) for 2 min at 90 °C as previously described (Koutrotsios et al., 2017). Peaks identification was based on a standard mixture of 37 known FAMEs (Supelco; Steinheim, Germany) and was confirmed by means of NIST05 mass spectra library.

Ergosterol was isolated and determined essentially as described by Sapozhnikova, Byrdwell, Lobato, and Romig (2014). Briefly, 100–200 mg of freeze-dried samples were spiked with standard cholesterol solution, as internal standard, and hot-saponified with 3 M KOH in methanol for 60 min at 60 °C. The unsaponifiable fraction was extracted with hexane and sterols were derivatizated to trimethylsilylethers (TMS) after treatment with BSTFA at 70 °C for 20 min. In order to avoid conversion of ergosterol in vitamin D_2, all manipulations were conducted under reduced light. Analysis of the TMS derivatives was carried out by GC–MS in an Agilent (Waldbronn, Germany) HP series GC 6890 N coupled with a HP 5973 mass selective (MS) detector operating under electron impact ionization (70 eV) on an HP-5MS capillary column as described by Koutrotsios et al. (2017). Ergosterol was quantitated by a 7-point calibration curve covering the range 0–600 μg by employing cholesterol as internal standard.

2.8. Determination of glucans

The content of total and α-glucans were assessed by using the Mushroom and Yeast Beta – Glucan assay kit (Megazyme Int., Bray, Ireland) according to the manufacturer's instructions; β-glucans content was determined by subtracting α-glucans content from total glucans content.

2.9. Extraction, derivatisation and determination of free amino acids

Free amino acids (FAAs) profiling of mushrooms and substrates was conducted as described by Tagkouli et al. (2020). The procedure consists of a solid phase extraction step followed by amino acids derivatisation and liquid/liquid extraction of the derivatives following the EZ:faast™ (Phenomenex®, Torrance, USA) Free (Physiological) Amino Acid Analysis by GC–MS protocol (https://phenomenex.blob.core.windows.net). An Agilent series GC 6890N gas chromatograph (Waldbronn, Germany), coupled with an HP5973 Mass Selective detector (EI, 70 eV), split–splitless injector and an HP7683 auto sampler was used for the analysis. The separation was achieved using a Phenomenex Zebron ZB-A amino acid analysis dedicated column (length: 10 m, internal diameter: 0.25 mm, film thickness: 25 μm), with high purity helium as the carrier gas, at 1.1 mL/min flow rate. A selective ion monitoring (SIM) GC–MS method was applied for the detection and identification of 21 amino acids, based on the ±0.05 RT presence of target and qualifier ions at the predetermined ratios, together with the electronic library "Agilent.L" provided with the Ez:faast kit. Quantification of FAAs was carried out employing norvaline as internal standard and constructing five-point reference curves for each amino acid by standard solutions provided with the kit (Tagkouli et al., 2020). For the quantification of GABA, which was not present in the standards of the kit, pure GABA (Sigma, Steinheim, Germany) was used. The *m/z* of the selected ions for each amino acid are provided in Supplementary Material (Table S3).

2.10. Determination of ergothioneine

Regarding the recovery of ergothioneine from *P. citrinopileatus* samples, a similar procedure (with different centrifugation conditions) to that reported by Sapozhnikova et al. (2014) was implemented as previously described (Tsiantas et al., 2021).

The identification and quantification of ergothioneine in mushrooms were conducted by using a recently developed liquid chromatography-mass spectrometry (LC-MS/MS) method (Tsiantas et al., 2021). For ergothioneine extraction, 10 mL of extraction solvent (water:methanol 1:4 v/v) were added to 100 mg of mushroom powder. The mixture was vigorously vortexed (Falc Instruments, Bergamo, Italy) for 20 min and then centrifuged (Centrifuge Z32 HK; Hermle, Wehingen, Germany) for other 20 min at 3650 rcf. Then, 8 mL of the supernatant were freeze-dried and the dry residue of the extracts was collected for further analysis. Methimidazole was used as the internal standard for LC-MS/MS analysis. A Kromasil C18 column (100 mm × 2.1 mm i.d, 3.5 μm particle size; Nouryon, Amsterdam, The Netherlands) was used for the chromatographic separation of ergothioneine and methimidazole. Analytes were separated using gradient elusion consisting of water with 0.1% formic acid (solvent A) and acetonitrile (solvent B). The gradient initialized with 30% of solvent A, reached at 50% in 10 min, and in 15 min the percentage of solvent A ramped to initial conditions (30%). The flow rate was set at 0.2 mL/min and the samples were diluted to acetonitrile:water 70:30 v/v. The injected volume was 10 μL and the column temperature was set at 25 °C. The mass spectrometer used was a 3D quadrupole ion trap LCQ FLEET (Thermo Fisher Scientific, Waltham, USA) with electrospray ionization (ESI) operated in positive mode. The mass transition of *m/z* 186.1 greater than 230.1 using single reaction monitoring (SRM) was used for ergothioneine determination, while methimazole was quantified using the parent ion with *m/z* 114.9. Ergothioneine content in mushroom samples was determined by the calibration curve Peak area ratio (a.u.) = $0.030C_{ergothioneine} + 0.011$ ($R^2 = 0.998$) at concentration range of 2.5–35 μg/mL. All measurements were conducted in triplicate. All LC-MS/MS spectra were processed by Xcalibur software (Thermo Fisher Scientific, Waltham, USA).

2.11. Determination of lovastatin

Lovastatin was extracted from freeze dried mushroom powder according to the process described in previous studies (Chen, Ho, Hsieh, Wang, & Mau, 2012; Tsiantas et al., 2021). In brief, acetonitrile (4 mL) was the solvent used for extracting lovastatin from 400 mg of dried mushrooms. Vigorous shaking was applied at 250 rpm for 2 h (Falc Instruments, Bergamo, Italy). The extract was separated from the sediment by centrifugation at 3650 rcf for 20 min. Then, 3 mL of the supernatant were evaporated until dryness. The dry residues were used for LC-MS/MS analysis.

For lovastatin LC-MS/MS analysis, an Acquity C18 column (100 mm × 2.1 mm i.d., 1.7 μm particle size; Waters, Milford, USA) was used for the elution of lovastatin and simvastatin, which was selected as the

internal standard of the developed LC-MS/MS-method. The autosampler tray and the column oven temperature was set at 10 °C and 25 °C, respectively. The samples were diluted in acetonitrile and the two analytes were separated using a 10 min isocratic elution consisting of water 0.1% formic acid (Solvent A, 40%) and acetonitrile (Solvent B, 60%). The injection volume was set at 10 μL. MS^2 detection was performed in ion trap mode of LTQ Orbitrap Velos mass spectrometer (Thermo Fisher Scientific, Waltham, USA) using electron spray ionization (ESI) on positive mode. The parent ions of lovastatin ($m/z = 427.3$) and simvastatin ($m/z = 441.3$) were fragmented to the quantitative ions (Q1) with $m/z = 325.1773$ (for lovastatin) and $m/z = 325.1772$ (for simvastatin). The optimized MS source parameters and the validation protocol of the developed LC-MS/MS method were thoroughly described by Tsiantas et al. (2021). The linearity of lovastatin's calibration curve [Peak area ratio (a.u.) = 33.6 $C_{lovastatin}$ + 0.23, R^2 = 0.999] was established over the concentration range of 0.01–0.25 μg/mL. All measurements were conducted in triplicate and LC-MS/MS spectra were processed by the Xcalibur software (Thermo Fisher Scientific, Waltham, USA).

2.12. Attenuated total reflection Fourier transform infrared (ATR-FTIR) analysis

The FTIR spectra of the substrates prior to the inoculation with the fungi and the produced mushrooms were recorded by a Spectrum Two FTIR spectrometer equipped with a Diamond ATR compartment (Perkin Elmer Inc., Waltham, USA) using the provided Spectrum 10 spectroscopy software. For each sample, 64 scans of the infrared region between 4000 and 450 cm^{-1} at a resolution of 4 cm^{-1} were recorded in triplicates and averaged. The recorded spectra were then ATR-corrected with a refractive index of 1.5, smoothed by the Savitzky-Golay algorithm [2 points each side (total window of 5 smoothing points) and a zero-order polynomial], and adaptively baseline corrected and normalised by the mean using the SpectraGryph 1.2.7 software (https://www.effemm2.de/spectragryph/).

2.13. Statistical analysis

All chemical analyses and assays were performed in five-fold. Results are presented as mean ± standard deviation (SD). Analysis of variance followed by Duncan's *t*-test at 5% level of probability for assessing differences between means (IBM SPSS statistics 21). Pearson's correlation coefficient was used for determining relationships (at significance levels of 0.05 and 0.01) between variables. A principal component analysis (PCA) was performed on the normalised – by the mean – spectra of mushrooms cultivated in different substrates (including all replicates) in order to detect sample groupings and the respective spectral regions and associated compounds. The PCA as well as the normalisation of the spectra was performed by R-studio 1.0.136/R3.3.3 software loaded with the "ade4" and "adegraphics" packages.

3. Results and discussion

3.1. Evaluation of cultivation parameters

Three cultivation substrates consisting of lignocellulosic residues/wastes were examined for their suitability to support production of *P. citrinopileatus* mushrooms. As regards the cultivation process, the GMW substrate was fully colonized by the mycelium within a period of 12 days after inoculation, while the respective period was significantly longer on WHS and OLW (17 and 18 days, respectively). The period for the appearance of the first fruitbodies (earliness) and the completion of the entire cultivation cycle was shorter in GMW (i.e., 18 and 54 days, respectively) compared with WHS (i.e., 22 and 59 days, respectively), although differences were not statistically significant (Table 1). This outcome could be attributed to the high content of GMW in easily degradable sugars that enhanced fungal growth and biomass development. In contrast, extended periods of incubation and cultivation (by 6 to 8 days, respectively) were noted in OLW (Table 1); this substrate contains inhibitory compounds (e.g., polyphenols) which delay the colonization of the respective substrate. Our results are in line with previous reports on the use of olive mill by-products – even composted – and olive pruning residues as substrates for the production of *Cyclocybe cylindracea*, *Hericium erinaceus* and *Pleurotus* spp. mushrooms (Koutrotsios et al., 2014, 2018; Koutrotsios, Larou, Mountzouris, & Zervakis, 2016; Zervakis et al., 2013).

Table 1
Cultivation parameters for *Pleurotus citrinopileatus* mushrooms produced on three substrates, i.e., GMW: grape marc plus wheat straw (1:1 w/w), OLW: olive mill by-products (leaves and two-phase olive mill waste, 1:1 w/w) and WHS: wheat straw. Values are expressed as means ± standard deviation (n = 5). Lack of letters in common indicates statistically significant differences (Duncan's *t*-test. $p < 0.05$) for comparison of treatment means between different substrates.

	Substrates		
Cultivation parameters	WHS	GMW	OLW
Incubation period (days)	17.00 ± 0.00[a]	12.00 ± 0.00[b]	18.00 ± 0.00[a]
Earliness (days)	21.75 ± 1.71[a]	18.25 ± 0.50[a]	27.00 ± 9.00[a]
Cultivation period (days)	59.00 ± 4.34[a]	54.00 ± 2.83[a]	62.00 ± 9.75[a]
Yield 1st flush (g)	117.00 ± 21.68[a]	100.25 ± 20.32[a]	41.6 ± 18.43[b]
Yield 2nd flush (g)	34.25 ± 7.36[b]	135.75 ± 18.63[a]	39.00 ± 8.85[b]
Yield 3rd flush (g)	15.50 ± 6.68[a]	38.75 ± 13.26[a]	36.20 ± 14.06[a]
Total yield (g)	166.75 ± 51.28[b]	274.75 ± 5.80[a]	129.00 ± 17.51[b]
B.E. (%)	53.70 ± 16.51[b]	78.52 ± 1.66 [a]	26.24 ± 3.56[c]
Productivity	0.84 ± 0.30[b]	1.46 ± 0.10[a]	0.46 ± 0.11[b]
Mushrooms weight (g)	8.55 ± 2.35[a]	8.62 ± 2.70[a]	9.46 ± 2.65[a]

The distribution of mushroom yield per flush showed great variability among the substrates tested. Approximately 70% of the total yield derived from the first flush in WHS, whereas <40% was noted in the first flush of the other two substrates. Such distribution in yields among flushes during the mushroom cropping period is quite uncommon among *Pleurotus* spp. since in most cases the first flush represents considerably more than 50% of the total yield. A similar fructification pattern was recently reported for *P. nebrodensis* which exhibited the highest production during the second flush in GMW-based substrates (Koutrotsios et al., 2018). In general, GMW supported significantly higher total yields (275 g/kg of substrate), followed by WHS and OLW (167 and 129 g/kg of substrate, respectively). Similarly, biological efficiency was significantly higher in GMW than in WHS (79% vs. 54%), whereas a much lower biological efficiency was noted in OLW (Table 1). The respective values previously reported for *P. citrinopileatus* varied considerably depending on the substrate used, e.g., 40 to 65% in various grass plants (Liang et al., 2009), 58% in wheat straw, (Kulshreshtha et al., 2013), and 89 to 95% in handmade paper and cardboard industrial wastes mixed with wheat straw (Kulshreshtha et al., 2013). Such variations not only depend on the nature of raw materials employed for the preparation of substrates but also on the type of supplementation applied (and consequently the C/N ratio) and the strain used. In the past, *N*-rich substrates provided high biological efficiency values for *C. cylindracea, H. erinaceus* and *Pleurotus ostreatus* (Koutrotsios et al., 2014, 2016), while considerable differentiation was recorded among strains of the same mushroom species in respect to the cultivation parameters examined (Koutrotsios et al., 2017).

Moreover, the productivity exhibited by the GMW substrate (i.e., 1.46) was significantly higher than the other two substrates (0.84 and 0.46 in WHS and OLW, respectively). Since both the duration of the cultivation period and the biological efficiency are taken into account for the calculation of the productivity parameter, GMW-based substrates could be considered as superior at supporting *P. citrinopileatus*

mushroom production in accordance with the outcome of previous relevant studies on *P. ostreatus, P. eryngii, P. nebrodensis* and *C. cylindracea* (Koutrotsios et al., 2014, 2018). As regards the quality of the fruitbodies formed, no noticeable differences were recorded in their appearance (including the size of individual pilei) among the substrates examined (Supplementary Material, Fig. S1).

3.2. Assessment of quality aspects in mushrooms cultivated on olive mill and winery by-products

3.2.1. Total phenolic content and antioxidant properties

P. citrinopileatus mushrooms are well-known for their antioxidant properties attributed to α- and γ-tocopherols, ascorbic acid and phenolic compounds (Lee, Huang, Liang, & Mau, 2007). In the present study, high TPC values (166.1–221.5 mg GAE/100 g d.w.) and high antioxidant activity of *P. citrinopileatus* methanolic extracts (radical scavenging activity: 40.3–55.7 mmol TE/100 g d.w.; reducing antioxidant potential: 12.4–12.8 mmol TE/100 g d.w.; total serum oxidizability: 4717–5115 *sec*) are reported. Previous studies have also shown high TPC and antioxidant potential of *P. citrinopileatus* extracts (Freitas et al., 2018; Lee et al., 2007); however, the different methods of sample processing and the various ways in which results are expressed do not allow direct comparisons.

The values determined for total phenolics and radical scavenging activity were significantly higher in fruitbodies produced on GMW as compared with WHS (control). On the other hand, reducing antioxidant potential and total serum oxidizability did not exhibit any significant difference between the substrates examined (Table 2). These results are in accordance with recent findings demonstrating the marked effect of the nature of cultivation substrate on TPC and antioxidant properties of *Pleurotus* mushrooms (Freitas et al., 2018; Koutrotsios et al., 2018), confirming that the content of organic compounds in the fruitbodies is influenced by the content of such ingredients in the respective cultivation substrates. Especially as regards TPC and total serum oxidizability, *P. citrinopileatus* showed considerably higher values in comparison to *P. ostreatus*, *P. eryngii* and *P. nebrodensis* cultivated on the same substrates (i.e., WHS, GMW and OLW; Koutrotsios et al., 2018). However, when radical scavenging activity and reducing antioxidant potential were compared, then the respective values for *P. citrinopileatus* were superior only to those of *P. ostreatus*. It is noteworthy that the TPC measured in *P. citrinopileatus* is considerably higher than the TPC assessed in 11 wild edible mushrooms (Gąsecka, Siwulski, & Mleczek, 2018). In addition, values of FRAP and total serum oxidizability in *P. citrinopileatus* mushrooms are positively correlated with the corresponding values of TPC in the substrates used ($r = 0.645$ and $r = 0.999$, $p < 0.01$ respectively).

Table 2
Antioxidant activities (DPPH and FRAP), and total phenolic (TPC), ergosterol, ergothioneine, lovastatin and glucan contents in *Pleurotus citrinopileatus* mushrooms cultivated on three substrates, i.e., GMW: grape marc plus wheat straw (1:1 w/w), OLW: olive mill by-products (leaves and two-phase olive mill waste, 1:1 w/w) and WHS: wheat straw. Values are expressed as means ± standard deviation (n = 5). Lack of letters in common indicates statistically significant differences (Duncan's *t*-test. $p < 0.05$) for comparison of treatment means between different substrates. TPC, total phenolic content; DPPH, radical scavenging activity; FRAP, reducing antioxidant potential; TSO, total serum oxidizability.

Antioxidant activities/ Content	Substrates		
	WHS	GMW	OLW
DPPH (mmol TE/100 g d.w.)	40.3 ± 8.6^{b}	55.7 ± 1.0^{a}	42.2 ± 9.7^{ab}
FRAP (mmol TE/100 g d.w.)	12.4 ± 0.33^{a}	12.8 ± 2.7^{a}	12.8 ± 2.3^{a}
TSO (*sec*)	4717 ± 375^{a}	4811 ± 272^{a}	5115 ± 480^{a}
TPC (mg GAE/100 g d.w.)	166.3 ± 36.9^{b}	221.5 ± 16.4^{a}	166.1 ± 5.3^{b}
Ergosterol (mg/g d.w.)	3.76 ± 0.42^{b}	5.53 ± 0.42^{a}	4.78 ± 0.56^{ab}
Ergothioneine (μg/g d.w.)	820.7 ± 25.2^{a}	631.8 ± 30.4^{b}	884.8 ± 24.5^{a}
Lovastatin (μg/g d.w.)	0.148 ± 0.005^{b}	0.220 ± 0.014^{a}	0.151 ± 0.009^{b}
α-glucans (% d.w.)	8.29 ± 2.46^{a}	5.67 ± 1.17^{a}	6.67 ± 2.38^{a}
β-glucans (% d.w.)	21.97 ± 1.07^{a}	22.74 ± 1.22^{a}	20.54 ± 0.13^{a}

3.2.2. Individual phenolics and triterpenic acids

Phenolic compounds are produced as secondary metabolites by plants and fungi as a result of ecological interactions, environmental pressure or stress conditions; their presence in edible mushrooms is linked to several beneficial properties, including antioxidant, antidiabetic, antimicrobial, anti-inflammatory, antitumor and antimutagenic activities; therefore, they have attracted considerable research interest (Heleno, Martins, Queiroz, & Ferreira, 2015).

Herein, seven phenolic components were identified in *P. citrinopileatus* mushrooms. Four phenolic acids, i.e., *p*-OH benzoic, *p*-OH phenylacetic, vanillic and cinnamic acids were measured in concentrations ranging from 0.09 to 0.87 μg/g d.w. (Fig. 1). More specifically, mushrooms grown on GMW substrate contained significantly higher concentrations of *p*-OH benzoic and *p*-OH phenylacetic acids, whereas vanillic acid showed a threefold higher concentration in mushrooms deriving from WHS and OLW than those from GMW. The content in cinnamic acid was significantly lower in mushrooms produced on the OLW substrate. In addition, cinnamic acid concentrations (0.09–0.16 μg/g d.w.; Fig. 1) were considerably lower to those reported for various wild mushrooms (0.43–46.04 μg/g d.w.; Vaz et al., 2011) but comparable to those estimated in other cultivated species (0.02–0.38 μg/g d.w.; Reis, Martins, Barros, & Ferreira, 2012). Based on the present data and those published by Koutrotsios et al. (2018), the content of *p*-OH benzoic and *p*-OH phenylacetic acids was significantly higher in *P. eryngii* and *P. ostreatus* mushrooms deriving from OLW, whereas considerably higher contents were obtained in *P. nebrodensis* and *P. citrinopileatus* mushrooms produced on GMW. Hence, the combination of strain/species and cultivation substrate has a pronounced effect in these bioactive compounds in *Pleurotus* mushrooms.

Resveratrol is a stilbenoid, produced by several plants and fungi; in *P. citrinopileatus* samples, resveratrol concentration ranged from 4.0 to 6.9 μg/100 g d.w. (Fig. 1). Mushrooms produced on the OLW-based substrate presented higher resveratrol content compared to the other cultivation media examined; however, differences were not significant. The resveratrol values obtained for *P. citrinopileatus* mushrooms were comparable to those recently reported for *P. ostreatus* mushrooms derived from the same substrates; however, *P. nebrodensis* and *P. eryngii* mushrooms exhibited considerably higher resveratrol content, e.g., up to 30 times for *P. nebrodensis* cultivated on OLW (Koutrotsios et al., 2018). Such data are indicative of the large differences in the concentration of bioactive compounds among mushrooms of closely-related species, or even among strains of the same species (Koutrotsios et al., 2017).

The two triterpenic (oleanolic and ursolic) acids were detected only in mushrooms produced on GMW and OLW. A significant correlation was noted between their content in fruitbodies and the respective substrates ($r = 0.99$, $p < 0.01$). The efficacy of mushrooms for selective absorption of organic compounds from their production substrates is evident and in accordance with the outcome of a recent study (Koutrotsios et al., 2018). An indicative GC–MS chromatogram is provided in Supplementary Material (Fig. S2a).

3.2.3. Ergosterol content

Mushrooms are a rich source of ergosterol, which is converted into vitamin D_2 following exposure to UV radiation (Phillips et al., 2011). In our study, the use of GMW and OLW led to an increase in ergosterol content by up to 32% and 21%, respectively, compared with the WHS control (Table 2). This outcome was linked to the squalene content of substrates; squalene is the first precursor in ergosterol biosynthesis in fungi, and it was found to be significantly correlated with the ergosterol concentration of *P. citrinopileatus* mushrooms ($r = 0.97$, $p < 0.01$). A

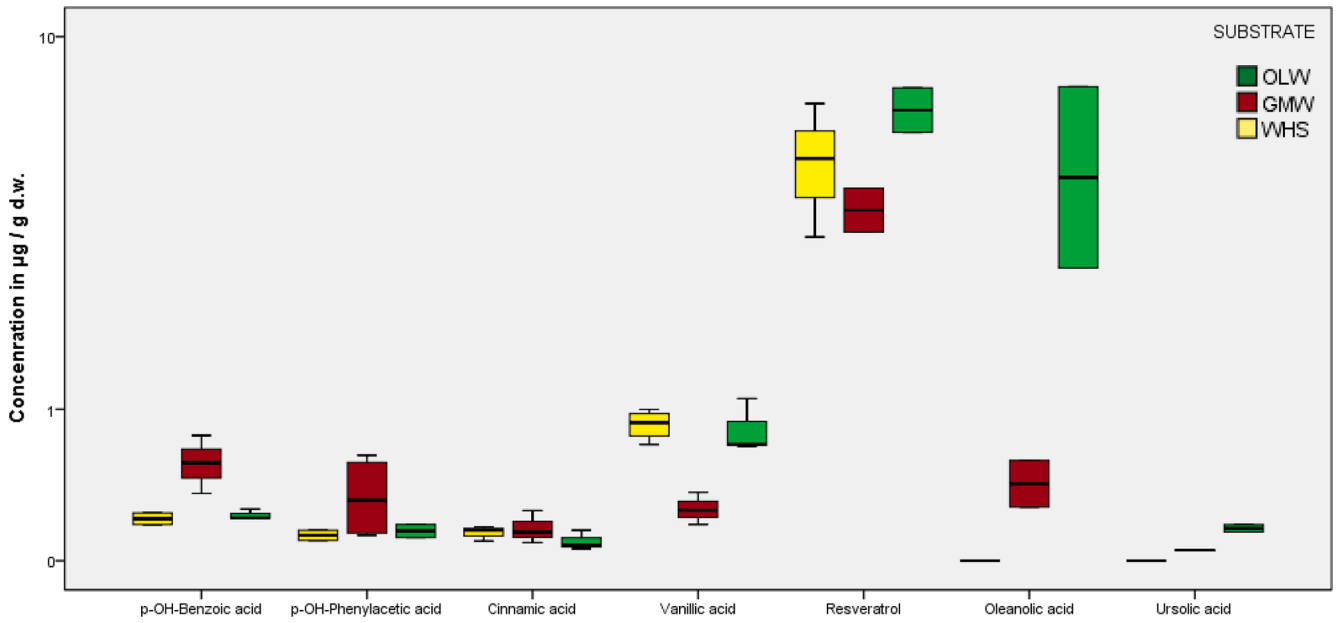

Fig. 1. Individual phenolic compounds and triterpenic acids in *Pleurotus citrinopileatus* mushrooms cultivated on three substrates, i.e., GMW: grape marc plus wheat straw (1:1 w/w), OLW: olive mill by-products (leaves and two-phase olive mill waste, 1:1 w/w) and WHS: wheat straw. Y-axis is presented as a logarithmic scale. Values (µg/g d.w.) are expressed as means, with the exception of resveratrol (µg/100 g d.w.). Lack of letters in common indicates statistically significant differences (Duncan's *t*-test; $p < 0.05$) for comparison of treatment means between different substrates.

similarly high correlation had previously been observed in fruitbodies of other *Pleurotus* spp. when various ratios of grape marc were added to WHS-based substrates (Koutrotsios et al., 2018). The ergosterol values found in our work are similar to those previously reported for *P. citrinopileatus* mushrooms obtained from commercial cultivation (i.e., 0.31 to 5.74 mg/g d.w.; Huang, Cai, & Xu, 2017; Krakowska et al., 2020; Lin, Chien, Wang, & Mau, 2016), and considerably higher than those measured in many other widely commercialized edible species (Huang et al., 2017; Phillips et al., 2011). An indicative GC–MS chromatogram is provided in Supplementary Material (Fig. S2b).

3.2.4. Glucans content

Research interest in mushroom glucans (i.e., a structural component of fungal cell walls) is steadily growing during the last 20 years due to their role in human health. The total glucan content of *P. citrinopileatus* mushrooms was 27.2–30.3% d.w with β-glucans corresponding to more than 70% of total glucans (i.e., 20.5–22.7% d.w.; Table 2). The cultivation substrates did not significantly affect the mushrooms glucan content in contrast to the outcome of previous studies on *Pleurotus ostreatus*, *P. eryngii*, *P. nebrodensis* and *H. erinaceus* (Koutrotsios et al., 2016, 2018). In general, the glucan content in *P. citrinopileatus* is similar to that reported for most cultivated species ranging from 10 to 40% d.w. (Bach, Helm, Bellettini, Maciel, & Haminiuk, 2017; Sari, Prange, Lelley, & Hambitzer, 2017).

3.2.5. Content in free amino acids

Mushrooms are characterized as a rich protein source and their amino acid composition is comparable to those of animal and dairy products (Tagkouli et al., 2020). In the frame of this work, 21 free amino acids (FAAs) including GABA were measured in *P. citrinopileatus* fruitbodies; glutamine, leucine, glutamic acid and alanine were – in descending order – the most abundant regardless of the substrate used (Table 3). Our results showed that amino acids in *P. citrinopileatus* mushrooms occur in amounts similar to those of other cultivated mushrooms (Bach et al., 2017).

On the other hand, the cultivation substrates exhibited a notable effect on mushrooms FAAs content. In particular, mushrooms produced on GMW demonstrated significantly higher values for most FAAs (with the exception of alanine, hydroxyproline, glutamic acid and ornithine) in comparison to those obtained from WHS and OLW. Hence, total FAAs ranged from 48.7 mg/g d.w. (OLW) and 50.5 mg/g d.w. (WHS) up to 87.5 mg/g d.w. (GMW). In addition, the eight essential amino acids content increased by 53% (leucine and phenylalanine) to 118% (histidine) in mushrooms cultivated on GMW in comparison to those harvested from the conventional substrate (WHS). Very notable was also the effect of the substrate on the production of GABA since fruitbodies obtained from GMW presented a 62% increase in GABA's content over those cultivated in WHS and a five-fold increase over those produced on OLW. Such results are in agreement with earlier findings reporting differences in the amino acids content of *Pleurotus* mushrooms ('florida' strain) deriving from various rice straw-based substrates (Shashirekha, Rajarathnam, & Bano, 2005), and in FAAs content of fruitbodies from other *Pleurotus* spp. produced on the same cultivation media as those of the present study (Tagkouli et al., 2020). An indicative GC–MS chromatogram is provided in Supplementary Material (Fig. S2c).

In seek of the relationships between the amino acid content in *P. citrinopileatus* mushrooms and their respective substrates, high correlation coefficients (0.9 to 1.0, $p < 0.05$ or $p < 0.01$) were found for all FAAs with the exception of aspartic acid, hydroxyproline, methionine, ornithine, thioproline, tryptophan and GABA (Table 3). This finding confirms the view that fungal cell walls are not a barrier to the uptake of amino acids, and that those required for the metabolic needs of fungi could be directly absorbed from their cultivation substrate (Braus, Pries, Düvel, & Valerius, 2004). The significantly higher content of FAAs in GMW – compared to OLW and WHS – may explain the significant improvement noted in the cultivation parameters during production of *P. citrinopileatus* on this particular substrate. This is further evidenced by the Pearson's correlation values obtained for total FAAs content vs. total mushroom yield ($r = 0.78$, $p < 0.05$) and vs. mushroom productivity ($r = 0.68$, $p < 0.05$).

Especially as regards mushrooms taste characteristics, glutamic and aspartic acids are responsible for the characteristic umami taste (MSG-like) in mushrooms; their total content ranged from 6.3 to 8.9 mg/g d.w. (Table 3). It is noteworthy that the respective values in literature vary considerably (i.e., from 0.05 to 46 mg/g d.w.; Zhang, Venkitasamy, Pan, & Wang, 2013) due to the variability among species and/or harvest

Table 3
Free amino acids (FAAs), and sum of branched chain, aromatic, MSG-like, bitter taste, sweet taste, tasteless and essential AAs content of *Pleurotus citrinopileatus* mushrooms cultivated in three substrates [i.e., GMW: grape marc plus wheat straw (1:1 w/w), OLW: olive mill by-products (leaves and two-phase olive mill waste, 1:1 w/w) and WHS: wheat straw] and Pearson's correlation coefficient from comparisons between AAs content in mushrooms and their respective substrates (the latter derive from the study by Tagkouli et al., 2020). Values (mg/g d.w.) are expressed as means ± standard deviation (n = 5). Lack of letters in common indicates statistically significant differences (Duncan's *t*-test, $p < 0.05$) for comparison of treatment means between different substrates. Essential AAs appear in bold typeface.

Free Amino Acids (FAAs)	Substrates			Pearson's correlation coefficient
	WHS	GMW	OLW	
Histidine[2,4]	0.95 ± 0.04^{b}	2.07 ± 0.82^{a}	0.88 ± 0.28^{b}	0.992*
Isoleucine[1]	1.82 ± 0.57^{b}	3.58 ± 1.08^{a}	2.03 ± 0.75^{b}	1.000**
Leucine[1,3]	7.69 ± 2.08^{b}	11.75 ± 3.61^{a}	8.76 ± 2.95^{b}	0.968*
Lysine[3]	2.15 ± 0.57^{b}	4.10 ± 1.38^{a}	2.19 ± 0.61^{b}	0.998**
Methionine[4]	1.02 ± 0.23^{b}	2.02 ± 0.59^{a}	0.92 ± 0.31^{b}	−0.111
Phenylalanine[2]	2.83 ± 0.79^{b}	4.33 ± 1.25^{a}	2.87 ± 0.90^{b}	1.000**
Threonine[4]	1.67 ± 0.63^{b}	2.99 ± 0.76^{a}	1.61 ± 0.43^{b}	0.989**
Valine[1,4]	2.68 ± 0.93^{b}	5.38 ± 1.32^{a}	2.79 ± 0.96^{b}	0.979*
Alanine[4]	3.84 ± 1.17^{b}	7.11 ± 1.72^{b}	4.73 ± 1.41^{b}	0.998**
Asparagine[4]	1.03 ± 0.29^{b}	2.28 ± 0.62^{a}	1.07 ± 0.28^{b}	0.913
Aspartic acid[4]	1.02 ± 0.28^{c}	2.68 ± 0.60^{a}	1.71 ± 0.90^{b}	0.589
Hydroxyproline	0.44 ± 0.15^{ab}	0.51 ± 0.09^{a}	0.33 ± 0.15^{b}	0.780
Glutamic acid[4]	5.19 ± 1.49^{a}	5.94 ± 1.64^{a}	4.47 ± 1.22^{a}	0.983*
Glutamine[4]	9.58 ± 3.78^{b}	15.78 ± 3.18^{a}	5.04 ± 1.76^{c}	0.907*
Glycine[4]	0.90 ± 0.34^{b}	1.81 ± 0.55^{a}	0.89 ± 0.22^{b}	0.911*
Ornithine	0.89 ± 0.60^{a}	0.99 ± 0.51^{a}	0.57 ± 0.20^{a}	0.680
Proline[4]	0.98 ± 0.46^{b}	1.85 ± 0.49^{a}	0.85 ± 0.17^{b}	0.951*
Serine[4]	2.37 ± 0.62^{b}	4.78 ± 0.97^{a}	2.61 ± 0.61^{b}	0.997**
Thioproline	0.84 ± 0.38^{c}	2.67 ± 0.74^{a}	1.64 ± 0.97^{b}	0.617
Tyrosine[2]	2.53 ± 0.70^{b}	3.94 ± 1.12^{a}	2.72 ± 0.72^{b}	0.999**
GABA	0.53 ± 0.32^{b}	0.86 ± 0.37^{a}	0.14 ± 0.04^{c}	0.767
Branched chain	11.77 ± 3.53^{b}	20.46 ± 6.10^{a}	12.92 ± 4.60^{b}	0.997**
Aromatic	7.04 ± 1.91^{b}	11.55 ± 3.27^{a}	6.96 ± 2.06^{b}	0.731
Umami taste (MSG-like)	6.64 ± 2.27^{b}	8.94 ± 2.32^{a}	6.27 ± 1.82^{b}	0.936*
Bitter taste	17.29 ± 4.94^{b}	30.09 ± 8.78^{a}	18.22 ± 6.16^{b}	0.872
Sweet taste	9.75 ± 3.01^{b}	18.17 ± 4.61^{a}	10.42 ± 2.83^{b}	0.987**
Tasteless	4.68 ± 1.18^{b}	8.04 ± 2.21^{a}	4.36 ± 1.33^{b}	0.978*
Essential	21.10 ± 6.04^{b}	37.18 ± 10.86^{a}	22.24 ± 7.44^{b}	0.914*
TOTAL	50.55 ± 14.2^{b}	87.52 ± 19.22^{a}	48.70 ± 12.60^{b}	0.885

*significant at $p < 0.05$.
**significant at $p < 0.01$.
[1] Branched chain AAs.
[2] Aromatic AAs.
[3] Ketogenic AAs.
[4] Glucogenic AAs.

stage but also due to sample processing and method of determination. In addition, significant differences were observed for other amino acid groups related to mushrooms taste and flavor depending on the respective cultivation substrates with those produced on GMW presenting notably higher values.

3.2.6. Ergothioneine content

Ergothioneine is a natural 2-thiol-amidazole amino acid with antioxidant properties that could play an important/beneficial role in inflammation, oxidative stress/damage, depression and cardiovascular diseases (Halliwell, Cheah, & Tang, 2018). In the present work, significantly higher concentration of ergothioneine was detected in fruitbodies cultivated on WHS and OLW compared to GMW substrate (821 and 885 vs. 632 μg/g d.w., respectively; Table 2). These values fall within the same wide range previously reported for other cultivated mushrooms, i.e., various species including *P. ostreatus* (210–2590 and 370–10400 μg/g d.w.; Dubost, Ou, & Beelman, 2007; Sapozhnikova et al., 2014), or several *Pleurotus* spp. including *P. citrinopileatus* (150–2850 μg/g d.w.; Chen et al., 2012; Krakowska et al., 2020), *P. eryngii* (1720–3000 μg/g d.w.; Rodriguez Estrada, Lee, Beelman, del Mar Jimenez-Gasco, & Royse, 2009), *P. citrinopileatus* (3890 μg/g d.w.; Lin et al., 2016), and *P. ostreatus* and *P. citrinopileatus* (150–3940 μg/g d.w.; Kalaras, Richie, Calcagnotto, & Beelman, 2017). Indicative LC-MS/MS chromatograms from our study are provided in Supplementary Material (Fig. S3a and Fig. S3b).

Earlier studies examining ergothioneine in mycelium biomass produced in liquid media demonstrated that ergothioneine content depended on the mushroom species investigated, and was largely influenced by the type of carbon and nitrogen sources available (e.g., fructose in combination with aspartic acid) or the presence of precursor compounds (e.g., histidine or methionine) (Lin et al., 2016). Nevertheless, the effect of certain amino acids on ergothioneine content in mycelia was not pronounced in mushrooms examined in this work. Despite that GMW was the substrate with the highest content in most of the FAAs measured (Tagkouli et al., 2020; this study), it produced fruitbodies with relatively lower ergothioneine content than the other two substrates used. In addition, although there is yet no solid evidence associating the phenolic content with ergothioneine concentration, it seems that mushrooms with high total phenolics present relatively inferior ergothioneine content (Dubost et al., 2007; this work). Since other factors (e.g., composition and water content of cultivation medium; Rodriguez Estrada, Lee, Beelman, Jimenez-Gasco, & Royse, 2009) are also involved in ergothioneine synthesis, further research is required to elucidate their interactions and role in ergothioneine production in mushrooms.

3.2.7. Lovastatin content

Edible mushrooms including those obtained from *Pleurotus* species are a valuable source of lovastatin, a compound belonging to the group of statins which are widely used as cholesterol-lowering drugs. Lovastatin exhibits a multidirectional effect in various diseases such as osteoporosis, neurodegenerative diseases, rheumatoid arthritis, ischemic heart disease and nonalcoholic fatty liver disease (Kała, Kryczyk-Poprawa, Rzewińska, & Muszyńska, 2020). In this work, the analysis of acetonitrile extracts and the use of the LC-MS/MS platform confirmed the presence of lovastatin in *P. citrinopileatus* mushrooms. Lovastatin concentration in mushrooms cultivated on the GMW substrate (0.220 μg/g d.w.) was significantly higher than in mushrooms cultivated on WHS or OLW substrates (0.148 and 0.151 μg/g d.w., respectively; Table 2). This outcome could be due to the higher content of GMW in organic nitrogen compared to other agricultural residues (Prandi et al., 2019). Previous studies on *P. ostreatus* and *Aspergillus terreus* reported increased lovastatin content in substrates rich in organic

nitrogen source(s) whereas non-organic nitrogen did not significantly influence lovastatin production (Alarcón & Águila, 2006; Hajjaj, Niederberger, & Duboc, 2001). Indicative LC-MS/MS chromatograms from our study are provided in Supplementary Material (Fig. S3c and Fig. S3d).

The wide range of lovastatin content reported in either wild or cultivated mushrooms (Chen et al., 2012; Kała et al., 2020; Lin et al., 2013), and the contradictory results regarding the presence or absence of this compound in *P. citrinopileatus* or other *Pleurotus* spp. (Chen et al., 2012; Krakowska et al., 2020; Lin et al., 2013), highlight the need for the application of reliable methodologies to assess lovastatin levels in mushrooms. Within this context, the MS-based methodology of high resolution and sensitivity developed and implemented for estimating lovastatin in edible mushrooms (Tsiantas et al., 2021) was adopted for the needs of the present study.

3.2.8. Content in fatty acids

The content of *P. citrinopileatus* mushrooms in seven fatty acids is presented in Supplementary Material (Supplementary Material; Table S4). Linoleic acid (C18:2n6) presented the highest content in all samples (54.5–70.5% of total fatty acids) followed by palmitic acid (C16:0; 12.3–14.3%) and oleic acid (C18:1n9; 3.9–4.9%). As regards the effect of different cultivation media, an increase in the short chain fatty acids (C14:0 and C15:0) content was observed in the GMW substrate, while the use of OLW substrate led to a significant increase in linoleic acid content. An indicative GC–MS chromatogram is provided in Supplementary Material (Fig. S2d).

3.3. Spectroscopic analysis

The recorded ATR-FTIR spectra of *P. citrinopileatus* mushrooms deriving from three different substrates demonstrated differences in several regions of absorption (Fig. 2a). Mushrooms produced in GMW revealed greater IR absorption intensities than mushrooms from the other two substrates at 1650, 1570, 1400 and 1250 cm^{-1}. Among them, the peak at 1650 cm^{-1} is related to the C═O stretching vibration in proteins (Amide I band) and carboxylates, or to the aromatic C═C stretching vibration in phenols (Socrates, 2001), while the peak at 1570 cm^{-1} is mostly associated with the N—H bending vibration of secondary amides (Amide II band), but also to the C—N stretching vibration of the –CO-NH- group (trans form) (Socrates, 2001). The peak at 1400 cm^{-1} corresponds to the symmetric stretching vibration of the COO^- group in fatty and amino acids as well as to the symmetric bending modes of methyl groups in skeletal proteins (Movasaghi, Rehman, & Rehman, 2008); the observed peak at 1255 cm^{-1} is attributed to the C—N stretching and N—H bending vibrations in proteins (Amide III band) (Movasaghi, Rehman, & ur Rehman, 2008; Socrates, 2001). The above-mentioned differences indicate an increased content in proteins and phenolic compounds (combinational peak at 1650 cm^{-1}) for mushrooms cultivated on the GMW substrate, which is in agreement with the contents in total amino acids and total phenolic compounds, respectively (Tables 2 and 3). On the other hand, the OLW substrate revealed the highest absorption intensities at the region 1650–1600 cm^{-1} (Fig. 2b) in accordance with the high values of total and individual phenolics measured in the initial materials used for mushroom production (Koutrotsios et al., 2018). Moreover, notable differences were also observed at 1200–1000 cm^{-1}, mostly related to the C—O stretching vibrations of carbohydrates but also associated with the symmetric PO_2^- and C—O—P stretching vibrations of lipids (peaks around 1080 and 1040 cm^{-1}; Socrates, 2001). Mushrooms cultivated on the OLW substrate present the highest absorption intensities in this region, followed by mushrooms cultivated on WHS and GMW in agreement with mushrooms content in linoleic acid as hereby established (Supplementary Material; Table S3).

PCA was performed on the normalized spectra of mushrooms (all replicates) cultivated in different substrates, and the score plot for the two principal components explaining 89.1% of total variance (PC1 vs. PC2) revealed a clear grouping of spectra according to the substrate used for the cultivation of *P. citrinopileatus* mushrooms (Fig. 3a). This grouping is also in agreement with the PCA performed taking into account the measurements of antioxidant activity (AAR and FRAP), ergosterol, α- and β-glucans, individual and total phenolic compounds and individual amino acids (Fig. 3b). Separation of spectra of *P. citrinopileatus* mushrooms cultivated on GMW substrate was achieved through PC1, whereas separation of mushroom spectra produced on WHS and OLW substrates was attributed to PC2.

The interpretation of PCA loadings for PC1 and PC2 allowed the identification of categories of compounds responsible for this separation (Supplementary Material; Fig. S4a and Fig. S4b). Hence, PC1 loadings revealed a positive correlation of the spectra obtained by mushrooms cultivated on GMW to the regions at 1586, 1508, 1358 and 1240 cm^{-1} (Supplementary Material; Fig. S4a). The regions at 1586 and 1508 cm^{-1} correspond to the phenyl ring and the C—C stretching or the C—H bending respectively (Movasaghi et al., 2008); the latter region is also related to the N—H bending and C—N stretching of the proteinic amide (Amide II band) (Movasaghi et al., 2008). The region at 1358 cm^{-1} is associated with the C—O stretching, C—H deformation and/or N—H

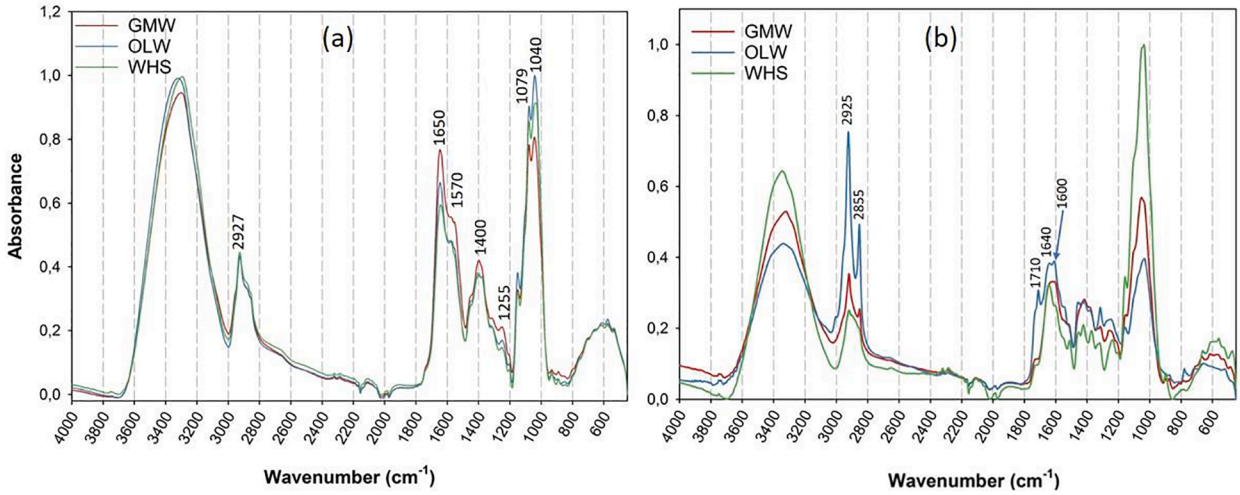

Fig. 2. Recorded ATR-FTIR spectra of (a) *Pleurotus citrinopileatus* mushrooms cultivated in three substrates and (b) the three substrates used for the production of *P. citrinopileatus* mushrooms, marked with the IR absorption regions of interest; GMW: mix of wheat straw and grape marc (1:1 w/w), OLW: olive mill by-products (leaves and two-phase olive mill waste 1:1 w/w) and WHS: wheat straw.

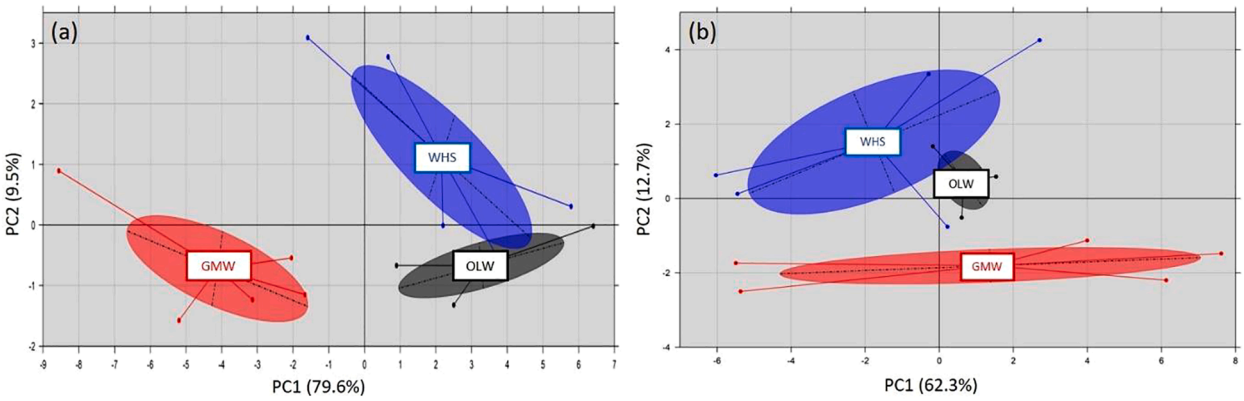

Fig. 3. Principal component analysis score plot revealing the grouping of *Pleurotus citrinopileatus* mushrooms in respect to the cultivation substrate used and on the basis of (a) the ATR-FTIR spectra recorded, and (b) the content in bioactive compounds (i.e., antioxidants, TPC, α- and β-glucans, ergosterol, individual phenolic compounds and individual amino acids).

deformation of the Amide III band, while the region at 1240 cm^{-1} to the C—N stretching of the Amide III band (Movasaghi et al., 2008; Socrates, 2001). These positively correlated regions are in agreement with the high phenolic content measured in mushrooms deriving from the GMW substrate (Table 2) as well as with the strong IR absorptions across the proteinic regions which were observed for the same mushrooms (Fig. 2). The interpretation of PC2 loadings revealed a positive correlation of the WHS group mainly to the spectral regions at 3166, 2907, 1425, 1285, 1036, 891 and 845 cm^{-1} (Supplementary Material; Fig. S4b). The regions at 3166 and 1285 cm^{-1} are related to the proteinic amide, and more specifically to the symmetric N—H stretching vibration from the overtone of the Amide II band (Socrates, 2001) and the N—H deformation of the Amide II band (Movasaghi et al., 2008), respectively. The rest of the regions are related to carbohydrates/polysaccharides, i.e., the region at 2907 cm^{-1} is attributed to the C—H stretching of carbohydrates, the region at 1425 cm^{-1} to the CH_2 deformation of polysaccharides, the region at 1036 cm^{-1} to the C—O stretching vibration in polysaccharides, the region at 891 cm^{-1} to the C—H deformation of the anomeric region of β-glucans, and the region at 845 cm^{-1} to the C—H deformation of the anomeric region of α-glucans (Movasaghi et al., 2008; Socrates, 2001).

4. Conclusions

Both olive mill and winery by-products are suitable for the cultivation of *Pleurotus citrinopileatus* mushrooms. Especially the latter appears better than the conventional (wheat-straw) substrate since it significantly shortens the incubation period and increases biological efficiency. Considerably higher concentrations of total phenolics, individual phenolic acids, ergosterol, essential and total amino acids were assessed in mushrooms cultivated on the GMW substrate. In addition, triterpenic acids were detected only in mushrooms produced in GMW and OLW, indicating that *P. citrinopileatus* selectively absorbs such compounds. The mushroom content in ergothioneine and lovastatin was also influenced by the type of substrate used. Moreover, ergosterol concentration in fruitbodies seems to depend on the amount of squalene in the respective substrate. On the other hand, glucans and fatty acids (with the exception of linoleic acid) were not significantly affected by the nature of the substrate. FTIR spectroscopy is a promising tool for monitoring various compounds in *P. citrinopileatus* fruitbodies and, when combined with the appropriate statistical methodologies, it can be used for qualitative screening of mushrooms cultivated on various substrates.

CRediT authorship contribution statement

Georgios Koutrotsios: Conceptualization, Methodology, Investigation, Validation, Formal analysis, Data curation, Writing – original draft. **Dimitra Tagkouli:** Methodology, Validation, Formal analysis, Investigation, Data curation, Writing – original draft. **Georgios Bekiaris:** Methodology, Validation, Formal analysis, Investigation, Writing – original draft. **Andriana Kaliora:** Methodology, Validation, Data curation, Writing - review & editing. **Thalia Tsiaka:** Methodology, Validation, Formal analysis, Investigation, Data curation, Writing – original draft. **Konstantinos Tsiantas:** Methodology, Validation, Formal analysis, Investigation, Data curation, Writing – original draft. **Iordanis Chatzipavlidis:** Validation, Resources, Data curation. **Panagiotis Zoumpoulakis:** Conceptualization, Methodology, Resources, Validation, Data curation, Writing - review & editing, Visualization, Supervision, Funding acquisition. **Nick Kalogeropoulos:** Conceptualization, Methodology, Resources, Validation, Data curation, Writing - review & editing, Visualization, Supervision, Funding acquisition. **Georgios I. Zervakis:** Conceptualization, Methodology, Resources, Validation, Data curation, Writing - review & editing, Visualization, Supervision, Project administration, Funding acquisition.

Declaration of Competing Interest

The authors declare that they have no known competing financial interests or personal relationships that could have appeared to influence the work reported in this paper.

Acknowledgements

This research has been co-financed by the European Union and Greek national funds (European Social Fund – ESF) through the Operational Program Competitiveness, Entrepreneurship and Innovation, under the call RESEARCH–CREATE–INNOVATE (project code: T1EDK–02560).

Appendix A. Supplementary data

Supplementary data to this article can be found online at https://doi.org/10.1016/j.foodchem.2021.131022.

References

Alarcón, J., & Águila, S. (2006). Lovastatin production by *Pleurotus ostreatus*: Effects of the C: N ratio. *Zeitschrift für Naturforschung C, 61*(1–2), 95–98.
Arnous, A., Makris, D. P., & Kefalas, P. (2002). Correlation of pigment and flavanol content with antioxidant properties in selected aged regional wines from Greece. *Journal of Food Composition and Analysis, 15*(6), 655–665.

Bach, F., Helm, C. V., Bellettini, M. B., Maciel, G. M., & Haminiuk, C. W. I. (2017). Edible mushrooms: A potential source of essential amino acids, glucans and minerals. *International Journal of Food Science and Technology, 52*(11), 2382–2392.

Braus, G. H., Pries, R., Düvel, K., & Valerius, O. (2004). In *Genetics and Biotechnology* (pp. 239–269). Berlin, Heidelberg: Springer Berlin Heidelberg.

Chen, S.-Y., Ho, K.-J., Hsieh, Y.-J., Wang, L.-T., & Mau, J.-L. (2012). Contents of lovastatin, γ-aminobutyric acid and ergothioneine in mushroom fruiting bodies and mycelia. *LWT, 47*(2), 274–278.

Dubost, N., Ou, B., & Beelman, R. (2007). Quantification of polyphenols and ergothioneine in cultivated mushrooms and correlation to total antioxidant capacity. *Food Chemistry, 105*(2), 727–735.

Freitas, A. C., Antunes, M. B., Rodrigues, D., Sousa, S., Amorim, M., Barroso, M. F., … Gomes, A. M. (2018). Use of coffee by-products for the cultivation of *Pleurotus citrinopileatus* and *Pleurotus salmoneo-stramineus* and its impact on biological properties of extracts thereof. *International Journal of Food Science & Technology, 53*(8), 1914–1924.

Gąsecka, M., Siwulski, M., & Mleczek, M. (2018). Evaluation of bioactive compounds content and antioxidant properties of soil-growing and wood-growing edible mushrooms. *Journal of Food Processing and Preservation, 42*(1), e13386.

Hajjaj, H., Niederberger, P., & Duboc, P. (2001). Lovastatin biosynthesis by *Aspergillus terreus* in a chemically defined medium. *Applied and Environmental Microbiology, 67*(6), 2596–2602.

Halliwell, B., Cheah, I. K., & Tang, R. M. Y. (2018). Ergothioneine – a diet-derived antioxidant with therapeutic potential. *FEBS Letters, 592*(20), 3357–3366.

Heleno, S. A., Martins, A., Queiroz, M. J. R. P., & Ferreira, I. C. F. R. (2015). Bioactivity of phenolic acids: Metabolites versus parent compounds: A review. *Food Chemistry, 173*, 501–513.

Huang, G., Cai, W., & Xu, B. (2017). Vitamin D_2, ergosterol, and vitamin B_2 content in commercially dried mushrooms marketed in China and increased vitamin D_2 content following UV-C irradiation. *International Journal for Vitamin and Nutrition Research, 87*(5-6), 1–10.

Kała, K., Kryczyk-Poprawa, A., Rzewińska, A., & Muszyńska, B. (2020). Fruiting bodies of selected edible mushrooms as a potential source of lovastatin. *European Food Research and Technology, 246*(4), 713–722.

Kalaras, M. D., Richie, J. P., Calcagnotto, A., & Beelman, R. B. (2017). Mushrooms: A rich source of the antioxidants ergothioneine and glutathione. *Food Chemistry, 233*, 429–433.

Kalogeropoulos, N., Yanni, A. E., Koutrotsios, G., & Aloupi, M. (2013). Bioactive microconstituents and antioxidant properties of wild edible mushrooms from the island of Lesvos, Greece. *Food and Chemical Toxicology, 55*, 378–385.

Koutrotsios, G., Kalogeropoulos, N., Kaliora, A. C., & Zervakis, G. I. (2018). Toward an increased functionality in oyster (*Pleurotus*) mushrooms produced on grape marc or olive mill wastes serving as sources of bioactive compounds. *Journal of Agricultural and Food Chemistry, 66*(24), 5971–5983.

Koutrotsios, G., Kalogeropoulos, N., Stathopoulos, P., Kaliora, A. C., & Zervakis, G. I. (2017). Bioactive compounds and antioxidant activity exhibit high intraspecific variability in *Pleurotus ostreatus* mushrooms and correlate well with cultivation performance parameters. *World Journal of Microbiology and Biotechnology, 33*(5), 98.

Koutrotsios, G., Larou, E., Mountzouris, K. C., & Zervakis, G. I. (2016). Detoxification of olive mill wastewater and bioconversion of olive crop residues into high-value-added biomass by the choice edible mushroom *Hericium erinaceus*. *Applied Biochemistry and Biotechnology, 180*(2), 195–209.

Koutrotsios, G., Mountzouris, K. C., Chatzipavlidis, I., & Zervakis, G. I. (2014). Bioconversion of lignocellulosic residues by *Agrocybe cylindracea* and *Pleurotus ostreatus* mushroom fungi–Assessment of their effect on the final product and spent substrate properties. *Food Chemistry, 161*, 127–135.

Krakowska, A., Zięba, P., Włodarczyk, A., Kała, K., Sułkowska-Ziaja, K., Bernaś, E., … Muszyńska, B. (2020). Selected edible medicinal mushrooms from *Pleurotus* genus as an answer for human civilization diseases. *Food Chemistry, 327*, 127084. https://doi.org/10.1016/j.foodchem.2020.127084.

Kulshreshtha, S., Mathur, N., Bhatnagar, P., & Kulshreshtha, S. (2013). Cultivation of *Pleurotus citrinopileatus* on handmade paper and cardboard industrial wastes. *Industrial Crops and Products, 41*, 340–346.

Lee, Y. L., Huang, G. W., Liang, Z. C., & Mau, J. L. (2007). Antioxidant properties of three extracts from *Pleurotus citrinopileatus*. *LWT-Food Science and Technology, 40*(5), 823–833.

Liang, Z. C., Wu, C. Y., Shieh, Z. L., & Cheng, S. L. (2009). Utilization of grass plants for cultivation of *Pleurotus citrinopileatus*. *International Biodeterioration & Biodegradation, 63*(4), 509–514.

Lin, S. Y., Chen, Y. K., Yu, H. T., Barseghyan, G. S., Asatiani, M. D., Wasser, S. P., & Mau, J. L. (2013). Comparative study of contents of several bioactive components in fruiting bodies and mycelia of culinary-medicinal mushrooms. *International Journal of Medicinal Mushrooms, 15*(3), 315–323.

Lin, S. Y., Chien, S. C., Wang, S. Y., & Mau, J. L. (2016). Nonvolatile taste components and antioxidant properties of fruiting body and mycelium with high ergothioneine content from the culinary-medicinal golden oyster mushroom *Pleurotus citrinopileatus* (Agaricomycetes). *International Journal of Medicinal Mushrooms, 18*(8), 689–698.

Movasaghi, Z., Rehman, S., & ur Rehman, D. I. (2008). Fourier transform infrared (FTIR) spectroscopy of biological tissues. *Applied Spectroscopy Reviews, 43*(2), 134–179.

Phillips, K. M., Ruggio, D. M., Horst, R. L., Minor, B., Simon, R. R., Feeney, M. J., … Haytowitz, D. B. (2011). Vitamin D and sterol composition of 10 types of mushrooms from retail suppliers in the United States. *Journal of Agricultural and Food Chemistry, 59*(14), 7841–7853.

Prandi, B., Faccini, A., Lambertini, F., Bencivenni, M., Jorba, M., Van Droogenbroek, B., … Sforza, S. (2019). Food wastes from agrifood industry as possible sources of proteins: A detailed molecular view on the composition of the nitrogen fraction, amino acid profile and racemisation degree of 39 food waste streams. *Food Chemistry, 286*, 567–575.

Reis, F. S., Martins, A., Barros, L., & Ferreira, I. C. F. R. (2012). Antioxidant properties and phenolic profile of the most widely appreciated cultivated mushrooms: A comparative study between in vivo and in vitro samples. *Food and Chemical Toxicology, 50*(5), 1201–1207.

Rodriguez Estrada, A. E., Lee, H.-J., Beelman, R. B., Jimenez-Gasco, M. D. M., & Royse, D. J. (2009). Enhancement of the antioxidants ergothioneine and selenium in *Pleurotus eryngii* var. *eryngii* basidiomata through cultural practices. *World Journal of Microbiology and Biotechnology, 25*(9), 1597–1607.

Royse, D.J., Baars, J., Tan, Q. (2017). Current overview of mushroom production in the world. In Edible and Medicinal Mushrooms: Technology and Applications, pp. 5-13. Diego, C.Z., Pardo-Giménez, A., Eds. John Wiley & Sons Ltd. 10.1002/9781119149446.ch2.

Sapozhnikova, Y., Byrdwell, W. C., Lobato, A., & Romig, B. (2014). Effects of UV-B radiation levels on concentrations of phytosterols, ergothioneine, and polyphenolic compounds in mushroom powders used as dietary supplements. *Journal of Agricultural and Food Chemistry, 62*(14), 3034–3042.

Sari, M., Prange, A., Lelley, J. I., & Hambitzer, R. (2017). Screening of beta-glucan contents in commercially cultivated and wild growing mushrooms. *Food Chemistry, 216*, 45–51.

Shashirekha, M. N., Rajarathnam, S., & Bano, Z. (2005). Effects of supplementing rice straw growth substrate with cotton seeds on the analytical characteristics of the mushroom, *Pleurotus florida* (Block & Tsao). *Food Chemistry, 92*(2), 255–259.

Socrates, G. (2001). *Infrared and Raman characteristic group frequencies: Tables and charts* (3rd/Ed.). Chichester, England: John Wiley & Sons Ltd.

Tagkouli, D., Kaliora, A., Bekiaris, G., Koutrotsios, G., Christea, M., Zervakis, G. I., & Kalogeropoulos, N. (2020). Free amino acids in three *Pleurotus* species cultivated on agricultural and agro-industrial by-products. *Molecules, 25*(17), 4015.

Tsiantas, K., Tsiaka, T., Koutrotsios, G., Siapi, E., Zervakis, G. I., Kalogeropoulos, N., & Zoumpoulakis, P. (2021). On the identification and quantification of ergothioneine and lovastatin in various mushroom species: assets and challenges of different analytical approaches. *Molecules, 26*, 1832. https://doi.org/10.3390/molecules26071832.

Vaz, J. A., Barros, L., Martins, A., Morais, J. S., Vasconcelos, M. H., & Ferreira, I. C. F. R. (2011). Phenolic profile of seventeen Portuguese wild mushrooms. *LWT – Food Science and Technology, 44*(1), 343–346.

Zervakis, G. I., Koutrotsios, G. & Katsaris, P. (2013). Composted versus raw olive mill waste as substrates for the production of medicinal mushrooms: an assessment of selected cultivation and quality parameters. BioMed Research International, 2013, Article ID 546830.

Zhang, Y., Venkitasamy, C., Pan, Z., & Wang, W. (2013). Recent developments on umami ingredients of edible mushrooms – A review. *Trends in Food Science and Technology, 33*(2), 78–92.

International Journal of
Molecular Sciences

MDPI

Review

Effects of Non-Polar Dietary and Endogenous Lipids on Gut Microbiota Alterations: The Role of Lipidomics

Konstantinos Tsiantas [1], Spyridon J. Konteles [1], Eftichia Kritsi [1], Vassilia J. Sinanoglou [1], Thalia Tsiaka [1,2,*] and Panagiotis Zoumpoulakis [1,2,*]

[1] Department of Food Science and Technology, University of West Attica, Ag. Spyridonos, 12243 Egaleo, Greece; ktsiantas@uniwa.gr (K.T.); skonteles@uniwa.gr (S.J.K.); ekritsi@uniwa.gr (E.K.); vsina@uniwa.gr (V.J.S.)
[2] Institute of Chemical Biology, National Hellenic Research Foundation, 48, Vas. Constantinou Ave., 11635 Athens, Greece
* Correspondence: tsiakath@uniwa.gr (T.T.); pzoump@uniwa.gr (P.Z.)

Abstract: Advances in sequencing technologies over the past 15 years have led to a substantially greater appreciation of the importance of the gut microbiome to the health of the host. Recent outcomes indicate that aspects of nutrition, especially lipids (exogenous or endogenous), can influence the gut microbiota composition and consequently, play an important role in the metabolic health of the host. Thus, there is an increasing interest in applying holistic analytical approaches, such as lipidomics, metabolomics, (meta)transcriptomics, (meta)genomics, and (meta)proteomics, to thoroughly study the gut microbiota and any possible interplay with nutritional or endogenous components. This review firstly summarizes the general background regarding the interactions between important non-polar dietary (i.e., sterols, fat-soluble vitamins, and carotenoids) or amphoteric endogenous (i.e., eicosanoids, endocannabinoids-eCBs, and specialized pro-resolving mediators-SPMs) lipids and gut microbiota. In the second stage, through the evaluation of a vast number of dietary clinical interventions, a comprehensive effort is made to highlight the role of the above lipid categories on gut microbiota and vice versa. In addition, the present status of lipidomics in current clinical interventions as well as their strengths and limitations are also presented. Indisputably, dietary lipids and most phytochemicals, such as sterols and carotenoids, can play an important role on the development of medical foods or nutraceuticals, as they exert prebiotic-like effects. On the other hand, endogenous lipids can be considered either prognostic indicators of symbiosis or dysbiosis or even play a role as specialized mediators through dietary interventions, which seem to be regulated by gut microbiota.

Keywords: nutrition; gut microbiota; phytosterols; fat-soluble vitamins; carotenoids; eicosanoids; endocannabinoids; lipid mediators; lipidomics

Citation: Tsiantas, K.; Konteles, S.J.; Kritsi, E.; Sinanoglou, V.J.; Tsiaka, T.; Zoumpoulakis, P. Effects of Non-Polar Dietary and Endogenous Lipids on Gut Microbiota Alterations: The Role of Lipidomics. *Int. J. Mol. Sci.* **2022**, *23*, 4070. https://doi.org/10.3390/ijms23084070

Academic Editors: Francesco Asnicar and Serena Manara

Received: 23 January 2022
Accepted: 31 March 2022
Published: 7 April 2022

1. Introduction

Currently, more and more researchers are embracing the view that microbes are equally as important for the human body as cells. Among the systems that harbor microbes, the gut comprises the densest populated microenvironment, consisting of more than 3.8×10^{13} microorganisms [1], while the collected genetic material of all gut microorganisms constitutes the gut microbiome (GM). In addition, the human diet contains compounds (i.e., carotenoids, polyphenols, and dietary fibers), that are not digested by human enzymes, reaching the gut intact, where they are further catabolized by the microbiome, resulting in the production of unique metabolites. Interestingly, these gut-produced metabolites, along with the host's other metabolites, shape the metabolic signature of the host, which can be mapped through the analyses of various biological fluids, such as urine, plasma, and feces. Taking into account the complexity of the GI tract, it is quite apparent that it is almost impossible to identify or quantify all the metabolites present in a biological

sample. To date, state-of-the-art technological platforms (i.e., metabolomics, metagenomics, and transcriptomics) can be used in order to monitor and describe the unique and highly dynamic metabolic processes or pathways that occur in the human gut. Moreover, the implementation of -omics approaches enable the detection of a wide spectrum of different metabolites in various tissues [2,3].

One of the most important factors shaping the composition and, consequently, the properties of the intestinal microbiome is dietary lipids [4]. For instance, high-fat diets are suspected to play a role in the promotion of gut dysbiosis, which is defined as the imbalance of microbial populations in favor of pathogenic communities, while several dietary lipids (i.e., phytosterols and carotenoids) may reverse these effects [5,6]. Lipids are organic bio-molecules, which play a variety of important biological roles, such as energy saving, maintaining the integrity of membranes, and transporting and degrading other compounds. The term "lipidome" refers to (a) either the lipids originating from anabolic and catabolic pathways (endogenous lipids) or (b) the uptake of exogenous lipids through diet (dietary lipids), while "lipidomics" is a term used to present the current analytical framework applied in order to explain alterations that involve the lipidome [7].

Lipidomics provides new approaches to screen the metabolic pathways of lipids and therefore helps to understand lipid metabolism and its role in health and disease through the detection of lipid metabolites or other nutritional biomarkers [2,8]. In addition, considering the significant impact of diet in lipid metabolism, clinical lipidomics is a new integrative biomedicine field focused on the combination of lipid science with clinical medicine and nutrition [9]. This type of lipidomics is considered to be the answer to why certain types of diets, foods or even nutrients promote or inhibit the development of various gut-related diseases.

Application-wise, the combination of -omics techniques with high-throughput lipidomics can maximize their potential by developing tools which will help to achieve the desired comprehensive lipid analysis. However, it is essential to overcome specific limitations that may arise during experimental design or analysis. For example, the isomeric diversity of specific lipids (mostly fatty acids) as well as the differences between mass spectrometer ion sources need to be addressed in order to allow lipidomics to rapidly progress [10]. In addition, the lack of corresponding internal standards can be a real setback and may lead to quantitative inaccuracies due to the high sample complexity [11]. This is why an integrated, multifocal lipidomics platform must be very carefully designed in order to provide useful, reliable, and reproducible results and to extract as much information as possible. For that reason, targeted (determination of specific compounds) and untargeted (holistic) approaches, using GC/LC-MS^2 techniques, are combined in metabolomics studies [10]. Regarding endogenous lipids, a new analytical field, known as lipid mediator (LM) metabolomics or metabololipidomics, is gaining ground. The expansion and implementation of this promising field will: (a) shed light on the pathways (biosynthesis or a biological role in inflammation) of bioactive lipids, suggesting novel pre-resolving mechanisms by which the host responds during inflammation, tissue damage, or the disturbance of homeostasis (gut dysbiosis) [12], (b) establish a benchmark for novel active resolution pharmacology approaches to control or even treat gut-related diseases, and (c) allow the direct correlation and assessment of the personalized metabolome with medicine and nutrition without the need for conjectures.

Despite the conflicting views that prevailed for years, lipids are now classified into eight major groups (1: fatty acyls-FA, 2: Glycerolipids-GL, 3: glycerophospholipids-GP, 4: sphingolipids-SP, 5: sterol lipids-ST, 6: prenol lipids-PR, 7: saccharolipids-SL, and 8: polyketides-PK) and several sub-classes (fatty acids, mono-, di-, or triglycerides, ceramides, isoprenoids, and acrylaminosugars). Assaying the impact of different dietary habits on configuring the intestinal microbial profile, the key role of lipid nutrients in host health management and in disease prevention must be underscored. Due to the Westernization of the human diet [13], researchers have scrutinized the effect of polar lipid intake, mainly fatty acids (i.e., ω-3, ω-6 PUFAs, MUFAs, etc.) and phospholipids, on the modification of

gut microflora and on the maintenance of intestinal immunity and homeostasis [13]. The overall impact of an unhealthy nutritional lifestyle includes the increase in non-commensal (i.e., *Firmicutes* and *Proteobacteria*) bacteria, intestinal barrier dysfunctions, the decrease in gut microbiota diversity and intestinal immunity, the reduction in the mucus layer, the lower levels of bacteria-generated butyrate, and the stimulation of chronic inflammation pathways [14]. On the other hand, the balanced supplementation of phospholipids and the ω-3/ω-6 PUFAs ratio (in favor of the ω-3 fatty acids) increase the abundance of commensal bacteria (i.e., *Bifidobacterium*, *Akkermansia*) and reduce the *Firmicutes*-to-*Bacteroidetes* ratio (F/B ratio) [15], precluding the onset of various non-communicable gut-related disorders [16–29].

However, in this review, only non-polar dietary or amphoteric endogenous lipids were examined (Figure 1). This decision was based: (a) on the already existing huge amount of published data regarding gut-related interactions with more polar lipid categories, such as fatty acids, phospholipids, and short-chain fatty acids or cholesterol, and at the same time (b) on the lack of collective knowledge regarding the interrelationship of the lipids under study, gut microbiota, and host's health state, which underlined the need for further investigation [13,15,30].

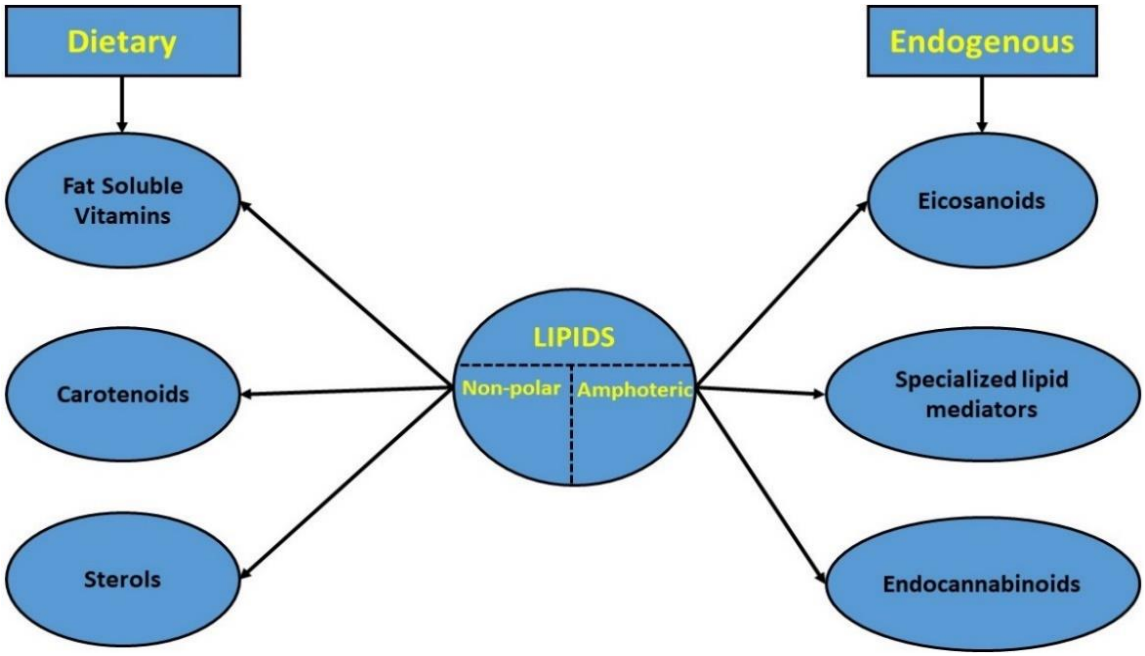

Figure 1. Classification of the studied lipid categories.

In particular, the dietary intake of these lipids could serve as a modulation strategy of gut microbiota functional ecology, to counteract any possible adverse health-related outcomes [30]. Nonetheless, data from both animal models and human interventions are still elusive and the effects of these nutrients are understudied. For example, despite the strong evidence that sterols (in particular phytosterols) affect the intestinal microbiome and the metabolism of the host by regulating microbiota composition (i.e., increase in *Bacteroides*, *Coprococcus*, *Oscillospira*, *Lactobacillus* and *Akkermansia* and decrease in *Desulfovibrio* genus, in a dose-dependent manner in the sterol-fed group), and cholesterol synthesis [31,32], the involved mechanisms and interactions have not been fully elucidated. Additionally, the metabolic fate and the effect on the intestinal microflora (and vice versa) of fat-soluble vitamins (FSVs) is still unclear. Recent findings show that this bidirectional relationship enhances important biological processes that take place in the gut (regulation, activation, and production of FSVs in the gut). In turn, these processes trigger many pivotal FSV-related functions, such as (i) the improvement of intestinal barrier integrity, (ii) the modulation of gut microbiota composition (i.e., increased *Proteobacteria* in the case of a high intake of

vitamin D or increased *Sutterella* in the case of a lower intake of vitamin E), and (iii) the regulation of the immune and inflammatory response [33,34]. The landscape is similar for carotenoids. So far, carotenoids' effect on gut microbiota composition has been investigated through (mainly) animal and human interventions focusing on specific metabolic diseases (i.e., obesity, diabetes type 2, etc.) or on diseases associated with metabolic syndromes, such as nonalcoholic fatty liver disease (NAFLD)).

At the same time, even less is known regarding the interplay between amphoteric endogenous lipids (i.e., eicosanoids, endocannabinoids, and specialized pro-resolving lipid mediators (SPMs)), the gut microbiota, and nutrition patterns. At present, the research interest in such molecules is mainly focused on their ability to act as "mediators" during the manifestation of various inflammatory conditions, related to either the intestine or the various axes where gut microbiota participate (gut–brain, gut–retinal, gut–kidney, and gut–liver). In any case, nutrition remains the most important factor that regulates this bidirectional relationship. Therefore, the employment of high-throughput lipidomics is crucial in order to further investigate the role of endogenous lipids in the pro- and anti-inflammatory pathways, as well as to mark novel prognostic markers of gut function.

Despite the increasing number of publications, the reciprocal relationship between lipids and gut microbiota must be further investigated in order to fill present knowledge gaps. Thus, the aim of the present comprehensive review is to unscramble the interrelation of nutrition and gut microbiome regulation, focusing on the role of non-polar dietary lipid nutrients and endogenous lipids by highlighting the use of lipidomic techniques. In detail, the sub-objectives of the current review are: (a) to review in depth the two-way interactions between dietary and endogenous lipids and the gut microbiota, (b) to evaluate the health impact of phytosterols, carotenoids, and lipophilic vitamins on the micromanagement of gut functional ecology, (c) to underline the use of lipidomics, implemented in several animal and human dietary clinical studies, for the elucidation of specialized biomarkers or endogenous mediators, and (d) to highlight the overall strengths and limitations of the up-to-date clinical studies.

2. Review Methodology

The adopted search strategy adopted and the method of article selection in this review were conducted in accordance with the Preferred Reporting Items for Systematic Reviews (PRISMA) statement (Figure 2). As a first step, the articles were evaluated on the basis of their title and abstract. The initial criteria for rejection or acceptance were defined as the presence or the absence of basic keywords (Figure 2) in the title. As a second step, the full text was also evaluated in terms of similarity to the main objectives of our study. With respect to studies published into 2021, the number of citations was also evaluated. Furthermore, in order to provide a comprehensive framework and remain impartial, four database sources, namely PubMed (Medline), Scopus (Elsevier), Google Scholar, and Frontiers (Health) were used. In addition, the search methodology was further divided into 5 categories according to the main objectives of the review (Figure 2), in which a combination of different keywords (i.e., gut microbiota, gut microbiota and dietary lipids, gut microbiota and (a) sterols, (b) phytosterols, (c) fat soluble vitamins, (d) carotenoids, (e) eicosanoids, (f) endocannabinoids, and (g) lipid mediators, and lipidomics and gut microbiota) and time frames was used, depending on the importance and timeliness of each. More specifically, for well-established scientific views or fundamental definitions, a ten-year time frame was chosen, while for specialized study subjects (i.e., clinical trials, interventions, and meta-analysis studies) a five-year time frame was selected.

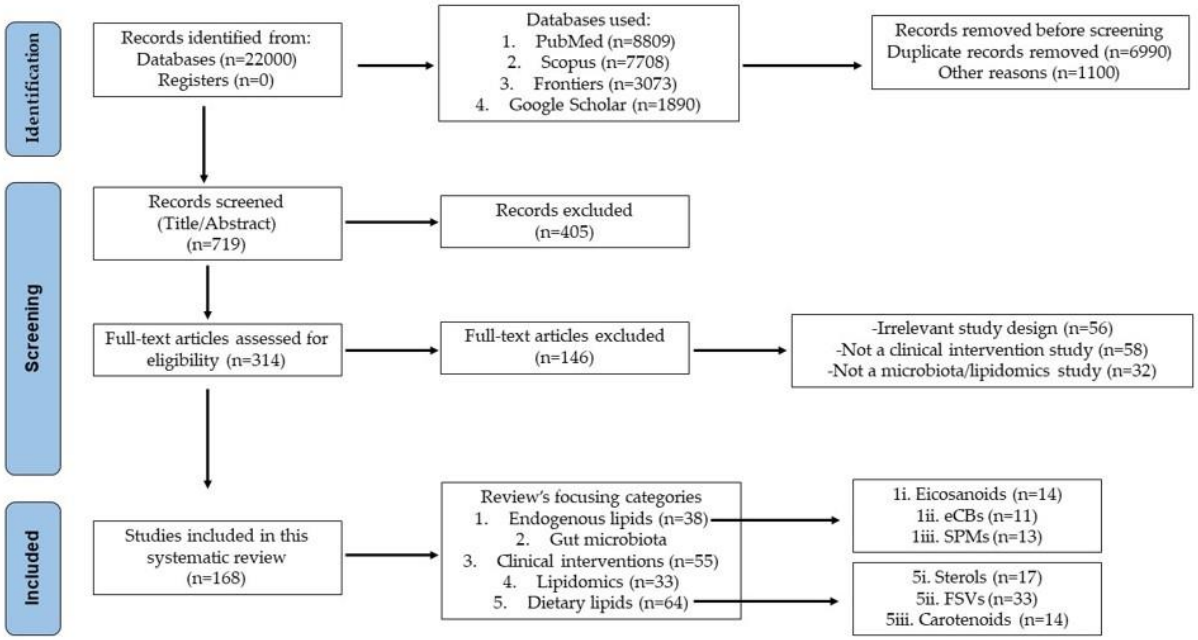

Figure 2. PRISMA flow diagram of the systematic review process.

3. Characteristics of the GI Microbiota

3.1. An Insight into Gut: What We Have Learnt So Far?

Although the definitions of the terms "microbiome" and "microbiota" are clearly different, these terms are commonly used interchangeably [35]. Nowadays, the study of the composition, structure, and functional properties of the human microbiome is a rapidly evolving scientific field. It is worth mentioning that the relationship between commensal bacterial and the host is an extremely dynamic system in which an intricate and mutually beneficial relationship, also known as symbiosis, is established [36]. The importance of this dynamic ecosystem is inextricably linked to various basic primary, as well as secondary functions, including the metabolism, immune system protection, the structural integrity of the epithelial barrier, and gut–brain axis communication [37] (Figure 3).

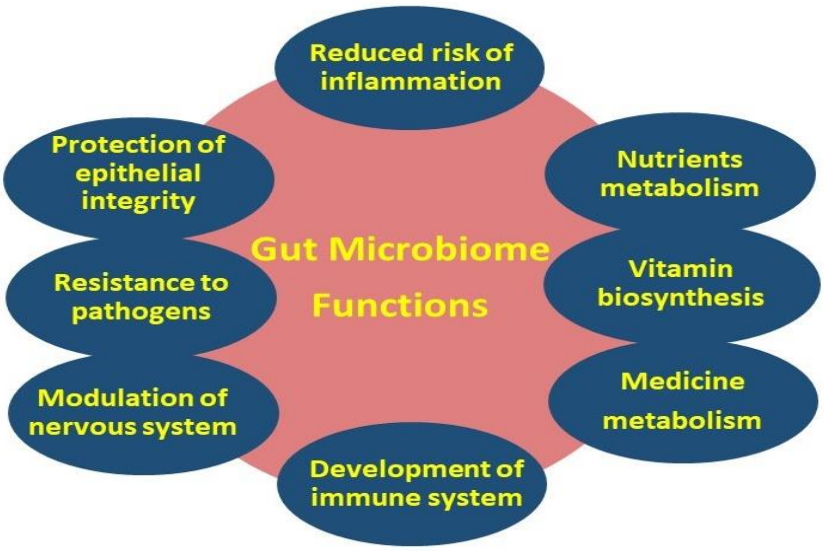

Figure 3. Primary (i.e., metabolism, gut–brain axis, and protection of epithelial integrity) and secondary (i.e., nutrients, vitamin and medicine metabolism, regulation of the immune and nervous systems, and resistance to pathogens) gut microbiome functions.

There is growing evidence that several gut disorders involve not only the GI system but distant organs as well [38]. Through a complex communication that includes the central nervous system as well as the autonomic and the intestinal nervous system, two-way interactions are created which affect both the gut microbiome and the lipids. Moreover, intestinal immune cells as well as the enteric nervous system affect the metabolism, absorption, and distribution of lipids, since they are key regulators of gut homeostasis [39]. Most recent studies link the gut with brain function (gut–brain axis), the host immune response, cell proliferation and vascularization, the regulation of intestinal endocrine functions, the modulation of energy biogenesis, the vitamin biosynthesis, and bile salts metabolism [40–44]. Focusing especially on lipid constituents, the gut–brain axis has the ability to regulate endogenous lipids (i.e., endocannabinoids, and SPMs) making them act "on demand" by exerting various bioactive properties, such as pro- or anti-inflammatory activities on the gut microbiota and immune system.

3.2. Gut Microbiota Stability and Composition: A Key Player in Various Gut-Related Diseases

As already stated, the gut microbiota presents a dynamic equilibrium that has adapted to harmoniously colonize the GI tract (symbiosis) [45]. Alteration in gut microbiota homeostasis can lead to undesirable situations, generally known as dysbiosis and abnormalities in the immune response of the intestinal microbiome. Gut dysbiosis is related to several chronic inflammatory conditions, also known as inflammatory bowel disease (IBD), including ulcerative colitis (UC) and Crohn's Disease (CD). Moreover, various multi-factorial diseases or metabolic disorders (e.g., duodenum cancer, obesity, diabetes, and metabolic and immune-mediated disorders) are linked to microbial imbalances, which are also associated with the intake of lipids and their interactions with certain bacterial populations, highlighting the need to further investigate the underlying mechanisms [46].

Taking into account some unquestionable data regarding the structure, functionality, and anatomy of the GI system, it is widely accepted that the latter is divided into the stomach, small intestine, which is further divided into (a) duodenum, (b) jejunum, and (c) ileum, and large intestine (LI), which includes the colon and cecum. Every "compartment" is characterized by different conditions, such as pH, nutrient availability, or oxygen availability, and thus, each organ promotes the growth of specific microbes. Despite the fact that the gut environment favors the growth of bacteria from seven predominant phyla (e.g., *Firmicutes*, *Bacteroides*, *Actinobacteria*, *Fusobacteria*, *Proteobacteria*, *Verrucomicrobia*, and *Cyanobacteria*), its diversity is limited since more than 85% of the total population is constituted by *Bacteroides* and *Firmicutes* [47]. More specifically, the species of *Bacteroides* and *Firmicutes* phyla belong to the genera (a) *Bacteroides* and *Prevotella* and (b) *Clostridium*, *Eubacterium* and *Ruminococcus*, respectively. The major genus belonging to the phylum *Actinobacteria* in the human gut is *Bifidobacterium*, while *Actinobacteria* contribute to a small fraction of the total bacteria [48]. In Table 1, the different major phyla and bacterial genera that colonize each organ of the GI system are summarized.

However, despite the various bacteria that colonize the GI system, even pathogen microorganisms can be found within it (i.e., *E. coli*, *H. pylori*, *C. jejuni*, *S. enterica*, and *B. fragili*) [54]. Furthermore, the fact that *Firmicutes* and *Bacteroides* are the predominant bacteria should not be considered as an infallible view, since significant differences can be observed in other phyla because of: (a) the current physio-pathological conditions, (b) the age (i.e., the microbiota is enriched during lactation and early years) and (c) the genetic background of the host, (d) the role of nutrition, and (e) geographical factors (i.e., levels of both *Firmicutes* and *Proteobacteria* were higher in European children, while *Firmicutes* were absent in West African children) [55].

Table 1. Bacteria phyla and genera in the GI tract.

Major phyla	Stomach	Duodenum	Jejunum	Ileum	Cecum	Colon	Refs.
Firmicutes	√	√	√	√		√	[49,50]
Bacteroides	√		√	√		√	
Actinobacteria	√	√			√	√	
Fusobacteria	√				√		
Proteobacteria	√			√	√		
Bacterial genera	**Stomach**	**Duodenum**	**Jejunum**	**Ileum**	**Cecum**	**Colon**	**Refs.**
Lactobacillus			√		√		[51,52]
Enterococcus			√	√			
Streptococcus			√	√			
Bacteroides				√			
Bifidobacterium						√	
Actinomycinae				√			
Peptostreptococcus	√						
Prevotella	√						
Veillonella	√						
Rothia	√						
Haemophilus	√						
Mucosa genera	**Stomach**	**Duodenum**	**Jejunum**	**Ileum**	**Cecum**	**Colon**	**Refs.**
Lactobacillus						√	[53]
Akkermansia						√	
Clostridium				√		√	
Enterobacteriaceae		√	√		√	√	

4. Dietary (Exogenous) Non-Polar Lipids

As has already been stated, lipid supplementation through the diet can affect (a) gut microbiota composition, (b) the metabolic end products, (c) other enzymatic indicators (i.e., alkaline phosphate (ALP), aspartate transaminase (AST), alanine transaminase (ALT), and high- or low-density lipoproteins (HDL-LDL)), and thus (d) the fate of gut-related diseases [5,14,48]. In this direction, a thorough review of the literature was conducted in order to evaluate the relationship between the intestinal microbiome and dietary non-polar lipids, such as (phyto)sterols, fat-soluble vitamins, and carotenoids.

4.1. Dietary Sterols: Are They an Inducer of Gut Dysbiosis?

Sterols, similarly to cholesterol, play an important role in the structure, integrity and properties of membranes. Phytosterols, which are plant-derived sterols, are found in abundance in Mediterranean diet models that promote beneficial changes in bacterial communities, while they are not present in a Western diet (high fat and cholesterol) [56]. In total, 20–80% of the cholesterol consumed daily (average recommended intake of 300 mg cholesterol per day) is absorbed, while the microbial absorption of phytosterols is only 2–3% (average intake of phytosterols is less than 500 mg per day) [57,58], which means that non-absorbed sterols can be further processed by the gut microbiome.

In particular, phytosterols are naturally occurring structural analogues of cholesterol, involved in altering certain lipid metabolic pathways. Thus, they are strongly related to the regulation of intestinal ecosystem and to the reduction in high hepatic cholesterol levels, which promotes gut dysbiosis in various liver abnormalities, such as steatosis, cirrhosis,

liver failure, NASH, NAFLD, and hepatocellular carcinoma [59,60]. The manifestation of these pathologies is associated with the depletion of *Bacteroides* and *Bifidobacterium* and the increased richness of *Mucispirillum*, *Desulfovibrio*, *Anaerotruncus*, and *Desulfovibrionaceae*. Updated evidence has confirmed the detrimental effect of dietary cholesterol in microbial populations and in gut bacterial metabolites (taurocholic acid (TCA) and 3-indolepropionic acid (IPA)) [61].

Nonetheless, according to estimations, the dietary intake of PS (150–400 mg phytosterols/day) does not reach the necessary established levels (1500–3100 mg phytosterols/day) in order to exert its hypocholesterolemic effect (and receive the corresponding health claim). Consequently, the above-mentioned levels can only be achieved in the daily diet through PS-enriched foods, such as dairy products (PS-enriched milk, cheese, and fermented milk products). Focusing on in vitro studies, Cuevas-Tena et al. [62] investigated the impact of plant sterol enrichment dose on the gut microbiota of lean and obese subjects using an in vitro fermentation model, also known as TIM-2. In this study, the "PS-enriched" supplement, but also β-sitosterol alone, was able to increase the proportion of the genera belonging to the *Firmicutes* phylum. This increase suggested a potential modification of the short-chain fatty acids (SCFAs) and of the microbial profile of both lean and obese populations. However, the authors suggest that the daily intake of PS over several weeks and the different fecal inocula may lead to different effects on gut microbiota composition. One year earlier, the same research team revealed that the presence of PS during batch-culture fermentation led to a decrease in *Erysipelotrichaceae* species and an increment in *Eubacterium hallii* [63].

Meanwhile, another in vitro dynamic model was used in order to examine the impact of plant-sterol- and galactooligosaccharide-enriched beverages on colonic metabolism and composition [64]. According to the authors, a higher diversity in the gut microbiome was found in the transverse and descending colon, where the production of sterol metabolites (coprostanol, methylcoprostanol, and sitostenone) also took place. In addition, despite the fact that the prebiotic effect of galactooligosaccharides was not detected, alterations in gut microbiota (an increase in the *Parabacteroides* genus and the *Synergistaceae* and *Lachnospiraceae* families) denoted an enhancement of sterol metabolism.

Furthermore, recent in vitro and in vivo studies confirmed that phytosterols, mainly β-sitosterol and stigmasterol, promoted gut symbiosis in cases of morbid obesity and hypercholesterolemia, by reducing the levels of the bacterial family *Erysipelotrichaceae* [65]. The supplementation of β-sitosterol in ruminants (sheep) lowered the abundance of the family *Lachnospiraceae* and increased the proportion of the genera *Prevotella* (*Bacteroidetes* phylum), presumably through the consequent increase in ruminal pH incited by the enrichment of the genus *Selenomonas* [66]. Although high-fat diets shift the F/B ratio toward the *Firmicutes* phylum in hamster models, plant sterols (i.e., soybean sterols) significantly attenuated this imbalance and improved gut microbiota diversity and richness of bacterial microenvironment (increase in *Bacteroides*, *Coprococcus*, *Oscillospira*, *Lactobacillus*, *Coprobacillus*, *Akkermansia*, and *Allobaculum* genera levels). The increased populations of these genera may present alleviating effects against high-fat-diet-related diseases, such as hypercholesterolemia and dyslipidemia [31,67].

Further intervention studies highlighted the potential modulating activity not only of free phytosterols, but also of their esters and their fully saturated derivatives, known as phytostanols. Namely, the relative abundance of *Anaerostipes* and *Bacteroidetes* species was increased in a high-dose diet of phytosterol esters (i.e., steryl esters). Phytosterol esters' regulatory action was intertwined, via bile acid metabolism, with hepatic steatosis prevention in adult participants [68]. Sitostanol also increased the levels of *Bacteroidetes* communities, while campestanol uptake reduced the quantity of SCFA butyrate, produced by *Firmicutes* species in human clinical studies [5,68,69]. Apart from being dietary derivatives of phytosterols, 5α/β stanols (coprostanol, cholestenol, 5α/β-sitostanol, 5α/β-campestanol), detected in human feces, can also be gut-produced metabolites of sterols and, thus, potential biomarkers of bacterial metabolism [70].

In summary, although the exact associations of (phyto)sterols and the intestinal microbiome are still under study, there is enough evidence showing that these compounds are excellent regulators of cholesterol and potential modifiers of the gut microbiota composition. At the same time, even though the body of evidence regarding the impact of phytosterols on gut microbiota alterations and on diet-induced health or disease conditions is growing, there are a limited number of well-designed and controlled human studies. Since the current knowledge concerning the use of phytosterols as new therapeutic targets remains quite an unexplored domain, further focus is required to classify phytosterols as phyto-therapeutics in the foreseeable future [5,65].

4.2. Fat-Soluble Vitamins (FSVs): The Master Player in Nutrition–Gut Microbiome Tug-of-War

According to an increasingly large body of clinical findings, malnutrition, especially the low supply of non-energy-delivering micronutrients, such as vitamins, is negatively affecting the configuration of gut microbiota diversity and the intestinal health. Vitamin deficiency plays an important role in the pathogenesis of several diseases, namely neuropsychiatric disorders (depression, autism, Parkinson disease, schizophrenia, and multiple sclerosis), cardiometabolic disorders, complications of lipid metabolism (metabolic syndrome, obesity, and hepatic disease), and child development impairments in different age groups [14,71,72]. Of note, vitamins also manipulate the communities of the microecosystems of mothers during pregnancy and of their offspring, both postpartum and during early childhood. For instance, vitamin D and retinol favor the growth of *Actinobacteria* and *Proteobacteria*, while vitamin E depleted them (mainly *Proteobacteria*) [73]. To date, mostly water-soluble vitamins (primarily those of B-group) have been in the spotlight of extensive research. However, many questions are left to be answered regarding the links between the intake or deficiency of fat-soluble vitamins, the resulting modification of the gut microbial ecosystem, and the contingent manifestation of various pathologies.

The Mediterranean diet is recommended as the ideal nutritional pattern in order to cope with the lack of FSVs, which are present in food items, such as vegetables, fruits, nuts, olive oil, dairy products, and fishes. The mutualistic interaction between vitamin uptake and gut microbiota composition is outlined with two different, yet firmly interrelated notions: (a) the impact of vitamins on shaping the microbial profile of pathogenic and nonpathogenic bacteria and (b) the role of microbiota in the synthesis, shuttling, and metabolism of vitamins and their metabolites [72]. Based on a brief overview of the impact of FSVs on microbial populations and health status control, the current data are quite controversial. On one hand, the administration of vitamins D, A, and K favored the prevalence of *Lactobacillus*. Nonetheless, in some cases, the intake of FSVs led to the increase of opportunistic pathogens or the depletion of synergistic bacteria belonging to several bacterial categories, such as *Proteobacteria*, *Deferribacteres*, *Enterobacteriacae*, *Clostridiaceae*, *Ruminococcus*, and *Odoribacter*, or *Verrucomicrobia*, *Bifidobacterium*, and symbiotic *Bacteroidetes*, respectively [14].

4.2.1. Vitamin A

Vitamin A (retinol) and its enzymatic oxidation product (retinoic acid) play a key role in the intestinal immune response through interactions with the intestinal microbiome [74]. A sheep model confirmed the potential of vitamin A as a putative diagnostic indicator for male infertility. The abnormalities in its absorption were linked to the deregulation of bile acid metabolism, which is related to lower levels of *Ruminococcaceae* [75]. The inclusion of vitamin A in obesogenic diet patterns in three-week-old male C57BL/6J mice precluded changes in microbiota α-diversity and enriched the abundance of *Lachnospiraceae* [76]. Another study, targeting the investigation of gut microbiota alterations at different lifetime points, demonstrated that vitamin A insufficiency played a pivotal role in the embryonic but also in the early-stage development of four-week-old healthy rats. Especially in the periods of gestation, lactation, and weaning, the populations of *Diaphorobacter* and *Psychrobacter* (increase) or *Propionibacterium*, *Ochrobactrum*, *Enterobacter*, and *Staphylococcus*

(increase) were affected. The effect of vitamin A was imprinted in the serum metabolome by the presence of retinol, which presented a positive and a negative correlation with *Faecalibacterium* and *Staphylococcus*, respectively [77].

4.2.2. Vitamin E

Vitamin E is considered a group of fat-soluble compounds and includes two main sub-categories: (a) α-, β-, γ-, and δ-tocopherols (TOHs) and (b) α-, β-, γ-, and δ-tocotrienols (T3), which are mainly presented in edible oils and several nuts [78]. Among these, a-tocopherol is one of the most important fat-soluble antioxidants of cellular membranes as it is the most biologically active form retrieved from human tissues. Additionally, it accounts for approximately 90% of the total vitamin E of the body [79].

In an experimental model, where five-week-old C57BL/6 male mice followed a high- and low-vitamin E diet, the phyla *Bacteroidetes* and *Verrucomicrobia* (*Akkermansia muciniphila* species) were related to lower body weight. More specifically, a dose-dependent relationship was highlighted between α-tocopherol and different gut microbial compositions, as the authors observed an increase in *Proteobacteria* and a decrease in *Verrucomicrobias* phylum [80]. Another study revealed that α-tocopherol supplementation was associated with changes in gut microbiota composition. Particularly, it was shown that a-tocopherol can reduce levels of *Bacteroides* and *Lactobacillaceae*, as well as the F/B ratio in humans [81]. δ-Tocotrienol, and its hydrogenated metabolite present in human feces, δTE-13′-carboxychromanol, can be considered as starting points against tumor growth [82]. Although they showed no significant effect on bacterial richness, they exhibited a modulating role in gut microbiota composition, by promoting the increase in health-promoting *Lactococcus* and *Bacteroides*. Focusing on δTE-13′-carboxychromanol, this tocotrienol metabolite counterbalanced the reduction in *Roseburia* in IBD patients and uniquely facilitated the elevation of *Eubacterium coprostanoloi* gene levels [82].

4.2.3. Vitamin K

Vitamin K consists of vitamin K1 (phylloquinone, PKs) and vitamin K2 (menaquinone, MKs). Vitamin K1 is a naturally occurring compound in green leafy vegetables, as it is directly related to photosynthesis, while vitamin K2 is found in animal products. Apart from their intake through diet, menaquinones (MKs) are also bacterial products of vitamin K, able to be remodeled in vivo. As proved by certain studies, vitamin K deficiency mostly affects female microbial composition with increased levels of *Lachnospiraceae* and *Ruminococcaceae* families [83]. A metagenomic analysis of the gut microbiota profiles of healthy volunteers and type 2 diabetes mellitus patients underlined the vital role of the phyla *Actinobacteria*, *Bacteroidetes*, and *Firmicutes*, mainly the *Erysipelotrichaceae* and *Corynebacterium* taxa, in the metabolic functionality of the diabetic gut microbiome related to the production of menaquinones [84]. According to the results of the aforementioned study, vitamin K2 emerged as a novel biomarker in the treatment of diabetes mellitus, also exerting other beneficial activities, such as enabling insoluble fiber digestion and refining immunomodulatory and nutritive molecules, such as SCFAs. Notably, MKs play a key role in gut microbiota homeostasis, promoting the growth of symbiotic bacteria. MK-7, one of the most studied vitamin K-related compounds, was reported to have protective effects against colon cancer during a study in male C57BL/6J mice [85]. In particular, the authors noticed a reduction in bacterial species promoting colorectal cancer, such as *Helicobacter apodemus*, *Helicobacter mesocricetorum*, *Allobaculum stercoricanis*, and *Adlercreutzia equolifaciens*.

4.2.4. Vitamin D

Despite the well-known contribution of vitamin D to calcium homeostasis and bone health [86], the forms of this vitamin (calcitriol, cholecalciferol-vit-D3, and ergocalciferol-vit-D2) also participate in the regulation of: (a) blood pressure, (b) inflammation, (c) immune response, and, most recently, (d) gut microbiota [87–90]. Unlike vitamins A, E, and K, which were supplemented mainly in animal studies, vitamin D has a leading role, among

lipid-soluble vitamins, in human clinical interventions. The aligned data in the literature provide a comprehensive insight into the crosstalk of the gut microbiota and vitamin D, primarily concerning the downregulation of inflammatory pathways. Though the effect of the gut microbiota signature on vitamin D metabolism is relatively established knowledge, the impact of vitamin D on gut microbial populations is still quite an uncharted field [91].

The administration of vitamin D in Crohn's disease patients in remission positively affected bacterial taxa and the abundance of *Megasphaera* and *Lactobacillus*. However, no changes were observed in the gut microbiota diversity of ulcerative colitis (UC) patients, despite the major increase in *Enterobacteriaceae* [92]. Oral supplementation of vitamin D3 in a study including twenty adults resulted in a dose-dependent increase in serum D3 metabolite, 25-hydroxyvitamin D [25(OH)D]. Consequently, this led to the enrichment of *Bacteroides* and *Parabacteroides* abundance, which was associated with the alleviation of IBD symptoms [93]. However, seasonal sunshine variability (winter vs. summer) is responsible for the fluctuations in the levels of circulating 25-hydroxyvitamin D in IBD patients. Thus, a cohort study that evaluated the effect of seasons on the relationship between vitamin D levels and gut microbiota, covarying in intestinal metabolic derangements, suggested that higher levels of sunshine reduced pathogenic genera, such as *Fusobacterium*, *Collinsella aerofaciens*, *Eggerthella lenta*, *Bacteroides*, *Helicobacter*, *Faecalibacterium prausnitzii*, and *Rhodococcus*, *a*nd increased species of *Pediococcus*, *Clostridium*, and *Escherichia/Shigella* [94]. *Faecalibacterium* and *Akkermansia* species, which were increased after D3 intake, also influenced the immune responses and health status in autoimmune intestinal pathologies, such as UC syndromes [92].

As proved in in vivo studies (three-week-old male C57/bl6 mice) related to the microbiota–pain interrelationship, suboptimal levels of vitamin D resulted in a restricted microbial diversity and in an increase in F/B ratio [95]. A multi-vitamin dietary supplement, including vitamin D and vitamin B, was administrated in overweight individuals. Shifts were observed in one phylum (*Actinobacteria* decrease) and three families (*Actinomycetaceae*, *Bifidobacteriaceae*, and *Corynebacteriaceae* decrease) after vitamin D supplementation, and in three phyla (*Bacteroidetes* increase, *Cyanobacteria* and *Proteobacteria* decrease) and three families (*Christensenellaceae*, *Lachnospiraceae*, and *Enterobacteriaceae* decrease) after a combined vitamin D and B supplementation [96]. A cirrhotic rat model suggested that calcitriol, the active form of vitamin D3, controlled bacterial translocation and gut permeability and enriched the populations of *Bacteroidales*, *Allobaculum*, *Ruminococcaceae*, *Muribaculaceae*, and *Anaerovorax* [97]. Recent studies in NAFLD subjects verified the impact of vitamin D in the delay of cell death caused by inflammation, through the remodeling of the relative bacterial abundances in favor of *Lactobacillus* and against *Acetatifactor*, *Oscillibacter*, *and Flavonifractor* [98].

Based on official guidelines, vitamin D is an essential nutrient in pre- and post-natal maternal diet and infant formulas, as the infant microbiome is rapidly evolving and altering up till early childhood years. According to the results of the CHILD (Canadian Healthy Infant Longitudinal Development) cohort study, the supplementation of vitamin D to both formula-fed and exclusively or partially breastfed infants negatively affected the concentrations of the *Megamonas* genus. In the group of exclusive breastfeeding, a diet rich in vitamin D during pregnancy was related to higher populations of *Haemophilus* and lower populations of *Bilophila* and *Lachnospiraceae*, while no compositional changes in the gut microbiota of partially breastfed or formula-fed infants were observed. Even though vitamin D supplementation of the mother or infant was not directly linked to Clostridioides difficile colonization, the maternal intake of vitamin-D-fortified milk minimized the risk of *C. difficile* colonization in infants [99]. Aligned data from the current literature highlight the importance of the feeding regimen in the foundation and constitution of the gut ecosystem in infants. The additional supplementation of vitamin D in the breastfed group stimulated the farming of *Bifidobacterium*, which are known to act as probiotics. On the contrary, no significant differences were noted in the gut taxonomy of formula-fed infants with or without vitamin D supplementation [100].

Additionally, the lack of vitamin D, which induced the abundance of *Erysipelotrichaceae* and *Veillonellaceae*, is the most common marker in the cases of osteoporosis in postmenopausal women. Nonetheless, it was intriguing that the presence of vitamin D in serum disclosed a negative correlation with *Enterobacteriaceae* and *Erwinia*. In addition, higher concentrations of vitamin D were affiliated with the amino acid metabolism, particularly with higher levels of the metabolites alanine, proline, tyrosine, valine, and leucine [101]. While the focus of current dietary interventions concerns chronic disease cases, little is known about the gut-regulated individualized responsiveness of healthy female subjects to vitamin D intake. The fact that the deficiency of vitamin D can be responsible for fragile bone health is a common observation. According to studies related to the effect of vitamin D on women, the dominating commensal phylum *Bacteroidetes* and taxa *Akkermansia* and *Bifidobacterium* were more abundant after vitamin D supplementation. Moreover, the variations in the gut microbiota diversity of bacterial genera were more prominent in the group of individuals who responded to vitamin D supplements than in the non-responders group, where the concentrations of *Bacteroides acidifaciens* were decreased [102].

Furthermore, several studies pointed out that the administration of FSVs, in total, yielded beneficial outcomes with regard to the state of the health of neuropsychiatric patients, by orchestrating the balance between bad and good microbes, through their biosynthesis and their interaction with gut microbiota [71]. Based on the results of a pilot study in an older Australian population, all vitamins (hydrophilic and lipophilic) are colon-delivered micronutrients, which instigate modifications in (a) the phyla of *Actinobacteria* (increase with vitamin A) and *Bacteroidetes* (reduction with vitamin D3), (b) the families of *Coriobacteriaceae* (increase with vitamin A), *Ruminococcaceae*, *Peptostreptococcacea* (increase with vitamin D3), and *Desulfovibrionaceae* (slight decrease with vitamin D3), (c) the genera of *Collinsella*, species *aerofaciens* (slight increase with vitamin A and D3) and *Bilophila* (slight decrease with D3), and (d) the species *Collinsella aerofaciens* (slight increase with vitamin E) and *Eubacterium hallii*, *Coprococcus comes*, and *Dorea longicatena* (increase with vitamin D3) [103].

In light of the dietary interventions under review, FSVs are wielded in the manipulation and restoration of gut microbiota, compared with the other two non-polar nutrients included in the present review. Nonetheless, the elucidation of the reciprocal interactions between lipid-soluble micronutrients and the gut microenvironment merits further research, in order to entrench specific guidelines for FSV supplementation and implementation in novel therapeutic strategies.

4.3. Carotenoids: Can They Balance Diet–Gut Microbiota Crosstalk?

Carotenoids, an important subgroup of terpenoids, are minor dietary phytochemicals present in red fruits or vegetables (orange, peaches, tomatoes, carrots, pumpkins, and peppers) and in green leafy vegetables (broccoli, spinach, and kale). These natural pigments are divided into two major groups: (a) xanthophylls, such as lutein, zeaxanthin, astaxanthin, etc., which contain >1 oxygen atom, and (b) carotenes, such as α-carotene and β-carotene, which contain no oxygen atoms and are the major precursors of vitamin A. Clinical trials have shown that carotenoids in low levels demonstrate beneficial effects, while overdoses are toxic [104]. However, carotenoids can protect against age-related eye diseases, metabolic syndromes, cardiovascular diseases, diabetes, inflammation, and, most recently proven, body composition changes [105–107]. Interestingly, carotenoids cannot be synthesized by the human body and thus can only be obtained through the diet. As fat-soluble compounds, carotenoid bioavailability is considered low (10–40%). However, their lipophilicity renders their absorption by the GI tract more efficient compared with that of hydrophilic molecules. Despite the accumulated data dealing with the interplay of the gut microbiome and other lipid dietary constituents, the bidirectional relationship between gut microbiota populations and carotenoids is as of yet poorly understood. There is no solid evidence concerning the impact of microbiota (a) on carotenoids and their bacterial

metabolites or (b) on the molecular triggers, which activate the beneficial health functions of carotenoids.

To date, a summarized effort in order to collect the most recent data regarding the interactions of carotenoids and the gut microbiota in both animal and human studies has been made (Table 2). It is worth mentioning that the majority of these studies focus on the impact that specific carotenoids have on certain intestinal-related diseases (e.g., obesity, NAFLD, and cancer-related diseases). Overall, carotenoids promote the increase in nonpathogenic bacteria, such as *Bifidobacterium* and *Lactobacillus*, and restore the balance of *Firmicutes/Bacteroides* fractions. More specifically, Xia et al. [108] showed that dietary tomato feeding, high in lycopene, prevents both high-fat diet (HFD)- or diethyl-nitrosamine (DEN)-induced inflammation through the potential modulation of the gut microbiota in male $BCO1^{-/-}BCO2^{-/-}$ double KO mice. In particular, tomato powder (TP) feeding increased gut microbiota richness and diversity, while it significantly decreased the relative abundance of the genera *Clostridium* and *Mucispirillum*. However, according to the authors, it was not possible to determine the individual beneficial effects that TP's ingredients (lycopene, apo-lycopenoids, vitamin E, vitamin C, β-carotene, phenolic compounds, and dietary fibers) may exert. A human study focusing on anti-obesity agents showed that lycosome GA lycopene (GAL) or a combination of GAL with dark chocolate (DC) supplementation led to dose-dependent gut microbiota changes, as indicated by an increase in the relative abundance of *Bifidobacterium adolescentis* and *Bifidobacterium longum* [109]. A lycopene-rich diet in postmenopausal women presented a direct and positive correlation with the *Oscillospira* genus, while lycopene consumption was inversely related to the *Pantoea* genus. However, the linkage between lycopene's contribution to bone and skeletal disorders remains to be ascertained [101].

Carotenoids' potential gut-modulating impact has been also correlated with fatty liver disease. During an animal study, astaxanthin supplementation was able to decrease *Bacteroides* and *Proteobacteria* in six-week-old male C57BL/6J mice, while at the same time elevated the abundance of *Akkermansia*, which is related to potential prebiotic effects against NAFLD [110]. Interestingly, Terasaki et al. [111] demonstrated that an alteration to the fecal microbiota by fucoxanthin was able to prevent colorectal cancer induced by azoxymethane (AOM) and dextran sulfate sodium (DSS) in five-week-old ICR male mice. This intervention exhibited higher concentrations of *Lachnospiraceae* and lower counts of *Bacteroidlales* and *Rikenellaceae*. As a result, fucoxanthin, a marine carotenoid, emerged as a promising therapeutic agent with chemopreventive activity against colorectal cancer [111].

The administration of capsaicin, the carotenoid of red spicy peppers, in obese eight-week-old female C57BL/6J WT and $TRPV1^{-/-}$ KO mice favored the populations of *Prevotella*, *Akkermansia*, and *Bacteroides* and successively the production of acetate and propionate, and at the same time impeded the increase in *Escherichia* numbers [112]. Another member of the red-colored spices family, capsanthin, conferring anti-atherogenic and anti-obesity effects by decreasing trimethylamine *N*-oxide formation, incited the accumulation of *Bacteroidetes*, *Bifidobacterium* and *Akkermansia* populations and suppressed the *Ruminococcus* class in animal models [113,114]. Notably, a one-month diet of Duroc pigs, enriched with β-carotene, did not elicit any changes in the diversity and richness of gut microbiota [115]. A two-arm, controlled, and randomized trial, where women in mid-pregnancy were enrolled and consumed a carotenoid-rich diet (carrots, apricots, sweet potatoes, bell peppers, oranges, mangos, tomatoes products, etc.) revealed positive correlations of serum α- and β-carotene with the alpha diversity of microbiota. In parallel, beta diversity was affected principally by the intake of β-carotene. Higher carotenoid intake resulted in higher levels of *Ruminococcaceae*, an enterotype for which the association with different dietary patterns is as of yet unclear [116].

However, the lack of a representative number of clinical trials involving humans and the inability to explain the mechanisms involved indicate the need for further research in this field.

Table 2. Recent studies highlighting carotenoid and gut microbiota interplay through their potential impact in various intestinal diseases and metabolic disorders.

Experimental Model/Disease	Supplementation	Methodology	Carotenoid Impact	Ref.
Lycopene				
Male BCO1 [1] $^{-/-}$ BCO2 [2] $^{-/-}$ double KO [3] mice/liver cancer	24-week treatment 1st group: HFD + DEN 2nd group: HFD + DEN + Tomato Powder	(1) Liver analysis (2) Lycopene analysis (3) Gut-microbiome analysis	(1) Increased diversity and richness of gut microbiome	[108]
Volunteers, (n = 30, 15 women and 15 men)/obesity	1-month treatment 1st group: 10 g DC + GAL 2nd group: 7 mg GAL-MSFA 3rd group: 30 mg GAL-MSFA 4th group: 30 mg GAL-PUFA 5th group: 10 g DC (control)	(1) Biochemical analysis (BMI, pulse rate, and blood diastolic pressure) (2) Gut microbiome analysis	(1) GA lycopene (GAL) had blood-lipid-lowering effects (2) GAL or DC-GAL increase the relative abundance of beneficial bifidobacteria and lactobacilli	[109]
Postmenopausal women (n = 92)/bone mineral density	Diet evaluation by a 116-item semi-quantitative food frequency questionnaire	(1) Sequencing of 16S rRNA (2) Fecal samples metabolomics analysis	(1) Increase in *Oscillospira* genus (2) Decrease in *Pantoea* genus	[101]
Astaxanthin (AST)				
Male C57BL/6J mice/alcoholic fatty liver disease	12-week treatment 1st group: Normal diet 2nd group: HFD (Control) 3rd group: HFD-Ethanol 4th group: HFD-AST 5th group: HFD-Ethanol-AST	(1) Serum liver analysis (2) Gut microbiome analysis	(1) Decreased Bacteroides-Proteobacteria (2) Increased *Akkermansia muciniphila* which acts as a potential prebiotic during NAFLD	[110]
Male (M)–Female (F) KO and wild-type mice/obesity and diabetes	8-week treatment 1st group: Control diet 2nd group: AST (control + 0.04% AST)	(1) AST fecal analysis (2) Energy expenditure (3) Gut microbiome profile	(1) ASTA affects gut microbiota composition in both (M)-(F) mice (2) The abundance of *Akkermansia* was 385% greater (3) Improvement of metabolic homeostasis only occurs in (M) mice	[117]

Table 2. *Cont.*

Experimental Model/Disease	Supplementation	Methodology	Carotenoid Impact	Ref.
		Fucoxanthin (Fx)		
ICR mice supplied with carcinogenesis agents/colorectal cancer	14-week treatment (3 times per week) 1st group: Oil diet (control) 2nd group: Oil diet + 5% Fx	(1) Gut microbiome analysis (2) Colorectal mucosa analysis	(1) Alteration of gut microbiome by Fx (2) Chemopreventive effect in colorectal cancer	[111]
Male BALB mice/obesity	4-week treatment 1st group: Normal chow diet (control) 2nd group: Normal chow diet + Fx 3rd group: HFD 4th group: HFD + Fx	(1) Cecal and fecal microbiome analysis	(1) Fx changed both cecal and fecal composition (2) Reduced F/B ratio	[118]
		Capsacinoids (CAP)		
C57BL/6J (TRPV1+/+) and B6.129X1-Trpv1tm1Jul/J (TRPV1$^{-/-}$) mice/obesity	12-week treatment 1st group: Standard lipid diet (control) 2nd group: HFD 3rd group: CAP + HFD-fed diet	(1) Triglyceride, cholesterol, and insulin analysis (2) Glucose tolerance tests (3) Gut microbiota analysis of feces by 16S rRNA gene sequencing (4) Fecal SCFAs determination by GC-MS	(1) Lower food intake and weight gain, glucose, triglyceride, insulin, and cholesterollevels in CAP + HFD-fed mice (2) Increase in *Akkermansia*, *Prevotella*, *Bacteroides*, *Odoribacter*, *Allobaculum*, and *Coprococcus* in CAP + HFD-fed mice (3) Decrease in *Desulfovibrio*, *Escherichia*, *Helicobacter*, and *Sutterella* in CAP + HFD-fed mice (4) Increase in acetate and propionate in CAP + HFD-fed mice	[112]
C57BL/6J mice/obesity	12-week treatment 1st group: Standard lipid diet (blank control group) 2nd group: HFD (experimental control group) 3rd group: HFD + CAP	(1) Glucose tolerance tests (2) Biochemical analysis, TMAO **** levels (3) Gut microbiota analysis in cecal content	(1) Reduced body weight, serum triglycerides, total cholesterol, low-density lipoprotein cholesterol, and TMAO * in CAP + HFD-fed diet (2) Increase in *Bacteroidetes*, *Bifidobacterium*, and *Akkermansia* in CAP + HFD-fed mice (3) Decrease in *Ruminococcus* and in the ratio of *Firmicutes/Bacteroidetes* in CAP + HFD-fed mice	[113]

Table 2. *Cont.*

Experimental Model/Disease	Supplementation	Methodology	Carotenoid Impact	Ref.
		Various Carotenoids		
Pregnant women (n = 27)	Gestational study at three different time points 1st group: 32-week gestation, pre-intervention 2nd group: 36-week gestation, mid-intervention 3rd group: 6 weeks after child is born, post-intervention Diet containing α- and β-carotene (AC and BC), lutein and zeaxantin (ZL), cryptoxanthin (CR), and *trans*-lycopene (TL)	(1) Plasma and fecal analysis (2) 16S rRNA DNA sequencing of fecal bacteria	(1) AC decreased *Akkermansia* and increased *Phascolarctobacterium* (2) BC increased *Ruminococcaceae UCG002* (3) TL decreased *Akkermansia*, *Escherichia Shigella*, *Phascolarctobacterium*, *Ruminococcaceae UCG002*,*Prevotella* and increase *Ruminococcus* (4) CR increased *Phascolarctobacterium* and decreased *Prevotella* (5) ZL increased *Akkermansia*, *Phascolarctobacterium* and decreased *Prevotella*	[116]
Rats	1-week treatment1st group: Normal diet (control group, n = 6) 2nd group: β-carotene supplementation (n = 6) 3rd group: Dextran sulfate sodium (DSS), ulcerative colitis model (n = 6) 4th group: Dextran sulfate sodium and β-carotene (n = 6)	(1) Enzyme analysis of inflammatory cytokines (2) Tissue analysis (3) 16S rRNA sequencing of fecal samples	(1) DSS increased *Proteobacteria* and *Bacteroidetes* and decreased *Firmicutes* and *Actinobacteria* (2) β-carotene reversed these changes (increased *Firmicutes* and *Actinobacteria* and decreased *Proteobacteria* and *Bacteroidetes*)	[119]

[1] β-carotene -15, 15′oxygenase (BCO1), [2] β-carotene -9-10′xygenase, [3] double knock out (DKO). * $p < 0.05$, **** $p < 0.0001$.

5. Endogenous Lipids

Despite their known contribution to membrane structure and energy storage, lipids are also signaling molecules. Endogenous bioactive lipids are part of a complex network that modulates a plethora of cellular and molecular processes involved in health and disease, while emphasis is placed on their role during inflammation, including gut-related diseases. Thus, it is currently being investigated whether these types of lipids act as promoters or suppressors of inflammation through their interaction with the gut microbiota. Bioactive lipids are: (a) divided into three main families (i.e., eicosanoids, endocannabinoids, and specialized pre-resolving lipid mediators—SPMs) and (b) generated from ω-6 or ω-3 essential polyunsaturated fatty acids (PUFA) precursors, which are esterified into membrane lipids and act by binding and activating specific G protein-coupled receptors (GPRs) [120].

5.1. Eicosanoids

According to the Lipids Metabolites and Pathways Strategy (LIPID MAPS), eicosanoids are lipid molecules of the fatty acyls group, produced by the oxidation of arachidonic acid. Arachidonic acid (AA) is one of the most important polyunsaturated fatty acids of cell membrane phospholipids, which acts as substrate for a variety of enzymes [121]. These enzymes (i.e., cyclooxygenases (COX), lipoxygenases (LOX), or cytochrome P450), through different biosynthetic pathways, result in the production of different types of eicosanoids (Figure 4) [122,123]. In terms of production, eicosanoids can be formed either by the majority of immune cells or by the intestinal epithelial cell, as the latest findings support [124]. However, even intestinal bacteria may be able to metabolize AA in order to produce eicosanoid metabolites [125]. In particular, LOXs derived from *Proteobacteria* sp. were able to produce various prostaglandins (PGs) through the fermentation of other bacterial metabolites (mostly short-chain fatty acids) in the large intestine [126].

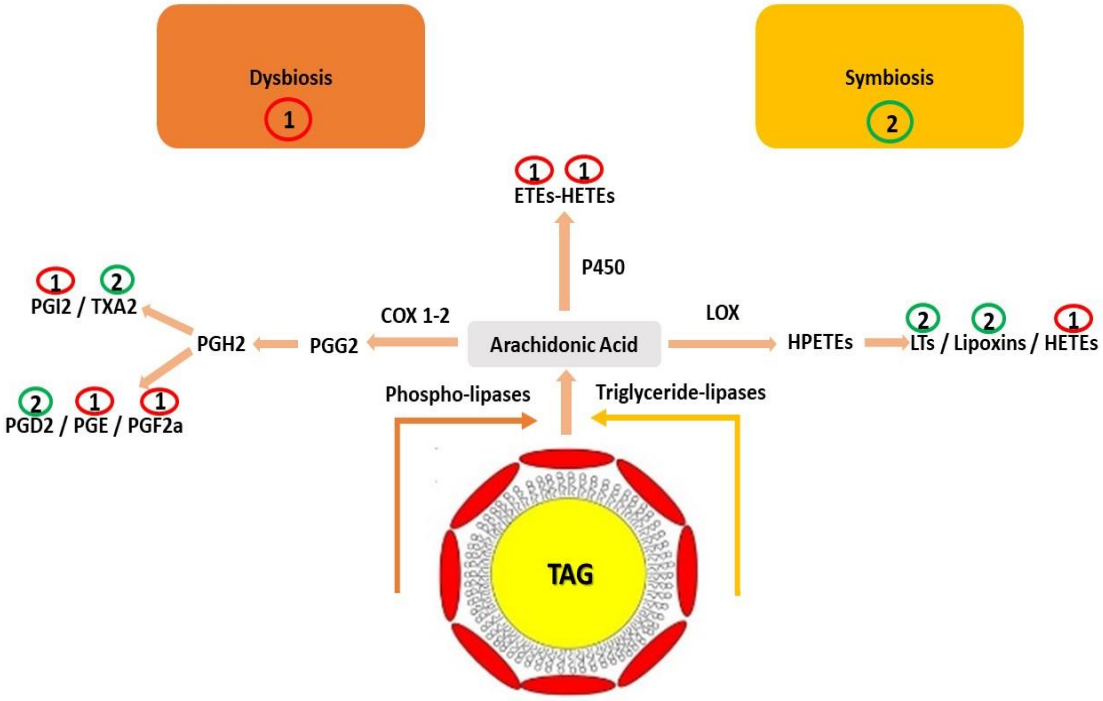

Figure 4. Schematic illustration of different enzymatic pathways (i.e., cyclooxygenase 1,2 (COX-1,2), lipoxygenase (LOX), and cytochrome 450 (CYP450)) of eicosanoids biosynthesis (i.e., prostaglandins (PGE, PGD, PGF, PGI, PGG), thromboxanes (TXs), leukotrienes (LTs), hydroxeicosatetraenoic acids (HETEs), and hydroperoxyeicosatetraenoic acids (HPETEs)) and their role in gut homeostasis [122]. Pink arrows indicate the different biosynthetic pathways, while red and green cycles are associated with gut dysbiosis or symbiosis, respectively.

Eicosanoids Clinical Effect

A few studies [124,127] revealed that eicosanoids can indirectly affect bacterial populations through their linkage with the normal growth function of the GI tract, as well as their potential role in the regulation of the intestinal epithelial response to injury. However, the exact mechanism, impact, or outcome that each specific eicosanoid has on the gut microbiota may differ significantly (Figure 4). For example, it is believed that PGE2 is related to the appearance of tumors, while PGD2 is characterized by a completely different action [128]. This has a significant impact on intestinal diseases and in particular IBD, since it appears that increased PG production occurs within the mucosa of patients with IBD. Prostaglandins (PG) production indicates a differentiated response, which may lead to a gradual re-shaping of the altered gut microbiota and consequently to a healing effect. Another study demonstrated that the COX-2-PGE2 pathway should be investigated as a target for primary non-responders to tumor necrosis factor (TNF) inhibitor therapy, as well as a prognostic biomarker for TNF inhibitor response in patients with ulcerative colitis [129].

Similarly, mice with leukotriene B4 (BLT4) receptor deficiency appear to be protected in inflammatory disease models of arthritis, asthma, and atherosclerosis. According to Jala et al. [130], when these mice were treated with various tumor factors, the tumor development and mortality were increased, while in germ-free mice, tumors appeared again after fecal transplantation. Microbiota analysis showed a defective host response (e.g., increased *A. muciniphila* sp., *Firmicutes* sp., and decreased *Bacteroides* sp.), reshaping the gut microbiota composition and consequently, promoting tumor growth in the large intestine. Interestingly, it seems that leukotriene inflammatory pathways which are related to tumor growth are clearly dependent on the action of the gut microbiota [130]. Meanwhile, there is evidence showing that LTs can have both positive and negative impacts on bowel-related diseases. For instance, it is widely accepted that the synthesis of leukotriene B4 is enhanced by the colonic mucosa of patients with IBD, helping the development of colitis, while on the other hand, recent data suggest that B4 promotes the intestinal damage repair of epithelial cell proliferation through a low-affinity BLT2 receptor [131].

On the other hand, the most recent approaches correlate LTs and PGs with specific dietary models based on the precursors from which they are derived. For example, the administration of krill oil, which is rich in *n*-3 PUFA such as EPA and DHA, showed pre-resolving properties and the ability to modulate gut microbiota composition (e.g., decreased abundance of *Rickettesiales* sp. and several species of *Lactobacillus* sp.) in a pig microbial-induced dysbiosis model [132]. Another study regarding linoleic acid (omega-6 PUFA) derived from sunflower or safflower showed that either itself or its metabolites (AA, PGE2, and LTB4) were able to enhance IBD [133]. In contrast, soybean or flaxseed a-linolenic acid (omega-3 PUFA) showed that either itself or its metabolic derivatives (EPA, DHA, PGE3, and LTB5) were able to reduce IBD [134]. Overall, the above conflicting results underscore the need for more clinical trials aiming toward the better use (at both the prognostic or therapeutic level) of the axis between nutrition and the role of gut microbiota.

5.2. Endocannabinoids

The endocannabinoid (eCB) family presents a complex system of different molecules such as ligands, analogs, and enzymes that are located in many organs and tissues, including the brain and the gut microbiota. According to several studies, eCBs exert immune-regulatory abilities followed by a high specialization that makes them "act on demand", consequently protecting epithelial barrier integrity and modulating GI motility [122,135]. Among the most studied of these ligands are *N*-arachidonoyethanolamide (AEA) and 2-arachidonoyglycerol (2-AG), which bind and activate type-1 and type-2 cannabinoid receptors (CB1 and CB2), while other eCB members include the following analogs: (1) O-arachidonoylethanolamine (AEA), *N*-oleoylethanolamine (OEA), and *N*-palmitoylethanolamine (PEA). These analogues are synthesized mostly by immune cells using specific enzymes such as the *N*-acylphospathidylethanolamine-hydrolyzing phospholipase D (NAPE-PLD) and diacyglycerol lipase (DAGL).

Endocannabinoid System–Intestinal Microbiota Interplay in Gut-Related Diseases

A new scientific field of increasing interest is related to the bidirectional interplay between eCBs and gut microbiota in various inflammatory diseases, such as IBD, rheumatoid arthritis, depression, and consequent pain. However, most of the published studies focus on the differential expression of its components in human IBD. For instance, during a knock-out endocannabinoid degradation study, an improvement in colon inflammation in a colitis C57B1/6 mice model was observed [136]. In contrast, another study, including human and mice stool, identified *N*-acyloethaloamines as a class of metabolites that are elevated in IBD and have the potential to shift the gut microbiota towards a more IBD-like composition (e.g., increased *Proteobacteria* and decreased *Bacteroides*) [137]. Therefore, as Mestre et al. [138] describe, while it is already known that the intestinal microbiome and endocannabinoids interact by affecting the basic functions of each other, there are no corresponding data regarding the mechanisms of action in IBD. Meanwhile, dysregulations of the gut–brain axis, and consequently in eCBs, were related to altered gut microbiota diversity (increased *Lactobacillaceae* and *Erysipelotrichaceae* or decreased butyrate-forming bacteria) in Parkinson's disease [139]. On the other hand, changes in the gut (reduced microbial alpha diversity) led to the increased excretion of PEA, which in turn led to a more severe clinical condition related to anhedonia/amotivation or other psychological disorders (e.g., depression and schizophrenia) [140].

Interestingly, it is believed that the gut microbiota and eCBs can communicate through signals that involve the gut–brain axis for the fine-tuning of energy, lipid, and glucose metabolism [141]. In addition, eCB enzymes also exert a key role in energy homeostasis and metabolism, including metabolic-related disorders such as obesity. In particular, NAPE-PLD regulates fat metabolism and absorption, while its deletion leads to insulin resistance, glucose tolerance, altered lipid and gut microbiota composition (e.g., increased *Alcaligenaceae*, *Bacteroidaceae*, *Clostridiaceae*, *Coriobacteriaceae*, *Erysipelotrichaceae*, and *Lactobacillaceae* families) in an adipose tissue-specific Napepld-deleted mice (cKO mice) model [142]. Notably, OEA and PEA acted as fat sensors through the mediation of the response to high-fat diets, resulting in the control of the thermogenic process as well as the reduction in the increased permeability of the GI tract that often occurs during obesity-driven dysbiosis [141].

Although these bioactive lipids appear to provide potential therapeutic abilities, their linkage with gut microbiota composition is indirect. For example, during a 2-day Mediterranean diet in Canadian men and women, specific gut bacterial families (e.g., *Veillonellaceae*, *Peptostreptococcaceae*, and *Akkemansiaceae*) were associated with variations in most *N*-acylethanolamines or 2-AG, independently of fat mass or dietary fatty acid intake [143]. The most commonly accepted mechanism by which the gut microbiota affects the endocannabinoid system involves the regulation of CB2 receptor gene expression. Thus, since the microbiome can affect several gut-related functions through eCBs, the alteration of gut microbiota composition may play a key role in gut-related diseases. This is the main reason why the beneficial role of probiotics on eCBs is being studied. Indeed, during an eCBs-targeted intervention, *L. acidophilus* induced CB2 expression, while the administration of A. muciniphila increased 2-AG [144]. In general, it has been found that *Lactobacillus acidophilus* and *Akkermansia muciniphila* increased the eCBs levels, while *Clostridium* spp was negatively correlated with 2-AG, 2-OG, and 2-PG [145]. However, in order to draw reliable data more human clinical trials are required.

5.3. Specialized Pro-Resolving Lipid Mediators: Ideal Molecules for Treating Gut-Related Diseases or Just Another Firework?

A new genus of lipid mediators, also known as specialized pro-resolving lipid mediators (SPMs), are synthesized mostly during inflammation, from ω-6 AA or even further from ω-3 PUFAs, eicosapentaenoic acid (EPA), docosahexaenoic acid (DHA), and docosapentaenoic acid (DPA), and it is believed that they play an important role in a wide range of gut-related metabolic disorders, including diabetes and IBD [146]. The same enzymes (i.e., COX, LOX, and P450) that are involved in eicosanoid synthesis are also associated

with the synthesis of these mediators, which takes place after the activation of immune cells such as neutrophils, monocytes, and macrophages. These types of endogenous lipids can: (a) promote the clearance of debris, infective pathogens, and macrophages, which are related to intestinal dysbiosis and (b) inhibit proinflammatory cytokines by enhancing the secretion of anti-inflammatory mediators, resulting in better tissue regeneration, analgesia, and increased functionality [147]. It is also believed that these EPA- and DHA-derived SPMs share similar protective actions with their precursor compounds in modulating innate inflammatory responses, lubricating the GI tract and joints as well as enabling early anticipation and treatment. The most important SPMs are:

- Arachidonic-acid-derived resolvins;
- Eicosapentaenoic-acid-derived resolvins (RvE1-3);
- Docosahexaenoic-acid-derived resolvins (RvD1-6);
- Protectin D1 (PD1);
- Maresins (MaR1 and MaR2);
- Lipoxins (lipoxins A4 and B4, LXA4-LXB4) [148].

What differentiates lipid mediators from other signaling-repair lipids is their role as immune-resolvents and not as immune suppressors. This was confirmed by a study in which lipid mediators may have played a pivotal role in the resolution of inflammation and the maintenance of gut integrity [149]. Based on this, it seems that SPMs demonstrate a key role during mucosal infections as well as various gut-related diseases, such as IBD, by promoting the killing of invading pathogens during dysbiosis and enhancing their clearance [150]. As far as inflammatory bowel disease is concerned, the supplementation with ω-3 DPA-derived protectin D1 and ω-3 DPA-derived resolving D5 showed strong protective effects against colitis and intestinal ischemia in eight to ten male C57BL/6 mice [151]. In addition, a recent study using male C57BL/6J mice revealed that MaR1 administration ameliorates the inflammation state in the colonic mucosa and may compensate for changes in the gut microbiota (e.g., increased *P. xylanivorans*) caused by obesity [152]. Similarly, with MaR1, the administration of fish oil or a high dose of resolvin D1 to six-week-old female C57BL/6J obese mice with resulted in the divergence of gut microbiota, which in turn affected body weight [153]. More specifically, microbiota analysis revealed that during resolvin D1 administration *Bacteroides* were increased, and *Desulfovibrio* were decreased, while suppression of the H2S-producing *Deltaproteobacteria* was also observed. Nevertheless, with respect to these promising findings regarding the potential effects of these mediators, clinical evidence with human tested models is still lacking. Overall, endogenous lipids, through signals that mostly involve the gut–brain axis, can play an important role in the design of novel personalized nutrition models by targeting gut microbiota alterations (Figure 5) [154].

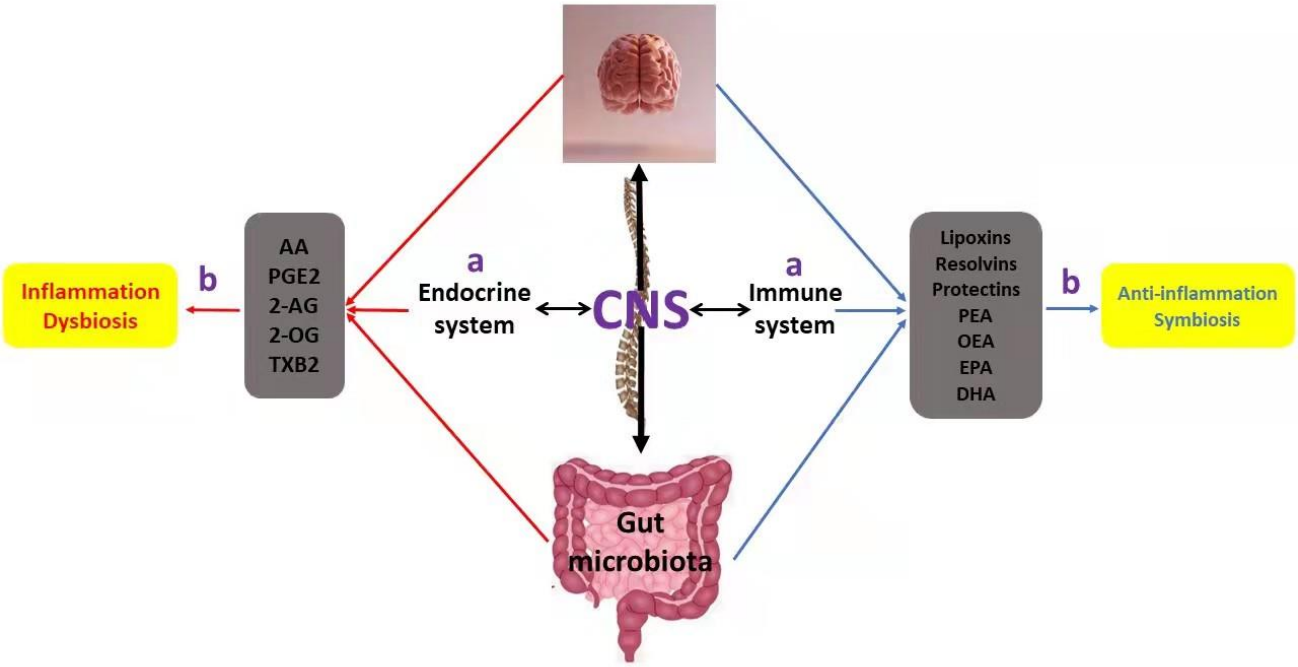

Figure 5. Schematic representation of: (a) the complex network also known as the gut–brain axis that involves different types of lipids, the gut microbiota, the central nervous system (CNS), and the endocrine and immune system, as well as (b) their impact on inflammation and gut homeostasis. Regarding bioactive lipids, red arrows and the left side indicate their pro-inflammatory activities, including dysbiosis, while blue arrows and the right side demonstrate their anti-inflammatory activities, which in turn drive a sustained net of gut symbiosis.

6. Lipidomics in Current Clinical Interventions: Present Status, Strengths, and Limitations

Although the current knowledge regarding the management of health and disease through the manipulation of the gut microbiome by diet is thriving, the relationship between dietary lipids and microbial populations still warrants more research. In this direction, in order to develop a benchmark for lipidomics, it is necessary to establish a world database in which all the required information (i.e., type of study, samples, techniques, disease, and metabolite outcomes) are recorded. An effort to gather the most recent data regarding lipidomics studies in animal studies and clinical interventions, which include non-polar and endogenous lipids, is presented in Table 3.

Table 3. Up-to-date lipidomic status of exogenous or endogenous lipids.

Experimental Model	Sample	Analytical Technique	Administrated/Studied Dietary Components	Lipid Species/Biomarkers Detected	Related Disorders	Ref.
Animal model (BALB/c nude mice)	Feces	GC-MS	Sitosterols	SCFAs (↑)	Colocteral cancer	[155]
Animal model (sheep)	Rumen fluid	GC-FID	β-Sitosterol	SCFAs	Rumen acidosis	[66]
Animal model (Syrian Golden hamsters)	Feces	GC-FID	Wood-plant sterols	(a) SCFAs (b) Neutral sterols (cholesterol, coprostanol, coprostanone, campesterol, and dihydrocholesterol) (↑) (c) Acidic sterols (deoxycholic acid, cholic acid, chenodeoxycholic acid, and lithocholic acid) (↑)	High-cholesterol diseases	[67]
Animal model (male Sprague Dawley rats)	Feces	UPLC-QTOFMS [1], GC-FID	Phytosterol-ester-fortified skimmed milk	(a) Bile acids metabolic products (i.e., 3alpha,12alpha,15beta-trihydroxy5beta-cholan-8(14)-en-24-oic acid, 2beta,3beta-dihydroxy-6-oxo5alpha-cholan-24-oic acid, 3alpha,11alpha-dihydroxy-12-oxo5beta-cholan-24-oic acid, and (23R)-23-Hydroxy-3,7-dioxo-5betacholan-24-oic acid) (↓) (b) Diglycerides (↓) (c) Novaxenicins A (↓) (d) PI(O-16:0/16:1(9Z)), PG (22:4(7Z,10Z,13Z,16Z)/22:6(4Z,7Z,10Z,13Z,16Z,19Z)), 11R-hexadecanoyloxy octadeca9Z,12Z,15Z-trienoic acid (↓) (e) SCFAs (isobutyric acid, valeric acid, and isovaleric acid) (↑)	NAFLD	[68]
Animal model Syrian Golden (hamsters)	Feces	GC-MS, GC-FID	Soybean sterols	Neutral sterols (coprostanol, campersterol, dihydrocholesterol, and cholesterol) (↑) Acid sterols (deoxycholic acid, cholic acid, chenodeoxycholic acid, and lithocholic acid) (↑) SCFAs (acetic, propionic, and butyric acid) (↑)	High-fat-diet-associated liver damages	[31]

Table 3. *Cont.*

Experimental Model	Sample	Analytical Technique	Administrated/Studied Dietary Components	Lipid Species/Biomarkers Detected	Related Disorders	Ref.
Human, randomized, double-blind, placebo-controlled parallel trial (adult participants)	Serum	GC-FID	Phytosterol-ester-enriched soymilk powder	Fatty acids, DHA, and EPA	NAFLD	[5]
Human, randomized, placebo-controlled crossover trial (adult participants)	Serum, Plasma	GC-MS/MS	Margarine enriched with plantstanol esters	(a) Sitosterol, campesterol (↓) (b) Sitostanol, campestanol (↑) (c) Lathosterol, desmosterol, and cholestenol (no significant changes) (d) 7b-OH-sitosterol, 7b-OH-campesterol, and oxyphytosterol (↓) (e) 7-keto-campesterol (no significant changes)	-	[69]
Human study (adult participants)	Feces	LC-MS/HRMS	-	Cholesterol, coprostanol, cholestanol, sitosterol, 5β-sitostanol, 5α-sitostanol, campesterol, 5β-campestanol, and 5α-campestanol	-	[70]
Human study (adult allograft participants)	Feces	GC-MS	-	(a) Campestanol, coprostanol, and epi-coprostanol (↓) (b) Cholestenone, cholesterylene, and γ-sitosterol (↑)	Kidney failure/kidney transplant	[156]
Animal model (sheep)	H&E-stained tissue samples	LC-MS	High-energy and medium-energy diet vs. normal diet, vitamin A absorption	(a) Viramin E, retinene, cholic acid, litocholic acid, and tauroursodeoxycholic acid (↓) (b) Retinol, glycocholic acid (↑)	Male infertility	[75]
Animal model (male C57BL/6J mice)	Cecal samples	GC-FID	Vitamin A	(a) SCFAs (acetate, propionate, butyrate, and valerate) (b) Branched short-chain fatty acids (BSCFAs) (isobutyrate and isovalerate)	Obesity	[76]

Table 3. *Cont.*

Experimental Model	Sample	Analytical Technique	Administrated/Studied Dietary Components	Lipid Species/Biomarkers Detected	Related Disorders	Ref.
Animal model (BALB/c nude mice)	Plasma, feces	LC-MS/MS	Vitamin E δ-tocotrienol (δTE) and δTE-13′-carboxychromanol (δTE-13′)	(a) Tocotrienols δTE, γTE in plasma and feces (↑) (b) δ-CEHC, sulfatedδTE-13′ with 2 double bonds, sulfated δTE-11′ in plasma (↑) (c) Unconjugated δTE-13′, δTE-13′ with 2 double bonds, 11′-COOH in feces (↑)	Colitis-associated colon cancer	[82]
Animal model (male C57BL/6J mice)	Spinal cord, jejunum, ileum, colon, and duodenum homogenized samples	LC-MS	Vitamin D	Anandamide (AEA) and 2-arachidonoylglycerol (2-AG)	Chronic pain	[95]
Human study (adult allograft participants)	Feces	GC-MS	-	γ- and δ-Tocopherols (↓)	Kidney failure/kidney transplant	[156]
Animal model (male C57BL/6J mice)	Feces	GC-MS	Capsaicin	SCFAs: (a) Acetate and propionate (↑) (b) Butyrate (no significant changes)	Obesity	[112]
Human study (adult allograft participants)	Feces	GC-MS	-	Squalene(↓)	Kidney failure/kidney transplant	[156]
Animal study (male C57BL/6J mice)	Liver tissues	HPLC-UV	Lycopene	(a) IL1β, IL6, IL12a (↓) (b) *Clostriduim*, *Mucispirillum* (↑)	High-fat-diet-promoted hepatocellular carcinoma	[108]
Human double-blinded study (obese participants)	Serum	HPLC-UV	Lycopene	(a) *Bifidobacterium adolescentis and longum* (↑) (b)	Obesity	[109]
Animal study (male C57BL/6J mice)	Fecesepatic and liver tissues	LC-MS, GC-FID	Astaxanthin	(a) *Akkermansia muciniphila* (↑) (b) Plasma glucagon-like peptide (↑) (c) IL-1β (↓)	Inflammation and metabolic homeostasis	[113]

Table 3. *Cont.*

Experimental Model	Sample	Analytical Technique	Administrated/Studied Dietary Components	Lipid Species/Biomarkers Detected	Related Disorders	Ref.
			Endogenous lipids			
Animal study (C57BL/6J-129/Sv mice)	Colons and small intestines	LC-MS	Eicosanoids	(a) PGE_2,PGD_2, 6-keto $PGF1_a$, and $PGG2_a$, (↓) (b) TXB_2,15-HETE (no significant changes) (c) Leukotrienes (ND)	Induced intestinal inflammation and tumorigenesis	[157]
Human study (UC verified patients)	Blood	GC-MS	Prostanoids	(a) PGE_2 in responders receiving a TNF stimulation (↓) (b) $PGF2_a$, TXB_2 (no significant differences) (c) PGI_2, PGD_2 (ND)	Ulcerative colitis	[129]
Animal study (male C57BL/6J obese mice)	White adipose tissue	LC-MS/MS	Lipoxin A4	(a) Lipoxin A4 in mice fed a high-fat diet (↓) (b) RvD1, RvD5 (c) Maresin 1	Obesity-induced adipose inflammation/kidney disease	[158]
In vitro and animal study (white Yorkshire-landrace pigs)	THP1 cells Gut luminal and serum	LC/ESI-MS	Short-, medium-, and long-chain fatty acids	(a) (↑) EPA, DHA, and acetate (b) (↓) SCFA	Intestinal inflammation	[132]
In vitro study	Caco-2 cells	LC-MS/MSGC-MS	Fatty acid ethanolamide, FAEs	(a)(↓) PEA, OEA (b) (↓) AEA	-	[159]
Animal study (C57BL/6J mice)	Plasma and adipose tissues	LC-ESI MS/MS	Phospholipids Ceramides Eicosanoids Cannabinoids	(a) (↓) PEA, OEA, and SEA in cKO mice (b) NEFA (no significant differences) (c) (↑) Triglyceride (d)(↑) Cholesterol		[142]
Animal study (C57BL/6J mice)	Colon tissues	LC-MS/MS	Cannabinoids	(a) (↓) 2-AG and 2-OG, and (↑) PGE_2 in PF-3845 inhibitor mice (b) (↑) 2-AG,2-OG, PGE_2 (no significant changes) in induced colitis mice (c) NAEs (no significant differences) in both PF-3845 and induced colitis mice	Experimental colitis	[136]
Human study (adult participants)	Plasma	LC-MS/MS	Dietary fatty acid for the determination of the circulation of endocannabinoidome	(a) 7 metabolites of NAEs were found (b) 6 metabolites of 2-MAGs were found	-	[143]

Table 3. *Cont.*

Experimental Model	Sample	Analytical Technique	Administrated/Studied Dietary Components	Lipid Species/Biomarkers Detected	Related Disorders	Ref.
Animal (mice) and human (healthy adult volunteers)	Blood	LC-MS/MS	Impact of resolvins (RvT) in infections	(a) Eicosanoids (b) SPMs (c) Novel 13-series resolvins (RvT1, RvT2, RvT3, and RvT4)	Bacterial infections	[160]
Human study	Urine	LC-MS/MS	Method validation for urinary ω-3 and ω-6 PUFA metabolites	More than 20 PUFA metabolites were identified and quantified	-	[161]
Animal (male mice and human) studies (healthy adults and IBD patients)	Gastrointestinal tissues/plasma	LC-MS/MS	Impact of lipid mediators on intestinal protection	(a) (↑) LTB_4, PGE_2, and TXB_2 in IBD patients (b) (↑) $RvD5_{n\text{-}3\ DPA}$ and $PD1_{n\text{-}3\ DPA}$ in IBD patients	IBD	[151]
Human study (healthy adults)	Human plasma/serum	LC-MS/MS	Identification of SPMs through o-3 supplementation	(a) RvE1, RvD1, LXB_4, 18-HEPE, and 17-HDHA in plasma (b) RvE1, RvD1, AT-LXA_4, 18-HEPE, and 17-HDHA in serum	-	[162]
Animal study (male C57BL/6J and male Slc:ICR mice)	Feces	CE-TOFMS	Impact of sCSDS [2] on the murine intestinal ecosystem	(a) 79 fecal metabolites were identified (b) 16 metabolites were significantly different in sCSDS mice	sCSDS	[163]

[1] quadrapole time-of-flight mass spectrometry (QTOFMS), [2] subchronic and mild social defeat strees (sCSDS).

It seems that sterols and other metabolites (mainly SCFA) were measured by GC-FID in mostly fecal samples. On the other hand, FSVs and other metabolites were mainly measured by LC-MS in serum or various tissue samples. Continuing, endogenous lipidomics was performed by using LC-ESI/MS or LC-MS/MS in almost every type of biological sample. However, in order to bridge any future gaps in the interpretation and evaluation of the findings of nutrition interventions derived from the implementation of lipidomic techniques, it is substantial to summarize the strong points and the limitations of present clinical studies. The strong points of the lipidomics studies are:

(a) The future design and actualization of cohort studies, which process a vast amount of information, such as lifestyle habits, sociodemographic and anthropometric factors, dietary patterns, and clinical results [164];
(b) The use of holistic –omics techniques (from metagenomics to untargeted metabolomics), the elucidation of novel biomarkers, and the determination of dietary constituents (i.e., carotenoids, vitamins, and sterols) in biological fluids (mainly plasma and feces), which will provide a multifaceted tool in disease diagnosis and treatment [116];
(c) The establishment of evidence in order to create tailored and personalized dietary approaches [155];
(d) The accomplishment of intervention studies, which will include pilot-testing of the dietary patterns that will be then adapted, and will collect more reliable and validated results [99].

On the other hand, the main limitations of current studies are abstracted hereupon:

(a) There is a restricted number of small-sample-size clinical trials concerning human subjects, while valid animal or in vitro models are absent. Therefore, the results of the studies cannot be generalized. In addition, most of the present studies refer to baseline and not to long-term or follow-up interventions (even across the lifespan), which are essential in order to produce representative results [164];
(b) The implementation of non-succinct enrollment criteria and the collection of self-reported questionnaires, related to volunteers' dietary tracking, may compromise the outcome of the studies due to the past chronic dietary habits or other possible confounders (for instance, Asian populations use plants oils with meat, while European populations consume plant oils in a Mediterranean vegetable-based diet) [99,164];
(c) Inter-individual variations in (socio)genetic factors (i.e., ethnicity or site-specific differences among the same ethnicity) and genetic polymorphisms in non-polar lipids metabolism may imperil the integrity and impartiality of the lipidomics results [116]. For example, populations with less dark skin present a higher risk of vitamin D deficiency [99];
(d) There is a lack of collective knowledge concerning the role of endogenous lipids, especially endocannabinoids and SPMs in clinical studies [154].

7. Conclusions

It is apparent that lipids (exogenous or endogenous) have a significant impact on gut microbiota and thus are able to lead the way for potential therapeutic approaches, either by targeting the specific causal pathways of gut-related diseases or by reshaping the composition of beneficial as well as detrimental bacterial populations. Regarding non-polar dietary lipids, phytosterols are considered to be promoters of symbiosis either through the production of SCFAs (i.e., in the case of sitosterols) or through the modulation of gut microbiota composition (i.e., in the case of stigmasterol and campesterol). Meanwhile, sterol metabolites (i.e., coprostanol, methylcoprostanol, and sitostenone) were also found to have a potential impact on gut microbiota composition, while the latest studies highlight their role as potential biomarkers of microbial metabolism.

In addition, taking into account recent data about the importance of FSVs, it seems that the FSVs–gut microbiota relationship is bidirectional, since FSVs can influence the composition as well as the function of the gut microbiota, while the latter can regulate the status (metabolism, absorption, and functions) of FSVs. This, however, can be a double-edged

sword, as it can either promote the necessary symbiosis or induce undesired interactions and enhance the manifestation of pathological conditions (i.e., vitamin K and its association with blood clotting). Thus, in order to elucidate many aspects of this two-way relationship, more human studies, including well-designed dietary or pharmacological approaches, as well as specific bioinformatics tools, are needed. In terms of carotenoid supplementation, numerous clinical interventions have taken place in the last three years. Carotenoids are considered to be phytochemicals with prebiotic-like effects allowing potential therapeutic interventions by regulating the composition of the gut microbiota. However, due to the high diversity of carotenoids, as well as the lack of a representative number of clinical trials involving humans, any kind of generalization would be hasty.

On the other hand, endogenous lipids are mostly involved in the gut–brain axis, which modulates important biological functions of the host, such as metabolism homeostasis and the immune response. More specifically, the impact of eicosanoids on the gut microbiota is controversial since different types of these endogenous lipids can have completely adverse effects. Notably, these interactions are clearly dependent on the action of the gut microbiota. Furthermore, a new scientific field of increasing interest is related to the effect of the interplay between eCBs and the gut microbiome in various inflammatory diseases, such as IBD and rheumatoid arthritis. Actually, eCBs are able to detect the gut microbiota composition or immune response changes and, consequently, maintain the necessary homeostasis. This also allows the modulation of specific eCB enzymes through microbial interventions (mostly prebiotics) that are associated with positive effects. However, considered to represent the "front line" of endogenous lipids are SPMs, the potential benefits of which are mostly related to the stimulation of inflammation. Surprisingly, these lipids "detect" the increased (pro-inflammatory) cytokines and through the production of anti-inflammatory mediators act as "extinguishers" of inflammation. However, despite these promising results, much more effort is needed, as this evidence has arisen from mostly in vitro or animal studies.

Regarding the lipidomics status of the presented studies, it seems that each lipid category is investigated using different analytical approaches. In general, GC-FID (in the case of sterols and SCFAs) and LC-MS (in the case of vitamins and carotenoids) are considered to be more suitable for the analysis of dietary lipids. In contrast, endogenous lipid analysis requires an increased resolving and separation power, which in turn will allow a higher sensitivity and broader lipidome coverage. This is why LC-MS/MS, LC-ESI/MS, or, most recently, LC/QC-TOF/MS fit better for the evaluation of endogenous lipids. Despite the analytical limitations in lipidomics so far, the availability of synthetic standards, as well as deuterium-labeled bioactive lipids, now permits the identification and quantification of existing (targeted approaches) or novel metabolites (untargeted approaches) in almost every human biological sample. However, several researchers believe that these studies should be accompanied by an assessment of the composition of the gut microbiome so that specific microbial changes can be associated with the corresponding functions, responses (in case of food intake), or diseases. In any case, lipid analysis must be constantly evolving and able to keep pace with new research data so that it always remains a useful and up-to-date tool for interpreting the complex interactions between the gut microbiota and nutrition. Going back to where we started, it seems that nutrition equally affects the interactions between endogenous lipids and the gut microbiota. However, there is growing evidence that correlates the type of the diet with the precursors (i.e., EPA, DHA, etc.) from which several endogenous lipids are derived. Indeed, more integrated approaches with emphasis on the Mediterranean diet (rich on ω-3 PUFA) can enhance the action of these mediators, while at the same time minimizing any pathological condition that may arise (i.e., cardiological or neurological disorders) according to clinical intervention studies. Overall, despite the differentiation between exogenous and endogenous lipids, the dietary factor remains the most important link that directly or indirectly modulates the intestinal microbiome, allowing prognostic or therapeutic interventions.

Author Contributions: Conceptualization, V.J.S. and P.Z.; methodology, K.T., S.J.K., E.K. and T.T.; data curation, K.T., S.J.K., E.K. and T.T.; writing—original draft preparation, K.T., S.J.K., E.K. and T.T.; writing—review and editing, S.J.K., T.T. and P.Z.; supervision, T.T., V.J.S. and P.Z.; project administration, P.Z. All authors have read and agreed to the published version of the manuscript.

Funding: This research was co-financed by the European Union and Greek national funds (European Social Fund—ESF) through the Operational Program Competitiveness, Entrepreneurship and Innovation, under the call RESEARCH–CREATE–INNOVATE (project code: T2EDK-03847).

Institutional Review Board Statement: Not applicable.

Informed Consent Statement: Not applicable.

Data Availability Statement: The data presented in this study are available on request from the corresponding author.

Conflicts of Interest: The authors declare no conflict of interest.

References

1. Sender, R.; Fuchs, S.; Milo, R. Revised estimates for the number of human and bacteria cells in the body. *PLoS Biol.* **2016**, *14*, e1002533. [CrossRef] [PubMed]
2. Ibáñez, C.; Mouhid, L.; Reglero, G.; Ramírez de Molina, A. Lipidomics insights in health and nutritional intervention studies. *J Agric. Food Chem.* **2017**, *65*, 7827–7842. [CrossRef]
3. Lamichhane, S.; Sen, P.; Dickens, A.M.; Oresic, M.; Bertram, H.C. Gut metabolome meets microbiome: A methodological perspective to understand the relationship between host and microbe. *Methods* **2018**, *149*, 3–12. [CrossRef] [PubMed]
4. Yang, Q.; Liang, Q.; Balakrishnan, B.; Belobrajdic, D.P.; Feng, Q.J.; Zhang, W. Role of dietary nutrients in the modulations of gut microbiota: A narrative review. *Nutrients* **2020**, *12*, 381. [CrossRef] [PubMed]
5. Dingeo, G.; Brito, A.; Samouda, H.; Iddir, M.; La Frano, M.R.; Bohn, T. Phytochemicals as modifiers of gut microbial communities. *Food Funct.* **2020**, *11*, 8444–8471. [CrossRef]
6. Sun, X.; Zhao, H.; Liu, Z.; Sun, X.; Zhang, D.; Wang, S.; Xu, Y.; Zhang, G.; Wang, D. Modulation of gut microbiota by fucoxanthin during alleviation of obesity in high-fat died fed-mice. *J. Agric. Food Chem.* **2020**, *68*, 5118–5128. [CrossRef] [PubMed]
7. Yang, K.; Han, X. Lipidomics: Techniques, applications, and outcomes related to biomedical sciences. *Trends Biochem. Sci.* **2016**, *41*, 954–969. [CrossRef] [PubMed]
8. Smilowitz, J.T.; Zivkovic, A.M.; Wan, Y.J.Y.; Watkins, S.M.; Nording, M.L.; Hammock, B.D.; German, J.B. Nutritional lipidomics: Molecular metabolism, analytics and diagnostics. *Mol. Nutr. Food Res.* **2013**, *57*, 1319–1335. [CrossRef] [PubMed]
9. Zhang, J.L.; Yan, F.; Wang, X. Clinical lipidomics: A new way to diagnose human diseases. *Clin. Trans. Med.* **2018**, *7*, e12.
10. De Castro, M.D.L.; Quiles-Zafra, R. Lipidomics: An omics discipline with a key role in nutrition. *Talanta* **2020**, *219*, 121197. [CrossRef] [PubMed]
11. O'Donnell, V.B.; Ekroos, K.; Liebisch, G.; Wakelam, M. Lipidomics: Current state of the art in a fast-moving field. *Rev. Syst. Biol. Med.* **2019**, *12*, e1466. [CrossRef] [PubMed]
12. Serhan, C.N. Discovery of specialized pro-resolving mediators marks the dawn of resolution physiology and pharmacology. *Mol. Asp. Med.* **2017**, *58*, 1–11. [CrossRef] [PubMed]
13. Fu, Y.; Wang, Y.; Gao, H.; Li, D.; Jiang, R.; Ge, L.; Tong, C.; Xu, K. Associations among dietary Omega-3 polyunsaturated fatty acids, the gut microbiota, and intestinal immunity. *Mediat. Inflamm.* **2021**, *2021*, 8879227. [CrossRef] [PubMed]
14. Stacchiotti, V.; Rezzi, S.; Eggersdorfer, M.; Galli, F. Metabolic and functional interplay between gut microbiota and fat-soluble vitamins. *Crit. Rev. Food. Sci Nutr.* **2020**, *61*, 3211–3232. [CrossRef] [PubMed]
15. Ye, Z.; Xu, Y.J.; Liu, Y. Influences of dietary oils and fats, and the accompanied minor content of components on the gut microbiota and gut inflammation: A review. *Trends Food Sci. Technol.* **2021**, *113*, 255–275. [CrossRef]
16. Shama, S.; Liu, W. Omega-3 fatty acids and gut microbiota: A reciprocal Interaction in nonalcoholic fatty liver disease. *Dig. Dis. Sci.* **2020**, *65*, 906–910. [CrossRef] [PubMed]
17. Amerikanou, C.; Kanoni, S.; Kaliora, A.C.; Barone, A.; Bjelanm, M.; d'Auria, G.; Gioxari, A.; Gosalbes, M.J.; Mouchti, S.; Stathopoulou, M.G.; et al. Effect of Mastiha supplementation on NAFLD: The MAST4HEALTH randomised, controlled trial. *Mol. Nutr. Food Res.* **2021**, *65*, 2001178. [CrossRef] [PubMed]
18. Wolters, M.; Ahrens, J.; Romaní-Pérez, M.; Watkins, C.; Sanz, Y.; Benítez-Páez, A.; Stanton, C.; Gunther, K. Dietary fat, the gut microbiota, and metabolic health—A systematic review conducted within the MyNewGut project. *Clin. Nutr.* **2018**, *8*, 1363–1369. [CrossRef] [PubMed]
19. Serini, S.; Calviello, G. Omega-3 PUFA responders and non-responders and the prevention of lipid dysmetabolism and related diseases. *Nutrients* **2020**, *12*, 1363. [CrossRef] [PubMed]
20. Liu, Y.; Ding, W.; Wang, H.L.; Dai, L.L.; Zong, W.H.; Wang, Y.Z.; Bi, J.; Han, W.; Dong, G.J. Gut microbiota and obesity-associated osteoarthritis. *Osteoarthr. Cartil.* **2019**, *27*, 1257–1265. [CrossRef] [PubMed]

21. Weir, T.L.; Trihka, S.; Thompson, H.J. Diet and cancer risk reduction: The role of diet-microbiota interactions and microbial metabolites. *Semin. Cancer Biol.* **2020**, *70*, 53–60. [CrossRef] [PubMed]
22. Bojkova, B.; Winklewski, P.J.; Wszedybyl-Winklewska, M. Dietary fat and cancer-which is good, which is bad, and the body of evidence. *Int. J. Mol. Sci.* **2020**, *21*, 4114. [CrossRef]
23. Wu, W.K.; Ivanova, E.; Orekhov, A.N. Gut microbiome: A possible common therapeutic target for treatment of atherosclerosis and cancer. *Semin. Cancer Biol.* **2021**, *70*, 85–97. [CrossRef]
24. Fan, Y.; Zhang, J. Dietary modulation of intestinal microbiota: Future opportunities in experimental autoimmune encephalomyelitis and multiple sclerosis. *Front. Microbiol.* **2019**, *10*, 740. [CrossRef]
25. Kendig, M.D.; Leigh, S.J.; Morris, M.J. Unravelling the impacts of western-style diets on brain, gut microbiota and cognition. *Neurosci. Biobehav. Rev.* **2021**, *128*, 233–243. [CrossRef] [PubMed]
26. Schverer, M.; O'Mahony, S.M.; O'Riordan, K.J.; Donoso, F.; Roy, B.L.; Stanton, C.; Dinan, T.G.; Schellekens, H.; Cryan, J.F. Dietary phospholipids: Role in cognitive processes across the lifespan. *Neurosci. Biobehav. Rev.* **2020**, *111*, 183–193. [CrossRef] [PubMed]
27. Robertson, R.C.; Oriach, C.S.; Murphy, K.; Moloney, G.M.; Cryan, J.F.; Dinan, T.G.; Ross, R.P.; Stanton, C. Omega-3 polyunsaturated fatty acids critically regulate behaviour and gut microbiota development in adolescence and adulthood. *Brain Behav. Immun.* **2017**, *59*, 21–37. [CrossRef] [PubMed]
28. Vander Wyst, K.B.; Ortega-Santos, C.P.; Toffoli, S.N.; Lahti, C.E.; Whisner, C.M. Diet, adiposity, and the gut microbiota from infancy to adolescence: A systematic review. *Obes. Rev.* **2021**, *22*, e13175. [CrossRef] [PubMed]
29. Tavella, T.; Rampelli, S.; Guidarelli, G.; Bazzocchi, A.; Gasperini, C.; Pujos-Guillot, E.; Comte, B.; Barone, M.; Biagi, E.; Candela, M.; et al. Elevated gut microbiome abundance of Christensenellaceae, Porphyromonadaceae and Rikenellaceae is associated with reduced visceral adipose tissue and healthier metabolic profile in Italian elderly. *Gut Microb.* **2021**, *13*, 1880221. [CrossRef] [PubMed]
30. Moszak, M.; Szulinska, M.; Walczak-Galezewska, M.; Bogdanski, P. Nutritional approach targeting gut microbiota in NAFLD-To date. *Int. J. Environ. Res. Public Health* **2021**, *18*, 1616. [CrossRef] [PubMed]
31. Li, X.; Zhang, Z.; Cheng, J.; Diao, C.; Yan, Y.; Liu, D.; Wang, H.; Zheng, F. Dietary supplementation of soybean-derived sterols regulates cholesterol metabolism and intestinal microbiota in hamsters. *J. Funct. Foods* **2019**, *59*, 242. [CrossRef]
32. Wang, H.; Liu, D.; Ji, Y.; Liu, Y.; Xu, L.; Guo, Y. Dietary supplementation of black rice anthocyanin extract regulates cholesterol metabolism and improves gut gicrobiota dysbiosis in C57BL/6J mice fed a high-fat and cholesterol diet. *Mol. Nutr. Food Res.* **2020**, *64*, 1900876. [CrossRef] [PubMed]
33. Steinert, R.E.; Lee, Y.K.; Sybesma, W. Vitamins for the gut microbiome. *Trends Mol. Med.* **2020**, *26*, 137–140. [CrossRef]
34. Goncalves, A.; Roi, S.; Nowicki, M.; Dhaussy, A.; Huertas, A.; Amiot, M.J.; Reboul, E. Fat-soluble vitamin intestinal absorption: Absorption sites in the intestine and interactions for absorption. *Food Chem.* **2015**, *172*, 155–160. [CrossRef] [PubMed]
35. Berg, G.; Rybakova, D.; Fischer, D.; Cernava, T.; Vergès, M.C.C.; Charles, T.; Chen, X.; Cocolin, L.; Eversole, K.; Corral, G.H.; et al. Microbiome definition re-visited: Old concepts and new challenges. *Microbiome* **2020**, *8*, 1–22.
36. Thursby, E.; Juge, N. Introduction to the human gut microbiota. *Biochem. J.* **2020**, *474*, 1823–1836. [CrossRef] [PubMed]
37. Cryan, F.; O'Riordan, K.J.; Cowan, C.S.M.; Sandhu, K.V.; Bastiaanssen, T.F.S.; Boehme, M.; Codagnone, M.G.; Cussoto, S.; Fulling, C.; Golubeva, A.V.; et al. The microbiota-gut-brain axis. *Physiol. Rev.* **2019**, *99*, 1877–2013. [CrossRef]
38. Schroeder, J.B.; Backhead, F. Signals from gut microbiota to distant organs in physiology and disease. *Nat. Med.* **2016**, *22*, 1079–1089. [CrossRef] [PubMed]
39. Bessac, A.; Cani, P.D.; Meunier, E.; Dietrich, G.; Knauf, C. Inflammation and gut-brain-axis during type 2 diabetes: Focus on the crosstalk between intestinal immune cells and enteric nervous system. *Front. Neurosci.* **2018**, *12*, 725. [CrossRef]
40. Fulde, M.; Hornef, M.W. Maturation of the enteric mucosal innate immune system during the postnatal period. *Immunol. Rev.* **2014**, *260*, 21–34. [CrossRef] [PubMed]
41. Kamada, N.; Chen, G.Y.; Inohara, N.; Nunez, G. Control of pathogens and pathobionts by the gut microbiota. *Nat. Immunol.* **2013**, *14*, 685–690. [CrossRef]
42. Neuman, H.; Debelius, J.W.; Knight, R.; Koren, O. Microbial endocrinology: The interplay between the microbiota and the endocrine system. *FEMS Microbiol. Rev.* **2015**, *39*, 509–521. [CrossRef]
43. Canfora, E.E.; Jocken, J.W.; Blaak, E.E. Short-chain fatty acids in control of body weight and insulin sensitivity. *Nat. Rev. Endocrinol.* **2015**, *11*, 577–591. [CrossRef] [PubMed]
44. Yano, J.M.; Yu, K.; Donaldson, G.P.; Shastri, G.G.; Ann, P.; Ma, L.; Nagler, C.R.; Ismagilov, R.F.; Mazmanian, S.K.; Hsiao, E.Y. Indigenous bacteria from the gut microbiota regulate host serotonin biosynthesis. *Cell* **2015**, *161*, 264–276. [CrossRef]
45. Hillman, E.T.; Lu, H.; Yao, T.; Nakatsu, C.H. Microbial ecology along the gastrointestinal tract. *Microbes Environ.* **2017**, *32*, 300–313. [CrossRef]
46. Sommer, F.; Anderson, J.M.; Bharti, R.; Raes, J.; Rosenstiel, P. The resilience of the intestinal microbiota influences health and disease. *Nat. Rev. Microbiol.* **2017**, *15*, 630–638. [CrossRef] [PubMed]
47. Rinninella, E.; Raoul, P.; Cintoni, M.; Franceschi, F.; Miggiano, G.A.D.; Gasbarrini, A.; Mele, M.C. What is the healthy gut microbiota composition? A changing ecosystem across age, environment, diet and disease. *Microorganisms* **2019**, *7*, 14. [CrossRef]
48. Sanchez-Tapia, M.; Tovar, A.R.; Torres, N. Diet as regulator of gut microbiota and its role in health and disease. *Arch. Med. Res.* **2019**, *50*, 259–268. [CrossRef] [PubMed]

49. Holmes, E.; Li, J.V.; Marchesi, J.R.; Nicholson, J.K. Gut microbiota composition and activity in relation to host metabolic phenotype and disease risk. *Cell Metab.* **2012**, *16*, 559–564. [CrossRef]
50. Flint, H.J.; Scott, K.P.; Louis, P.; Duncan, S.H. The role of gut microbiota in nutrition and health. *Nat. Rev. Gastroenterol. Hepatol.* **2012**, *9*, 577–590. [CrossRef]
51. Arumugam, M.; Raes, J.; Pelletier, E.; Le Paslier, D.; Yamada, T.; Mende, D.R.; Fernades, G.R.; Tap, J.; Bruls, T.; Batto, J.M.; et al. Enterotypes of the human gut microbiome. *Nature* **2011**, *12*, 174–180. [CrossRef]
52. Evgenik, A.; Evgenik, M. Exploring the impact of intestinal ion transport on the gut microbiota. *Comput. Struct. Biotechnol. J.* **2021**, *19*, 134–144.
53. Clemente, J.C.; Ursell, L.K.; Parfrey, L.W.; Knight, R. The impact of the gut microbiota on human health: An integrative view. *Cell* **2012**, *148*, 1258–1270. [CrossRef] [PubMed]
54. Holister, B.; Gao, C.; Versalovic, J. Compositional and functional features of Gastrointestinal Microbiome and Their Effects on Human Health. *Gastroenterology* **2014**, *146*, 1449–1458. [CrossRef] [PubMed]
55. Hasan, N.; Yang, H. Factors affecting the composition of the gut microbiota, and its modulation. *PeerJ* **2019**, *7*, e7502. [CrossRef] [PubMed]
56. García-Montero, C.; Fraile-Martínez, O.; Gómez-Lahoz, A.M.; Pekarek, L.; Castellanos, A.J.; Noguerales-Fraguas, F.; Coca, S.; Guijarro, L.G.; García-Honduvilla, N.; Asúnsolo, A.; et al. Nutritional components in Western diet versus Mediterranean diet at the gut microbiota-immune system interplay. Implications for health and disease. *Nutrients* **2021**, *13*, 699. [CrossRef] [PubMed]
57. Lecerf, J.M.; de Lorgeril, M. Dietary cholesterol: From physiology to cardiovascular risk. *Br. J. Nutr.* **2021**, *106*, 6–14. [CrossRef]
58. Racette, S.B.; Lin, X.; Lefevre, M.; Spearie, C.A.; Most, M.M.; Ma, L.; Ostlund, R.E. Dose effects of dietary phytosterols on cholesterol metabolism: A control feeding study. *Am. J. Clin. Nutr.* **2010**, *91*, 32–38. [CrossRef]
59. García-Llatas, G.; Rodríguez-Estrada, M.T. Current and new insights on phytosterols oxides in plant sterol-enriched food. *Chem. Phys. Lipids* **2021**, *164*, 607–624. [CrossRef] [PubMed]
60. Feng, S.M.; Dai, Z.Q.; Liu, A.N.; Wang, H.; Chen, J.S.; Luo, Z.S.; Yang, C.S. Beta-Sitosterol and stigmasterol ameliorate dextran sulfate sodium-induced colitis in mice fed a high fat Westernstyle diet. *Food Funct.* **2017**, *8*, 4179–4186. [CrossRef]
61. Zhang, X.; Coker, O.O.; Chu, E.S.; Fu, K.; Lau, H.C.H.; Wang, Y.X.; Chan, A.W.; Wei, H.; Yang, X.; Sung, J.Y.; et al. Dietary cholesterol drives fatty liver-associated liver cancer by modulating gut microbiota and metabolites. *Gut* **2021**, *70*, 761–774. [CrossRef] [PubMed]
62. Cuevas-Tena, M.; Alegria, A.; Lagarda, M.J.; Venema, K. Impact of plant sterols enrichment dose on gut microbiota from lean and obese subjects using TIM-2 in vitro fermentation model. *Funct. Foods* **2019**, *54*, 164–174. [CrossRef]
63. Cuevas-Tena, M.; del Pulgar, E.M.G.; Benítez-Páez, A.; Sanz, Y.; Alegría, A.; Lagarda, J.M. Plant sterols and human gut microbiota relationship: An in vitro colonic fermentation study. *J. Funct. Foods* **2018**, *44*, 322–329. [CrossRef]
64. Blanco-Morales, V.; Garcia-Llatas, G.; Yebra, M.J.; Sentandreu, V.; Lagarda, M.J.; Alegría, A. Impact of a Plant Sterol- and Galactooligosaccharide-Enriched Beverage on Colonic Metabolism and Gut Microbiota Composition Using an in vitro Dynamic Model. *J. Agric. Food Chem.* **2020**, *68*, 1884–1895. [CrossRef]
65. Vezza, T.; Canet, F.; de Maranon, A.M.; Banuls, C.; Rocha, M.; Víctor, V.M. Phytosterols: Nutritional health players in the management of obesity and its related disorders. *Antioxidants* **2020**, *9*, 1266. [CrossRef] [PubMed]
66. Xia, G.L.; Sun, J.; Fan, Y.T.; Zhao, F.F.; Ahmed, G.; Jin, Y.; Zhang, Y.; Wang, H. β-Sitosterol attenuates high grain diet-induced inflammatory stress and modifies rumen fermentation and microbiota in sheep. *Animals* **2020**, *10*, 171. [CrossRef]
67. Li, X.; Wang, H.; Wang, T.; Zheng, F.; Wang, H.; Wang, C. Dietary wood pulp-derived sterols modulation of cholesterol metabolism and gut microbiota in high-fat-diet-fed hamsters. *Food Funct.* **2019**, *10*, 775–785. [CrossRef] [PubMed]
68. Song, L.; Zhao, X.G.; Ouyang, P.L.; Guan, Q.; Yang, L.; Peng, F.; Du, H.; Yin, F.; Yan, W.; Yu, W.J.; et al. Combined effect of n3 fatty acids and phytosterol esters on alleviating hepatic steatosis in non-alcoholic fatty liver disease subjects: A double-blind placebo-controlled clinical trial. *Br. J. Nutr.* **2020**, *123*, 1148–1158. [CrossRef] [PubMed]
69. Baumgartner, S.; Mensink, R.P.; Smet, E.D.; Konings, M.; Fuentes, S.; de Vos, W.; Plat, J. Effects of plant sterol ester consumption on fasting plasma oxy(phyto)sterol concentrations as related to fecal microbiota characteristics. *J. Steroid Biochem.* **2017**, *169*, 46–53. [CrossRef] [PubMed]
70. Schott, H.F.; Krautbauer, S.; Horing, M.; Liebisch, G.; Matysik, S.A. Validated, fast method for quantification of sterols and gut microbiome derived 5α/β-stanols in human feces by isotope dilution LC-high-resolution MS. *Anal. Chem.* **2018**, *90*, 8487–8494. [CrossRef] [PubMed]
71. Tong, J.; Satyanarayanan, S.K.; Su, H. Nutraceuticals and probiotics in the management of psychiatric and neurologicaldisorders: A focus on microbiota-gut-brain-immune axis. *Brain Behav. Immun.* **2020**, *90*, 403–419. [CrossRef] [PubMed]
72. Biesalski, H.K. Nutrition meets the microbiome: Micronutrients and the microbiota. *Ann. N. Y. Acad. Sci.* **2016**, *1372*, 53–64. [CrossRef] [PubMed]
73. Maher, S.E.; O'Brien, E.C.; Moore, R.L.; Byrne, D.F.; Geragthy, A.A.; Saldova, R.; Murphy, E.F.; Sinderen, D.V.; Cotter, P.D. The association between the maternal diet and the maternal and infant gut microbiome: A systematic review. *Br. J. Nutr.* **2020**, *4*, 1–29. [CrossRef] [PubMed]
74. Xiao, L.; Cui, T.; Liu, S.; Chen, B.; Wang, Y.; Yang, T.; Li, T.; Chen, J. Vitamin A supplementation improves the intestinal mucosal barrier and facilitates the expression of tight junction proteins in rats with diarrhea. *Nutrition* **2019**, *57*, 97–108. [CrossRef] [PubMed]

75. Zhang, T.; Sun, P.; Geng, Q.; Fan, H.; Gong, Y.; Hu, Y.; Shan, L.; Sun, Y.; Shen, W.; Zhou, Y. Disrupted spermatogenesis in a metabolic syndrome model: The role of vitamin A metabolism in the gut–testis axis. *Gut* **2022**, *71*, 78–87. [CrossRef]
76. Biyong, E.F.; Alfos, S.; Dumetz, F.; Helbling, J.C.; Aubert, A.; Brossaud, J.; Foury, A.; Moisan, M.P.; Laye, S.; Richard, E.; et al. Dietary vitamin A supplementation prevents early obesogenic diet-induced microbiota, neuronal and cognitive alterations. *Int. J. Obes.* **2021**, *45*, 588–598. [CrossRef]
77. Chen, B.; Liu, S.; Feng, D.; Xiao, L.; Yang, T.; Li, T.; Sun, W.; Chen, J. Vitamin A Deficiency in the Early-Life Periods Alters a Diversity of the Colonic Mucosal Microbiota in Rats. *Front. Nutr.* **2020**, *4*, 580780. [CrossRef] [PubMed]
78. Azzi, A. Many tocopherols, one vitamin E. *Mol. Aspects Med.* **2018**, *61*, 92–103. [CrossRef]
79. Galli, F.; Azzi, A.; Birringer, M.; Cook-Mills, J.M.; Eggersdorfer, M.; Frank, J.; Cruciani, G.; Lorkowski, S.; Ozer, N.K. Vitamin E: Emerging Aspects and New Directions. *Free Radical Bio. Med.* **2017**, *102*, 16–36. [CrossRef] [PubMed]
80. Choi, Y.; Lee, S.; Kim, S.; Lee, J.; Ha, J.; Oh, H.; Lee, Y.; Kim, Y.; Yoon, Y. Vitamin E (α-tocopherol) consumption influences gut microbiota composition. *Int. J. Food Sci. Nutr.* **2020**, *71*, 221–225. [CrossRef] [PubMed]
81. Kim, D.J.; Yoon, S.; Ji, S.C.; Yang, J.; Kim, Y.K.; Lee, S.; Yu, K.S.; Jang, I.J.; Chung, J.Y.; Cho, J.Y. Ursodeoxycholic acid improves liver function via phenylalanine/tyrosine pathway and microbiome remodeling in patients with liver dysfunction. *Sci. Rep.* **2018**, *8*, 11874. [CrossRef] [PubMed]
82. Yang, C.; Zhao, Y.; Im, C.; Nakatsu, C.; Jones-Hall, Y.; Jiang, Q. Vitamin E delta-tocotrienol and metabolite 13′-carboxychromanol inhibit colitis-associated colon tumorigenesis and modulate gut microbiota in mice. *J. Nutr. Biochem.* **2021**, *89*, 108567. [CrossRef] [PubMed]
83. Ellis, J.L.; Karl, P.; Oliverio, A.M.; Fu, X.; Soares, J.W.; Wolfe, E.B.; Hernandez, C.J.; Mason, J.B.; Booth, S.L. Dietary vitamin K is remodeled by gut microbiota and influences community composition. *Gut Microbes* **2021**, *13*, 1887721. [CrossRef]
84. Dash, N.R.; Al Bataineh, M.T. Metagenomic analysis of the gut microbiome reveals enrichment of menaquinones (vitamin K2) pathway in diabetes mellitus. *Diabetes Metab. J.* **2021**, *45*, 77–85. [CrossRef] [PubMed]
85. Zhang, Y.; Ma, C.; Zhao, J.; Xu, H.; Hou, Q.; Zhang, H. Lactobacillus casei and vitamin K2 prevent intestinal tumorigenesis in mice via adiponectin-elevated different signaling pathways. *Oncotarget* **2017**, *8*, 24719–24727. [CrossRef]
86. Fleet, J.C. The role of vitamin D in the endocrinology controlling calcium homeostasis. *Mol. Cell. Endocrinol.* **2017**, *453*, 36–45. [CrossRef] [PubMed]
87. Beveridge, L.A.; Struthers, A.D.; Khan, F.; Jorde, R.; Scragg, R.; Macdonald, H.M.; Alvarez, J.A.; Boxer, R.S.; Dalbeni, A.; Gepner, A.D.; et al. Effect of Vitamin D Supplementation on blood pressure: A systematic review and meta-analysis incorporating individual patient data. *JAMA Intern. Med.* **2015**, *175*, 745–754. [CrossRef] [PubMed]
88. Calton, E.K.; Keane, K.N.; Newsholme, P.; Soares, M.J. The impact of vitamin D levels on inflammatory status: A systematic review of immune cell studies. *PLoS ONE* **2015**, *10*, e0141770. [CrossRef]
89. Clark, A.; Mach, N. Role of vitamin D in the hygiene hypothesis: The interplay between Vitamin D, Vitamin D receptors, gut microbiota, and immune response. *Front. Immunol.* **2016**, *7*, 627. [CrossRef] [PubMed]
90. Fakhoury, H.M.A.; Peter, K.R.; AlKattan, W.; Al Anouti, F.; Elahi, M.A.; Karras, S.N.; Grant, W.B. Vitamin D and intestinal homeostasis: Barrier, microbiota, and immune modulation. *J. Ster. Biochem. Mol. Biol.* **2020**, *200*, 105663. [CrossRef]
91. Garcia-Serna, A.M.; Morales, E. Neurodevelopmental effects of prenatal vitamin D in humans: Systematic review and meta-analysis. *Mol. Psychiatry* **2020**, *25*, 2468–2481. [CrossRef] [PubMed]
92. Yamamoto, E.A.; Jørgensen, T.N. Relationships between Vitamin D, gut microbiome, and systemic autoimmunity. *Front. Immunol.* **2020**, *10*, 3141. [CrossRef] [PubMed]
93. Charoenngam, N.; Holick, M.F. Immunologic effects of vitamin D on human health and disease. *Nutrients* **2020**, *12*, 2097. [CrossRef] [PubMed]
94. Soltys, K.; Stuchlikova, M.; Hlavaty, T.; Gaalova, B.; Budis, J.; Gazdarica, J.; Krajcovicova, A.; Zelinkova, Z.; Szemes, T.; Kuba, D.; et al. Seasonal changes of circulating 25-hydroxyvitamin D correlate with the lower gut microbiome composition in inflammatory bowel disease patients. *Sci Rep.* **2020**, *10*, 6024. [CrossRef]
95. Guida, F.; Boccella, S.; Belardo, C.; Iannotta, M.; Piscitelli, F.; de Filippis, F.; Paino, S.; Ricciardi, F.; Marabese, I.; Luongo, L.; et al. Altered gut microbiota and endocannabinoid system tone in vitamin D deficiency-mediated chronic pain. *Brain Behav. Immun.* **2018**, *67*, 230–245. [CrossRef] [PubMed]
96. Jiang, S.; Zhu, Q.; Mai, M.; Yang, W.; Du, G. Vitamin B and vitamin D as modulators of gut microbiota in overweight individuals. *Int. J. Food Sci. Nutr.* **2020**, *71*, 1001–1009.
97. Lee, P.; Hsieh, Y.; Huo, T.; Yang, U.; Lin, C.; Li, C.; Huang, Y.; Hou, M.; Lin, H.; Lee, K. Active Vitamin D 3 Treatment Attenuated Bacterial Translocation via Improving Intestinal Barriers in Cirrhotic Rats. *Mol. Nutr. Food Res.* **2020**, *65*, 2000937. [CrossRef]
98. Zhang, X.; Shang, X.; Jin, S.; Ma, Z.; Wang, H.; Na, A.O.; Yang, J.; Du, J. Vitamin D ameliorates high-fat-diet-induced hepatic injury via inhabiting pyroptosis and alters gut microbiota in rats. *Arch. Biochem. Biophys.* **2021**, *705*, 108894. [CrossRef] [PubMed]
99. Drall, K.M.; Field, C.J.; Haqq, A.M.; de Souza, R.J.; Tun, T.M.; Morales-Lizcano, N.P.; Konya, T.B.; Guttman, D.S.; Azad, M.B.; Becker, A.B.; et al. Vitamin D supplementation in pregnancy and early infancy in relation to gut microbiota composition and C. difficile colonization: Implications for viral respiratory infections. *Gut Microbes* **2020**, *12*, 1799734. [CrossRef] [PubMed]
100. Lei, W.T.; Huang, K.Y.; Jhong, J.H.; Chen, C.H.; Weng, S.L. Metagenomic analysis of the gut microbiome composition associated with vitamin D supplementation in Taiwanese infants. *Sci. Rep.* **2021**, *11*, 2856. [CrossRef] [PubMed]

101. Palacios-Gonzalez, B.; Ramirez-Salazar, E.G.; Rivera-Paredez, B.; Quiterio, M.; Flores, Y.N.; Macias-Kauffer, L.; Moran-Ramos, S.; Denova-Gutierez, E.; Ibarra-González, I.; Vela-Amieva, M.; et al. A multi-omic analysis for low bone mineral density in postmenopausal women suggests a relationship between diet, metabolites and microbiota. *Microorganisms* **2020**, *8*, 1630. [CrossRef]
102. Singh, P.; Rawat, A.; Alwakeel, M.; Sharif, E.; Al Khodor, S. The potential role of vitamin D supplementation as a gut microbiota modifier in healthy individuals. *Sci. Rep.* **2020**, *10*, 1–14. [CrossRef]
103. Pham, H.; Waterhouse, M.; Baxter, C.; Romero, B.D.; McLeod, D.S.A.; Armstrong, B.K.; Ebeling, P.R.; English, D.R.; Hartel, G.; Kimlin, M.G.; et al. The effect of vitamin D supplementation on acute respiratory tract infection in older Australian adults: An analysis of data from the D-Health Trial. *Lancet Diabetes Endocrinol.* **2021**, *9*, 69–81. [CrossRef]
104. Tanaka, T.; Shnimizu, M.; Moriwaki, H. Cancer chemoprevention by carotenoids. *Molecules* **2012**, *17*, 3202–3242. [CrossRef]
105. Tsiaka, T.; Fotakis, C.; Lantzouraki, D.Z.; Tsiantas, K.; Siapi, E.; Sinanoglou, V.J.; Zoumpoulakis, P. Expanding the role of sub-exploited DOE-High energy extraction and metabolomic profiling towards agro-byproduct valorization: The case of carotenoid-rich apricot pulp. *Molecules* **2020**, *25*, 2702. [CrossRef] [PubMed]
106. Mounien, L.; Tourniaire, F.; Landrier, J.F. Anti-obesity effect of carotenoids: Direct impact on adipose tissue and adipose tissue-driven indirect effects. *Nutrients* **2019**, *11*, 1562. [CrossRef]
107. Melendez-Martinez, A.J.; Stinco, C.M.; Mapelli-Brahm, P. Skin Carotenoids in Public Health and Nutricosmetics: The Emerging Roles and Applications of the UV Radiation-Absorbing Colourless Carotenoids Phytoene and Phytofluene. *Nutrients* **2019**, *11*, 1093. [CrossRef] [PubMed]
108. Xia, H.; Liu, C.; Li, C.C.; Fu, M.; Takahashi, S.; Hu, K.Q.; Aizawa, K.; Hiroyuki, S.; Wu, G.; Zhao, L.; et al. Dietary tomato powder inhibits high-fat diet-promoted hepatocellular carcinoma with alteration of gut microbiota in mice lacking carotenoid cleavage enzymes. *Cancer Prev. Res.* **2018**, *11*, 797–810. [CrossRef] [PubMed]
109. Wiese, M.; Bashmakov, Y.; Chalyk, N.; Nielsen, D.S.; Krych, L.; Kot, W.; Klochkov, V.; Pristensky, D.; Bandaletova, T.; Chernyshova, M.; et al. Prebiotic effect of lycopene and dark chocolate on gut microbiome with systemic changes in liver metabolism, skeletal muscles and skin in moderately obese persons. *Biomed. Res. Int.* **2019**, *2019*, 4625279. [CrossRef] [PubMed]
110. Liu, H.; Liu, M.; Fu, X.; Zhang, Z.; Zhu, L.; Zheng, X.; Liu, J. Astaxanthin prevents alcoholic fatty liver disease by modulating mouse gut microbiota. *Nutrients* **2018**, *10*, 1298. [CrossRef] [PubMed]
111. Terasaki, M.; Uehara, O.; Ogasa, S.; Sano, T.; Kubota, A.; Kojima, H.; Tanaka, T.; Maeda, H.; Miyashita, K.; Mutoh, M. Alteration of fecal microbiota by fucoxanthin results in prevention of colorectal cancer in AOM/DSS mice. *Carcinogenesis* **2020**, *42*, 210–219. [CrossRef] [PubMed]
112. Wang, Y.; Tang, C.; Tang, Y.; Yin, H.; Liu, X. Capsaicin has an anti-obesity effect through alterations in gut microbiota populations and short-chain fatty acid concentrations. *Food Nutr. Res.* **2020**, *64*, 3525. [CrossRef] [PubMed]
113. Wu, T.; Gao, Y.; Hao, J.; Geng, J.; Zhang, J.; Yin, J.; Liu, R.; Sui, W.; Gong, L.; Zhang, M. Capsanthin extract prevents obesity, reduces serum TMAO levels and modulates the gut microbiota composition in high-fat diet induced obese C57BL/6J mice. *Food Res. Int.* **2020**, *128*, 108774. [CrossRef] [PubMed]
114. Iglesias-Carres, L.; Hughes, M.D.; Steele, C.N.; Ponder, M.A.; Davy, K.P.; Neilson, A.P. Use of dietary phytochemicals for inhibition of trimethylamine N-oxide formation. *J. Nutr. Biochem.* **2021**, *91*, 108600. [CrossRef]
115. Gonzalez-Prendes, R.; Pena, R.N.; Sole, E.; Seradj, A.R.; Estany, J.; Ramayo-Caldas, Y. Modulatory effect of protein and carotene dietary levels on pig gut microbiota. *Sci. Rep.* **2019**, *9*, 14582. [CrossRef] [PubMed]
116. Schmidt, K.M.; Haddad, E.N.; Sugino, K.Y.; Vevang, K.R.; Peterson, L.A.; Koratkar, R.; Gross, M.D.; Kerver, J.M.; Comstock, S.S. Dietary and plasma carotenoids are positively associated with alpha diversity in the fecal microbiota of pregnant women. *J. Food Sci.* **2021**, *86*, 602–613. [CrossRef] [PubMed]
117. Wu, L.; Lyu, Y.; Srinivasagan, R.; Wu, J.; Ojo, B.; Tang, M.; El-Rassi, G.D.; Metzinger, K.; Smith, B.J.; Lucas, A.E.; et al. Astaxanthin Shifted Gut Microbiota Is Associated with Inflammation and Metabolic Homeostasis in Mice. *J. Nutr.* **2020**, *150*, 2687–2698. [CrossRef] [PubMed]
118. Guo, B.; Yang, B.; Pang, X.; Chen, T.; Chen, F.; Cheng, K.W. Fucoxanthin modulates cecal and fecal microbiota differently based on diet. *Food Funct.* **2019**, *10*, 5644–5655. [CrossRef]
119. Zhu, L.; Song, Y.; Liu, H.; Wu, M.; Gong, H.; Lan, H.; Zheng, X. Gut microbiota regulation and anti-inflammatory effect of β-carotene in dextran sulfate sodium-stimulated ulcerative colitis in rats. *J. Food Sci.* **2021**, *86*, 2118–2130. [CrossRef]
120. Leuti, A.; Fazio, D.; Fava, M.; Piccoli, A.; Oddi, S.; Maccarrone, M. Bioactive lipids, inflammation and chronic diseases. *Adv. Drug Deliv. Rev.* **2020**, *159*, 133–169. [CrossRef] [PubMed]
121. Innes, J.K.; Calder, P.C. Omega-6 fatty acids and inflammation. *Prostaglandins Leukot. Essent. Fat. Acids* **2018**, *132*, 41–48. [CrossRef]
122. Chiurchiu, V.; Maccarrone, M. Bioactive lipids and chronic inflammation: Managing the fire within. *Front. Immunol.* **2018**, *9*, 38. [CrossRef] [PubMed]
123. Biringer, R.G. The enzymology of human eicosanoid pathways: The lipoxygenase branches. *Mol. Biol. Rep.* **2020**, *47*, 7189–7207. [CrossRef]
124. Ferrer, R.; Moreno, J. Role of eicosanoids on intestinal epithelial homeostasis. *Biochem. Pharmacol.* **2010**, *80*, 431–438. [PubMed]
125. Bezirtzoglou, E.E.V. Intestinal cytochromes P450 regulating the intestinal microbiota and its probiotic profile. *Microb. Ecol. Health D.* **2012**, *23*, 18370. [CrossRef] [PubMed]
126. An, J.U.; Hong, S.H.; Oh, D.K. Regiospecificity of a novel bacterial lipoxygenase from Myxococcus xanthus for polyunsaturated fatty acids. *BBA-MOL Cell Biol.* **2018**, *1863*, 823–833. [CrossRef] [PubMed]

127. Huang, N.; Wang, M.; Peng, J.; Wei, H. Role of arachidonic acid-derived eicosanoids in intestinal innate immunity. *Crit. Rev. Food Sci. Nutr.* **2020**, *61*, 2399–2410. [CrossRef]
128. Mizuno, R.; Kawada, K.; Sakai, Y. Prostaglandin E2/EP Signaling in the tumor microenvironment of colorectal cancer. *Int. J. Mol. Sci.* **2019**, *20*, 6254.
129. Li, Y.; Soendergaard, C.; Bergenheim, F.H.; Aronoff, D.M.; Milne, G.; Riis, L.B.; Seidelin, J.B.; Jensen, K.B.; Nielsen, O.H. COX-2–PGE2 Signaling Impairs Intestinal Epithelial Regeneration and Associates with TNF Inhibitor Responsiveness in Ulcerative Colitis. *EBioMedicine* **2018**, *36*, 497–507. [CrossRef] [PubMed]
130. Jala, V.R.; Maturu, P.; Bodduluri, S.R.; Krishnan, E.; Mathis, S.; Subbarao, K.; Wang, M.; Jenson, A.B.; Proctor, M.L.; Rouchka, E.C.; et al. Leukotriene B4-receptor-1 mediated host response shapes gut microbiota and controls colon tumor progression. *Oncoimmunology* **2017**, *6*, e1361593. [CrossRef]
131. Wawrzyniak, P.; Noureddine, N.; Wawrzyniak, M.; Lucchinetti, E.; Kramer, S.D.; Rogler, G.; Zaugg, M.; Hersberger, M. Nutritional lipids and mucosal inflammation. *Mol. Nutr. Food Res.* **2020**, *65*, 1901269. [CrossRef] [PubMed]
132. Liu, F.; Smith, A.D.; Solano-Aguilar, G.; Wang, T.Y.Y.; Pham, Q.; Beshah, E.; Tang, Q.; Urban, J.F.; Xue, C.; Robert, W.L.; et al. Mechanistic insights into the attenuation of intestinal inflammation and modulation of the gut microbiome by krill oil using in vitro and in vivo models. *Microbiome* **2020**, *8*, 83. [CrossRef]
133. Yao, Q.; Li, H.; Fan, L.; Zhang, Y.; Zhao, S.; Zheng, N.; Wang, J. Dietary Regulation of the Crosstalk between Gut Microbiome and Immune Response in Inflammatory Bowel Disease. *Foods* **2021**, *10*, 368. [CrossRef]
134. Ajabnoor, S.M.; Thorpe, G.; Abdelhamid, A.; Hooper, L. Long-term effects of increasing omega-3, omega-6 and total polyunsaturated fats on inflammatory bowel disease and markers of inflammation: A systematic review and meta-analysis of randomized controlled trials. *Eur. J. Nutr.* **2021**, *60*, 2293–2316. [CrossRef] [PubMed]
135. Cani, P.D.; Plovier, M.; van Hul, M.; Geurts, L.; Delzenne, N.M.; Druart, C.; Everard, A. Endocannabinoids–at the crossroads between the gut microbiota and host metabolism. *Nat. Rev. Endocrinol.* **2016**, *12*, 133–143. [CrossRef] [PubMed]
136. Sałaga, M.; Mokrowiecka, A.; Zakrzewski, P.K.; Cygankiewicz, A.; Leishman, E.; Sobczak, M.; Zatorski, H.; Małecka-Panas, E.; Kordek, R.; Storr, M.; et al. Experimental colitis in mice is attenuated by changes in the levels of endocannabinoid metabolites induced by selective inhibition of fatty acid amide hydrolase (FAAH). *J. Crohn's Colitis* **2014**, *8*, 998–1009.
137. Fornelos, N.; Franzosa, E.A.; Bishai, J.; Annand, J.W.; Oka, A.; Lloyd-Price, J.; Arthur, T.D.; Garner, A.; Avila-Pacheco, J.; Haiser, H.J.; et al. Growth effects of N-acylethanolamines on gut bacteria reflect altered bacterial abundances in inflammatory bowel disease. *Nat. Microbiol.* **2020**, *5*, 486–497. [CrossRef]
138. Mestre, L.; Carrillo-Salinas, F.J.; Mecha, M.; Feliu, A.; Guazaet, C. Gut microbiota, cannabinoid system and neuroimmune interactions: New perspectives in multiple sclerosis. *Biochem. Pharmacol.* **2018**, *157*, 51–66. [CrossRef] [PubMed]
139. Kaur, G.; Behl, T.; Bungau, S.; Kumar, A.; Uddin, M.S.; Mehta, V.; Zengin, G.; Mathew, B.; Shah, M.A.; Arora, S. Dysregulation of the gut-brain axis, dysbiosis and influence of numerous factors on gut microbiota associated Parkinson's Disease. *Curr. Neuropharmacol.* **2020**, *19*, 233–247. [CrossRef]
140. Minichino, A.; Jackson, M.A.; Francesconi, M.; Steves, C.J.; Menni, C.; Burnet, P.W.J.; Lennox, B.R. Endocannabinoid system mediates the association between gut-microbiota diversity and anhedonia/amotivation in a general population cohort. *Mol. Psychiatry* **2021**, *26*, 6269–6276. [CrossRef] [PubMed]
141. Iannotti, F.A.; Di Marzo, V. The Gut Microbiome, Endocannabinoids and Metabolic Disorders. *J. Endocrinol.* **2020**, *248*, 83–97. [CrossRef]
142. Geurts, L.; Everard, A.; van Hul, M.; Essaghir, A.; Duparc, T.; Matamoros, S.; Plovier, H.; Castel, J.; Denis, R.G.P.; Bergiers, M.; et al. Adipose tissue NAPE-PLD controls fat mass development by altering the browning process and gut microbiota. *Nat. Commun.* **2015**, *6*, 6495. [CrossRef] [PubMed]
143. Castonguay-Paradis, S.; Lacroix, S.; Rochefort, G.; Parent, L.; Perron, J.; Martin, C.; Lamarche, B.; Raymond, F.; Flamand, N.; di Marzo, V.; et al. Dietary fatty acid intake and gut microbiota determine circulating endocannabinoidome signaling beyond the effect of body fat. *Sci. Rep.* **2020**, *10*, 15975. [CrossRef] [PubMed]
144. Jansma, J.; Brinkman, F.; van Hemert, S.; El Aidy, S. Targeting the endocannabinoid system with microbial interventions to improve gut integrity. *Prog. Neuro-Psychopharmacol. Biol. Psychiatry* **2021**, *106*, 110169. [CrossRef] [PubMed]
145. Forte, N.; Fernandez-Rilo, A.C.; Palomba, L.; di Marzo, V.; Cristino, L. Obesity affects the microbiota-gut-brain axis and the regulation thereof by endocannabinoids and related mediators. *Int. J. Mol. Sci.* **2020**, *21*, 1554. [CrossRef] [PubMed]
146. Zhu, L.; Sha, L.; Li, K.; Wang, Z.; Wang, T.; Li, Y.; Liu, P.; Dong, X.; Dong, Y.; Zhang, X.; et al. Dietary flaxseed oil rich in omega-3 suppresses severity of type 2 diabetes mellitus via anti-inflammation and modulating gut microbiota in rats. *Lipids Health Dis.* **2020**, *19*, 20. [CrossRef] [PubMed]
147. Serhan, C.N.; Levy, B.D. Resolvins in inflammation: Emergence of the pro-resolving superfamily of mediators. *J. Clin. Investig.* **2018**, *128*, 2657–2669. [CrossRef] [PubMed]
148. Doyle, R.; Sadlier, D.M.; Godson, C. Pro-resolving lipid mediators: Agents of anti-ageing? *Semin. Immunol.* **2018**, *40*, 36–48. [CrossRef] [PubMed]
149. Quiros, M.; Nusrat, A. Saving problematic mucosae: SPMs in intestinal mucosal inflammation and repair. *Trends Mol. Med.* **2019**, *25*, 124–135. [CrossRef] [PubMed]
150. Chiang, N.; Serhan, C.N. Specialized pro-resolving mediator network: An update on production and actions. *Essays Biochem.* **2020**, *65*, 443–446.

151. Gobbetti, T.; Dalli, J.; Colas, R.A.; Federici-Canova, D.; Aursnes, M.; Bonnet, D.; Alric, L.; Vergnolle, M.; Deraison, C.; Hansen, T.V.; et al. Protectin D1n-3 DPA and resolvin D5n-3 DPA are effectors of intestinal protection. *Proc. Natl. Acad. Sci. USA* **2017**, *114*, 3963–3968. [CrossRef] [PubMed]
152. Leon, I.C.; Quesada-Vazquez, S.; Sainz, N.; Guruceage, E.; Escote, X.; Moreno-Aliaga, M.J. Effects of Maresin 1 (MaR1) on colonic inflammation and gut dysbiosis in diet-induced obese mice. *Microorganisms* **2020**, *8*, 1156. [CrossRef] [PubMed]
153. Lam, Y.Y.; Ha, C.W.Y.; Hoffmann, J.M.A.; Oscarsson, J.; Dinudom, A.; Mather, T.J.; Cook, D.I.; Hunt, N.H.; Caterson, I.D.; Holmes, A.J.; et al. Effects of dietary fat profile on gut permeability and microbiota and their relationships with metabolic changes in mice. *Obesity* **2015**, *23*, 1429–1439. [CrossRef] [PubMed]
154. Baptista, L.C.; Sun, Y.; Carter, C.S.; Buford, T.W. Crosstalk between the gut microbiome and bioactive lipids: Therapeutic targets in cognitive frailty. *Front. Nutr.* **2020**, *7*, 17. [CrossRef] [PubMed]
155. Ma, H.; Yu, Y.; Wang, M.; Li, Z.; Xu, H.; Tian, C.; Zhang, J.; Ye, X.; Li, X. Correlation between microbes and colorectal cancer: Tumor apoptosis is induced by sitosterols through promoting gut microbiota to produce short-chain fatty acids. *Apoptosis* **2019**, *24*, 168–183. [CrossRef] [PubMed]
156. Kouidhi, S.; Zidi, O.; Alhujaily, M.; Souai, N.; Mosbah, A.; Belali, T.M.; Ghedira, K.; El Kossai, L.; El Manaa, J.; Mnif, W.; et al. Fecal Metabolomics Reveals Distinct Profiles of Kidney Transplant Recipients and Healthy Controls. *Diagnostics* **2021**, *11*, 807. [CrossRef]
157. Montrose, D.C.; Nakanishi, M.; Murphy, R.C.; Zarini, S.; McAleer, J.P.; Vella, A.T.; Rosenberg, D.W. The role of PGE2 in intestinal inflammation and tumorgenesis. *Prostaglandins Other Lipid Mediat.* **2015**, *116–117*, 26–36.
158. Börgeson, E.; Johnson, A.M.; Lee, Y.S.; Till, A.; Syed, G.H.; Ali-Shah, S.T.; Guiry, P.J.; Dalli, J.; Colas, R.A.; Serhan, C.N.; et al. Lipoxin A4 attenuates obesity-induced adipose inflammation and associated liver and kidney disease. *Cell Metabol.* **2015**, *22*, 125–137. [CrossRef]
159. Igarashi, M.; Watanabe, K.; Tsuduki, T.; Kimura, I.; Kubota, N. NAPE-PLD controls OEA synthesis and fat absorption by regulating lipoprotein synthesis in an in vitro model of intestinal epithelial cells. *FASEB J.* **2019**, *33*, 3167–3179. [CrossRef] [PubMed]
160. Dalli, J.; Chiang, N.; Serhan, C.N. Elucidation of novel 13-series resolvins that increase with atorvastatin and clear infections. *Nat. Med.* **2015**, *21*, 1071–1075. [CrossRef]
161. Sasaki, A.; Fukuda, H.; Shiida, N.; Tanaka, N.; Furugen, A.; Ogura, J.; Shuto, S.; Mano, N.; Yamaguchi, H. Determination of ω-6 and ω-3 metabolites in human urine samples using UPLC/MS/MS. *Anal. Bioanal. Chem.* **2015**, *407*, 1625–1639. [CrossRef] [PubMed]
162. Norrris, P.C.; Skulas-Ray, C.; Riley, I.; Richter, C.K.; Kris-Etherton, P.M.; Jensen, G.L.; Serhan, C.N.; Maddipati, K.O. Identification of specialized pro-resolving mediator clusters from healthy adults after intravenous low-dose endotoxin and omega-3 supplementation: A methodological validation. *Sci. Rep.* **2018**, *8*, 18050. [CrossRef] [PubMed]
163. Aoki-Yoshida, A.; Aoki, R.; Moriya, N.; Goto, T.; Kubota, Y.; Toyoda, A.; Takayama, Y.; Suzuki, C. Omics studies of the murine intestinal ecosystem exposed subchronic and mild social defeat stress. *J. Proteome Res.* **2016**, *15*, 3126–3138. [CrossRef] [PubMed]
164. Miao, J.S.; Lin, Y.; Mao, G.D.; Chen, F.F.; Zeng, H.L.; Dong, Z.; Jiang, J.; Wang, C.; Xiao, M.; Shuai, M.; et al. Erythrocyte n-6 polyunsaturated fatty acids, gut microbiota, and incident type 2 diabetes: A prospective cohort study. *Diabetes Care* **2020**, *43*, 2435–2443. [CrossRef] [PubMed]

nutraceuticals

MDPI

Review

Design and Development of Novel Nutraceuticals: Current Trends and Methodologies

Thalia Tsiaka [1], Eftichia Kritsi [1,*], Konstantinos Tsiantas [1], Paris Christodoulou [2], Vassilia J. Sinanoglou [1] and Panagiotis Zoumpoulakis [1,*]

[1] Department of Food Science and Technology, University of West Attica, Ag. Spyridonos, 12243 Egaleo, Greece; tsiakath@uniwa.gr (T.T.); ktsiantas@uniwa.gr (K.T.); vsina@uniwa.gr (V.J.S.)
[2] Institute of Chemical Biology, National Hellenic Research Foundation, 48 Vas. Constantinou Avenue, 11635 Athens, Greece; pchristodoulou@eie.gr
* Correspondence: ekritsi@uniwa.gr (E.K.); pzoump@uniwa.gr (P.Z.)

Abstract: Over the past few years, nutraceuticals have gained substantial attention due to the health-promoting and disease-preventing functions behind their nutritional value. The global prevalence of nutraceuticals is reflected in the increasing number of commercially available nutraceuticals and their wide range of applications. Therefore, a unique opportunity emerges for their further exploration using innovative, reliable, accurate, low cost, and high hit rate methods to design and develop next generation nutraceuticals. Towards this direction, computational techniques constitute an influential trend for academic and industrial research, providing not only the chemical tools necessary for further mechanism characterization but also the starting point for the development of novel nutraceuticals. In the present review, an overview of nutraceuticals is discussed, underscoring the crucial role of chemoinformatic platforms, chemolibraries, and in silico techniques, as well as their perspectives in the development of novel nutraceuticals. This review also aims to record the latest advances and challenges in the area of nanonutraceuticals, an innovative field that capitalizes on the assets of nanotechnology for the encapsulation of bioactive components in order to improve their release profile and therapeutic efficacy.

Keywords: nutraceuticals; chemolibraries; natural products databases; chemoinformatics; computational chemistry tools; novel drug delivery; nanonutraceuticals

Citation: Tsiaka, T.; Kritsi, E.; Tsiantas, K.; Christodoulou, P.; Sinanoglou, V.J.; Zoumpoulakis, P. Design and Development of Novel Nutraceuticals: Current Trends and Methodologies. *Nutraceuticals* **2022**, *2*, 71–90. https://doi.org/10.3390/nutraceuticals2020006

Academic Editor: Luisa Tesoriere

Received: 15 March 2022
Accepted: 20 April 2022
Published: 23 April 2022

1. Introduction

Nowadays, public awareness of health issues and concerns have created a new flourishing economy based on food-derived bioactive compounds which present health-promoting and disease-preventing functions, commonly referred to as nutraceuticals. Nutraceuticals constitute an emerging sector in the pharmaceutical and food industry, receiving considerable interest due to their functions [1]. The increased scientific community interest in the field of nutraceuticals is reflected in the fact that more than 8000 manuscripts have been published in the last decade, highlighting the unforeseen worldwide response (Figure 1).

Recent studies have revealed that several nutraceuticals are promising agents for the prevention and treatment of various diseases, such as allergies, Alzheimer's disease, cardiovascular and eye disorders, cancer, obesity, diabetes, and Parkinson's disease, as well as the regulation of immune system function and inflammation [2]. Therefore, nutraceuticals have attracted substantial interest which offers novel opportunities for the development of innovative products that will cover consumer needs for health-enhancing foods [3]. Based on the increasing number of commercially available nutraceuticals and their wide range of applications, the global nutraceutical market accounted for $289.8 billion in the year 2021 and is expected to grow to $438.9 billion by the year 2026, with a compound annual growth rate of 8.7% for the aforementioned period [4]. Furthermore, following the outbreak of the

COVID-19 pandemic, the nutraceutical market is expected to increase due to the possible beneficial effects of these products on the human immune system function [5]. Additionally, the number of nutraceutical-based patents has increased, highlighting the crucial role of nutraceuticals worldwide [6].

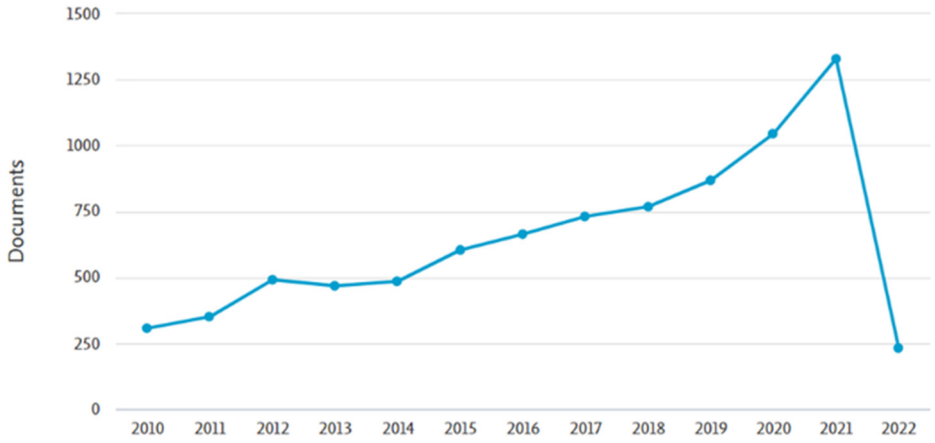

Figure 1. Number of published manuscripts for the period 2010–2022, derived from the bibliographic database "SCOPUS" (https://pubmed.ncbi.nlm.nih.gov/?term=nutraceuticals&filter=simsearch3.fft&filter=years.2010-2022/ Last access: 11 April 2022).

Currently, the nutraceutical industry conforms to the practices of conventional food or pharmaceutical technology. However, current advances in the field of nanotechnology are the driving force behind the novel research strategies followed in nutraceutical development. Presently, nanosystems (structures or molecules of at least one dimension with a size from 1 to 100 nm) are incorporated in many different areas of food and health sciences. For instance, nanoengineered materials have been applied (a) for the nanopacking and improvement of the sensory attributes of foods, (b) for the smart delivery and nanofortification of functional and fortified products, and (c) for personalized treatment in nanomedicine [7]. The implementation of nano-scale materials for the encapsulation and delivery of nutraceuticals coined the concept of nanonutraceuticals [8].

Although the mechanism of action of nanoparticles is not yet fully elucidated and may differ according to the selected nanosystem, the beneficial biological properties of nanonutraceuticals are mainly attributed to the biological action of the loaded bioactive compounds [9]. For instance, nanonutraceuticals can act through the scavenging of free radicals, the improvement of antioxidant potential, and the chelation of transition metals. Various molecular pathways (including NF-κB, interleukin 6 and 1β, and TNF-α) and enzymatic functions (acetylcholinesterase, inducible nitric oxide synthase, superoxide dismutase, NADPH oxidase, etc.) are affected [10]. In addition, these nanoformulations protect the encapsulated bioactive molecules from oxidation or the action of gastrointestinal tract enzymes. Thus, through targeted delivery, they facilitate their slow and controlled release, elongate their activity, and enhance their bioefficacy [7,8].

Moreover, in recent decades, in silico virtual screening has emerged as a substantial research tool, defined as a set of computational methods that analyze large libraries of chemical compounds to identify potential hit candidates [11]. Among them, natural product (NP) libraries constitute the main tool for the discovery of novel nutraceuticals by applying virtual screening strategies. A remarkable number of academia, pharmaceutical, and food companies utilize these methods, worldwide, highlighting their contribution to the design and development process of novel compounds [12]. Computational techniques provide a wide range of possibilities to speed up the design of nutraceuticals and reduce the associated risks and costs [13].

In the field of nutraceuticals, in silico applications are still in their infancy, offering a unique opportunity for further investigation and exploitation. Recent publications have

revealed new pathways toward the discovery of novel nutraceuticals by using in silico approaches [14]. The present comprehensive review is focused on the innovative concept of nutraceuticals and, in particular, on the latest advances in that field which concern the implementation of nanotechnology for the formulation of nanonutraceuticals. Furthermore, the current overview delves into the use of these state-of-the-art nanoformulations in the food and healthcare fields and also into their limitations and regulatory frameworks. In addition, it emphasizes the applications of computational methodologies and tools that facilitate the design and discovery of novel nutraceuticals. This overview illustrates the potential of computational techniques to drive the first screening steps of the nutraceutical industry in detail. Moreover, a prospective analysis of the impact of these techniques in the field of nutraceuticals is discussed.

2. Review Methodology

The present review focuses on collecting data regarding the current knowledge in the field of nutraceuticals in terms of in silico applications and nanotechnology advents. In order to structure this overview, a thorough bibliographic search was employed in different search engines, mainly Scopus and Google Scholar. The selected time frame was between 2015 and 2022. The period of the search was limited from 2020 to 2022, only for the terms related to nanonutraceuticals, since these concepts and their applications have been discussed in other recent review papers. The keywords used for the collection of papers were 'Nutraceuticals AND market', 'Natural products databases', 'In silico screening', 'Computational techniques', 'Nanonutraceuticals', 'Nanofibers', 'Nanoparticles', 'Liposomes', 'Nanoemulsions'. The type of documents that were examined included original articles, reviews, and book chapters, published in the English language. The pipeline of the research methodology is illustrated in Figure 2 by a PRISMA flowchart.

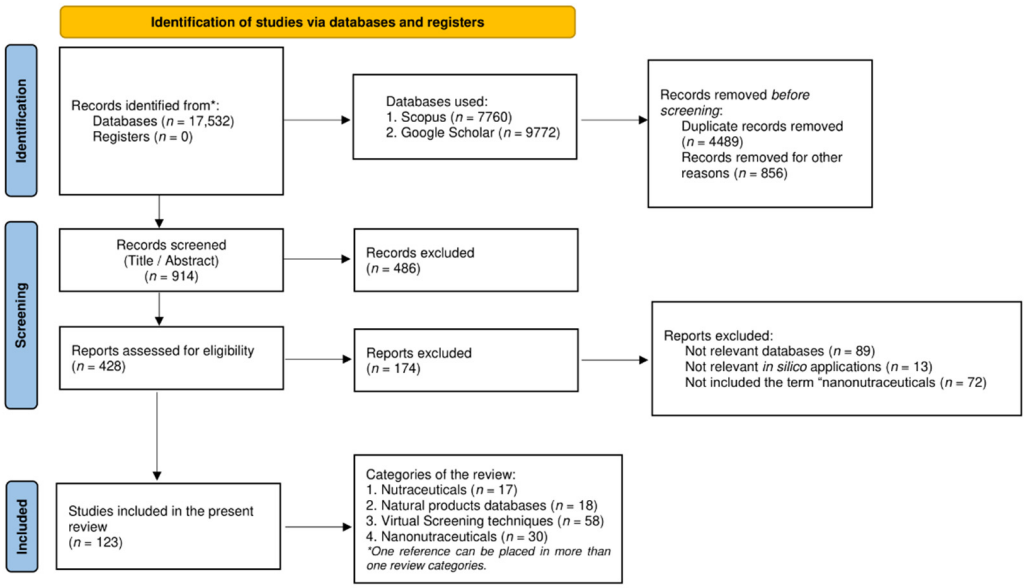

Figure 2. PRISMA flowchart of the review process.

3. Current Knowledge in the Field of Nutraceuticals

3.1. Nutraceuticals: Definition and Introduction

The term 'nutraceutical' originated from the plausible combination of the words 'nutrient' and 'pharmaceuticals' and was invented in 1989 by Dr. Stephen De Felice (Chairman of the Foundation for Innovation in Medicine) [15]. According to the present definition, 'nutraceutical' refers to 'a food (or part of a food) that provides medical or health benefits, including the prevention and/or treatment of a disease' [16]. The described terminology has evolved through the years, characterizing 'nutraceutical' as 'a product isolated or purified from foods that are generally sold in medicinal forms not usually associated

with food' [17]. Based on literature data, there are a plethora of definitions that describe 'nutraceuticals', by referring to them as 'food, food components or nutrients providing health benefits behind their nutritional value' [18]. To date, there is a controversy over the specific definition of 'nutraceutical products' based on their deliberate usage. Even though there is no clear definition of 'nutraceuticals' globally, the term includes health-promoting and disease-preventing functions behind the nutritional value of these products [19].

3.2. Nutraceuticals Classification

Since no scientific consensus has been reached yet over the classification of nutraceuticals, various criteria have been applied for their categorization (Figure 3). The key categories of nutraceuticals are herbal and botanical products (natural extracts or concentrates), nutrients (fatty acids, amino acids, vitamins, and minerals), functional foods, and dietary supplements, while their major natural sources are animals, plants, and microbes. If classified as nutritional ingredients, they can be divided into probiotics, prebiotics, antioxidant vitamins, polyunsaturated fatty acids, dietary fibers, polyphenols, and carotenoids [20]. Tablets, pills, creams, capsules, liquids, and powders are the most common forms touted in the global market [21]. On the basis of their health benefits, nutraceuticals serve several functions against various ailments, such as neurodegenerative and cardiovascular diseases, metabolic syndromes, congenital abnormalities, bone-related pathologies (osteoarthritis, osteoporosis), and cancer [21,22]. The term 'established nutraceuticals' includes the products with confirmed health-promoting effects, while the lack of validated clinical evidence describes the group of 'potential nutraceuticals' [20].

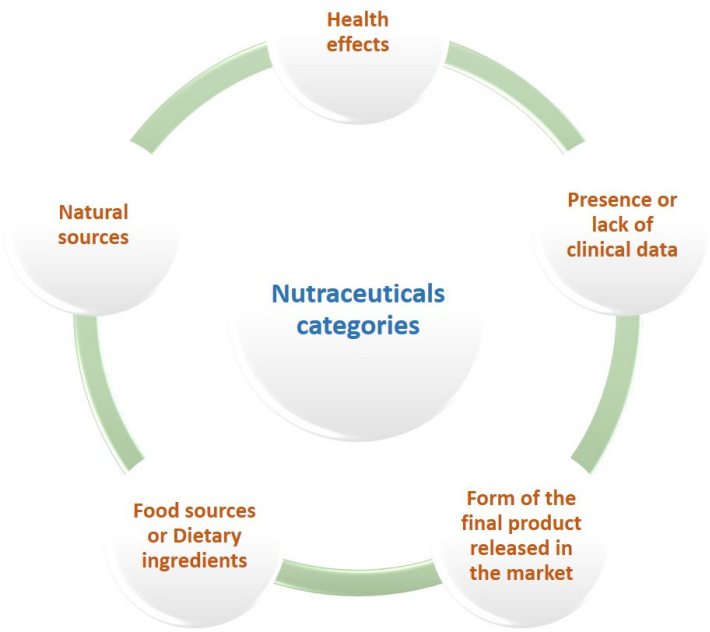

Figure 3. Criteria used for the classification of nutraceuticals into different categories.

3.3. Regulatory Framework and Official Guidelines

Whilst nutraceuticals, as a concept, attract the interest of the current global market, there are still challenges that should be faced in order to bring nutraceuticals from bench top to bedside. Essential issues, such as the safety, toxicity, efficacy, and quality of the final products require further scrutiny to ensure consumers' acceptance and reduce health risks. Therefore, the adoption of a shared international regulatory system, which at this point resides in the grey area between pharma and food regulations, is a key requirement.

For instance, the United States Food and Drug Administration (FDA) classifies nutraceuticals as 'dietary supplements' and therefore no safety or efficacy reports are demanded before approval. On the other hand, Canadian authorities have established a

broader categorization of nutraceuticals, where they can be designated as drugs, foods, or natural health products. According to the Japanese regulatory bodies, which are governed by stricter legislation, nutraceuticals are termed as 'Foods in General', 'Food with Health Claims', and 'Food for Specified Health Uses' [3,22], while European directives remain quite equivocal since nutraceuticals can be considered as food supplements or medicinal products, according to European Food Safety Authority (EFSA) [3,23].

Focusing on the future perspectives of nutraceuticals, the official international and local authorities should set forth collective legislation that will provide a clear definition of nutraceuticals by describing a solid scientific rationale and common practices or responsibilities regarding their manufacturing, approval, and labeling [23].

4. Novel Approaches in Nutraceuticals' Discovery

4.1. Natural Products (NPs) Databases (Chemo-Libraries)

Chemo libraries consist of the main resources for in silico applications and have emerged as a fundamental tool in the initial steps of computer-aided molecular discovery [24]. These databases are repositories of chemicals, mainly composed of synthetic and natural compounds, which provide information about their chemical scaffolds, their computable structural properties, and their vendors.

The natural compounds databases constitute the main tool for the discovery of novel nutraceuticals by applying virtual screening strategies. Natural compounds have been the center of attention of the scientific community in recent decades, rendering them in the limelight as an attractive and promising target for the discovery of novel bioactive compounds. In comparison to synthetic compounds, the key areas in which they excel are: (a) their structural diversity and complexity, often bearing numerous stereogenic centers and fused ring systems, which are poorly represented in synthetic compounds, (b) their abundance, and (c) their acceptance from consumers. It is noted that in 2017, the natural products market reached 11.5 billion USD and it is expected to rise with an annual CAGR of 19.7% between 2018 and 2026 [25].

Focusing on this knowledge-intensive scientific field, the current section attempts to present an overview of free and open access databases consisting of compounds with natural origins. These databases could be divided into two major classes, including (a) Virtual and (b) Physical Natural Product libraries. The major difference between virtual and physical libraries is that the first library contains only the chemical structures in an easily retrievable format, appropriate for computational applications, while physical libraries provide not only the chemical scaffold of NPs but also the available suppliers [26].

Virtual Natural Product Libraries

Up-to-date, only the COlleCtion of Open Natural prodUcTs (COCONUT: https://coconut.naturalproducts.net, accessed on 11 April 2022), a free of charge and open access natural compounds database, efficiently aggregates the natural compounds chemical structures collected from various open sources (most compounds were added from the Ayurveda, Alkamid, CMNPD, and CyanoMetDB databases). Particularly, COCONUT contains 406,747 unique natural compounds in a readable format (.SMILES file) which are easily and quickly downloaded. Apart from chemical structures, COCONUT provides information about the stereochemical forms, organisms, natural geographical presence, and diverse pre-computed molecular properties of natural compounds [27].

The Natural Products Atlas (NPAtlas: https://www.npatlas.org/, accessed on 11 April 2022) constitutes another recently created open-access database, incorporating 24,594 natural compounds. It is a well-annotated database, including detailed information (structure, name, organisms source, isolation references, total syntheses, and cases of structural reassignment) about natural compounds, but unfortunately, it involves only microbial natural compounds [28].

The FooDB (https://foodb.ca/, accessed on 11 April 2022), a food-related chemical database, obtains >23,000 food chemicals in a searchable and downloadable format. Up to today, it is the most informative public resource of food ingredients, offering a unique

opportunity for the identification of dietary components by performing virtual screening methods [29].

Based on the proven beneficial effects of functionally useful plants, as food and medicine, the Collective Molecular Activities of Useful Plants database (CMAUP: http://bidd.group/CMAUP/index.html, accessed on 11 April 2022) collected and classified in a downloadable format 47,645 plant ingredients derived from 5645 plants. The novelty of the aforementioned freely available database is that it possesses information not only for the chemical structure, name, and predicted physicochemical properties of the ingredients but also reports the ZINC code pointing out potential suppliers [30].

Marine natural products (MNPs) are considered important sources of biologically active agents that regulate a variety of biological functions, offering a major impact on human health [31–34]. The Comprehensive Marine Natural Products database (CMNPD: https://www.cmnpd.org/, accessed on 11 April 2022) is a freely available database that provides abundant information. The complete dataset could be downloaded via https://docs.cmnpd.org/downloads (accessed on 11 April 2022) in a ready-to-use format for virtual screening [35].

Another database conveniently downloadable in a readable format is the South African Natural Compounds Database (SANCDB: https://sancdb.rubi.ru.ac.za/, accessed on 11 April 2022), comprising more than 1000 compounds isolated from the plant and marine life in South Africa. Compared to other natural databases, SANCDB incorporates available analogues from MolPort (https://www.molport.com/, accessed on 11 April 2022) and Mcule (https://mcule.com/, accessed on 11 April 2022), two commercially available vendors, overcoming the major problem of the commercial availability of the compounds. Additionally, it facilitates virtual screening, including chemical scaffolds in a ready-to-dock format [36]. Table 1 enlists the most common free access and downloadable virtual natural compounds databases.

Table 1. List of the most significant open-access virtual natural compounds databases.

Database Name	NP Type	No. of Compounds	VS Format	Link
COCONUT [27]	Generalistic	406,747	.SMILES and .SDF	https://coconut.naturalproducts.net accessed on 11 April 2022
NPAtlas [28]	Microbial	24,594	.SMILES and .SDF	https://www.npatlas.org/ accessed on 11 April 2022
FooDB [29]	Food Ingredients	23,883	.MOL, .SDF, .PDB, and .SMILES	https://foodb.ca/ accessed on 11 April 2022
CMAUP [30]	Plant Ingredients	5645	.SMILES	http://bidd.group/CMAUP/index.html accessed on 11 April 2022
CMNPD [35]	Marine	>31,000	.SDF	https://www.cmnpd.org/ accessed on 11 April 2022
SANCDB [36]	Chemical compounds of South African biodiversity	1012	.SDF and .SMILES	https://sancdb.rubi.ru.ac.za/ accessed on 11 April 2022
NuBBEDB [37]	NPs and derivatives from plants and microorganisms native	2218	.MOL2	https://nubbe.iq.unesp.br/portal/nubbe-search.html accessed on 11 April 2022

Table 1. *Cont.*

Database Name	NP Type	No. of Compounds	VS Format	Link
TIPdb [38]	Phytochemicals originated in Taiwan	>9000 Focused on anticancer, antiplatelet, and antituberculosis	.SDF	https://cwtung.kmu.edu.tw/tipdb/ accessed on 11 April 2022
TCM database@Taiwan [39]	Generalistic	>20,000	.MOL2	http://tcm.cmu.edu.tw/ accessed on 11 April 2022
ChEBI [40]	Generalistic	>12,000	.SDF and .SMILES	https://www.ebi.ac.uk/chebi/ accessed on 11 April 2022

Physical Natural Product Libraries

The ZINC 15 database (http://zinc15.docking.org, accessed on 11 April 2022) constitutes the most comprehensive resource, which includes readily purchasable compounds (over 230 million compounds in a ready-to-dock format), overcoming the limitations of the compounds' commercial availability. Particularly, the field of natural compounds consists of over 80,000 ready-to-use compounds, derived from a plethora of vendors. In addition, it categorizes natural compounds according to the following vendors: Analyticon Discovery (www.ac-discovery.com, accessed on 11 April 2022), AfroDB [41], Compound cloud (https://compoundcloud.bioascent.com/, accessed on 11 April 2022), Indofine (www.indofinechemical.com, accessed on 11 April 2022), MolPort (www.molport.com, accessed on 11 April 2022), MicroSource Natural Products (www.msdicovery.com, accessed on 11 April 2022), Nubbe (www.nubbe.iq.unesp.br, accessed on 11 April 2022), Specs (www.specs.net, accessed on 11 April 2022), TimTec (www.timtec.net, accessed on 11 April 2022) and UEFS (www.uefs.br, accessed on 11 April 2022), offering a direct assessment of purchasability and price of compounds. Therefore, ZINC 15 combines the information about the structure collection and potential suppliers, rendering it an ideal tool for virtual screening applications. Another advantage of the ZINC 15 database of particular interest is that, apart from chemical structures and vendors, it provides physicochemical properties and analogs of the compounds that can also be examined as potential hits [42].

Analyticon Discovery (https://ac-discovery.com/, accessed on 11 April 2022) is a free access database, that provides a continuously growing collection of purified natural compounds. In particular, the library could be divided into the following subsets: (a) MEGx which offers about 5000 purified natural compounds originating from plants and microorganisms, (b) MACROx comprises over of 1800 macrocycle compounds, and (c) FRGx with over 200 fragments. Additionally, Analyticon Discovery includes a semisynthetic NP-derived compound subset (NATx) with over 26,000 compounds. Finally, polyphenols and flavonoids collections are also available, offering a unique opportunity for further exploration in the fields of the development of novel taste-modulating or health-promoting ingredients for the food industry [26].

Ambinter (https://www.ambinter.com/, accessed on 11 April 2022) and Greenpharma (www.greenpharma.com, accessed on 11 April 2022) constitute two collaborative companies, offering a set of ~8000 natural compounds (alkaloids, phenols, phenolic acids, terpenoids, and others) in .SDF format ready to use for virtual screening. Additionally, the above-mentioned companies propose more than 11,000 semi-synthetic derivatives of natural compounds [26].

One of the largest natural compound libraries is InterBioScreen (https://www.ibscreen.com/, accessed on 11 April 2022), listing over 68,000 well-annotated natural compounds derived from a variety of sources, such as plants and microorganisms. The presented library is easily and quickly downloaded in a readable format (.SMILES and .SDF) [26].

The MolPort (https://www.molport.com/, accessed on 11 April 2022) database is another natural compound vendor of paramount importance since it stores in downloadable

files over 10,000 unique natural and over 100,000 natural-like products from a variety of suppliers (.SMILES and .SDF). Therefore, its usage facilitates in silico screening applications since it possesses available-to-purchase natural products.

A collection of more than 3000 natural compounds and 396 food additive-related compounds are supplied from MedChemExpress (https://www.medchemexpress.com/, accessed on 11 April 2022). For data accessibility, a query is required, and purchasable compounds in .SDF format is received. The main advantage of the present database is that all compounds have indicated bioactivity and safety.

INDOFINE Chemical Company (https://indofinechemical.com/, accessed on 11 April 2022) includes around 1900 NPs and semisynthetic compounds, in a ready-to-screen format (.SDF), focused on flavonoids. The library consists of flavonoids, flavones, isoflavones, flavanones, coumarins, chromones, chalcones, and lipids especially. The chemical scaffolds of Indofine are offered and are classified according to compound types.

The most common free access and downloadable physical natural compounds databases are presented in Table 2.

Table 2. List of the most significant open-access physical natural compounds databases.

Database Name	NP Type	No. of Compounds	VS Format	Link
ZINC 15 [42]	Generalistic	>80,000	.MOL2 .SDF .SMILES	https://zinc15.docking.org/ accessed on 11 April 2022
Analyticon Discovery [26]	MEGx plants and microorganisms	5000 NC	.SDF via request	https://ac-discovery.com/ accessed on 11 April 2022
	MACROx Macrocycle compounds	>1800		
	FRGx Fragments	>200		
Ambinter and GreenPharma [26]	Generalistic	>8000	.SDF	https://www.ambinter.com/ accessed on 11 April 2022
InterBioScreen [26]	Plants and Microorganisms	>68,000	.SDF .SMILES	https://www.ibscreen.com/ accessed on 11 April 2022
Indofine	Generalistic	>1900	.SDF	https: //indofinechemical.com/ accessed on 11 April 2022
MolPort	Generalistic	>10,000	.SDF .SMILES	https://www.molport.com/ accessed on 11 April 2022
MedChemExpress	Generalistic	>3000	.SDF	https://www. medchemexpress.com/ accessed on 11 April 2022
	Food additive-related compounds	396		

4.2. Virtual Screening (VS) Techniques

As it is generally known, the identification of bioactive molecules constitutes an expensive, time-consuming, and laborious inter-disciplinary process. As a result, innovative approaches are continuously developed, aiming to optimize and simplify this procedure. Among them, Virtual Screening (VS) is one of the most important and widespread strategies that has been applied for the determination of potentially bioactive molecules. In recent years, a variety of tools and software that can be performed in VS were utilized to reduce the selection of promising compounds that will be tested experimentally. Particularly, VS objectives are to accelerate the discovery process, increase the number of compounds to be tested experimentally, and rationalize their choice [13,43]. Additionally, the classification

of NPs into libraries contributes effectively to VS, facing and tackling issues related to the extraction, purification, and purchasability of NPs [26].

The most commonly used methods for VS of NP libraries include Molecular Docking, Quantitative Structure-Activity Models (QSAR), Molecular Docking, Pharmacophore Modeling, and Molecular Dynamics (MD) Simulations. The main advantage of these methods is that they lead to reducing the selection of compounds that will be tested experimentally [44].

In the field of nutraceuticals, in silico approaches such as QSAR, molecular docking, and molecular dynamic simulations have been utilized, aiming to unravel bioactive food components with health-promoting and disease-preventing properties [45]. The present section provides a brief description of the fundamental idea of the above techniques as well as their state-of-the-art applications in the field of nutraceuticals.

Quantitative Structure-Activity Relationship (QSAR)

In general, Quantitative Structure-Activity Relationship (QSAR) analysis is a ligand-based computational technique that attempts to correlate the structural properties (chemical structures) and the biological activity of a compounds' dataset [46]. The underlying principle of QSAR models is based on the hypothesis that structurally similar compounds may exhibit similar biological activities [47]. The creation of QSAR models is causally linked with equations that relate a dependent variable (i.e., an observed activity) with a number of calculated descriptors, including physicochemical, constitutional, and topological properties [48,49]. For this purpose, various multivariate statistical regression (Multiple Linear Regression—MLR, Principal Component Analysis—PCA, and Partial Least Square Analysis—PLS) and Machine Learning (ML) tools are applied in an effort to generate appropriate algorithms [50]. Table 3 presents a list of available software for molecular descriptor calculations. The building of the model is followed by the validation process in which the accuracy of the method is verified. The produced model can be used as a prediction tool to prioritize compounds that have the potential to display biological activity and to reduce the number of the compounds that will be tested experimentally [51]. Therefore, it is a widely used process with a broad spectrum of applications in the pharmaceutical landscape [52]. Regarding nutraceuticals, the relationship between food ingredients and a variety of properties has already been studied on several occasions [53].

Table 3. List of several available softwares to calculate molecular descriptors.

Name	Availability	Link
Open Babel	Free	http://openbabel.org accessed on 11 April 2022
RDKit	Free	http://www.rdkit.org/ accessed on 11 April 2022
Dragon	Free	https://chm.kode-solutions.net/pf/dragon-7-0/ accessed on 11 April 2022
Chemistry Development Kit (CDK)	Free	https://cdk.github.io/ accessed on 11 April 2022
Qikprop	Commercial	https://www.schrodinger.com/products/qikprop accessed on 11 April 2022

Molecular Docking

Molecular Docking is the most commonly used in silico technique, which predicts the interaction between a small molecule (ligand) and a protein (receptor) at the atomic level. This approach enables the characterization of the behavior of small molecules in the binding site of a target protein as well as the elucidation of the fundamental biochemical

process behind this interaction [54]. It is a structure-based approach which requires a high-resolution 3D illustration of the examined target derived from (a) X-ray crystallography [55], (b) Nuclear Magnetic Resonance Spectroscopy [56], and (c) Cryo-Electron Microscopy [57]. Until now, numerous computational tools and algorithms have been developed, including commercial or free-of-charge software (Table 4). Molecular Docking finds a plethora of applications mainly in the field of drug discovery and design [58]. It should be noted that during recent years, a constantly increasing interest has been observed concerning the applications of molecular docking in food science [59].

Table 4. The most commonly used ligand-receptor Molecular Docking software.

Name	Availability	Link
AutoDock [60]	Free/Open Source	https://autodock.scripps.edu/ accessed on 11 April 2022
AutoDock Vina [61]	Free	https://vina.scripps.edu/ accessed on 11 April 2022
Dock [62]	Free	http://dock.compbio.ucsf.edu/ accessed on 11 April 2022
GOLD [63]	Commercial	https://www.ccdc.cam.ac.uk/solutions/csddiscovery/components/gold/ accessed on 11 April 2022
Glide [64]	Commercial/License requirement	https://www.schrodinger.com/products/glide accessed on 11 April 2022
Molecular Operating Environment (MOE) [65] Molecular Operating Environment (MOE), 2020.09 Chemical Computing Group ULC, 1010 Sherbooke St. West, Suite #910, Montreal, QC, Canada, H3A 2R7, 2022	Commercial	https://www.chemcomp.com/Products.htm accessed on 11 April 2022
PyRx [66]	Open Source	https://pyrx.sourceforge.io/downloads accessed on 11 April 2022
OEDocking [67–69]	Commercial	https://www.eyesopen.com/oedocking accessed on 11 April 2022
HADDOCK (High Ambiguity Driven protein-protein DOCKing) [70]	Docking Web Server/registration requirement	https://wenmr.science.uu.nl/haddock2.4/ accessed on 11 April 2022
SwissDock [71]	Docking Web Server	http://www.swissdock.ch/ accessed on 11 April 2022

In the nutraceutical landscape, molecular docking studies have been employed to provide information about the initial steps of nutraceutical research that precede the in vitro studies [45]. Herein, the most relevant applications of molecular docking in the assessment of the potential health-promoting benefits of nutraceuticals are reviewed.

Pharmacophore Modeling

A pharmacophore model illustrates in a 3D arrangement, the chemical features, which are crucial for the molecular recognition of a ligand by a macromolecule, offering a putative explanation for the binding affinity of structurally diverse ligands to a common target [72]. It can be generated either in a structure-based way, by predicting the potential interactions between the target and the ligand, or in a ligand-based way, by overlaying a group of active molecules and creating common chemical features that may be responsible for their

bioactivity [73]. Currently, a variety of 3D pharmacophore modeling generators have been constructed, containing commercially available software and academic programs (Table 5) [74].

Once a pharmacophore model is created, it can be exploited as a query to screen a chemical library. Compounds that satisfy the query pharmacophore features are retrieved and expected to exhibit bioactivity. The described process, commonly known as Pharmacophore-based Virtual Screening, represents a mainstream tool of VS with a plethora of applications in the drug discovery process [75,76].

Table 5. List of several 3D pharmacophore modeling software.

Name	Availability	Link
Catalyst [77]	Commercial	Not available
FLAP [78]	Commercial	https://www.moldiscovery.com/software/flap/ accessed on 11 April 2022
LigandScout [79]	Commercial	Not available
MOE	Commercial	https://www.chemcomp.com/ accessed on 11 April 2022 Chemical Computing Group. Molecular operating environment (MOE). Montreal, QC, Canada; 2010
Pharmer [80]	Free for academic use	http://pharmer.sourceforge.net accessed on 11 April 2022
PHASE [81]	Commercial	https://www.schrodinger.com/products/phase accessed on 11 April 2022
Pharmmaker [82]	Free	http://prody.csb.pitt.edu/pharmmaker/ accessed on 11 April 2022
PharmaGist [83]	Freely available webserver	https://bioinfo3d.cs.tau.ac.il/PharmaGist/php.php accessed on 11 April 2022

Molecular Dynamics Simulations (MD simulation)

Molecular Dynamics Simulation is another powerful computational tool that captures the behavior of proteins, ligand-protein complexes, and other biomolecules in full atomic detail and at very fine temporal resolution [84]. It is a well-established technique which provides a molecular perspective to observe the behavior of atoms, molecules, and particulates [85]. Based on Newton's equation of motion, MD predicts the physical movements of atoms and molecules using interatomic potentials or molecular mechanics force fields, offering the opportunity to comprehend the overall behavior of molecular systems during the motion of individual atoms [84].

Up to now, several force fields [86] and tools have been developed and are available for MD simulations. GROMACS [87], AMBER [88,89], Nanoscale MD (NAMD) [90], CHARMM-GUI [91], and DESMOND are the most commonly used tools for MD simulations.

In recent years, the impact of MD simulations in molecular biology and drug discovery has expanded drastically [92]. MD simulations have gained ground in deciphering functional mechanisms of proteins and other biomolecules, unraveling the structural basis of disease, and designing and optimizing the production of small molecules [84].

Applications of in Silico Screening Techniques in the Field of Nutraceuticals

Although the application of in silico screening for the discovery of novel nutraceuticals is still in its first steps, studies proving the significant role of these methodologies have

been carried out. Therefore, in this section, relevant applications of in silico techniques in the evaluation of the potential health benefits of nutraceuticals are described.

Nowadays, the outbreak of severe acute respiratory syndrome coronavirus 2 (SARS-CoV-2), a life-threatening disease causing thousands of deaths daily, is responsible for a current global health crisis. Therefore, the scientific community has the made treatment and prevention of SARS-CoV-2 infection its first priority [93]. It has been proven that nutraceuticals contribute effectively to reducing the chances of SARS-CoV-2 infection, but also in alleviating COVID-19 symptoms [94].

Towards this direction, Gyebi et al. (2021) performed a structure-based virtual screening to suggest inhibitors of 3-Chymotrypsin-Like Protease ($3CL^{pro}$) of SARS-CoV-2 from *Vernonia amygdalina* and *Occinum gratissimum*. In particular, they applied docking studies in the active site of $3CL^{pro}$, aiming to predict the binding affinity of an in-house library, which includes 173 phytochemicals from *Vernonia amygdalina* and *Occinum gratissimum*. Docking results defined a hit list of 10 phytochemicals with strong binding affinities in the catalytic center of $3CL^{pro}$ from three related strains of coronavirus (SARS-CoV, MERS-CoV, and HKU4). Subsequently, drug-likeness prediction revealed two terpenoids, neoandrographolide and vernolide, as the most promising inhibitors of SARS-CoV-2 $3CL^{pro}$. The selected compounds were subjected to Molecular Dynamics simulations and the results showed that the examined terpenoid-enzyme complexes exhibited strong interactions and structural stability, which could be adapted in experimental models for the development of preventive nutraceuticals against coronavirus diseases [95]. Furthermore, Kodchakorn et al. (2020) employed a combination of in silico screening techniques to determine natural compounds with high calculated binding affinity on the homology structure of coronavirus protease (SARS-CoV-2 PR). Molecular Docking and Molecular Dynamics simulations were applied to eight natural compounds (Andrographolide, anthocyanin-β-D-glucoside, capsaicin, curcumin, cyanidin, cyanidin-3-*O*-glucoside, sesamin, and hesperidin). Result analysis indicated that all natural compounds presented favorable binding affinities, providing preliminary data for the development of novel nutraceuticals [96]. On the other hand, Kumar et al. (2019) utilized Molecular Docking to screen a library, consisting of 106 well-known nutraceuticals, against four SARS-CoV-2 targets (S protein (Receptor Binding Domain)-ACE2 complex, M^{pro}, PL^{pro}, and Nsp15). The results suggested that among the tested nutraceuticals, folic acid and its derivatives, such as tetrahydrofolic acid and 5-methyl tetrahydrofolic acid, were the most promising and could serve as a starting material for further in vitro and in vivo experiments [14]. Recently, Baig et al. (2022) studied the in silico inhibitory activity of 58 compounds, derived from the miraculous herb *Nigella sativa*, against the SARS-CoV-2 target in an effort to propose potential compounds as SARS-CoV-2 inhibitors. Three compounds, α-hederin, rutin, and nigellamine A2 were identified as the most promising molecules and further investigation is necessary to prove the ability of *Nigella sativa* to inhibit SARS-CoV-2 targets [97].

5. Nanotechnology: A Powerful Toolbox in the Field of Nutraceuticals

5.1. Health Effects and Limitations of Nanonutraceuticals

Nanonutraceuticals outweigh traditional nutraceutical formulations since they can (a) enhance the solubility and stability of the encapsulated natural bioactive compounds and (b) increase their absorption and biological efficacy by diminishing the off-target release and minimizing their side effects [8]. The up-to-date reported nanosized delivery systems include polymeric nanonutraceuticals (nanocapsules and nanospheres), carbon-based nanomaterials (i.e., fullerene and graphene particles), lipid-based formulations (solid lipid nanoparticles (SLNs), lipid nanocapsules, micelles, nanosuspensions, lipid–polymer hybrid nanoparticles, nanostructured lipid carriers, and liposomes), metal-based nanoparticles (silver and gold nanoparticles), dendrimers, nanoemulsions, exosomes, niosomes, quantom dots, nanoshells, nanofilms, and nanofibers. In the majority of cases, the therapeutic cargo of these nanocarriers is attributed to biologically active constituents, such as minerals, vitamins, polyphenols (i.e., resveratrol, rutin, tannins, anthocyanins, catechins and flavonoids,

curcuminoids, berberine, etc.), carotenoids (lycopene, β-carotene, astaxanthin, etc.), ω-3 fatty acids, phytosterols, and probiotics (*Lactobacillus* and *Bifidobacterium* bacteria). When these nanovehicles are loaded with phytochemicals (i.e., curcumin, resveratrol, vitamin E, etc.), they are specified as nano-phytomedicines or nano-phytoceuticals. The first insights concerning these nanoformulations showed that they act as more efficient delivery systems of phytoconstituents [98,99].

Based on the latest scientific evidence, the role of nutraceuticals in the prevention and treatment of several pathologies is multifarious. The scope of health-related applications of nanonutraceuticals is extended from the display of antioxidant, antimicrobial, anti-inflammatory, wound healing, pain relief, and immunomodulatory properties to the management of age-related neurogenerative conditions (i.e., Alzheimer's and Parkinson's disease), cancer, diabetes, skin diseases and recently, of pre- and post-COVID-19 infections [99,100]. Recent examples of nanonutraceuticals in therapeutics and healthcare are presented in Table 6.

Table 6. Potential therapeutical effects of recent nanonutraceuticals.

Nanonutraceuticals	Bioactive Compounds	Disease	References
Bovine serum albumin nanoparticles (BSAnp)	Chrysin (Flavonoid)	Potential use in cancer treatment	[101]
Poly (lactic-co-glycolic acid) (PLGA)-polyvinyl alcohol (PVA)-Chitosan nanoemulsion	Costunolide (Sesquiterpene lactone)	Possible anticancer and cardiac muscles protection	[102]
Chitosan-modified solid lipid nanoparticles (SLNs)	Thymoquinone (Monoterpene)	Possible anticancer, antidiabetic, antimicrobial, hepatoprotective, anti-inflammatory, and central nervous system protective activity	[103,104]
Micro-micelles	Sinacurcumin (Curcuminoid)	Possible antiviral properties against COVID-19	[99]
Nanocomposites	Glycyrrhizic acid (Triterpene glycoside)	Possible anti-inflammatory effects against COVID-19	[99]
Nanoparticles	Vitamin E/Squalene (Endogenous lipid)	Decrease in pro-inflammatory cytokines and increase in IL-10 in COVID-19 cases	[99]

Special focus should be paid to the tuning of probiotics and prebiotics to their nano-sized products, known as nanoprobiotics and nanoprebiotics, respectively. According to the International Scientific Association for Probiotics and Prebiotics (ISAPP) definition, live microorganisms confer beneficial effects on human health by modulating the immune system, producing antimicrobial compounds, interacting with the gut microbiota of the host, and improving gut barrier integrity are characterized as probiotics. The substrates or natural compounds that the host microbiota use to improve the health of the host are acknowledged as prebiotics [105]. The encapsulation of probiotics and prebiotics to nanoplatforms reduces any possible side effects, enhances their stability, absorption, and bioactivity, increases their fermentability and indigestibility in the GI tract, and triggers their selective stimulation and targeted activity [106,107].

Nonetheless, the research community should address some issues regarding the toxicity and safety implications as well as the manufacturing challenges of nanonutraceuticals. At first, these nanoformulations must be fully characterized on the basis of their physicochemical properties, especially their size and shape, which may induce tissue damage or inadvertent permeation of non-targeted cell membranes. In addition, further clinical data from in vivo animal models should be collected and evaluated to decipher the mecha-

nisms of action of these nanoproducts, improve their absorption and metabolism by the gastrointestinal (GI) tract, and eliminate any possible immunotoxicity. Furthermore, the commercialization of nanoproducts is strongly related to the establishment of scaled-up cost-effective processes, which ensure the reproducibility, reliability, and high quality of the final product. The outcomes of these trials will lead to the establishment of guidelines and standardized protocols for the safe monitoring of nanonutraceuticals, which, eventually, will curb the concerns of the consumers regarding their use [8,108].

5.2. The Latest Updates Regarding Nanonutraceuticals Applications

Based on the most recent projections regarding the demands of the current nutraceuticals market [4], nanonutraceuticals will be at the forefront of research and industry strategies in the upcoming years. Indicative examples of the newest applications of nanoformulations, recorded in the last two years (2021–2022) are exhibited in Table 7.

Table 7. Examples of nanonutraceuticals reported in the last two years (2021–2022).

Nanonutraceuticals	Bioactive Compounds	Properties	References
Nanoemulsion of monoglyceride oleogels	Curcumin	Higher encapsulation efficiency/Decelerate curcumin release	[109]
Nanoemulsion of PLGA and PVA natural polymers	Thymoquinone	Reduce cisplatin-induced kidney inflammation without hindering its anti-tumor activity	[110]
Almond oil nanoemulsion	Thymoquinone	Gastroprotective activities	[111]
α-Cyclodextrin nanoemulsion	Costunolide	Enhanced anticancer properties	[112]
Oil-in-water nanoemulsions	Resveratrol	Improved solubility, bioavailability, in vivo efficacy, and cytotoxic activity	[113]
Solid lipid nanoparticles	Berberine	Higher bioavailability and anticancer effect	[114]
Ufasomes	Oleuropein	Higher antioxidant activity	[115]
Liposomes	Thymoquinone	Reduced toxicity, increased cell absorption and permeability/enhanced bioavailability and anticancer efficacy	[116,117]
Liposomes	Quercetin and mint oil	Protection against oral cavities	[118]
Corn starch-sodium alginate nanofibers	*Bifidobacteria* and lactic acid bacteria	Protection of their probiotic activity in a food model and a simulated gastrointestinal system	[119,120]
Food-derived hydrogel nanostructures	Lupin- and soybean glycinin-derived peptides	Antioxidant activity/ DPP-IV and ACE inhibitors	[121,122]
Nanoparticles	Soy isoflavones	Activity against the neurogenerative effect of D-galactose	[123]

The entrapment of curcumin in monoglycerides oleogels, which formed oil nanoemulsions of high stability, resulted in higher encapsulation efficiency and a more controlled release of this bioactive molecule [109]. Nanoparticles increased the solubility and bioavailability of thymoquinone and have been used in a cancer mice model as a complementary therapy to prevent cases of nephrotoxicity caused by the cisplatin chemotherapy [110]. Thymoquinone nanoemulsions also exhibited strong anti-ulcer properties [111]. Costunolide is another natural anticancer agent of the sesquiterpene group whose anti-tumor properties were enhanced when it was loaded in an α-cyclodextrin nanoemulsion [112]. Oil-in-water nanoemulsions of resveratrol demonstrated higher cytotoxic activity and improved significantly the solubility, bioavailability, and in vivo efficacy of this polyphenol [113].

Lipid nanocarriers, such as solid lipid nanoparticles (SLNs), enhanced the therapeutic effect of phytoconstituents, such as berberine, due to their lipid nature that facilitates the

absorption and the targeted delivery of the bioactive compounds [114]. The combination of two unsaturated fatty acids, oleic and linoleic acid, formed liposomes, known as ufasomes, which achieved delivery of less or non-polar molecules, such as oleuropein, and increased their antioxidant activity [115]. Liposomes containing phosphatidylcholine and the liquid lipid Plurol Oleique also acted as carriers for the ocular delivery of thymoquinone and decreased its possible adverse effects (i.e., the toxicity of high doses, low cell absorption, and permeability) [116]. Liposomal formulations (cationic liposomal formulation) containing thymoquinone were also investigated for their anticancer properties [117]. Furthermore, phospholipid liposomes loaded with quercetin and mint oil were used against oral cavities [118].

Corn starch and sodium alginate-based nanofibers were applied as coatings to protect the probiotic activity of Bifidobacteria and lactic acid bacteria in yogurts and under gastrointestinal conditions in a simulated system [119,120]. Moreover, a nanostructured hydrogel formed by a lupin-derived peptide proved to have significant antioxidant properties, paving the way for the implementation of food-derived peptides in nanotechnology [122]. A year later, the same research group used synthetic analogues of lupin β-conglutin and soybean glycinin bioactive peptides in gel nanoformulation as DPP-4 and ACE inhibitors [121]. Based on the results of Faruk et al. (2022), a soybean nano-isoflavone presented potential therapeutic activity against the degenerative effect of D-galactose [123].

To sum up, there is mounting evidence that the engineering of natural products into nanoformulations is emerging as a straightforward approach, able to improve the low solubility, reduced bioavailability, low stability, non-site specific targeting, and possible degradation of conventional nutraceuticals by gastrointestinal fluid.

6. Conclusions

In the last few years, a new perception has been shaped in the general public regarding the incorporation of natural products and functional foods into everyday life. Thus, the market of nutraceuticals greatly expanded due to their acknowledged health benefits against several pathologies and their increased therapeutic efficacy compared to known conventional formulations. Rapid progress in the field of natural compound databases and chemoinformatics tools facilitates the design and development of novel nutraceuticals with enhanced bioactivities by applying in silico screening methodologies. Furthermore, the combination of in silico techniques with modern nanonization strategies is the key driver in all the innovations related to nutraceuticals. Therefore, nanonutraceuticals are considered the next generation nutraceuticals since they present improved properties, such as enhanced stability and solubility and improved absorption and bioavailability, and thus, more targeted delivery and upgraded therapeutic efficacy. Nonetheless, further investigation and clinical data are required to draw safe conclusions regarding the toxicity and safety of these nanoformulations. Finally, it is important to stress that both the research community as well as international and local authorities should establish shared legislation and common protocols to ensure the safety of consumers.

Author Contributions: Conceptualization, T.T., E.K. and P.Z.; methodology, T.T. and E.K.; investigation, K.T., P.C. and V.J.S.; data curation, T.T., K.T., P.C. and E.K.; writing—original draft preparation, T.T., K.T., P.C. and E.K.; writing—review and editing, T.T., V.J.S., E.K. and P.Z.; visualization, K.T. and P.C.; supervision, E.K. and P.Z.; project administration, V.J.S. and P.Z. All authors have read and agreed to the published version of the manuscript.

Funding: This research received no external funding.

Institutional Review Board Statement: Not applicable.

Informed Consent Statement: Not applicable.

Data Availability Statement: Not applicable.

Conflicts of Interest: The authors declare no conflict of interest.

References

1. Dikmen, B.Y.; Filazi, A. Chapter 69—Nutraceuticals: Turkish Perspective. In *Nutraceuticals*; Gupta, R.C., Ed.; Academic Press: Boston, MA, USA, 2016; pp. 971–981.
2. Nasri, H.; Baradaran, A.; Shirzad, H.; Rafieian-Kopaei, M. New Concepts in Nutraceuticals as Alternative for Pharmaceuticals. *Int. J. Prev. Med.* **2014**, *5*, 1487–1499. [PubMed]
3. Chopra, A.S.; Lordan, R.; Horbańczuk, O.K.; Atanasov, A.G.; Chopra, I.; Horbańczuk, J.O.; Jóźwik, A.; Huang, L.; Pirgozliev, V.; Banach, M.; et al. The Current Use and Evolving Landscape of Nutraceuticals. *Pharmacol. Res.* **2022**, *175*, 106001. [CrossRef] [PubMed]
4. BCC Research. Nutraceuticals Market Size, Share & Growth Analysis Report. Available online: https://www.bccresearch.com/market-research/food-and-beverage/nutraceuticals-global-markets.html (accessed on 13 March 2022).
5. Mordor Intelligence. Global Nutraceuticals Market Size, Share, Trends, Growth (2022–27). Available online: https://www.mordorintelligence.com/industry-reports/global-nutraceuticals-market-industry (accessed on 13 March 2022).
6. Daliu, P.; Santini, A.; Novellino, E. A Decade of Nutraceutical Patents: Where Are We Now in 2018? *Expert Opin. Ther. Patents* **2018**, *28*, 875–882. [CrossRef] [PubMed]
7. Aguilar-Pérez, K.M.; Ruiz-Pulido, G.; Medina, D.I.; Parra-Saldivar, R.; Iqbal, H.M. Insight of Nanotechnological Processing for Nano-Fortified Functional Foods and Nutraceutical—Opportunities, Challenges, and Future Scope in Food for Better Health. *Crit. Rev. Food Sci. Nutr.* **2021**, 1–18. [CrossRef] [PubMed]
8. Paolino, D.; Mancuso, A.; Cristiano, M.C.; Froiio, F.; Lammari, N.; Celia, C.; Fresta, M. Nanonutraceuticals: The New Frontier of Supplementary Food. *Nanomaterials* **2021**, *11*, 792. [CrossRef] [PubMed]
9. Daliu, P.; Santini, A.; Novellino, E. From Pharmaceuticals to Nutraceuticals: Bridging Disease Prevention and Management. *Expert Rev. Clin. Pharmacol.* **2019**, *12*, 1–7. [CrossRef]
10. Hesari, M.; Mohammadi, P.; Khademi, F.; Shackebaei, D.; Momtaz, S.; Moasefi, N.; Farzaei, M.H.; Abdollahi, M. Current Advances in the Use of Nanophytomedicine Therapies for Human Cardiovascular Diseases. *Int. J. Nanomed.* **2021**, *16*, 3293–3315. [CrossRef]
11. Murugan, N.A.; Podobas, A.; Gadioli, D.; Vitali, E.; Palermo, G.; Markidis, S. A Review on Parallel Virtual Screening Softwares for High-Performance Computers. *Pharmaceuticals* **2022**, *15*, 63. [CrossRef]
12. Suay-García, B.; Bueso-Bordils, J.I.; Falcó, A.; Antón-Fos, G.M.; Alemán-López, P.A. Virtual Combinatorial Chemistry and Pharmacological Screening: A Short Guide to Drug Design. *Int. J. Mol. Sci.* **2022**, *23*, 1620. [CrossRef]
13. Haga, J.H.; Ichikawa, K.; Date, S. Virtual Screening Techniques and Current Computational Infrastructures. *Curr. Pharm. Des.* **2016**, *22*, 3576–3584. [CrossRef]
14. Kumar, R.; Singh, A.K.; Gupta, A.; Pandey, A.K. In-Silico Approaches to Study Therapeutic Efficacy of Nutraceuticals. In *Phytochemistry: An In-Silico and In-Vitro Update: Advances in Phytochemical Research*; Kumar, S., Egbuna, C., Eds.; Springer: Singapore, 2019; pp. 479–490.
15. Andlauer, W.; Fürst, P. Nutraceuticals: A Piece of History, Present Status and Outlook. *Food Res. Int.* **2002**, *35*, 171–176. [CrossRef]
16. De Felice, S.L. The Nutraceutical Revolution: Its Impact on Food Industry R&D. *Trends Food Sci. Technol.* **1995**, *6*, 59–61. [CrossRef]
17. Pandey, M.; Verma, R.; Saraf, S. Nutraceuticals: New Era of Medicine and Health. *Asian J. Pharm. Clin. Res.* **2010**, *3*, 2010.
18. Andrew, R.; Izzo, A.A. Principles of Pharmacological Research of Nutraceuticals. *Br. J. Pharmacol.* **2017**, *174*, 1177–1194. [CrossRef] [PubMed]
19. Aronson, J.K. Defining "Nutraceuticals": Neither Nutritious nor Pharmaceutical. *Br. J. Clin. Pharmacol.* **2017**, *83*, 8–19. [CrossRef]
20. Ansari, S.; Chauhan, B.; Kalam, N.; Kumar, G. Current Concepts and Prospects of Herbal Nutraceutical: A Review. *J. Adv. Pharm. Technol. Res.* **2013**, *4*, 4–8. [CrossRef]
21. De, S.; Gopikrishna, A.; Keerthana, V.; Girigoswami, A.; Girigoswami, K. An Overview of Nanoformulated Nutraceuticals and Their Therapeutic Approaches. *Curr. Nutr. Food Sci.* **2021**, *17*, 392–407. [CrossRef]
22. Blaze, J. A Comparison of Current Regulatory Frameworks for Nutraceuticals in Australia, Canada, Japan, and the United States. *Innov. Pharm.* **2021**, *12*, 8. [CrossRef]
23. Santini, A.; Cammarata, S.M.; Capone, G.; Ianaro, A.; Tenore, G.C.; Pani, L.; Novellino, E. Nutraceuticals: Opening the Debate for a Regulatory Framework: Nutraceutical Regulatory Framework. *Br. J. Clin. Pharmacol.* **2018**, *84*, 659–672. [CrossRef]
24. Lagunin, A.A.; Goel, R.K.; Gawande, D.Y.; Pahwa, P.; Gloriozova, T.A.; Dmitriev, A.V.; Ivanov, S.M.; Rudik, A.V.; Konova, V.I.; Pogodin, P.V.; et al. Chemo- and Bioinformatics Resources for in Silico Drug Discovery from Medicinal Plants beyond Their Traditional Use: A Critical Review. *Nat. Prod. Rep.* **2014**, *31*, 1585–1611. [CrossRef]
25. Global Natural & Organic Personal Care Market 2018–2026: Growth Trends, Key Players and Competitive Strategies. Available online: https://www.prnewswire.com/news-releases/global-natural--organic-personal-care-market-2018-2026-growth-trends-key-players-and-competitive-strategies-300675255.html (accessed on 13 March 2022).
26. Chen, Y.; de Bruyn Kops, C.; Kirchmair, J. Data Resources for the Computer-Guided Discovery of Bioactive Natural Products. *J. Chem. Inf. Model.* **2017**, *57*, 2099–2111. [CrossRef] [PubMed]
27. Sorokina, M.; Merseburger, P.; Rajan, K.; Yirik, M.A.; Steinbeck, C. COCONUT Online: Collection of Open Natural Products Database. *J. Cheminform.* **2021**, *13*, 2. [CrossRef] [PubMed]
28. van Santen, J.A.; Jacob, G.; Singh, A.L.; Aniebok, V.; Balunas, M.J.; Bunsko, D.; Neto, F.C.; Castaño-Espriu, L.; Chang, C.; Clark, T.N.; et al. The Natural Products Atlas: An Open Access Knowledge Base for Microbial Natural Products Discovery. *ACS Cent. Sci.* **2019**, *5*, 1824–1833. [CrossRef] [PubMed]

29. Naveja, J.J.; Rico-Hidalgo, M.P.; Medina-Franco, J.L. Analysis of a Large Food Chemical Database: Chemical Space, Diversity, and Complexity. *F1000Research* **2018**, *7*, 993. [CrossRef]
30. Zeng, X.; Zhang, P.; Wang, Y.; Qin, C.; Chen, S.; He, W.; Tao, L.; Tan, Y.; Gao, D.; Wang, B.; et al. CMAUP: A Database of Collective Molecular Activities of Useful Plants. *Nucleic Acids Res.* **2019**, *47*, D1118–D1127. [CrossRef]
31. Choudhary, A.; Naughton, L.M.; Montánchez, I.; Dobson, A.D.W.; Rai, D.K. Current Status and Future Prospects of Marine Natural Products (MNPs) as Antimicrobials. *Mar. Drugs* **2017**, *15*, 272. [CrossRef]
32. Pradhan, B.; Nayak, R.; Patra, S.; Jit, B.P.; Ragusa, A.; Jena, M. Bioactive Metabolites from Marine Algae as Potent Pharmacophores against Oxidative Stress-Associated Human Diseases: A Comprehensive Review. *Molecules* **2021**, *26*, 37. [CrossRef]
33. Ghosh, S.; Sarkar, T.; Pati, S.; Kari, Z.A.; Edinur, H.A.; Chakraborty, R. Novel Bioactive Compounds From Marine Sources as a Tool for Functional Food Development. *Front. Mar. Sci.* **2022**, *9*, 832957. [CrossRef]
34. Khanam, S.; Prakash, A. Biomedical Applications and Therapeutic Potential of Marine Natural Products and Marine Algae. *IP J. Nutr. Metab. Health Sci.* **2021**, *4*, 76–82. [CrossRef]
35. Lyu, C.; Chen, T.; Qiang, B.; Liu, N.; Wang, H.; Zhang, L.; Liu, Z. CMNPD: A Comprehensive Marine Natural Products Database towards Facilitating Drug Discovery from the Ocean. *Nucleic Acids Res.* **2021**, *49*, D509–D515. [CrossRef]
36. Diallo, B.N.; Glenister, M.; Musyoka, T.M.; Lobb, K.; Tastan Bishop, Ö. SANCDB: An Update on South African Natural Compounds and Their Readily Available Analogs. *J. Cheminform.* **2021**, *13*, 37. [CrossRef] [PubMed]
37. Pilon, A.C.; Valli, M.; Dametto, A.C.; Pinto, M.E.F.; Freire, R.T.; Castro-Gamboa, I.; Andricopulo, A.D.; Bolzani, V.S. NuBBEDB: An Updated Database to Uncover Chemical and Biological Information from Brazilian Biodiversity. *Sci. Rep.* **2017**, *7*, 7215. [CrossRef] [PubMed]
38. Tung, C.W.; Lin, Y.C.; Chang, H.S.; Wang, C.C.; Chen, I.S.; Jheng, J.L.; Li, J.H. TIPdb-3D: The Three-Dimensional Structure Database of Phytochemicals from Taiwan Indigenous Plants. *Database* **2014**, *2014*, bau055. [CrossRef] [PubMed]
39. Chen, C.Y.C. TCM Database@Taiwan: The World's Largest Traditional Chinese Medicine Database for Drug Screening In Silico. *PLoS ONE* **2011**, *6*, e15939. [CrossRef] [PubMed]
40. Degtyarenko, K.; de Matos, P.; Ennis, M.; Hastings, J.; Zbinden, M.; McNaught, A.; Alcántara, R.; Darsow, M.; Guedj, M.; Ashburner, M. ChEBI: A Database and Ontology for Chemical Entities of Biological Interest. *Nucleic Acids Res.* **2008**, *36*, D344–D350. [CrossRef]
41. Ntie-Kang, F.; Zofou, D.; Babiaka, S.B.; Meudom, R.; Scharfe, M.; Lifongo, L.L.; Mbah, J.A.; Mbaze, L.M.; Sippl, W.; Efange, S.M.N. AfroDb: A Select Highly Potent and Diverse Natural Product Library from African Medicinal Plants. *PLoS ONE* **2013**, *8*, e78085. [CrossRef]
42. Sterling, T.; Irwin, J.J. ZINC 15—Ligand Discovery for Everyone. *J. Chem. Inf. Model.* **2015**, *55*, 2324–2337. [CrossRef]
43. da Silva Rocha, S.F.L.; Olanda, C.G.; Fokoue, H.H.; Sant'Anna, C.M.R. Virtual Screening Techniques in Drug Discovery: Review and Recent Applications. *Curr. Top. Med. Chem.* **2019**, *19*, 1751–1767. [CrossRef]
44. Lin, X.; Li, X.; Lin, X. A Review on Applications of Computational Methods in Drug Screening and Design. *Molecules* **2020**, *25*, 1375. [CrossRef]
45. Carpio, L.E.; Sanz, Y.; Gozalbes, R.; Barigye, S.J. Computational Strategies for the Discovery of Biological Functions of Health Foods, Nutraceuticals and Cosmeceuticals: A Review. *Mol. Divers.* **2021**, *25*, 1425–1438. [CrossRef]
46. Neves, B.J.; Braga, R.C.; Melo-Filho, C.C.; Moreira-Filho, J.T.; Muratov, E.N.; Andrade, C.H. QSAR-Based Virtual Screening: Advances and Applications in Drug Discovery. *Front. Pharmacol.* **2018**, *9*, 1275. [CrossRef] [PubMed]
47. Akamatsu, M. Current State and Perspectives of 3D-QSAR. *Curr. Top. Med. Chem.* **2002**, *2*, 1381–1394. [CrossRef] [PubMed]
48. Rybińska-Fryca, A.; Sosnowska, A.; Puzyn, T. Representation of the Structure—A Key Point of Building QSAR/QSPR Models for Ionic Liquids. *Materials* **2020**, *13*, 2500. [CrossRef] [PubMed]
49. Roy, K.; Kar, S.; Das, R.N. Chemical Information and Descriptors. In *Understanding the Basics of QSAR for Applications in Pharmaceutical Sciences and Risk Assessment*; Elsevier: Amsterdam, The Netherlands, 2015; pp. 47–80.
50. Dudek, A.Z.; Arodz, T.; Gálvez, J. Computational Methods in Developing Quantitative Structure-Activity Relationships (QSAR): A Review. *Comb. Chem. High Throughput Screen* **2006**, *9*, 213–228. [CrossRef]
51. Cherkasov, A.; Muratov, E.; Fourches, D.; Varnek, A.; Baskin, I.; Cronin, M.; Dearden, J.; Gramatica, P.; Martin, Y.; Todeschini, R.; et al. QSAR Modeling: Where Have You Been? Where Are You Going To? *J. Med. Chem.* **2013**, *57*, 4977–5010. [CrossRef]
52. Achary, P.G.R. Applications of Quantitative Structure-Activity Relationships (QSAR) Based Virtual Screening in Drug Design: A Review. *Mini Rev. Med. Chem.* **2020**, *20*, 1375–1388. [CrossRef]
53. Pripp, A.H.; Isaksson, T.; Stepaniak, L.; Sørhaug, T.; Ardö, Y. Quantitative Structure Activity Relationship Modelling of Peptides and Proteins as a Tool in Food Science. *Trends Food Sci. Technol.* **2005**, *16*, 484–494. [CrossRef]
54. Meng, X.Y.; Zhang, H.X.; Mezei, M.; Cui, M. Molecular Docking: A Powerful Approach for Structure-Based Drug Discovery. *Curr. Comput. Aided Drug Des.* **2011**, *7*, 146–157. [CrossRef]
55. Smyth, M.S.; Martin, J.H. X Ray Crystallography. *Mol. Pathol.* **2000**, *53*, 8–14. [CrossRef]
56. Sugiki, T.; Kobayashi, N.; Fujiwara, T. Modern Technologies of Solution Nuclear Magnetic Resonance Spectroscopy for Three-Dimensional Structure Determination of Proteins Open Avenues for Life Scientists. *Comput. Struct. Biotechnol. J.* **2017**, *15*, 328–339. [CrossRef]
57. Nakane, T.; Kotecha, A.; Sente, A.; McMullan, G.; Masiulis, S.; Brown, P.M.G.E.; Grigoras, I.T.; Malinauskaite, L.; Malinauskas, T.; Miehling, J.; et al. Single-Particle Cryo-EM at Atomic Resolution. *Nature* **2020**, *587*, 152–156. [CrossRef] [PubMed]

58. Pinzi, L.; Rastelli, G. Molecular Docking: Shifting Paradigms in Drug Discovery. *Int. J. Mol. Sci.* **2019**, *20*, 4331. [CrossRef] [PubMed]
59. Tao, X.; Huang, Y.; Wang, C.; Chen, F.; Yang, L.; Ling, L.; Che, Z.; Chen, X. Recent Developments in Molecular Docking Technology Applied in Food Science: A Review. *Int. J. Food Sci. Technol.* **2020**, *55*, 33–45. [CrossRef]
60. Morris, G.M.; Huey, R.; Lindstrom, W.; Sanner, M.F.; Belew, R.K.; Goodsell, D.S.; Olson, A.J. AutoDock4 and AutoDockTools4: Automated Docking with Selective Receptor Flexibility. *J. Comput. Chem.* **2009**, *30*, 2785–2791. [CrossRef] [PubMed]
61. Trott, O.; Olson, A.J. AutoDock Vina: Improving the Speed and Accuracy of Docking with a New Scoring Function, Efficient Optimization, and Multithreading. *J. Comput. Chem.* **2010**, *31*, 455–461. [CrossRef] [PubMed]
62. Allen, W.J.; Balius, T.E.; Mukherjee, S.; Brozell, S.R.; Moustakas, D.T.; Lang, P.T.; Case, D.A.; Kuntz, I.D.; Rizzo, R.C. DOCK 6: Impact of New Features and Current Docking Performance. *J. Comput. Chem.* **2015**, *36*, 1132–1156. [CrossRef]
63. Jones, G.; Willett, P.; Glen, R.C.; Leach, A.R.; Taylor, R. Development and Validation of a Genetic Algorithm for Flexible Docking11Edited by F. E. Cohen. *J. Mol. Biol.* **1997**, *267*, 727–748. [CrossRef]
64. Friesner, R.A.; Murphy, R.B.; Repasky, M.P.; Frye, L.L.; Greenwood, J.R.; Halgren, T.A.; Sanschagrin, P.C.; Mainz, D.T. Extra Precision Glide: Docking and Scoring Incorporating a Model of Hydrophobic Enclosure for Protein-Ligand Complexes. *J. Med. Chem.* **2006**, *49*, 6177–6196. [CrossRef]
65. Corbeil, C.R.; Williams, C.I.; Labute, P. Variability in Docking Success Rates Due to Dataset Preparation. *J. Comput. Aided Mol. Des.* **2012**, *26*, 775–786. [CrossRef]
66. Dallakyan, S.; Olson, A.J. Small-Molecule Library Screening by Docking with PyRx. *Methods Mol. Biol.* **2015**, *1263*, 243–250. [CrossRef]
67. McGann, M. FRED and HYBRID Docking Performance on Standardized Datasets. *J. Comput. Aided Mol. Des.* **2012**, *26*, 897–906. [CrossRef] [PubMed]
68. McGann, M. FRED Pose Prediction and Virtual Screening Accuracy. *J. Chem. Inf. Model.* **2011**, *51*, 578–596. [CrossRef] [PubMed]
69. Kelley, B.P.; Brown, S.P.; Warren, G.L.; Muchmore, S.W. POSIT: Flexible Shape-Guided Docking for Pose Prediction. *J. Chem. Inf. Model.* **2015**, *55*, 1771–1780. [CrossRef] [PubMed]
70. van Zundert, G.C.P.; Rodrigues, J.P.G.L.M.; Trellet, M.; Schmitz, C.; Kastritis, P.L.; Karaca, E.; Melquiond, A.S.J.; van Dijk, M.; de Vries, S.J.; Bonvin, A.M.J.J. The HADDOCK2.2 Web Server: User-Friendly Integrative Modeling of Biomolecular Complexes. *J. Mol. Biol.* **2016**, *428*, 720–725. [CrossRef] [PubMed]
71. Bitencourt-Ferreira, G.; de Azevedo, W.F. Docking with SwissDock. *Methods Mol. Biol.* **2019**, *2053*, 189–202. [CrossRef]
72. Seidel, T.; Bryant, S.D.; Ibis, G.; Poli, G.; Langer, T. 3D Pharmacophore Modeling Techniques in Computer-Aided Molecular Design Using LigandScout. In *Tutorials in Chemoinformatics*; John Wiley & Sons, Ltd.: Hoboken, NJ, USA, 2017; pp. 279–309.
73. Yang, S.Y. Pharmacophore Modeling and Applications in Drug Discovery: Challenges and Recent Advances. *Drug Discov. Today* **2010**, *15*, 444–450. [CrossRef] [PubMed]
74. Schaller, D.; Šribar, D.; Noonan, T.; Deng, L.; Nguyen, T.N.; Pach, S.; Machalz, D.; Bermudez, M.; Wolber, G. Next Generation 3D Pharmacophore Modeling. *WIREs Comput. Mol. Sci.* **2020**, *10*, e1468. [CrossRef]
75. Grabowski, M.; Murgueitio, M.S.; Bermudez, M.; Rademann, J.; Wolber, G.; Weindl, G. Identification of a Pyrogallol Derivative as a Potent and Selective Human TLR2 Antagonist by Structure-Based Virtual Screening. *Biochem. Pharmacol.* **2018**, *154*, 148–160. [CrossRef]
76. Grabowski, M.; Murgueitio, M.S.; Bermudez, M.; Wolber, G.; Weindl, G. The Novel Small-Molecule Antagonist MMG-11 Preferentially Inhibits TLR2/1 Signaling. *Biochem. Pharmacol.* **2020**, *171*, 113687. [CrossRef]
77. Barnum, D.; Greene, J.; Smellie, A.; Sprague, P. Identification of Common Functional Configurations Among Molecules. *J. Chem. Inf. Comput. Sci.* **1996**, *36*, 563–571. [CrossRef]
78. Baroni, M.; Cruciani, G.; Sciabola, S.; Perruccio, F.; Mason, J.S. A Common Reference Framework for Analyzing/Comparing Proteins and Ligands. Fingerprints for Ligands and Proteins (FLAP): Theory and Application. *J. Chem. Inf. Model.* **2007**, *47*, 279–294. [CrossRef] [PubMed]
79. Wolber, G.; Langer, T. LigandScout: 3-D Pharmacophores Derived from Protein-Bound Ligands and Their Use as Virtual Screening Filters. *J. Chem. Inf. Model.* **2005**, *45*, 160–169. [CrossRef] [PubMed]
80. Koes, D.R.; Camacho, C.J. Pharmer: Efficient and Exact Pharmacophore Search. *J. Chem. Inf. Model.* **2011**, *51*, 1307–1314. [CrossRef]
81. Dixon, S.L.; Smondyrev, A.M.; Knoll, E.H.; Rao, S.N.; Shaw, D.E.; Friesner, R.A. PHASE: A New Engine for Pharmacophore Perception, 3D QSAR Model Development, and 3D Database Screening: 1. Methodology and Preliminary Results. *J. Comput. Aided Mol. Des.* **2006**, *20*, 647–671. [CrossRef] [PubMed]
82. Lee, J.Y.; Krieger, J.M.; Li, H.; Bahar, I. Pharmmaker: Pharmacophore Modeling and Hit Identification Based on Druggability Simulations. *Protein Sci.* **2020**, *29*, 76–86. [CrossRef]
83. Schneidman-Duhovny, D.; Dror, O.; Inbar, Y.; Nussinov, R.; Wolfson, H.J. PharmaGist: A Webserver for Ligand-Based Pharmacophore Detection. *Nucleic Acids Res.* **2008**, *36*, W223–W228. [CrossRef]
84. Hollingsworth, S.A.; Dror, R.O. Molecular Dynamics Simulation for All. *Neuron* **2018**, *99*, 1129–1143. [CrossRef]
85. Chen, G.; Huang, K.; Miao, M.; Feng, B.; Campanella, O.H. Molecular Dynamics Simulation for Mechanism Elucidation of Food Processing and Safety: State of the Art. *Compr. Rev. Food Sci. Food Saf.* **2019**, *18*, 243–263. [CrossRef]
86. González, M.A. Force Fields and Molecular Dynamics Simulations. *École Thématique Société Française Neutron* **2011**, *12*, 169–200. [CrossRef]

87. Pronk, S.; Páll, S.; Schulz, R.; Larsson, P.; Bjelkmar, P.; Apostolov, R.; Shirts, M.R.; Smith, J.C.; Kasson, P.M.; van der Spoel, D.; et al. GROMACS 4.5: A High-Throughput and Highly Parallel Open Source Molecular Simulation Toolkit. *Bioinformatics* **2013**, *29*, 845–854. [CrossRef]
88. Case, D.A.; Cheatham, T.E., III; Darden, T.; Gohlke, H.; Luo, R.; Merz, K.M., Jr.; Onufriev, A.; Simmerling, C.; Wang, B.; Woods, R.J. The Amber Biomolecular Simulation Programs. *J. Comput. Chem.* **2005**, *26*, 1668–1688. [CrossRef] [PubMed]
89. Salomon-Ferrer, R.; Götz, A.W.; Poole, D.; Le Grand, S.; Walker, R.C. Routine Microsecond Molecular Dynamics Simulations with AMBER on GPUs. 2. Explicit Solvent Particle Mesh Ewald. *J. Chem. Theory Comput.* **2013**, *9*, 3878–3888. [CrossRef] [PubMed]
90. Phillips, J.C.; Braun, R.; Wang, W.; Gumbart, J.; Tajkhorshid, E.; Villa, E.; Chipot, C.; Skeel, R.D.; Kalé, L.; Schulten, K. Scalable Molecular Dynamics with NAMD. *J. Comput. Chem.* **2005**, *26*, 1781–1802. [CrossRef] [PubMed]
91. Brooks, B.R.; Brooks, C.L., III; Mackerell, A.D., Jr.; Nilsson, L.; Petrella, R.J.; Roux, B.; Won, Y.; Archontis, G.; Bartels, C.; Boresch, S.; et al. CHARMM: The Biomolecular Simulation Program. *J. Comput. Chem.* **2009**, *30*, 1545–1614. [CrossRef] [PubMed]
92. Shukla, R.; Tripathi, T. Molecular Dynamics Simulation of Protein and Protein–Ligand Complexes. In *Computer-Aided Drug Design*; Singh, D.B., Ed.; Springer: Singapore, 2020; pp. 133–161.
93. Tagde, P.; Tagde, S.; Tagde, P.; Bhattacharya, T.; Monzur, S.M.; Rahman, M.H.; Otrisal, P.; Behl, T.; ul Hassan, S.S.; Abdel-Daim, M.M.; et al. Nutraceuticals and Herbs in Reducing the Risk and Improving the Treatment of COVID-19 by Targeting SARS-CoV-2. *Biomedicines* **2021**, *9*, 1266. [CrossRef] [PubMed]
94. Savant, S.; Srinivasan, S.; Kruthiventi, A.K. Potential Nutraceuticals for COVID-19. *Nutr. Diet. Suppl.* **2021**, *13*, 25–51. [CrossRef]
95. Gyebi, G.A.; Elfiky, A.A.; Ogunyemi, O.M.; Ibrahim, I.M.; Adegunloye, A.P.; Adebayo, J.O.; Olaiya, C.O.; Ocheje, J.O.; Fabusiwa, M.M. Structure-Based Virtual Screening Suggests Inhibitors of 3-Chymotrypsin-Like Protease of SARS-CoV-2 from Vernonia Amygdalina and Occinum Gratissimum. *Comput. Biol. Med.* **2021**, *136*, 104671. [CrossRef]
96. Kodchakorn, K.; Poovorawan, Y.; Suwannakarn, K.; Kongtawelert, P. Molecular Modelling Investigation for Drugs and Nutraceuticals against Protease of SARS-CoV-2. *J. Mol. Graph. Model.* **2020**, *101*, 107717. [CrossRef]
97. Baig, A.; Srinivasan, H. SARS-CoV-2 Inhibitors from Nigella Sativa. *Appl. Biochem. Biotechnol.* **2022**, *194*, 1051–1090. [CrossRef]
98. Gupta, S.; Tejavath, K.K. Nano Phytoceuticals: A Step Forward in Tracking Down Paths for Therapy Against Pancreatic Ductal Adenocarcinoma. *J. Clust. Sci.* **2022**, 1–21. [CrossRef]
99. Dubey, A.K.; Chaudhry, S.K.; Singh, H.B.; Gupta, V.K.; Kaushik, A. Perspectives on Nano-Nutraceuticals to Manage Pre and Post COVID-19 Infections. *Biotechnol. Rep.* **2022**, *33*, e00712. [CrossRef] [PubMed]
100. Shende, P.; Mallick, C. Nanonutraceuticals: A Way towards Modern Therapeutics in Healthcare. *J. Drug Deliv. Sci. Technol.* **2020**, *58*, 101838. [CrossRef]
101. Ferrado, J.B.; Perez, A.A.; Ruiz, M.C.; León, I.E.; Santiago, L.G. Chrysin-Loaded Bovine Serum Albumin Particles as Bioactive Nanosupplements. *Food Funct.* **2020**, *11*, 6007–6019. [CrossRef] [PubMed]
102. El-Far, A.H.; Godugu, K.; Salaheldin, T.A.; Darwish, N.H.E.; Saddiq, A.A.; Mousa, S.A. Nanonutraceuticals: Anti-Cancer Activity and Improved Safety of Chemotherapy by Costunolide and Its Nanoformulation against Colon and Breast Cancer. *Biomedicines* **2021**, *9*, 990. [CrossRef] [PubMed]
103. Sikk, A.M. Review on Defensive Roles of Thymoquinone Nanobiosensoring Prospective in Opposition to Cancer. *J. Cancer Clin. Res.* **2021**, *4*, 297–299.
104. Rahat, I.; Rizwanullah, M.; Gilani, S.J.; Bin-Jummah, M.N.; Imam, S.S.; Kala, C.; Asif, M.; Alshehri, S.; Sharma, S.K. Thymoquinone Loaded Chitosan—Solid Lipid Nanoparticles: Formulation Optimization to Oral Bioavailability Study. *J. Drug Deliv. Sci. Technol.* **2021**, *64*, 102565. [CrossRef]
105. Sanders, M.E.; Merenstein, D.J.; Reid, G.; Gibson, G.R.; Rastall, R.A. Probiotics and Prebiotics in Intestinal Health and Disease: From Biology to the Clinic. *Nat. Rev. Gastroenterol. Hepatol.* **2019**, *16*, 605–616. [CrossRef]
106. Ashaolu, T.J. Emerging Applications of Nanotechnologies to Probiotics and Prebiotics. *Int. J. Food Sci. Technol.* **2021**, *56*, 3719–3725. [CrossRef]
107. Durazzo, A.; Nazhand, A.; Lucarini, M.; Atanasov, A.G.; Souto, E.B.; Novellino, E.; Capasso, R.; Santini, A. An Updated Overview on Nanonutraceuticals: Focus on Nanoprebiotics and Nanoprobiotics. *Int. J. Mol. Sci.* **2020**, *21*, 2285. [CrossRef]
108. Rambaran, T.F. A Patent Review of Polyphenol Nano-Formulations and Their Commercialization. *Trends Food Sci. Technol.* **2022**, *120*, 111–122. [CrossRef]
109. Palla, C.A.; Aguilera-Garrido, A.; Carrín, M.E.; Galisteo-González, F.; Gálvez-Ruiz, M.J. Preparation of Highly Stable Oleogel-Based Nanoemulsions for Encapsulation and Controlled Release of Curcumin. *Food Chem.* **2022**, *378*, 132132. [CrossRef] [PubMed]
110. Harakeh, S.; Qari, Y.; Tashkandi, H.; Almuhayawi, M.; Saber, S.H.; aljahdali, E.; El-Shitany, N.; Shaker, S.; Lucas, F.; Alamri, T.; et al. Thymoquinone Nanoparticles Protect against Cisplatin-Induced Nephrotoxicity in Ehrlich Carcinoma Model without Compromising Cisplatin Anti-Cancer Efficacy. *J. King Saud Univ. Sci.* **2022**, *34*, 101675. [CrossRef]
111. Radwan, M.F.; El-Moselhy, M.A.; Alarif, W.M.; Orif, M.; Alruwaili, N.K.; Alhakamy, N.A. Optimization of Thymoquinone-Loaded Self-Nanoemulsion for Management of Indomethacin-Induced Ulcer. *Dose-Response* **2021**, *19*, 155932582110136. [CrossRef]
112. Alhakamy, N.A.; Badr-Eldin, S.M.; Ahmed, O.A.A.; Aldawsari, H.M.; Okbazghi, S.Z.; Alfaleh, M.A.; Abdulaal, W.H.; Neamatallah, T.; Al-hejaili, O.D.; Fahmy, U.A. Green Nanoemulsion Stabilized by In Situ Self-Assembled Natural Oil/Native Cyclodextrin Complexes: An Eco-Friendly Approach for Enhancing Anticancer Activity of Costunolide against Lung Cancer Cells. *Pharmaceutics* **2022**, *14*, 227. [CrossRef] [PubMed]

113. Rinaldi, F.; Maurizi, L.; Forte, J.; Marazzato, M.; Hanieh, P.; Conte, A.; Ammendolia, M.; Marianecci, C.; Carafa, M.; Longhi, C. Resveratrol-Loaded Nanoemulsions: In Vitro Activity on Human T24 Bladder Cancer Cells. *Nanomaterials* **2021**, *11*, 1569. [CrossRef] [PubMed]
114. Javed Iqbal, M.; Quispe, C.; Javed, Z.; Sadia, H.; Qadri, Q.R.; Raza, S.; Salehi, B.; Cruz-Martins, N.; Abdulwanis Mohamed, Z.; Sani Jaafaru, M.; et al. Nanotechnology-Based Strategies for Berberine Delivery System in Cancer Treatment: Pulling Strings to Keep Berberine in Power. *Front. Mol. Biosci.* **2021**, *7*, 624494. [CrossRef]
115. Cristiano, M.C.; Froiio, F.; Mancuso, A.; Cosco, D.; Dini, L.; Di Marzio, L.; Fresta, M.; Paolino, D. Oleuropein-Laded Ufasomes Improve the Nutraceutical Efficacy. *Nanomaterials* **2021**, *11*, 105. [CrossRef]
116. Landucci, E.; Bonomolo, F.; De Stefani, C.; Mazzantini, C.; Pellegrini-Giampietro, D.E.; Bilia, A.R.; Bergonzi, M.C. Preparation of Liposomal Formulations for Ocular Delivery of Thymoquinone: In Vitro Evaluation in HCEC-2 e HConEC Cells. *Pharmaceutics* **2021**, *13*, 2093. [CrossRef]
117. Rachamalla, H.K.; Bhattacharya, S.; Ahmad, A.; Sridharan, K.; Madamsetty, V.S.; Mondal, S.K.; Wang, E.; Dutta, S.K.; Jan, B.L.; Jinka, S.; et al. Enriched Pharmacokinetic Behavior and Antitumor Efficacy of Thymoquinone by Liposomal Delivery. *Nanomedicine* **2021**, *16*, 641–656. [CrossRef]
118. Castangia, I.; Manconi, M.; Allaw, M.; Perra, M.; Orrù, G.; Fais, S.; Scano, A.; Escribano-Ferrer, E.; Ghavam, M.; Rezvani, M.; et al. Mouthwash Formulation Co-Delivering Quercetin and Mint Oil in Liposomes Improved with Glycol and Ethanol and Tailored for Protecting and Tackling Oral Cavity. *Antioxidants* **2022**, *11*, 367. [CrossRef]
119. Ghorbani, S.; Maryam, A. Encapsulation of Lactic Acid Bacteria and Bifidobacteria Using Starch-sodium Alginate Nanofibers to Enhance Viability in Food Model. *J. Food Process. Preserv.* **2021**, *45*, e16048. [CrossRef]
120. Atraki, R.; Azizkhani, M. Survival of Probiotic Bacteria Nanoencapsulated within Biopolymers in a Simulated Gastrointestinal Model. *Innov. Food Sci. Emerg. Technol.* **2021**, *72*, 102750. [CrossRef]
121. Pugliese, R.; Bartolomei, M.; Bollati, C.; Boschin, G.; Arnoldi, A.; Lammi, C. Gel-Forming of Self-Assembling Peptides Functionalized with Food Bioactive Motifs Modulate DPP-IV and ACE Inhibitory Activity in Human Intestinal Caco-2 Cells. *Biomedicines* **2022**, *10*, 330. [CrossRef] [PubMed]
122. Pugliese, R.; Arnoldi, A.; Lammi, C. Nanostructure, Self-Assembly, Mechanical Properties, and Antioxidant Activity of a Lupin-Derived Peptide Hydrogel. *Biomedicines* **2021**, *9*, 294. [CrossRef]
123. Faruk, E.M.; Fouad, H.; Hasan, R.A.A.; Taha, N.M.; El-Shazly, A.M. Inhibition of Gene Expression and Production of INOS and TNF-α in Experimental Model of Neurodegenerative Disorders Stimulated Microglia by Soy Nano-Isoflavone/Stem Cell-Exosomes. *Tissue Cell* **2022**, *76*, 101758. [CrossRef]

antioxidants

MDPI

Article

A Randomized Controlled Trial on *Pleurotus eryngii* Mushrooms with Antioxidant Compounds and Vitamin D_2 in Managing Metabolic Disorders

Stamatia-Angeliki Kleftaki [1], Charalampia Amerikanou [1], Aristea Gioxari [1,2], Dimitra Z. Lantzouraki [3], George Sotiroudis [3], Konstantinos Tsiantas [4], Thalia Tsiaka [3,4], Dimitra Tagkouli [1], Chara Tzavara [1], Lefteris Lachouvaris [5], Georgios I. Zervakis [6], Nick Kalogeropoulos [1], Panagiotis Zoumpoulakis [3,4] and Andriana C. Kaliora [1,*]

1 Department of Nutrition and Dietetics, School of Health Science and Education, Harokopio University, 70 El. Venizelou Ave., 17676 Athens, Greece
2 Department of Nutritional Science and Dietetics, School of Health Science, University of the Peloponnese, Antikalamos, 24100 Kalamata-Messinia, Greece
3 Institute of Chemical Biology, National Hellenic Research Foundation, 48, Vas. Constantinou Ave., 11635 Athens, Greece
4 Department of Food Science and Technology, University of West Attica, Ag. Spyridonos, 12243 Egaleo, Greece
5 Dirfis Mushrooms P.C., Kathenoi, 34018 Euboea, Greece
6 Laboratory of General and Agricultural Microbiology, Department of Crop Science, Agricultural University of Athens, 11855 Athens, Greece
* Correspondence: akaliora@hua.gr; Tel.: +30-2109549266

check for updates

Citation: Kleftaki, S.-A.; Amerikanou, C.; Gioxari, A.; Lantzouraki, D.Z.; Sotiroudis, G.; Tsiantas, K.; Tsiaka, T.; Tagkouli, D.; Tzavara, C.; Lachouvaris, L.; et al. A Randomized Controlled Trial on *Pleurotus eryngii* Mushrooms with Antioxidant Compounds and Vitamin D_2 in Managing Metabolic Disorders. *Antioxidants* **2022**, *11*, 2113. https://doi.org/10.3390/antiox11112113

Academic Editors: Wlodzimierz Opoka and Bożena Muszyńska

Received: 23 September 2022
Accepted: 25 October 2022
Published: 26 October 2022

Publisher's Note: MDPI stays neutral with regard to jurisdictional claims in published maps and institutional affiliations.

Abstract: This study examined the effects of a *Pleurotus eryngii* mushroom snack on metabolically unhealthy patients. After harvest, mushrooms were baked and subjected to UV-B irradiation to enhance vitamin D_2 content. A randomized controlled trial was conducted for three months with two arms. Both groups received conventional nutritional counseling for metabolic disorders, while the intervention group had to consume the snack daily as well. We collected blood samples at the beginning and the end of the study to determine biochemical measurements and serum 25(OH)D2 and to evaluate inflammation and oxidative stress. One hundred patients consented and were randomized. Comparatively to the control group, snack consumption regulated glucose levels and reduced body weight, fat, waist and hip circumferences. In addition, 25(OH)D2 increased significantly in the intervention group. The levels of LDL and SGOT were lower only in the intervention group. Levels of IL-6 and ox-LDL decreased in the mushroom group, while the overall physical health increased. These findings suggest potential antidiabetic, antiobesity, anti-inflammatory and antioxidant health benefits of the snack to metabolically unhealthy individuals.

Keywords: *Pleurotus eryngii*; metabolically unhealthy; antioxidants; glucose levels; inflammation; oxidative stress; vitamin D; physical health

1. Introduction

Obesity is a chronic relapsing disease, characterized by excessive body fat accumulation. It is associated with a series of disorders, which are threatening for the global public health and economy [1]. During the last few decades, there has been a significant global increase in obesity rate. According to WHO, the prevalence of overweight and obesity cases in the adult population is 39% and 13%, respectively [2]. In recent years, there has been a growing interest in metabolic disorders that represent a cluster of abnormalities, including abdominal adiposity, dyslipidemia, glucose intolerance, insulin resistance and hypertension [3]. There are many health and economic consequences associated with obesity and metabolic disorders, such as type 2 diabetes mellitus (T2DM), cardiovascular disease

(CVD), nonalcoholic fatty liver disease (NAFLD), certain types of cancer, obstructive sleep apnea and depression [4,5].

In order to address the obesity epidemic, a series of approaches have been proposed, including changes in diet. More specifically, there is an increasing interest in the consumption of functional foods which may improve cardiometabolic health [6]. In this respect, edible mushrooms may be a great choice since they demonstrate various medicinal and functional properties [7,8]. Pleurotus species are among the most widely cultivated mushrooms and account for approximately 20% of the respective total global production [9]; they are rich in proteins, fibers, essential amino acids, carbohydrates, water-soluble vitamins, and minerals [10]. In particular, the fruitbodies of *Pleurotus eryngii (P. eryngii)*, also known as "King Oyster mushroom", present a high content of bioactive compounds, such as ergosterol, beta-glucan, and ergothioneine [11,12]. In addition, they are a good source of vitamin D_2, which is produced by the conversion of ergosterol to ergocalciferol after exposure to UV light [13]. As a result, *P. eryngii* exhibits a variety of pharmacological activities and important nutritional value, and has gained a great deal of research attention in recent years due to its antioxidant, immunoregulatory, antihyperlipidemic, and other activities [14].

Although there is a variety of literature on the cardioprotective activities of *P. eryngii* extracts in vitro, as well as in animal studies [15–19], no human clinical trials exist in this field. Our interest in the potential benefits of *P. eryngii* on metabolic parameters was further reinforced by our recent study that showed that a meal with *P. eryngii* can ameliorate postprandial glycemia and appetite, and can regulate ghrelin levels at the postprandial state [20].

Thus, the aim of the present study was to investigate the effects of a *P. eryngii* mushroom snack administered daily for 3 months in metabolically unhealthy patients as regards the improvement in biochemical, inflammatory, oxidative stress, and lifestyle parameters.

2. Materials and Methods

2.1. Study Design

The protocol was reviewed and approved by the Ethics Committee of Harokopio University (ID protocol: 62/03-07-2018). The trial was conducted in accordance with the Helsinki Declaration and the Data Protection Act 1998 and was registered with clinicaltrials.gov (ID Number: NCT04081818). Eligible subjects were enrolled in the study after being informed in detail about its nature and all procedures and having given their written consent for participation. The study took place in Harokopio University of Athens, Greece in 2020 and 2021.

One hundred and eighty metabolically unhealthy subjects were recruited according to predetermined inclusion and exclusion criteria in a randomized controlled trial (Figure 1). Eligible subjects were between the ages of 18 and 76 years and diagnosed with metabolic disorders. They also had a stable weight for at least 3 months before enrollment and a moderately active lifestyle. Exclusion criteria included pregnancy and lactation, untreated thyroid disease, any use of supplements within 3 months pre-intervention, a history of drug and/or alcohol abuse, and psychiatric or mental disorders.

After giving their consent, participants were randomized to the control or intervention group for 3 months. Both arms were given standard nutritional counseling for metabolic disorders throughout the 3-month trial, whereas the intervention group had also to consume the snack daily for 3 months. Randomization was carried out by an independent biostatistician, and compliance was monitored biweekly through phone calls. All baseline assessments were repeated at follow-up.

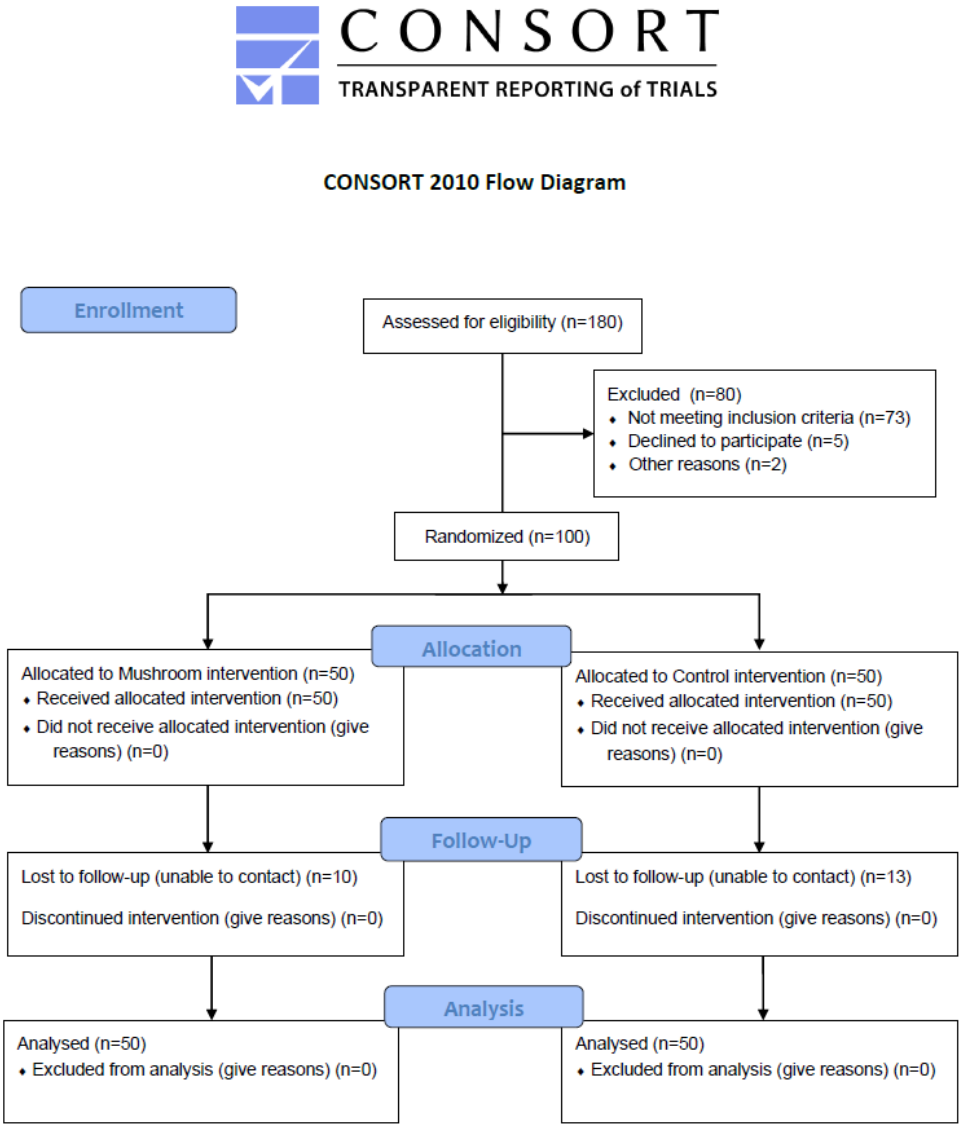

Figure 1. Study Flow diagram.

2.2. Snack Preparation

Following harvest, mushrooms were initially cut into 2 mm-thick slices; then, yeast extract (as a flavor enhancer) and garlic flavor powder were added at a ratio of 0.5% (*w*/*w*), and the slices were baked at 120 °C for 20 min in a professional oven. After baking, the sliced mushrooms were subjected to UV-B irradiation (290–315 nm; 39 W lamps positioned at 20 cm from one another; mushrooms were placed at a distance of 20 cm from the light source, and were subjected to illumination for 120 min) to enhance vitamin D2 content. For the intervention, sachets made of aluminum foil were filled with the generated mushroom product ('snack', 6 g in each sachet) and were hermetically sealed. The nutritional composition and caloric content of the snack are presented in Table 1, while the glucan content was ≈2.5 g [12]. To ensure food safety, microbiological tests that are necessary for the food sector, including both control of safety and of hygiene criteria, as the applicable law requires them (Regulation 2073/2005), were carried out in an accredited laboratory. Finally, an experienced panel (Laboratory of Food Chemistry and Technology, School of Chemical Engineering, National Technical University of Athens) carried out the sensory testing of the mushroom snack (data not shown).

Table 1. Nutritional composition of the snack.

	Snack (6 g)
Energy content (Kcal)	18.42
Available carbohydrates (g)	1.77
Fat (g)	0.288
Protein (g)	1.35
Salt (g)	0.08
Vitamin D_2 (μg)	20

2.3. Outcomes

The primary outcome of the study was the changes in insulin sensitivity, and more specifically changes in fasting glucose levels after the 3 months' intervention.

Secondary outcomes included changes in vitamin 25(OH)D2 levels, anthropometric measures, biochemical parameters, inflammatory and oxidative stress markers, as well as changes in quality of life.

2.4. Medical, Dietary, and Quality-of-Life Assessment

Detailed medical history was obtained including personal, family, medical history, and medication.

Dietary intake was assessed using a 24 h recall record (four non-consecutive days of the week) and was analyzed using Nutritionist Pro™ (Axxya Systems, Stafford, TX, USA) software (version 7.1.0).

Physical activity level was evaluated via the International Physical Activity Questionnaire Short Form (IPAQ-SF). This 7-day recall instrument measures frequency and duration of walking, moderate, and vigorous physical activity [21].

Self-esteem was evaluated via the Rosenberg Self-Esteem scale. It includes a 10-item scale that estimates global self-worth by measuring both positive and negative feelings about the self. There is a 4-point rating scale (1 to 4) from strongly agree to strongly disagree. The total score ranges from 10 to 40 points. Higher scores indicate higher self-esteem [22].

As obesity is considered a risk factor for depressive disorders, the 10-item questionnaire Center for Epidemiologic Studies Depression Scale Revised (CESD-R-10) was applied pre- and post-intervention. Subjects scoring $\geq$16 (range 0–60) are considered at risk for prevalent depression [23].

Additionally, the insomnia level was evaluated via the Athens Insomnia Scale (AII) which records the assessment of any sleep difficulty. It consists of eight items that assess nocturnal sleep problems and daytime dysfunction. A higher score indicates greater severity of insomnia symptoms [24].

Finally, the subjects completed questionnaires regarding their physical and mental health (Short Form-12 Physical Composite Score (PCS-12) and Mental Composite Score (MCS-12). The questionnaires include 12 questions with dichotomous responses (yes/no), ordinal (excellent to poor), or expressed by a frequency (always to never). The higher the score, the better the health status [25].

2.5. Anthropometric Measurements

Body weight, body fat, fat free mass (FFM), total body water (TBW), and visceral fat rating were measured with bioelectrical impedance analysis (Tanita BC-418, Tokyo, Japan). Height was measured using a stadiometer (Seca Mode 220, Hamburg, Germany) with subjects not wearing shoes, their shoulders in a relaxed position, and their arms hanging freely. Waist circumference (WC) was determined at the midpoint between the lower margin of the last palpable rib and the top of the iliac crest in a standing position at the end of gentle expiration. Hip circumference (HP) measurement was taken around the widest portion of the buttocks. Body mass index (BMI) was computed as weight (kg)/height $(m)^2$.

2.6. Blood Collection

Blood samples (20 mL) were collected after an overnight fast for biochemical and laboratory analyses. Blood samples were centrifuged at 3000 rpm for 10 min at 20 °C for plasma and serum isolation. EDTA was used as an anticoagulant for plasma isolation. All samples were stored at −80 °C until further laboratory analysis.

2.7. Laboratory Analyses

2.7.1. Biochemical Analyses

Serum glucose, insulin, urea, uric acid, creatinine, total cholesterol (TC), HDL-C, low-density lipoprotein cholesterol (LDL-C), triglycerides (TG), alanine aminotransferase (ALT), aspartate aminotransferase (AST), γ-glutamyl transferase (γ-GT), alkaline phosphatase (ALP), uric acid, lactate dehydrogenase (LDH), iron (Fe), ferritin, albumin, C-reactive protein (CRP) were measured in serum with an automatic biochemical analyser (Cobas 8000 analyser, Roche Diagnostics GmbH, Mannheim, Germany).

2.7.2. Evaluation of Inflammation and Oxidative Stress

Interleukin-6 (IL-6), tumor necrosis factor α (TNFα), leptin, adiponectin (R&D Systems, Inc., Minneapolis, MN, USA), MPO (Thermo Fisher Scientific Inc., Waltham, MA, USA), oxLDL (Mercodia, AB, Uppsala, Sweden) and 8-isoprostanes (Abcam, Cambridge, UK) were measured applying ELISA as indicators of chronic inflammatory grade and oxidative stress. All ELISA measurements were conducted in duplicate.

2.7.3. 25(OH)D2 and 25(OH)D3 Using Liquid Chromatography–Tandem Mass Spectrometry (LC-MS/MS)

Reagents and Standards

Standards of 25-Hydroxy vitamin D_2, 25-Hydroxy vitamin D_3 as well as vitamin D_2 deuterated (25-Hydroxy Vitamin D_2-d6), used as internal standard (IS) were purchased from Santa Cruz Biotechnology (Dallas, TX, USA), while D_3 deuterated (25-Hydroxy Vitamin D_3-d6, IS) was acquired from Glentham Life Sciences (Leafield, UK). All standard stock solutions were prepared in methanol and stored at −18 °C. All solvents were of a liquid chromatography–mass spectrometry (LC-MS) grade. More specifically, acetonitrile and formic acid were provided from Carlo Erba (Reuil, France), whereas water, hexane and methanol were purchased from Fischer Scientific (Hampton, VA, USA) and Sharlau (Barcelona, Spain), respectively.

25(OH)D2 and 25(OH)D3 Extraction Procedure

The extraction of vitamins 25(OH)D2 and 25(OH)D3 was performed as described in a previously published work with slight modifications [26–28]. Briefly, frozen serum samples (280 μL) were thawed, mixed gently (multi vortex V-32, BioSan, Riga, Latvia) with another 280 μL acetonitrile containing 0.1% formic acid and finally spiked with 40 μL of a combined mixture of the internal standards' solution at concentrations 0.5 and 4.0 μg mL^{-1} of 25(OH)D2-d6 and 25(OH)D3-d6, respectively. The mixture was incubated for 30 min in 7 °C in order to induce protein precipitation. Then, 1200 μL of hexane was added to the above solution followed by a 5 min vortex. The new solution was incubated for another 25 min at 7 °C and then centrifuged at 10 °C and 12,000 rpm (Centrifuge Z32 HK, Hermle, Wehingen, Germany). After centrifugation, 900 μL of the upper organic phase was transferred to a new Eppendorf tube. Next, 1000 μL of hexane was added to the remaining solution and treated as previously described (vortex, incubation, centrifugation and collection of 1000 μL of the supernatant). The merged organic layers (1900 μL total) were centrifuged for 15 min at 10 °C and 1700 μL of the supernatant was collected in order to remove the solvent by using a nitrogen pump. Prior to analysis, the dry residue was reconstituted using a mixture of 2-propanol (35 μL) and methanol (50 μL), followed by a 10 min centrifugation (12,000 rpm at 10 °C). Finally, the supernatant was inserted in Liquid chromatography–mass spectrometry (LC-MS) vials.

25(OH)D2 and 25(OH)D3 Analysis

LC-MS analysis was used for the identification and quantification of 25(OH)D2 and 25(OH)D3. LC-MS included an API 3200 QTrap triple quadrupole/Linear ion trap mass spectrometer (AB Sciex, Foster City, CA, USA) coupled to an Agilent 1200 HPLC system (Agilent, Waldbronn, Germany). All spectra were processed by the Analyst software (version 1.4.2, AB Sciex, Foster City, CA, USA). In addition, for the separation of the four analytes, a Poroshell HPH-C18 column was used (2.1 particle size, 50 mm i.d., 2.7 μm). The elution of the analytes was performed by using a gradient system with two solvents (Solvent A, water with 0.1% formic acid and Solvent B: methanol with 0.1% formic acid) at flow rate 0.150 mL min^{-1}. More specifically, the gradient started with 23% of solvent A, reduced to 0% over 8 min of analysis, and, in 23 min, percentage of solvent A ramped to initial conditions (23%), which remained till the end of the analysis. The injection volume was set at 5 μL. The MS/MS parameters for all the analytes were optimized with the direct infusion of a mixed standard methanol solution (1 mg mL^{-1}) of the analytes. Tandem mass spectrometry analysis of all samples was performed in a positive mode using an electrospray chemical ionization (ESI) source.

The identification and quantification of the two forms of vitamin D were based on the fragmentation of the precursor ions into the respective product ions using a multiple monitoring reaction (MRM) technique. More specifically, product fragments of deuterated 25-Hydroxy vitamin D2 (*m/z* 419.3 > 355.4) were observed at a retention time (RT) of 12. 86 min, while product fragments of 25-Hydroxy vitamin D2 (*m/z* 413.4 > 355.4) were identified at a retention time of 12.91 min. Similarly, a product ion of 25-Hydroxy D3 (*m/z* 401.4 > 365.3) was detected at a retention time of 12.63 min, while a product ion of deuterated 25-Hydroxy D3 (*m/z* 407.5 > 371.4) was identified at a retention time of 12.68 min.

A mixture of plasma samples (pooled), which contained traces of the investigated analytes and 20 uL of each internal standard (25(OH)D2-d6 and 25(OH)D3 -d6), was used for the construction of calibration curves. The developed method exhibited good linearity (Peak area = 5.2456(±0.1362) × C 25(OH)D2 + 0.0004(±0.0130), R2 = 0.995 and Peak area = 8.2914(± 0.3029) × C 25(OH)D3–0.028(± 0.031), R2 = 0.993, respectively) within a wide range of concentrations (0.0001 to 0.25 μg mL^{-1}, n = 10). The method showed also good (a) intra-day (repeatability) (4.28% and 4.0%, for 25(OH)D2 and 25(OH)D3, respectively) and inter-day precision (reproducibility) (10.28% and 9.51%, for 25(OH)D2 and 25(OH)D3, respectively), (b) accuracy (115.1% and 86.42%, for 25(OH)D2 and 25(OH)D3, respectively) and (c) recovery (95.38% and 73.43%, for 25(OH)D2 and 25(OH)D3, respectively), as calculated by the *Official Journal of the European Communities* guidelines [29]. The limit of detection (LOD) was determined at 0.29 ng mL^{-1} for 25(OH)D2 and at 0.48 ng mL^{-1} for 25(OH)D3, whilst the limit of quantification (LOQ) was 0.00095 μg mL^{-1} and 0.00158 μg mL^{-1} for 25(OH)D2 and 25(OH)D3, respectively.

2.8. Sample Size Determination and Statistical Analysis

Continuous variables are presented with mean and standard deviation (SD). Quantitative variables are presented with absolute and relative frequencies. All analyses were conducted on an intention-to-treat basis. For the comparison of proportions, chi-square and Fisher's exact tests were used. For the comparison of means between the control and intervention group, Student's t-test was computed. To reduce the bias implicit in utilizing only complete cases, multiple imputation procedures for all data were implemented. Differences in changes of study variables during the follow-up period between the two study groups were evaluated using repeated measurements analysis of variance (ANOVA). All *p* values reported are two-tailed. Statistical significance was set at 0.05 and analyses were conducted using SPSS statistical software (version 24.0, IBM, New York, NY, USA).

A repeated-measures power analysis was conducted for a single within-subjects factor assessed over two time points. For this design, 50 participants per group achieve a power of 0.94 for the between-subjects main effect at an effect size of 0.30; a power of 0.95 for the

within-subjects main effect at an effect size of 0.20; and a power of 0.95 for the interaction effect at an effect size of 0.20.

3. Results

3.1. Subject Characteristics

A total of 100 participants (35 males, 65 females) were randomized in two equally sized groups. Participant characteristics are shown in Table 2 and were similar in both groups.

Table 2. Demographics in control and intervention groups. The results are given as N (%) of the total number.

		Group		*p*
		Control	**Intervention**	
		N (%)	**N (%)**	
Gender	Men Women	21 (42) 29 (58)	14 (28) 36 (72)	0.142 +
Age. mean (SD)		53.7 (10.8)	54.9 (11.8)	0.610 ‡
Nationality	Greek Other	48 (96.0) 2 (4.0)	48 (98.0) 1 (2.0)	>0.999 +
Family status	Married Divorced Single In a relationship Widowed	39 (78) 2 (4) 5 (10) 2 (4) 2 (4)	38 (77.6) 3 (6.1) 5 (10.2) 1 (2) 2 (4.1)	>0.999 ++
Children	0 1 2 3	16 (32) 8 (16) 19 (38) 7 (14)	9 (18.4) 7 (14.3) 26 (53.1) 7 (14.3)	0.376 +
Educational level	None Primary Secondary University Other	1 (2) 0 (0) 19 (38) 20 (40) 10 (20)	0 (0) 2 (4.1) 20 (40.8) 21 (42.9) 6 (12.2)	0.482 ++
Years of education, mean (SD)		15.3 (3.1)	14.7 (3.8)	0.436 ‡
Occupation	Full time in public sector Full time in private sector Part time in public sector Part time in private sector Freelancer Household Unemployed Pensioner	26 (52) 11 (22) 0 (0) 0 (0) 4 (8) 1 (2) 0 (0) 8 (16)	20 (40.8) 4 (8.2) 2 (4.1) 1 (2) 4 (8.2) 6 (12.2) 1 (2) 11 (22.4)	0.071 ++
Menstruation [1]	No Yes	18 (62.1) 11 (37.9)	24 (70.6) 10 (29.4)	0.475 +
Overweight	No Yes	0 (0) 50 (100)	1 (2) 48 (98)	0.495 ++
Hypertension	No Yes	13 (26) 37 (74)	8 (16) 42 (84)	0.220 +
Diabetes	No Yes	34 (68) 16 (32)	28 (56) 22 (44)	0.216 +
Dyslipidemia	No Yes	5 (10) 45 (90)	6 (12) 44 (88)	0.749 +
Smoking	Daily Occasionally Daily for stopped smoking Occasionally but stopped smoking No	10 (20) 1 (2) 15 (30) 3 (6) 21 (42)	9 (18) 2 (4) 12 (24) 3 (6) 24 (48)	0.949 ++
Alcohol consumption	Daily 4–6 times/week 1–3 times/week 1–2 times/month Rarely Never	1 (2) 2 (4) 14 (28) 13 (26) 13 (26) 7 (14)	2 (4.1) 3 (6.1) 13 (26.5) 6 (12.2) 14 (28.6) 11 (22.4)	0.544 ++

[1] only in women; + Pearson's chi-square test; ++ Fisher's exact test; ‡ Student's *t*-test.

No side effects were reported. Additionally, as recorded through biweekly phone calls from experienced dieticians, the overall protocol compliance was >80%.

3.2. Effect on Biochemical Indices

Regarding the biochemical measurements (Table 3), glucose decreased only in the intervention group after 3 months, while it remained unchanged in the control group, with the degree of change being significantly different between the two groups. LDL and SGOT decreased only in the intervention group and the between group differences changes were not significant. Additionally, glucose levels were different between groups in post-intervention as well as albumin levels in pre- as well as in post-intervention, but no other significant differences were observed in albumin.

Table 3. (a): Changes in biochemical measurements after 3 months in control vs. the intervention group; (b): Changes in lipid profile, hepatic enzymes and markers of renal function after 3 months in control vs. the intervention group.

(a)

	Group	**Pre Mean (SD)**	**Post Mean (SD)**	**Change Mean (SD)**	**P2**	**P3**
Glucose (mg/dL)	Control	104 (34.7)	107 (37)	3 (19.3)	0.283	**0.001**
	Intervention	101.6 (26.8)	90.7 (15.4)	−10.9 (20.2)	**<0.001**	
	P1	0.704	**0.005**			
Insulin (µIU/mL)	Control	16.7 (12.1)	15.9 (11.4)	−0.9 (12.9)	0.617	0.915
	Intervention	18.8 (13.8)	17.6 (10.2)	−1.1 (11.7)	0.519	
	P1	0.444	0.425			
ALP (U/L)	Control	67.1 (17.8)	70 (22.7)	2.9 (13.6)	0.110	0.059
	Intervention	73.3 (21.5)	71.4 (24.6)	−2 (11.4)	0.279	
	P1	0.122	0.775			
Fe (µg/dL)	Control	82.5 (31)	81 (30.6)	−1.5 (35)	0.772	0.261
	Intervention	78.2 (28.4)	84.9 (30)	6.7 (37)	0.196	
	P1	0.471	0.529			
Ferritin (ng/mL)	Control	91.6 (106.2)	101.7 (104.4)	10.1 (41.3)	0.165	0.119
	Intervention	98.8 (81.6)	92.7 (83.7)	−6 (59.2)	0.410	
	P1	0.709	0.638			
Albumin (g/dL)	Control	4.35 (0.29)	4.39 (0.25)	0.04 (0.32)	0.359	0.180
	Intervention	4.62 (0.28)	4.58 (0.35)	−0.04 (0.31)	0.327	
	P1	**<0.001**	**0.003**			
CRP (mg/L)	Control	4.94 (5.81)	5.46 (4.89)	0.52 (5.23)	0.411	0.906
	Intervention	4.29 (4.04)	4.91 (4.45)	0.63 (3.48)	0.327	
	P1	0.518	0.561			
LDH (U/L)	Control	179.6 (125.8)	161.9 (38.8)	−17.7 (118.9)	0.176	0.603
	Intervention	161.6 (40.7)	153.5 (42.2)	−8.1 (51.5)	0.540	
	P1	0.341	0.304			

Table 3. *Cont.*

(b)						
	Group	**Pre Mean (SD)**	**Post Mean (SD)**	**Change Mean (SD)**	**P2**	**P3**
TC (mg/dL)	Control	186.3 (32.8)	182 (40)	−4.3 (40.7)	0.419	0.643
	Intervention	200.3 (50.9)	196.6 (55.2)	−3.7 (33.5)	0.485	
	P1	0.105	0.134			
TG (mg/dL)	Control	143.5 (93.1)	134.6 (81.2)	−9 (73.4)	0.440	0.921
	Intervention	162 (94.1)	154.6 (82.3)	−7.3 (89.7)	0.532	
	P1	0.330	0.225			
HDL (mg/dL)	Control	47.1 (11.6)	48.0 (12.8)	0.9 (6.9)	0.327	0.072
	Intervention	51 (9.6)	49.6 (9.8)	−1.4 (5.2)	0.117	
	P1	0.074	0.479			
LDL (mg/dL)	Control	115.9 (27.2)	110.7 (36.5)	−5.2 (27.6)	0.153	0.498
	Intervention	129.0 (43.2)	120.4 (38.4)	−8.6 (22.7)	**0.019**	
	P1	0.073	0.203			
SGOT (iu/L)	Control	18.8 (7.8)	17.7 (6.6)	−1.2 (7.9)	0.212	0.461
	Intervention	18.8 (6.7)	15.9 (5.7)	−2.9 (5.1)	**0.003**	
	P1	0.999	0.162			
SGPT (iu/L)	Control	20.8 (11.1)	21.2 (12.1)	0.5 (8.6)	0.751	0.230
	Intervention	22.5 (12)	20.5 (10.1)	−2.1 (12)	0.169	
	P1	0.451	0.730			
γ-GT (iu/L)	Control	25.9 (16.4)	24.8 (19.2)	−1.1 (10.3)	0.564	0.373
	Intervention	27.8 (24.2)	24.4 (19.4)	−3.4 (15.1)	0.070	
	P1	0.639	0.923			
Urea (mg/dL)	Control	31.5 (8)	32.1 (9)	0.6 (8)	0.656	0.875
	Intervention	30.2 (6.9)	31.1 (10.4)	0.9 (10.5)	0.509	
	P1	0.367	0.587			
Uric acid-(mg/dL)	Control	5.14 (1.17)	5.39 (1.1)	0.25 (0.98)	0.086	0.103
	Intervention	5.29 (1.34)	5.2 (1.46)	−0.09 (1.07)	0.552	
	P1	0.545	0.476			
Creatinine (mg/dL)	Control	0.78 (0.2)	0.87 (0.49)	0.09 (0.45)	0.144	0.973
	Intervention	0.74 (0.13)	0.83 (0.41)	0.09 (0.42)	0.161	
	P1	0.247	0.642			

P1: *p*-value for group comparison, P2: *p*-value for time comparison, P3: Repeated measures ANOVA. Level of significance was set at 0.05. Values in bold point to significant differences. Effects reported include differences between the groups in the degree of change over the follow-up period; ALP: alkaline phosphatase, Fe: iron, CRP: C-reactive protein, LDH: lactate dehydrogenase. TC: total cholesterol, TG: triglycerides, HDL: high-density lipoprotein, LDL: low-density lipoprotein, SGOT: serum glutamic oxaloacetic transaminase, SGPT: serum glutamic pyruvic transaminase, γ-GT: γ-glutamyl transferase.

3.3. 25(OH)D2 and 25(OH)D3 Levels

As for 25(OH)D2 and 25(OH)D3 (Table 4), no significant differences occurred at baseline and at follow-up between the two groups. During follow-up, 25(OH)D2 increased significantly only in the intervention group. Consequently, the degree of change of 25(OH)D2 differed significantly between the two groups. No significant time differences were found in 25(OH)D3.

Table 4. Changes in 25(OH)D2 and 25(OH)D3 after 3 months in control vs. intervention group, by group.

	Group	Pre Mean (SD)	Post Mean (SD)	Change Mean (SD)	P2	P3
25(OH)D3 ng/mL	Control	24.5 (10.4)	22.5 (10.2)	−2.0 (15.1)	0.293	0.358
	Intervention	24.2 (10.9)	24.6 (11.0)	0.4 (15.4)	0.804	
	P1	0.867	0.316			
25(OH)D2 ng/mL	Control	3.86 (4.85)	4.84 (5.07)	0.98 (6.3)	0.154	**0.014**
	Intervention	3.11 (3.78)	6.50 (4.69)	3.39 (4.2)	**<0.001**	
	P1	0.392	0.091			

P1: *p*-value for group comparison, P2: *p*-value for time comparison, P3: Repeated measures ANOVA. Level of significance was set at 0.05. Values in bold point to significant differences. Effects reported include differences between the groups in the degree of change over the follow-up period.

3.4. Effect on Anthropometric Characteristics

Table 5 presents changes in anthropometric characteristics after 3 months in both groups. Weight, fat (kg and %), BMI, waist and hip circumferences decreased only in the intervention group after 3 months, while they remained unchanged in the control, with the mean changes being significantly different between the two groups. When comparing pre- and post- levels in the groups, no significant changes were observed. Only TBW was lower in the intervention group than in the control group at follow-up, without the differences in mean changes being significant.

Table 5. Changes in anthropometric measurements after 3 months in control vs. intervention group.

	Group	Pre Mean (SD)	Post Mean (SD)	Change Mean (SD)	P2	P3
Weight (kg)	Control	96.1 (16.7)	96.6 (16.8)	0.5 (10.9)	0.787	**0.031**
	Intervention	95.9 (20.3)	90.5 (21.3)	−5.4 (16)	**0.006**	
	P1	0.960	0.112			
Fat (kg)	Control	37.7 (12.6)	37.2 (11.7)	−0.6 (5.1)	0.427	0.186
	Intervention	39.6 (12.2)	37.7 (11.7)	−2 (5.3)	**0.009**	
	P1	0.447	0.826			
Fat (%)	Control	38.9 (8.2)	38.5 (8)	−0.4 (4.8)	0.590	**0.040**
	Intervention	41.4 (7)	39.0 (7.2)	−2.4 (4.8)	**0.001**	
	P1	0.108	0.757			
FFM (kg)	Control	58.4 (10.2)	57.8 (9.7)	−0.6 (2.6)	0.136	0.460
	Intervention	54.4 (12.3)	54.2 (12)	−0.2 (2.8)	0.651	
	P1	0.080	0.103			
TBW (kg)	Control	43.4 (7.2)	44.6 (7.7)	1.3 (5.3)	0.281	0.435
	Intervention	41.1 (10.4)	41.2 (9.2)	0.1 (10.7)	0.982	
	P1	0.219	**0.040**			
Visceral	Control	14.7 (5.2)	15 (5.7)	0.4 (2)	0.236	0.212
	Intervention	13.8 (4.7)	13.7 (5.3)	−0.2 (2.2)	0.560	
	P1	0.402	0.216			
BMI (kg/m^2)	Control	34.1 (6.2)	34.4 (6.2)	0.2 (4.1)	0.760	**0.026**
	Intervention	34.8 (6.7)	32.8 (6.8)	−2 (5.5)	**0.005**	
	P1	0.635	0.970			

Table 5. *Cont.*

	Group	Pre Mean (SD)	Post Mean (SD)	Change Mean (SD)	P2	P3
WC (cm)	Control	112.4 (11.8)	112.2 (10.7)	−0.2 (4.6)	0.534	0.343
	Intervention	111.5 (15.1)	110.1 (14.5)	−1.4 (4.8)	**0.050**	
	P1	0.718	0.456			
HC (cm)	Control	117 (13)	116.5 (13)	−0.5 (5.1)	0.760	**0.041**
	Intervention	122.5 (20.1)	117.2 (14.3)	−5.2 (15.4)	**0.002**	
	P1	0.110	0.791			
SBP (mm/Hg)	Control	132.2 (16)	132.5 (14.7)	0.3 (14.8)	0.926	0.896
	Intervention	138.1 (19.5)	137.8 (21.5)	−0.3 (25.5)	0.926	
	P1	0.102	0.151			
DBP (mm/Hg)	Control	76.7 (9.8)	76.9 (9.2)	0.2 (6.2)	0.848	0.550
	Intervention	80.1 (11.4)	79.4 (9.2)	−0.7 (8.1)	0.513	
	P1	0.119	0.179			

P1: *p*-value for group comparison, P2: *p*-value for time comparison, P3: Repeated measures ANOVA. Level of significance was set at 0.05. Values in bold point to significant differences. Effects reported include differences between the groups in the degree of change over the follow-up period. FFM: free fat mass, TBW: total body water, BMI: body mass index, WC: waist circumference, HC: hip circumference, SBP: systolic blood pressure, DBP: diastolic blood pressure.

3.5. Effect on Inflammatory and Oxidative Stress Biomarkers

Changes in inflammatory and oxidative stress biomarkers are presented in Table 6. IL-6 and oxLDL decreased in the intervention group after 3 months and remained unchanged in the control group, with the mean changes being significantly different between the two groups. At baseline and at follow-up, both groups had similar values.

Table 6. Changes in inflammatory and oxidative stress markers after 3 months in control vs. intervention group.

	Group	Pre Mean (SD)	Post Mean (SD)	Change Mean (SD)	P2	P3
Leptin (ng/mL)	Control	43.6 (45)	41.7 (42.8)	−1.9 (28)	0.604	0.501
	Intervention	54.8 (91.5)	56.6 (95.5)	1.8 (24.4)	0.664	
	P1	0.439	0.325			
IL-6 (pg/mL)	Control	2.8 (1.9)	2.9 (1.6)	0.1 (1.7)	0.702	**0.047**
	Intervention	3.2 (2.3)	2.7 (2)	−0.6 (1.6)	**0.016**	
	P1	0.353	0.452			
Adiponectin (µg/mL)	Control	12.4 (10.7)	10.9 (7.6)	−1.6 (8.4)	0.111	0.530
	Intervention	9.2 (9.5)	8.5 (7.9)	−0.7 (4.8)	0.475	
	P1	0.110	0.123			
MPO (ng/mL)	Control	125.6 (184.1)	162.6 (140.9)	37.0 (196)	0.137	0.900
	Intervention	178.6 (164.4)	211.1 (201.1)	32.5 (149.1)	0.190	
	P1	0.133	0.165			
oxLDL (U/L)	Control	81.29 (37.72)	80.88 (47.28)	−0.41 (40.05)	0.946	**0.020**
	Intervention	92.84 (53.12)	71.92 (44.09)	−20.92 (46.11)	**0.001**	
	P1	0.213	0.330			
TNF- α (pg/mL)	Control	1.21 (0.75)	1.19 (0.65)	−0.01 (0.96)	0.903	0.890
	Intervention	1.43 (0.64)	1.39 (0.59)	−0.04 (0.68)	0.750	
	P1	0.116	0.117			
8-isoprostane pg/mL)	Control	1893.1 (3753.8)	1912.7 (2878.1)	19.6 (3123.1)	0.872	0.856
	Intervention	1112.6 (1679.1)	1799.5 (2828.1)	686.9 (2957.6)	0.681	
	P1	0.779	0.518			

P1: *p*-value for group comparison, P2: *p*-value for time comparison, P3: Repeated measures ANOVA. Level of significance was set at 0.05. Values in bold point to significant differences. Effects reported include differences between the groups in the degree of change over the follow-up period. MPO: myeloperoxidase, oxLDL: oxidized LDL, TNF-α: tumor necrosis factor- α.

3.6. Effect on the Quality of Life

Finally, regarding quality of life, changes after the intervention are presented in Table 7. Physical health score was significantly higher in the intervention group at follow-up and the degree of change after 3 months differed significantly between the two groups. Additionally, PCS-12 and physical activity (total MET- min/week) were higher in the intervention group and pre- and post-intervention accordingly. No significant changes were observed in the quality-of-life scores that derive from all the other questionnaires.

Table 7. Changes in QoL, depression, insomnia, self-esteem and physical activity.

	Group	**Pre Mean (SD)**	**Post Mean (SD)**	**Change Mean (SD)**	**P2**	**P3**
AII	Control	6 (3.8)	5.5 (3.9)	−0.5 (2.8)	0.273	0.073
	Intervention	5.9 (4.1)	6.5 (4)	0.7 (3.7)	0.147	
	P1	0.831	0.201			
CESD-R-10	Control	18.9 (10.3)	17 (9.9)	−1.9 (8.0)	0.168	0.129
	Intervention	15.8 (9.7)	16.8 (11.3)	1 (10.6)	0.438	
	P1	0.123	0.909			
Rosenberg Self-Esteem scale	Control	31.1 (4)	31.4 (5.5)	0.2 (4.5)	0.729	0.840
	Intervention	30.8 (4.4)	30.8 (5)	0 (4.4)	0.951	
	P1	0.652	0.594			
PCS-12	Control	44.9 (9.2)	42.9 (9.2)	−2 (9.2)	0.139	**0.002**
	Intervention	43.9 (9.6)	48.1 (8.7)	4.1 (9.8)	**0.003**	
	P1	0.624	**0.004**			
MCS-12	Control	45.4 (10.2)	47.4 (9.9)	2.0 (7.0)	0.066	0.579
	Intervention	48.5 (8.6)	49.6 (9.6)	1.2 (8.1)	0.285	
	P1	0.113	0.267			
IPAQ-SF (MET-min/week)	Control	902.8 (916.3)	1326.9 (1685)	424.1 (1778.5)	0.240	0.293
	Intervention	2159.3 (2306.7)	2047.1 (2313.7)	−112.2 (3111.5)	0.755	
	P1	**0.001**	0.078			

P1: *p*-value for group comparison, P2: *p*-value for time comparison, P3: Repeated measures ANOVA. Level of significance was set at 0.05. Values in bold point to significant differences. Effects reported include differences between the groups in the degree of change over the follow-up period. AII: Athens Insomnia Scale, CESD-R: Center for Epidemiologic Studies Depression Scale Revised, PCS-12: Physical Composite Score, MCS-12: Mental Composite Score, IPAQ-SF: International Physical Activity Questionnaire (short form).

4. Discussion

During the last few decades, functional ingredients of foods have attracted research interest in the prevention and management of obesity and related metabolic disorders. Several bioactive compounds of mushrooms have been documented to have beneficial impacts on various metabolic markers.The consumption of mushrooms has been associated with cardioprotective effects, such as hypocholesterolemic, antihyperglycemic, antihypertensive, anti-inflammatory and antioxidant properties [30]. To the best of our knowledge, this is the first randomized controlled clinical trial exploring the effect of vitamin D2-enhanced *P. eryngii* snack on parameters related to metabolic disorders.

We succeeded in proving our primary hypothesis that the daily consumption of the snack regulates glucose levels compared with the control group. Our findings are in accordance with the existing literature, as it has been shown that mushrooms possess an antidiabetic effect mainly due to their polysaccharide content [31] and by increasing glucokinase activity [32]. *P. ostreatus* exhibits similar effects, with a 7-day consumption of a cooked mushroom meal in exchange for vegetables to hospitalized patients with insulin resistance, resulting in a 22% reduction in fasting glucose [33].

During follow-up, 25(OH)D2 levels increased significantly only in the intervention group with the degree of change being significantly different between the intervention and the control group. No significant differences were found in 25(OH)D3. Recently, Hu et al. showed that UV irradiation increases vitamin D2 concentration in *P. ostreatus* mushrooms in ethanol suspension, thus enhancing their nutritional value [34]. Several studies have demonstrated that UV irradiation of edible mushrooms results in a high rate of ergosterol conversion to vitamin D2; in addition, serum 25(OH)D levels are increased as shown in some clinical trials [35]. Other clinical trials showed that serum 25(OH)D did not significantly increase by consumption of UV-exposed mushrooms [36]. Although most studies have investigated D3 supplementation and its benefits on human health, D2 has also been shown to exhibit beneficial effects. Hence, D2 improves the quality of life in osteoarthritis subjects [37], and it regulates endothelial function [38] and arterial stiffness [39]. Endothelial dysfunction is not only a consequence of insulin resistance but also impairs insulin signaling to further reduce insulin sensitivity, thereby resulting in a destructive cycle in metabolic disorders and diabetes [40].

Additionally, participants of the intervention group exhibited a reduction in body weight, fat, waist, and hip circumference, whereas no significant alterations appeared in the control group, with the mean changes being different between the two intervention groups. This may be due to better appetite regulation as also shown in our previous study where *P. eryngii* mushrooms ameliorate appetite and suppress ghrelin levels postprandially owed to their beta-glucan content [20]. Moreover, it has been shown that a meal enriched with powder from dried oyster mushrooms can increase GLP-1 postprandially and decrease hunger rate for the same reasons [41]. In a long-term (1 year) clinical trial with obese patients that substituted mushrooms for red meat lower BMI and waist circumference were reported [42].

The results of the present investigation suggest that *P. eryngii* might improve lipid profile. LDL levels decreased only in the intervention group although mean changes were not different between the intervention and the control group. Polysaccharides in mushrooms, including chitosans and glucans can reduce LDL levels [43,44]. However, modest weight loss in obese individuals may also provide lower fasting glucose and LDL levels [45]. Our findings are in consistency with those of Choudhury et al. [46] who showed a reduction in TC and LDL-C levels of obese hypertensive non-diabetic males administered with 3 g of *P. ostreatus* powder in capsule form daily for 3 months. Similar results were also found in another study where lipid levels, including TC and LDL-C were significantly different after the consumption of *Agaricus bisporus* cooked with olive oil [47]. In contrast, other studies reported that LDL-C remains unchanged [48,49].

As for SGOT/AST levels, consumption of several mushroom species, including those of the genus Pleurotus, can reduce AST levels according to results obtained from animal models [50]. Pleurotus species can generate the paths for diffraction of different liver enzymes and reduce the levels of serum enzyme activities [51].

As obesity is associated with chronic low-grade inflammation and oxidative stress, studying them in clinical trials of obese and metabolic patients is essential. Insulin signaling is impaired and chronic inflammation is induced by such markers [52]. In the present, a decrease in IL-6 and ox-LDL was found in the mushroom group, which did not appear in the control, the mean changes being significantly different between groups. To the best of our knowledge, this study is the first to demonstrate that *P. eryngii* mushrooms regulate inflammation and oxidative stress in humans. The CRP alterations after mushroom intake were not accompanied by IL-6 and oxLDL differences when compared with the control [53]. Similarly, other trials failed to report any significant effects on inflammatory markers [54,55]. The presence of lovastatin, a member of the statins family that lower TC and LDL levels and reduce the risk of coronary heart disease [56] and the antioxidants ergothioneine [11] and selenium [57] have been detected in relatively high amounts in *P. eryngii*. Added to the above, the increase in vitamin D2 content via UV radiation has been shown to ameliorate inflammation in humans [58,59]. However, when examining

the effects of such complex matrices on metabolic health, it should be emphasized that the overall activity may be due to the synergistic effects of all compounds rather than the individual activities of specific constituents. DPPH and FRAP experiments in the extracts from the snack have shown a noticeable antioxidant capacity (399.92 ±10.14 μmol Trolox equivalents/100 g and 16.31 ± 0.07 μmol ascorbic acid equivalents/100 g, respectively). This may be due to the remaining antioxidant content in mushrooms, but also due to the antioxidants that arise from baking (i.e., the Maillard reaction products) and contribute to the overall antioxidant capacity.

With regard to the quality of life, PCS-12 was significantly higher in the intervention group at follow-up with a significant difference in the degree of mean change between the two groups. PCS-12 is a very good marker for explaining variations in the quality of life across BMI and seems to be lower in obese patients compared to normal-weight controls [60]. In our study, the 4.1-point increase in PCS-12 in the intervention group may be explained by the regulation of several metabolic parameters, such as glucose, weight, BMI, fat, and of course by the overall improvement in the inflammatory and oxidative stress status. Additionally, the quality of life may have been improved due to an improvement in the quality of sleep and, more specifically, in snoring (snoring was stopped successfully in 23% of the participants at follow-up in the intervention group, whereas no participant stopped snoring in the control group).

Overall, the results of our randomized controlled clinical trial should be viewed in light of the fact that the trial could not be blinded; thus, a degree of bias is inevitable. However, we believe that the above is counterbalanced by several strengths, such as the adequate power of the study, and the satisfying degree of compliance, as verified by consistent phone calls with the participants, as well as with follow-up increased levels of vitamin 25(OH)D2 only in the intervention group. Finally, another strength was the very careful selection of the participants according to tight inclusion and exclusion criteria, as well as the successful randomization process mitigating possible bias in the study.

5. Conclusions

In conclusion, the consumption for 3 months of a snack prepared from *P. eryngii* mushrooms with enhanced content of vitamin D_2 and with other bioactive compounds was associated with a significant reduction in glucose, body weight, BMI, and body fat, in parallel with an increase in serum 25(OH)D2 and quality of life. Additionally, the snack resulted in an improved profile of inflammatory and oxidative stress status. Overall, these findings suggest potential antidiabetic, antiobesity, anti-inflammatory, and antioxidant health benefits of the snack to metabolically unhealthy individuals. In light of the increase in the obesity epidemic and the resulting metabolic disorders, such data are considered of great importance. However, essential information about the synergistic activity of the components of *P. eryngii* that are beneficial to metabolic health is needed to exploit further the value of the results.

Author Contributions: Conceptualization, A.C.K.; methodology, A.C.K.; formal analysis, C.T.; investigation, S.-A.K., C.A., A.G., D.Z.L., G.S., K.T., T.T., L.L. and D.T.; writing—original draft preparation, S.-A.K.; writing—review and editing, S.-A.K., C.A., A.G., D.Z.L., G.S., K.T., T.T., L.L., G.I.Z., N.K., P.Z. and A.C.K.; supervision, A.C.K. All authors have read and agreed to the published version of the manuscript.

Funding: The implementation of the doctoral thesis of S.-A.K. was co-financed by Greece and the European Union (European Social Fund) through the Operational Program "Human Resource Development, Education and Lifelong Learning", 2014–2020, within the framework of the Action "Strengthening human resources through the implementation of doctoral research-Sub-Action 2: IKY grant program for doctoral candidates of Greek universities". Additionally, this work has been co-financed by the European Union and Greek national funds (European Social Fund—ESF) through the Operational Program Competitiveness, Entrepreneurship, and Innovation, under the call RESEARCH-CREATE-INNOVATE (project code: T1EDK-02560).

Institutional Review Board Statement: The study was conducted in accordance with the Declaration of Helsinki and the Data Protection Act 1998, and was registered at clinicaltrials.gov (ID Number: NCT04081818). Additionally, the study was approved by the Ethics Committee of Harokopio University (ID protocol: 62/03-07-2018).

Informed Consent Statement: Informed consent was obtained from all subjects involved in the study.

Data Availability Statement: All data are included within the article.

Acknowledgments: We are grateful to patients for participating in this study.

Conflicts of Interest: The authors declare no conflict of interest.

References

1. Blüher, M. Obesity: Global epidemiology and pathogenesis. *Nat. Rev. Endocrinol.* **2019**, *15*, 288–298. [CrossRef] [PubMed]
2. WHO. *Obesity and Overweight 2016*; WHO: Geneva, Switzerland, 2016.
3. Frasca, D.; Blomberg, B.B.; Paganelli, R. Aging, Obesity, and Inflammatory Age-Related Diseases. *Front. Immunol.* **2017**, *8*, 1745. [CrossRef] [PubMed]
4. Swinburn, B.A.; Sacks, G.; Hall, K.D.; McPherson, K.; Finegood, D.T.; Moodie, M.L.; Gortmaker, S.L. The Global Obesity Pandemic: Shaped by Global Drivers and Local Environments. *Lancet* **2011**, *378*, 804–814. [CrossRef]
5. Zheng, R.; Zhou, D.; Zhu, Y. The long-term prognosis of cardiovascular disease and all-cause mortality for metabolically healthy obesity: A systematic review and meta-analysis. *J. Epidemiol. Community Health* **2016**, *70*, 1024–1031. [CrossRef]
6. Alkhatib, A.; Tsang, C.; Tiss, A.; Bahorun, T.; Arefanian, H.; Barake, R.; Khadir, A.; Tuomilehto, J. Functional Foods and Lifestyle Approaches for Diabetes Prevention and Management. *Nutrients* **2017**, *9*, 1310. [CrossRef]
7. Gargano, M.L.; van Griensven, L.J.L.D.; Isikhuemhen, O.S.; Lindequist, U.; Venturella, G.; Wasser, S.P.; Zervakis, G.I. Medicinal mushrooms: Valuable biological resources of high exploitation potential. *Plant Biosyst.* **2017**, *151*, 548–565. [CrossRef]
8. Bhambri, A.; Srivastava, M.; Mahale, V.G.; Mahale, S.; Karn, S.K. Mushrooms as Potential Sources of Active Metabolites and Medicines. *Front. Microbiol.* **2022**, *13*, 837266. [CrossRef]
9. Royse, D.J.; Baars, J.; Tan, Q. Current Overview of Mushroom Production in the World. In *Edible and Medicinal Mushrooms*; John Wiley & Sons: Hoboken, NJ, USA, 2017; pp. 5–13.
10. Raman, J.; Jang, K.Y.; Oh, Y.L.; Oh, M.; Im, J.H.; Lakshmanan, H.; Sabaratnam, V. Cultivation and Nutritional Value of Prominent *Pleurotus* spp.: An Overview. *Mycobiology* **2020**, *49*, 1–14. [CrossRef]
11. Chen, S.-Y.; Ho, K.-J.; Hsieh, Y.-J.; Wang, L.-T.; Mau, J.-L. Contents of lovastatin, γ-aminobutyric acid and ergothioneine in mushroom fruiting bodies and mycelia. *LWT* **2012**, *47*, 274–278. [CrossRef]
12. Koutrotsios, G.; Kalogeropoulos, N.; Kaliora, A.; Zervakis, G.I. Toward an increased functionality in oyster (*Pleurotus*) mushrooms produced on grape marc or olive mill wastes serving as sources of bioactive compounds. *J. Agric. Food Chem.* **2018**, *66*, 5971–5983. [CrossRef]
13. Cardwell, G.; Bornman, J.F.; James, A.P.; Black, L.J. A Review of Mushrooms as a Potential Source of Dietary Vitamin D. *Nutrients* **2018**, *10*, 1498. [CrossRef] [PubMed]
14. Zhang, B.; Li, Y.; Zhang, F.; Linhardt, R.J.; Zeng, G.; Zhang, A. Extraction, structure and bioactivities of the polysaccharides from *Pleurotus eryngii*: A review. *Int. J. Biol. Macromol.* **2020**, *150*, 1342–1347. [CrossRef] [PubMed]
15. Kim, J.-I.; Kang, M.-J.; Im, J.; Seo, Y.-J.; Lee, Y.-M.; Song, J.-H.; Lee, J.-H.; Kim, M.-E. Effect of king oyster mushroom (*Pleurotus eryngii*) on insulin resistance and dyslipidemia in db/db mice. *Food Sci. Biotechnol.* **2010**, *19*, 239–242. [CrossRef]
16. Chen, J.; Yong, Y.; Xing, M.; Gu, Y.; Zhang, Z.; Zhang, S.; Lu, L. Characterization of polysaccharides with marked inhibitory effect on lipid accumulation in *Pleurotus eryngii*. *Carbohydr. Polym.* **2013**, *97*, 604–613. [CrossRef]
17. Chen, J.; Yong, Y.; Xia, X.; Wang, Z.; Liang, Y.; Zhang, S.; Lu, L. The excreted polysaccharide of *Pleurotus eryngii* inhibits the foam-cell formation via down-regulation of CD36. *Carbohydr. Polym.* **2014**, *112*, 16–23. [CrossRef] [PubMed]
18. Chen, L.; Zhang, Y.; Sha, O.; Xu, W.; Wang, S. Hypolipidaemic and hypoglycaemic activities of polysaccharide from *Pleurotus eryngii* in Kunming mice. *Int. J. Biol. Macromol.* **2016**, *93*, 1206–1209. [CrossRef]
19. Nakahara, D.; Nan, C.; Mori, K.; Hanayama, M.; Kikuchi, H.; Hirai, S.; Egashira, Y. Effect of mushroom polysaccharides from *Pleurotus eryngii* on obesity and gut microbiota in mice fed a high-fat diet. *Eur. J. Nutr.* **2020**, *59*, 3231–3244. [CrossRef]
20. Kleftaki, S.A.; Simati, S.; Amerikanou, C.; Gioxari, A.; Tzavara, C.; Zervakis, G.I.; Kalogeropoulos, N.; Kokkinos, A.; Kaliora, A.C. *Pleurotus eryngii* improves postprandial glycaemia, hunger and fullness perception, and enhances ghrelin suppression in people with metabolically unhealthy obesity. *Pharmacol. Res.* **2022**, *175*, 105979. [CrossRef]
21. Craig, C.L.; Marshall, A.L.; Sjöström, M.; Bauman, A.E.; Booth, M.L.; Ainsworth, B.E.; Pratt, M.; Ekelund, U.L.F.; Yngve, A.; Sallis, J.F.; et al. International physical activity questionnaire: 12-country reliability and validity. *Med. Sci. Sport.* **2003**, *35*, 1381–1395. [CrossRef]
22. Rosenberg, M. *Society and the Adolescent Self-Image*; Princeton University Press: Princeton, NJ, USA, 1965.
23. Björgvinsson, T.; Kertz, S.J.; Bigda-Peyton, J.S.; McCoy, K.L.; Aderka, I.M. Psychometric properties of the CES-D-10 in a psychiatric sample. *Assessment* **2013**, *20*, 429–436. [CrossRef]

24. Soldatos, C.R.; Dikeos, D.G.; Paparrigopoulos, T.J. Athens Insomnia Scale: Validation of an instrument based on ICD-10 criteria. *J. Psychosom. Res.* **2000**, *48*, 555–560. [CrossRef]
25. Ware John, E.; Susan, D. *Keller, and Mark Kosinski. SF-12: How to Score the SF-12 Physical and Mental Health Summary Scales*; Health Institute, New England Medical Center: Boston, MA, USA, 1995.
26. Abu Kassim, N.S.; Shaw, P.N.; Hewavitharana, A.K. Simultaneous determination of 12 vitamin D compounds in human serum using online sample preparation and liquid chromatography-tandem mass spectrometry. *J. Chromatogr. A* **2018**, *1533*, 57–65. [CrossRef] [PubMed]
27. Baecher, S.; Leinenbach, A.; Wright, J.A.; Pongratz, S.; Kobold, U.; Thiele, R. Simultaneous quantification of four vitamin D metabolites in human serum using high performance liquid chromatography tandem mass spectrometry for vitamin D profiling. *Clin. Biochem.* **2012**, *45*, 1491–1496. [CrossRef] [PubMed]
28. Holick, M.F. Vitamin D status: Measurement, interpretation, and clinical application. *Ann. Epidemiol.* **2009**, *19*, 73–78. [CrossRef]
29. 2002/657/EC: Commission Decision of 12 August 2002 Implementing Council Directive 96/23/EC. Available online: https://op.europa.eu/el/publication-detail/-/publication/ed928116-a955-4a84-b10a-cf7a82bad858/language-en (accessed on 10 August 2022).
30. Ganesan, K.; Xu, B. Anti-Obesity Effects of Medicinal and Edible Mushrooms. *Molecules* **2018**, *23*, 2880. [CrossRef]
31. Das, A.; Chen, C.-M.; Mu, S.-C.; Yang, S.-H.; Ju, Y.-M.; Li, S.-C. Medicinal Components in Edible Mushrooms on Diabetes Mellitus Treatment. *Pharmaceutics* **2022**, *14*, 436. [CrossRef]
32. Jayasuriya, W.J.; Wanigatunge, C.A.; Fernando, G.H.; Abeytunga, D.T.; Suresh, T.S. Hypoglycaemic activity of culinary Pleurotus ostreatus and P. cystidiosus mushrooms in healthy volunteers and type 2 diabetic patients on diet control and the possible mechanisms of action. *Phytother. Res.* **2015**, *29*, 303–309. [CrossRef]
33. Khatun, K.; Mahtab, H.; Khanam, P.A.; Sayeed, M.A.; Khan, K.A. Oyster mushroom reduced blood glucose and cholesterol in diabetic subjects. *Mymensingh Med. J.* **2007**, *16*, 94–99. [CrossRef]
34. Hu, D.; Chen, W.; Li, X.; Yue, T.; Zhang, Z.; Feng, Z.; Li, C.; Bu, X.; Li, Q.X.; Hu, C.Y.; et al. Ultraviolet Irradiation Increased the Concentration of Vitamin D2 and Decreased the Concentration of Ergosterol in Shiitake Mushroom (*Lentinus edodes*) and Oyster Mushroom (*Pleurotus ostreatus*) Powder in Ethanol Suspension. *ACS Omega* **2020**, *23*, 7361–7368. [CrossRef]
35. Taofiq, O.; Fernandes, A.; Barros, L.; Barreiro, M.F.; Ferreira, I.C. UV-irradiated mushrooms as a source of vitamin D2: A review. *Trends Food Sci. Technol.* **2017**, *70*, 82–94. [CrossRef]
36. Cashman, K.D.; Kiely, M.; Seamans, K.M.; Urbain, P. Effect of Ultraviolet Light–Exposed Mushrooms on Vitamin D Status: Liquid Chromatography–Tandem Mass Spectrometry Reanalysis of Biobanked Sera from a Randomized Controlled Trial and a Systematic Review plus Meta-Analysis. *J. Nutr.* **2016**, *146*, 565–575. [CrossRef] [PubMed]
37. Manoy, P.; Yuktanandana, P.; Tanavalee, A.; Anomasiri, W.; Ngarmukos, S.; Tanpowpong, T.; Honsawek, S. Vitamin D Supplementation Improves Quality of Life and Physical Performance in Osteoarthritis Patients. *Nutrients* **2017**, *26*, 799. [CrossRef] [PubMed]
38. Siasos, G.; Tousoulis, D.; Oikonomou, E.; Maniatis, K.; Kioufis, S.; Kokkou, E.; Vavuranakis, M.; Zaromitidou, M.; Kassi, E.; Miliou, A.; et al. Vitamin D3, D2 and arterial wall properties in coronary artery disease. *Curr. Pharm. Des.* **2014**, *20*, 5914–5918. [CrossRef] [PubMed]
39. Forouhi, N.G.; Menon, R.K.; Sharp, S.J.; Mannan, N.; Timms, P.M.; Martineau, A.R.; Rickard, A.P.; Boucher, B.J.; Chowdhury, T.A.; Griffiths, C.J.; et al. Effects of vitamin D2 or D3 supplementation on glycaemic control and cardiometabolic risk among people at risk of type 2 diabetes: Results of a randomized double-blind placebo-controlled trial. *Diabetes Obes. Metab.* **2016**, *18*, 392–400. [CrossRef]
40. Tran, V.; De Silva, T.M.; Sobey, C.G.; Lim, K.; Drummond, G.R.; Vinh, A.; Jelinic, M. The Vascular Consequences of Metabolic Syndrome: Rodent Models, Endothelial Dysfunction, and Current Therapies. *Front. Pharmacol.* **2020**, *11*, 148. [CrossRef]
41. Dicks, L.; Jakobs, L.; Sari, M.; Hambitzer, R.; Ludwig, N.; Simon, M.C.; Stehle, P.; Stoffel-Wagner, B.; Helfrich, H.P.; Ahlborn, J.; et al. Fortifying a meal with oyster mushroom powder beneficially affects postprandial glucagon-like peptide-1, non-esterified free fatty acids and hunger sensation in adults with impaired glucose tolerance: A double-blind randomized controlled crossover trial. *Eur. J. Nutr.* **2022**, *61*, 687–701. [CrossRef]
42. Poddar, K.H.; Ames, M.; Hsin-Jen, C.; Feeney, M.J.; Wang, Y.; Cheskin, L.J. Positive effect of mushrooms substituted for meat on body weight, body composition, and health parameters. A 1-year randomized clinical trial. *Appetite* **2013**, *71*, 379–387. [CrossRef]
43. Friedman, M. Mushroom Polysaccharides: Chemistry and Antiobesity, Antidiabetes, Anticancer, and Antibiotic Properties in Cells, Rodents, and Humans. *Foods* **2016**, *5*, 80. [CrossRef]
44. Kozarski, M.; Klaus, A.; Niksic, M.; Jakovljevic, D.; Helsper, J.P.; Van Griensven, L.J. Antioxidative and immunomodulating activities of polysaccharide extracts of the medicinal mushrooms *Agaricus bisporus*, *Agaricus brasiliensis*, *Ganoderma lucidum* and *Phellinus linteus*. *Food Chem.* **2011**, *129*, 1667–1675. [CrossRef]
45. Wing, R.R.; Lang, W.; Wadden, T.A.; Safford, M.; Knowler, W.C.; Bertoni, A.G.; Hill, J.O.; Brancati, F.L.; Peters, A.; Wagenknecht, L.; et al. Benefits of modest weight loss in improving cardiovascular risk factors in overweight and obese individuals with type 2 diabetes. *Diabetes Care* **2011**, *34*, 1481–1486. [CrossRef]
46. Choudhury, M.B.K.; Hossain, M.S.; Hossain, M.M.; Kakon, A.J.; Choudhury, M.A.K.; Ahmed, N.U.; Rahman, T. *Pleurotus ostreatus* improves lipid profile of obese hypertensive nondiabetic males. *Bangladesh J. Mushroom* **2013**, *7*, 37–44.
47. Abd-alwahab, W.I.; Al-dulaimi, F.K.; Abdulqader, A.T. Effect of mushroom cooked in olive oil on some physiological and biochemical parameters of human. *EurAsian J. BioSciences* **2018**, *12*, 393–397.

48. Sayeed, M.A.; Banu, A.; Khatun, K.; Khanam, P.A.; Begum, T.; Mahtab, H.; Haq, J.A. Effect of edible mushroom (*Pleurotus ostreatus*) on type-2 diabetics. *Ibrahim. Med. Coll. J.* **2014**, *8*, 6–11. [CrossRef]
49. Schneider, I.; Kressel, G.; Meyer, A.; Krings, U.; Berger, R.G.; Hahn, A. Lipid lowering effects of oyster mushroom (*Pleurotus ostreatus*) in humans. J. Funct. *Foods* **2011**, *3*, 17–24.
50. Fontes, A.; Ramalho-Santos, J.; Zischka, H.; Azul, A.M. Mushrooms on the plate: Trends towards NAFLD treatment, health improvement and sustainable diets. *Eur. J. Clin. Investig.* **2021**, *52*, e13667. [CrossRef]
51. Ren, Z.; Li, J.; Xu, N.; Zhang, J.; Song, X.; Wang, X.; Gao, Z.; Jing, H.; Li, S.; Zhang, C.; et al. Anti-hyperlipidemic and antioxidant effects of alkali-extractable mycelia polysaccharides by *Pleurotus eryngii* var tuolensis. *Carbohydr. Polym.* **2017**, *175*, 282–292. [CrossRef]
52. Jung, U.J.; Choi, M.S. Obesity and its metabolic complications: The role of adipokines and the relationship between obesity, inflammation, insulin resistance, dyslipidemia and nonalcoholic fatty liver disease. *Int. J. Mol. Sci.* **2014**, *15*, 6184–6223. [CrossRef]
53. Rizzo, G.; Goggi, S.; Giampieri, F.; Baroni, L. A review of mushrooms in human nutrition and health. *Trends Food Sci. Technol.* **2021**, *117*, 60–73. [CrossRef]
54. Volman, J.J.; Mensink, R.P.; van Griensven, L.J.; Plat, J. Effects of alpha-glucans from Agaricus bisporus on ex vivo cytokine production by LPS and PHA-stimulated PBMCs; a placebo-controlled study in slightly hypercholesterolemic subjects. *Eur. J. Clin. Nutr.* **2010**, *64*, 720–726. [CrossRef]
55. Morales, D.; Shetty, S.A.; López-Plaza, B.; Gómez-Candela, C.; Smidt, H.; Marín, F.R.; Soler-Rivas, C. Modulation of human intestinal microbiota in a clinical trial by consumption of a β-D-glucan-enriched extract obtained from Lentinula edodes. *Eur. J. Nutr.* **2021**, *60*, 3249–3265. [CrossRef]
56. Zhang, Y.; Chen, Z.; Wen, Q.; Xiong, Z.; Cao, X.; Zheng, Z.; Zhang, Y.; Huang, Z. An overview on the biosynthesis and metabolic regulation of monacolin K/lovastatin. *Food Funct.* **2020**, *11*, 5738–5748. [CrossRef] [PubMed]
57. Maseko, T.; Howell, K.; Dunshea, F.R.; Ng, K. Selenium-enriched Agaricus bisporus increases expression and activity of glutathione peroxidase-1 and expression of glutathione peroxidase-2 in rat colon. *Food Chem.* **2014**, *146*, 327–333. [CrossRef] [PubMed]
58. Stepien, M.; O'Mahony, L.; O'Sullivan, A.; Collier, J.; Fraser, W.D.; Gibney, M.J.; Nugent, A.P.; Brennan, L. Effect of supplementation with vitamin D2-enhanced mushrooms on vitamin D status in healthy adults. *J. Nutr. Sci.* **2013**, *2*, E29. [CrossRef] [PubMed]
59. Drori, A.; Shabat, Y.; Ben Ya'acov, A.; Danay, O.; Levanon, D.; Zolotarov, L.; Ilan, Y. Extracts from Lentinula edodes (Shiitake) Edible Mushrooms Enriched with Vitamin D Exert an Anti-Inflammatory Hepatoprotective Effect. *J. Med. Food* **2016**, *19*, 383–389.
60. Wee, C.C.; Davis, R.B.; Hamel, M.B. Comparing the SF-12 and SF-36 health status questionnaires in patients with and without obesity. *Health Qual. Life Outcomes* **2008**, *6*, 11. [CrossRef]

metabolites

MDPI

Article

Metabolomic Profiling of Second-Trimester Amniotic Fluid for Predicting Preterm Delivery: Insights from NMR Analysis

Charalampos Kolvatzis [1,*], Paris Christodoulou [2], Ioannis Kalogiannidis [1], Konstantinos Tsiantas [2], Ioannis Tsakiridis [1], Charikleia Kyrkou [3], Antigoni Cheilari [4], Nikolaos S. Thomaidis [5], Panagiotis Zoumpoulakis [2], Apostolos Athanasiadis [1] and Alexandra-Maria Michaelidou [3]

1 Third Department of Obstetrics and Gynecology, School of Medicine, Faculty of Health Sciences, Aristotle University of Thessaloniki, 54642 Thessaloniki, Greece; ikalogia@auth.gr (I.K.); igtsakir@auth.gr (I.T.); apathana@auth.gr (A.A.)
2 Department of Food Science and Technology, University of West Attica, Ag. Spyridonos, 12243 Egaleo, Greece; pchristodoulou@uniwa.gr (P.C.); ktsiantas@uniwa.gr (K.T.); pzoump@uniwa.gr (P.Z.)
3 Department of Food Science and Technology, Faculty of Agriculture, Forestry and Natural Environment, School of Agriculture, Aristotle University of Thessaloniki, 54124 Thessaloniki, Greece; kyrkoucg@agro.auth.gr (C.K.); amichail@agro.auth.gr (A.-M.M.)
4 Department of Pharmacognosy and Natural Products Chemistry, Faculty of Pharmacy, National and Kapodistrian University of Athens, Panepistimiopolis Zografou, 17551 Athens, Greece; cheilarianti@pharm.uoa.gr
5 Laboratory of Analytical Chemistry, Department of Chemistry, National and Kapodistrian University of Athens, Panepistimiopolis Zografou, 15771 Athens, Greece; ntho@chem.uoa.gr
* Correspondence: kolvatzis@auth.gr

Abstract: Preterm delivery (PTD) is a notable pregnancy complication, affecting one out of every ten births. This study set out to investigate whether analyzing the metabolic composition of amniotic fluid (AF) collected from pregnant women during the second trimester of pregnancy could offer valuable insights into prematurity. The research employed ^{1}H–NMR metabolomics to examine AF samples obtained from 17 women who gave birth prematurely (between 29^{+0} and 36^{+5} weeks of gestation) and 43 women who delivered at full term. The application of multivariate analysis revealed metabolites (dimethylglycine, glucose, myo-inositol, and succinate) that can serve as possible biomarkers for the prognosis and early diagnosis of preterm delivery. Additionally, pathway analysis unveiled the most critical metabolic pathways relevant to our research hypothesis. In summary, these findings suggest that the metabolic composition of AF in the second trimester can be a potential indicator for identifying biomarkers associated with the risk of PTD.

Keywords: amniotic fluid; preterm delivery; NMR metabolomics; multivariate analysis

Citation: Kolvatzis, C.; Christodoulou, P.; Kalogiannidis, I.; Tsiantas, K.; Tsakiridis, I.; Kyrkou, C.; Cheilari, A.; Thomaidis, N.S.; Zoumpoulakis, P.; Athanasiadis, A.; et al. Metabolomic Profiling of Second-Trimester Amniotic Fluid for Predicting Preterm Delivery: Insights from NMR Analysis. *Metabolites* **2023**, *13*, 1147. https://doi.org/10.3390/metabo13111147

Academic Editors: Eleftherios Panteris and Olga Deda

Received: 23 October 2023
Revised: 9 November 2023
Accepted: 9 November 2023
Published: 12 November 2023

1. Introduction

Spontaneous preterm delivery (PTD), affecting one out of every ten births, is recognized as a syndrome influenced by multiple contributing factors [1]. Among the spectrum of suspected causes of PTD, infection and/or inflammation characterized as the body's response to signals of microbial or non-microbial danger stand out as the only pathological processes for which a confirmed causal connection with PTD has been established, along with a clearly defined molecular pathophysiology [2].

Infants born prematurely, particularly those born before 34 weeks of gestation, have an elevated risk of mortality and health problems. Furthermore, infants born during the late preterm period, i.e., 34–37 weeks of gestation, face increased health complications and a higher probability of developing health conditions like obesity, metabolic syndrome, hypertension, and type 2 diabetes later in life [3].

Prediction and early diagnosis of PTD are often challenging because of their complexity [4]. Hence, it is not surprising that metabolomics, utilizing advanced techniques such

as Nuclear Magnetic Resonance Spectroscopy (NMR), Gas Chromatography–Mass Spectrometry (GC-MS), and Liquid Chromatography–Mass Spectrometry (LC-MS/MS), have gained prominence in identifying biomarkers and pathways crucial to the development and progression of this syndrome [4–10].

Among the various options, amniotic fluid (AF) emerges as a particularly promising biofluid; it serves as a dynamic repository, reflecting the metabolic profile of the developing fetus. Research studies [11–15] suggest that conducting a metabolomic analysis on AF obtained during the prenatal period holds the potential to identify metabolic deviations before PTD occurs. However, a recent study using untargeted LC-MS mid-trimester amniotic fluid metabolic profiling on two groups of 37 pregnant women (full term/preterm) that underwent amniocentesis showed no evidence of metabolite differentiation for spontaneous PTD [16].

Studies in this area have employed diverse metabolomics techniques, and the consensus on critical metabolites serving as biomarkers remains elusive [10]. The apparent inconsistency highlights the intricate nature of the PTD syndrome and implies the presence of unexplored aspects. Within this context, our study aims to bridge this gap by identifying potential predictive biomarkers for spontaneous PTD within second-trimester AF using NMR analysis.

2. Materials and Methods

2.1. Study Design and Population

This prospective cohort study investigated AF samples between 2013 and 2014 at the Third Department of Obstetrics and Gynecology, School of Medicine, Faculty of Health Sciences, Aristotle University of Thessaloniki, Greece. The study was approved by the Aristotle University of Thessaloniki Research Ethics Committee (Prot. No. 1.662/21 November 2018) and conducted in compliance with the declaration of Helsinki. No incentives were provided, and all the participants signed a relevant informed written consent.

Data Collection and Eligibility Criteria

All the pregnant women in singleton pregnancies who underwent amniocentesis (between 16 and 22 weeks of gestation) for prenatal screening were eligible to participate in the study; a small amount of AF was donated and kept at −80 °C. Detailed obstetric and medical histories were recorded for each woman in the study.

Exclusion criteria were (1) multiple pregnancies, (2) short cervical length at second-trimester ultrasound (<25 mm), and (3) preterm prelabor rupture of membranes, placental ischemic disease, and iatrogenic PTD. In addition, pregnant women who had a miscarriage before 24 weeks or PTD within the first 3 weeks of amniocentesis were excluded from the analysis.

With regards to the indications of amniocentesis, increased risk of fetal genetic abnormality after combined first-trimester ultrasound and biochemical screening, detection of ultrasound markers at first- and second-trimester screenings associated with an increased likelihood of chromosomal abnormalities (e.g., nasal bone hypoplasia, short femur, and hyperechoic bowel), maternal desire, and high risk of vertical transmission of congenital infection were the most common ones, as recommended by the majority of the guidelines [17].

Pregnancy outcomes were collected to determine the gestational age at delivery (preterm <37 weeks or term >37 weeks), mode of delivery (vaginal/cesarean), birthweight, and possible complications during pregnancy. The metabolomic profile of the AF was checked and compared according to the week of delivery and birthweight.

2.2. NMR Metabolomics Analysis

2.2.1. Sample Preparation

Amniotic fluid samples were thawed at room temperature (25 °C) and extracted according to a common method established in the literature [13]. Specifically, 10 mL of AF

was centrifuged (14,000 rpm, 4 °C, 10 min), and 1 mL of the supernatants was lyophilized overnight until dry. The dry residues were then reconstituted into 540 μL of phosphate buffer (0.2 M, Na_2HPO_4 $2H_2O$, and NaH_2PO_4, pH = 7.0) in D_2O and 60 μL (5 mM) of *d6*- trimethylsilyl propionic acid sodium salt (TSP) as the internal standard.

2.2.2. ^{1}H–NMR Analysis

For ^{1}H–NMR measurement, 600 μL of the final samples was transferred to 5 mm NMR tubes (LabScape, Bruker, Germany). The NMR spectra were acquired at 300 K, after a 5 min resting period for temperature stabilization, on a Bruker Ascend 500 MHz NMR spectrometer equipped with a 5 mm double resonance broadband inverse (BBI) detection probe. Experiments were performed in automation mode, using a SampleCase-24 sample changer operated by IconNMR. Data acquisition and processing were performed with TopSpin 4.1.4 (Bruker Italia Slr, Milan, Italy). Metabolic profiling 1D NMR spectra were acquired using water suppression. T2-edited Carr-Purcell-Meiboom-Gill (CPMG) experiments were acquired with d1 = 6 s; AQ = 4.92 s; FID data points = 96 k; SW = 20 ppm; ns = 32. The transmitter offset was set manually to achieve optimal suppression of the residual water signal for both experiments. FIDs were zero-filled and multiplied by an exponential weighting function corresponding to a line broadening of 0.3 Hz before Fourier transformation. Chemical shift values were referenced to the residual TSP signal (0.00 ppm).

2.2.3. Data Processing

All ^{1}H–NMR spectra were phase-corrected using TopSpin 4.1.4 software. Then, the .zip file of all files was uploaded to the NMRProcFlow open-access web tool [18] to proceed with chemical shift calibration, baseline correction, and S/N ratio identification as well as alignment normalization and bucketing. For alignment, an interactive philosophy was performed, meaning that each interval had been chosen separately performing CluPA, as well as the least squares method [2]. All spectra were normalized using the Probabilistic Quotient Normalization (PQN) method [3], and an intelligent bucketing module was performed within the 0.8–8.5 spectra region.

2.2.4. Metabolites Screening

A series of 2D TOCSY and HSQC experiments were acquired for metabolite identification. More specifically, the above validation NMR experiments were acquired using a phase-sensitive MLEV sequence with d1 = 4 s; FID data points = 2 k (F2) and 256 (F1); SW = 20 ppm; ns = 32; and mixing time (d9) = 0.08 sec with suppression of the residual water signal. Furthermore, phase-sensitive HSQC-DEPT experiments were acquired using Echo/Antiecho-TPPI gradient selection with decoupling during acquisition (hsqcedetgpsisp2.3) with FID data points = 4 k (F2) and 288 (F1); SW = 12 ppm (F2) and 180 (F1); and ns = 160 in non-uniform sampling (NUS) acquisition mode with a NUS level of 50%.. To aid in rapid and efficient metabolite identification, Metabominer [19], an easy-to-use software tool, along with 2D TOCSY and HSQC experiments and data from the literature were used. Briefly, an automated pick-picking list from each spectrum (TOCSY and HSQC) was generated from MestreNOVA software and loaded in the Metabominer tool to (a) screen metabolites from Metabominers' biofluids database and (b) refine the identified compounds by superimposing the spectral images to the Metabominers' generated spectra.

2.3. Statistical Analysis

2.3.1. Demographics

As all demographic parameters did not follow the normal distribution, the Mann–Whitney U test was used for group comparisons. The statistical significance level was set at 5%. The demographics were statistically analyzed with SPSS (Statistical Package for the Social Sciences) v.26 (SPSS, Inc., Chicago, IL, USA).

2.3.2. Metabolomics

The MetaboAnalyst 5.0 was facilitated for both univariate/multivariate analyses and pathway analysis [5]. For multivariate analysis, -Pareto scaling was used, and unsupervised/supervised models (PCA/PLS-DA) were extracted at a confidence level of 95%. Feature selection of the PLS-DA model was based on variable importance projection (VIP) scores > 1.0 to reveal the variable that mostly contributes to the discrimination of the studied groups. The validation of the models was evaluated in terms of accuracy (>90.0 %), the goodness-of-fit R^2 ($0 \leq R^2 \leq 1$), and the predictive ability Q^2 ($0 \leq Q^2 \leq 1$) values. The PLS-DA results were further cross-validated by carrying out permutation tests with 1000 random permutations.

In terms of univariate analysis, non-parametric Wilcoxon *t*-tests were performed ($p < 0.05$). For the elucidation of metabolites as possible biomarkers, Receiver Operating Characteristic (ROC) curves were acquired. Finally, pathway analysis was performed by Metaboanalyst 5.0 platform.

3. Results

In total, 60 AF samples were used in the analyses; 43 were term and 17 were preterm. The mean duration of gestation was 38.5 (±0.9) weeks for the term group and 35.3 (±2.8) weeks for the preterm group ($p < 0.001$). Similarly, the mean birthweight was statistically different with term neonates having a mean birthweight of 3340 g (±380.77), while the preterm ones weighed 2695 g (±553.85) ($p < 0.001$). All parameters investigated are presented in Table 1.

Table 1. Sample demographics and pregnancy outcome data by group ($n = 60$).

	Preterm ($n = 17$)	**Full Term ($n = 43$)**	**Mann–Whitney U Test**
	% (n)	**% (n)**	***p* Value**
Sex			
Boy	58.8% (10)	51.2% (22)	0.595
Girl	41.2% (7)	48.8% (21)	
Delivery			
Cesarean section	17.6% (3)	7% (3)	0.218
Normal delivery	82.4% (14)	93% (40)	
	Mean (SD)	**Mean (SD)**	
Gestational age (weeks)	35.3 (2.8)	38.5 (0.9)	<0.001
Amniocentesis (week)	20.31 (2.46)	19.68 (1.82)	0.479
Age (years)	36.54 (2.70)	37.29 (3.63)	0.548
Weight (Kg)	71.82 (10.54)	73.16 (9.11)	0.755
Weight gain (Kg)	12.9 (6.4)	12.9 (5.9)	0.786
Neonatal weight (g)	2695.29 (553.85)	3340.23 (380.77)	<0.001
Neonatal weight (z-scores)	−0.886 (1.06)	0.350 (0.730)	<0.001
Neonatal length (cm)	51.2 (2.2)	51.2 (1.6)	0.744

SD = standard deviation.

3.1. NMR Analysis

A total of 27 metabolites including aliphatic and aromatic amino acids, sugars, and organic acids were assigned by the combination of 2D NMR spectroscopy (2D-HSQC, 2D TOCSY) and available online tools such as Metabominer and the literature data, as described in Section 2.2.4. The identified metabolites of the acquired AF samples are displayed in Figure 1, while the characteristic chemical shifts are represented in Supplementary Table S1.

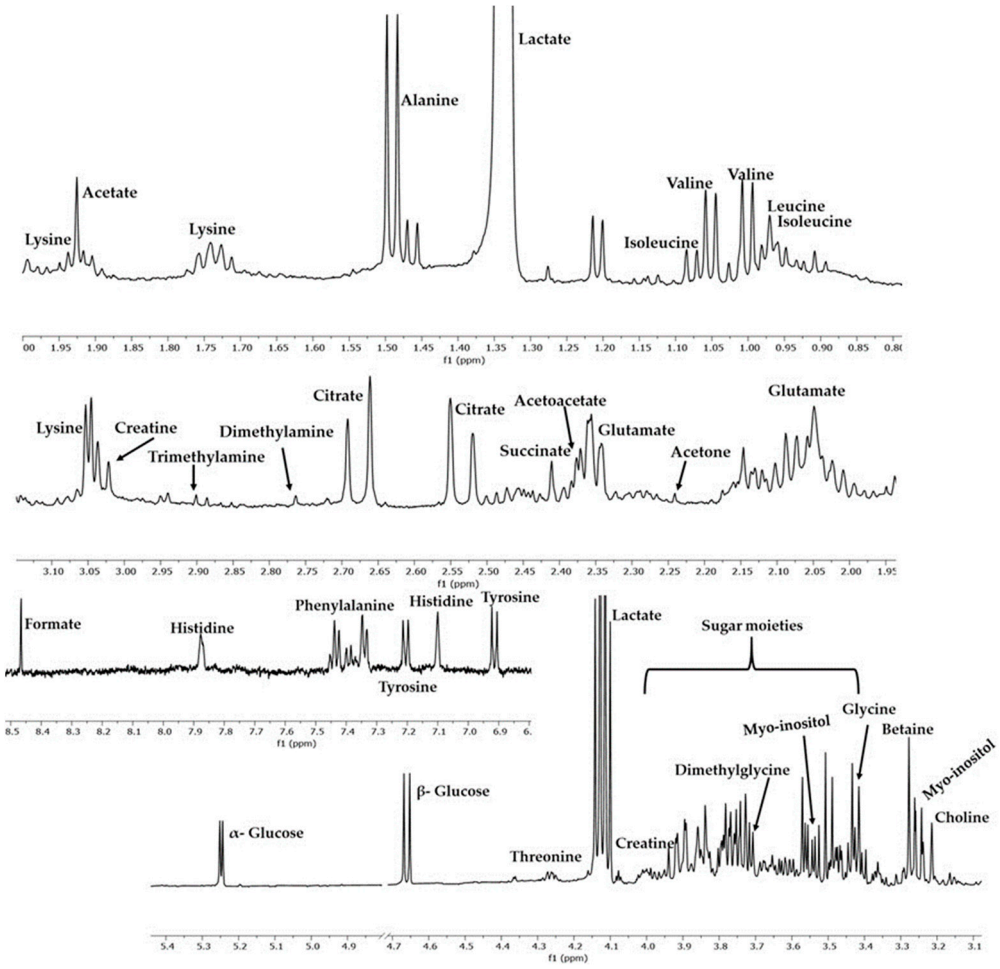

Figure 1. ^{1}H NMR spectra of AF sample with annotation of the identified metabolites.

The spectra matrix underwent intelligent bucketing to reduce the spectra data and facilitate subsequent statistical analysis. A total of 170 buckets were annotated according to the assignment procedure (Supplementary Table S2). The new matrix was subjected to both multivariate and univariate analysis.

3.2. Statistics

3.2.1. Overview of the Studied Samples

Principal Component Analysis (PCA) was conducted on the annotated NMR profile (170 annotated intelligent buckets, Supplementary Table S2) to gain an overview of the sample space. The resulting scores plot (Figure 2) revealed a pattern between the two studied groups along the first principal component, accounting for 34.3% of the metabolic variance in the studied AF samples.

3.2.2. Data Reduction Method for Unique Potential Biomarker Discovery

Digging deeper into the annotated metabolites (Supplementary Table S2), it is observed that a significant number of buckets correspond to more than one metabolite. Considering that the purpose of this study is the development of reliable potential prognostic markers for PTD, we applied a robust statistical methodology based on the annotated spectra buckets.

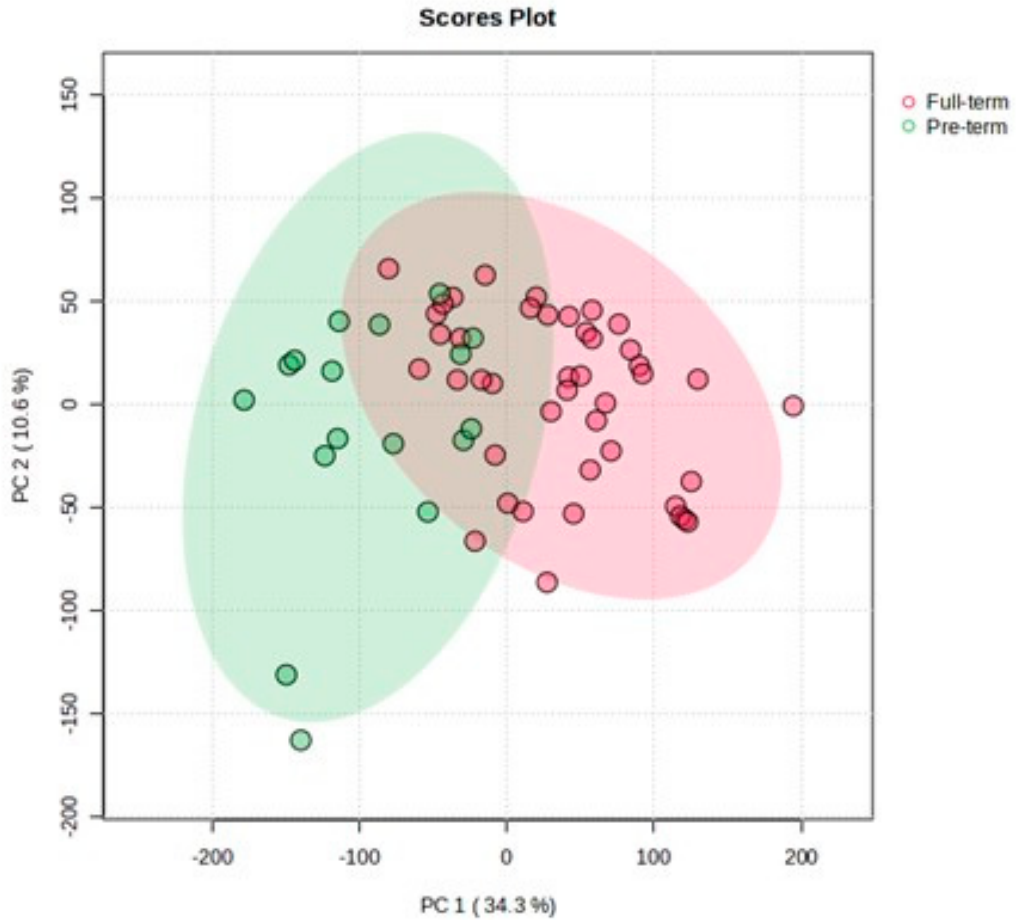

Figure 2. PCA score plot of the studied AF samples; No. of components = 2, n = 60, confidence level = 95%; red dots correspond to full-term samples, while green dots correspond to preterm samples.

In detail, a gradual bucketing reduction method was implemented by including buckets that characterize unique metabolites to avoid the metabolites' overlapping phenomenon. This procedure led to the reduction of the feature space to 94 out of 170 annotated intelligent buckets. Notably, the 94 buckets corresponded to the initial number of assigned metabolites (n = 27).

Moreover, the reduced feature space (n = 94) was subjected to biomarker analysis considering the area under the ROC curve (AUROC) and the p values promoting potential biomarkers with a good predictive ability and strong statistical significance (AUROC > 0.75 and $p < 0.05$). These values are in accordance with the literature [10,20].

Applying the above criteria, the process concluded with 25 intelligent buckets corresponding to 12 unique metabolites (Supplementary Table S3). Finally, to exclude multiple buckets corresponding to the same metabolite, buckets that demonstrated the higher AUROC (n = 12) were kept for further statistical analyses (Supplementary Table S4). The whole procedure is shown in Figure 3.

3.2.3. Discriminant and Pathway Analysis

Discriminant analysis was applied to define the metabolites that confirm the discrimination of the two sample categories (full term/preterm). Supervised partial least-squares discriminant analysis (PLS-DA) was employed, using the full-term/preterm classification as the response variable and the 12 potential biomarkers as the independent variables. The extracted 3D score plot manifested the separation of the studied groups across the first component (Figure 4A). The variable importance projection (VIP) plot was then retrieved to identify the variables with the greater discriminative ability (VIP > 1) among the two

studied groups. Indicatively, PTB is associated with a lower abundance of dimethylglycine, glucose, and myo-inositol; while in the full-term birth, the production of succinate is fostered (Figure 4B). The model was validated by permutation test statistics (Figure 4C). The box plots of the four promoted metabolites are shown in Figure 5.

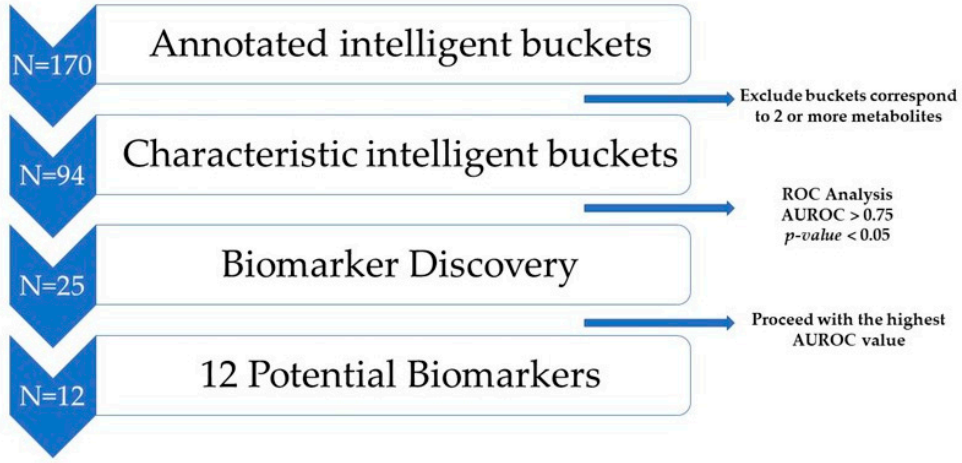

Figure 3. Overview of the buckets' reduction methodology.

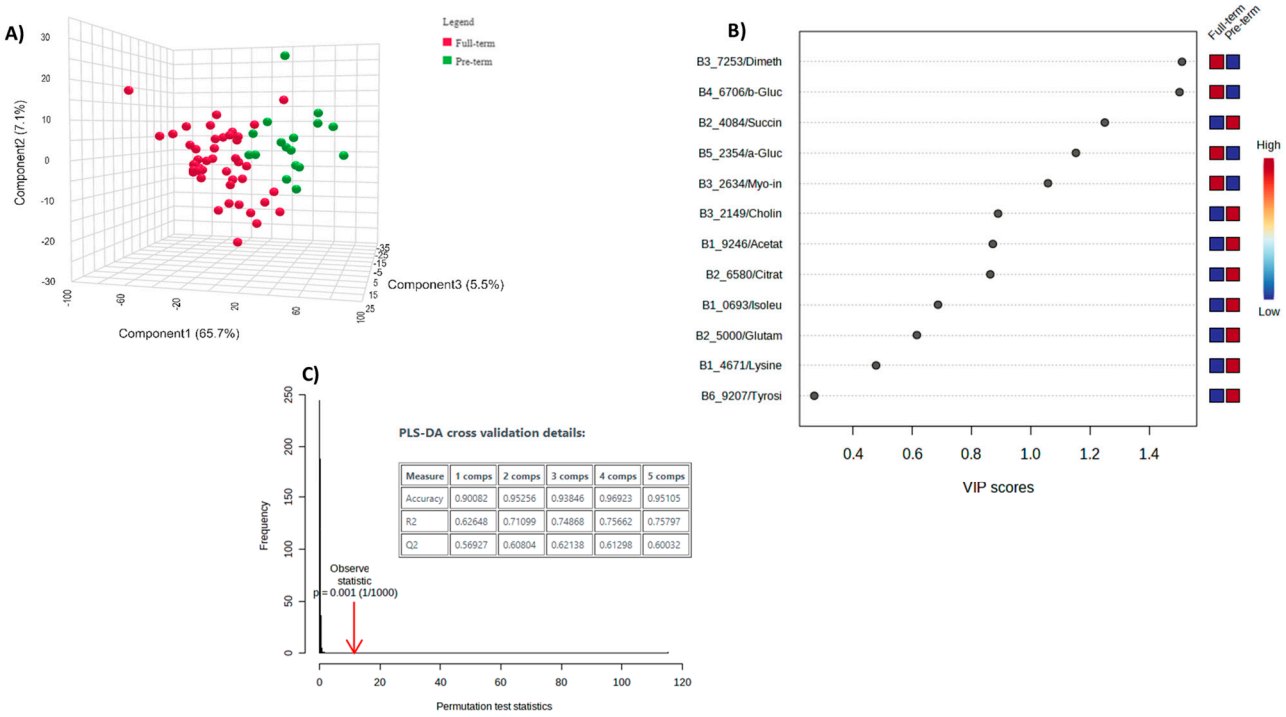

Figure 4. PLS-DA analysis for the AF samples of 60 volunteers. (**A**) Score plot of PLS-DA analysis ($R^2X(cum) = 0.75$, $Q^2(cum) = 0.61$, accuracy = 0.93, comp No. = 3). The green and red dots correspond to preterm and term classification, respectively; (**B**) VIP plot of the studied metabolites. (**C**) Validation of the PLS-DA analysis, by permutation test statistics, indicates that the extracted model is significantly different from a model built on random data. The permutation tests were carried out with 1000 random permutations, thus providing significance of the model at the 0.001 level.

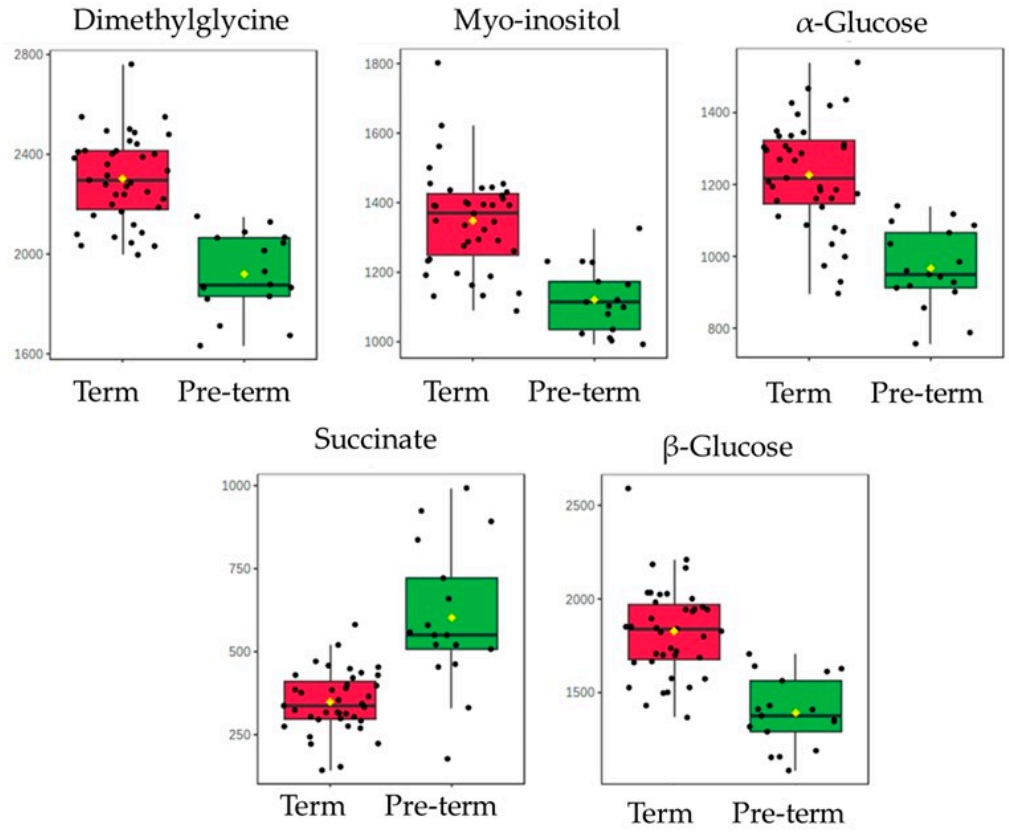

Figure 5. Box plot of the promoted metabolites from the discriminant analysis.

Finally, metabolites exhibiting AUROC > 0.75 (Supplementary Table S4) in AF samples were subjected to pathway analysis to relate the promoted metabolic patterns to specific pathways. The results (Supplementary Figure S1) depicted that seven metabolic pathways were significantly enriched ($p < 0.05$) containing at least two compounds, while two of them (alanine, aspartate, and glutamate metabolism and the citrate cycle) had the largest impact (>0.1) (Table 2).

Table 2. Results of the pathway analysis of the AF samples (in bold, the pathways of importance are depicted).

No.	Pathway	Total	Expected	Hits	Raw *p*	log (*p*)	Holm Adjust	FDR	Impact
1	Aminoacyl-tRNA biosynthesis	48	0.34	4	0.0002	3.6417	0.0192	0.02	0.00
2	Alanine, aspartate, and glutamate metabolism	28	0.20	3	0.0008	3.1015	0.0657	0.03	0.20
3	Glyoxylate and dicarboxylate metabolism	32	0.23	3	0.0012	2.9282	0.0968	0.03	0.03
4	Butanoate metabolism	15	0.11	2	0.0046	2.3397	0.3705	0.10	0.00
5	Citrate cycle (TCA cycle)	20	0.14	2	0.0081	2.0906	0.6494	0.14	0.12
6	Glycolysis/ Gluconeogenesis	26	0.18	2	0.0136	1.8676	1.0000	0.19	0.03

Table 2. *Cont.*

No.	Pathway	Total	Expected	Hits	Raw *p*	log (*p*)	Holm Adjust	FDR	Impact
7	Glycine, serine, and threonine metabolism	33	0.23	2	0.0214	1.6686	1.0000	0.26	0.07
8	Phenylalanine, tyrosine, and tryptophan biosynthesis	4	0.03	1	0.0281	1.5511	1.0000	0.30	0.50
9	Nitrogen metabolism	6	0.04	1	0.0419	1.3778	1.0000	0.35	0.00
10	D-Glutamine and D-glutamate metabolism	6	0.04	1	0.0419	1.3778	1.0000	0.35	0.50

4. Discussion

The present study explores the possibility of identifying potential concentration patterns of markers that characterize PTD. Among these 60 asymptomatic women, 43 delivered at term, while 17 delivered prematurely.

Our study supports the hypothesis that PTD is characterized by several changes in the metabolic profile of the fetus as reflected in second-trimester amniotic fluid [10]. The multivariate analysis highlighted that dimethylglycine, glucose, myo-inositol and succinate possessed the highest discriminative ability between the two studied groups. Moreover, pathway analysis revealed the most important metabolic pathways involved in our research hypothesis.

In accordance with prior research results [13], we have observed decreased glucose levels in second-trimester amniotic fluid samples obtained from women that delivered preterm. The decrease in glucose levels may be linked to increased glycolysis, potentially occurring under stressful conditions and reduced utilization of the respiratory chain pathway (as indicated by the rise in succinate levels) partly due to disrupted transplacental flow [15]. Furthermore, a meta-analysis conducted by Liu et al. (2017) supported our observations, indicating that lower glucose levels in early- or mid-trimester AF are associated with PTD [21]. Previous studies have convincingly demonstrated that decreased levels of glucose in AF are linked to the presence of microorganisms in the amniotic cavity and/or an inflammatory response [21–24]. These findings align with the notion that intraamniotic infection or inflammation (subclinical) plays a causative role in PTD [21].

Our analysis revealed that during the second trimester, women who later experienced PTD exhibited higher levels of succinate in their AF compared to women who carried their pregnancies to term. This discovery aligns with a recent study conducted by Virgiliou et al. in 2017 [14], which observed elevated fumarate levels in mid-trimester AF derived from women who delivered prematurely. Ansari et al. [22] and others [25–27] have proposed that succinate and fumarate, vital metabolites in both host and microbial processes, act as potent allosteric inhibitors of 2OG-dependent dioxygenases. Notably, this group of enzymes includes members of the histone demethylase family. Emerging evidence highlights a strong correlation between epigenetic events, particularly histone methylation, T-cell activation, differentiation, and commitment [22,25,26]. Hence, it is plausible that the generation, utilization, and translocation of these metabolites from the mitochondria to the cytosol, facilitating dynamic histone methylation within the nucleus, could potentially contribute to the occurrence of PTD. Given the immunomodulatory effects of succinate, as demonstrated by Al-Mushrif et al. in 2000 albeit in a slightly different setting [23], this finding needs further investigation.

Another noteworthy discovery that aligns with the existing literature [14] pertains to the reduced levels of myo-inositol found in the AF of PTD cases. Myo-inositol is a vital nutrient essential for the growth and viability of human cells. It is worth mentioning that myo-inositol has previously been identified as a significant marker in AF for women experiencing preterm labor without intraamniotic infection or inflammation [14,28,29]. Numerous assumptions may document myo-inositol's potential role in fetal development and metabolic maturity. Myo-inositol acts as a structural basis for several secondary messengers found in eukaryotic cells, including inositol phosphates, phosphatidylinositol, and phosphatidylinositol phosphate lipids. These secondary messengers are pivotal in various cellular processes, including the regulation of intracellular calcium, gene expression, and lipid metabolism [30]. Current data suggest that a higher content of placental myo-inositol might postpone the initiation of labor by suppressing the synthesis and production of placental eicosanoids. This suppression could result from either a decrease in the availability of arachidonic acid for eicosanoid synthesis or a reduction in the activity of enzymes responsible for eicosanoid production. Moreover, myo-inositol could potentially redirect arachidonic acid metabolism towards generating anti-inflammatory eicosanoids rather than pro-inflammatory ones, thereby regulating the overall equilibrium of pro-inflammatory and anti-inflammatory factors to inhibit the onset of preterm labor. Furthermore, the administration of myo-inositol for the prevention of prematurity has been a subject of study [26].

Dimethylglycine is a derivative of the amino acid glycine. It is important to note that glycine, choline, betaine, and dimethylglycine are interconnected compounds with related metabolic pathways. While a previous metabolomic analysis of healthy pregnant individuals' AF indicated increased levels of both choline and N-dimethylglycine during the transition from the second to the third trimester [31], there is limited information available regarding dimethylglycine levels in AF among cases of PTD. In the context of our study, dimethylglycine was found to be decreased in AF samples from women who delivered prematurely. Deciphering the role of dimethylglycine in relation to PTD is interesting since current data suggest that dimethylglycine may be engaging in different pathways that influence the regulation of the labor process itself. These effects might be related, at least in part, to its function in bolstering cellular antioxidant activity. It is well-documented that spontaneous PTD is associated with oxidative stress and disturbances in the body's redox system, often linked with inflammation [14]. Dimethylglycine is involved in multiple metabolic pathways and can facilitate the recycling of other antioxidants, such as glutathione, which is a vital cellular antioxidant [32]. By aiding in the regeneration of other antioxidants, dimethylglycine could indirectly contribute to mitigating oxidative stress and safeguarding cells from damage caused by reactive oxygen species (ROS). Another viable scenario involves its role as a methyl donor. The transfer of a methyl group from betaine to homocysteine, catalyzed by the enzyme betaine-homocysteine methyltransferase, results in the production of methionine and dimethylglycine. Consequently, a deficiency in methyl donors may result in disturbances in metabolism and function [24].

Interestingly, as previously discussed, a recent study [16] found no significant differences in metabolite profiles associated with spontaneous PTD. This outcome may be attributed to variations in stratification and research protocols.

The strengths of this study are evident in its approach to data collection and the rigorous statistical methods applied. The collection of samples during the pre-clinical phase, when women show no symptoms, has the potential to identify individuals at high risk early on. This approach aligns with the findings of Souza et al. in 2019 [4], suggesting that it can help uncover the triggers of preterm labor. Furthermore, a meticulously statistical approach was adopted to thoroughly assess the candidate biomarkers' diagnostic and prognostic potential. This method yielded a concise set of features that represented the most reliable and noteworthy markers, characterized by AUROC values exceeding 0.75. Regarding limitations, the study's sample size may pose constraints on the broader applicability of its findings. Additionally, for future investigations, the integration of metabolomic techniques

with advanced molecular microbiological methods could offer a deeper exploration of the intricate connections between microbiota and metabolites.

5. Conclusions

To conclude, NMR metabolomics' analysis led to the identification of glucose, succinate, myo-inositol, and dimethylglycine as potential biomarkers of PTD. The results overall support previous data, while they underscore the dynamic nature of AF composition, reflecting the physiological changes occurring throughout pregnancy. The identified specific metabolites and their fluctuations have the potential to serve as biomarkers for monitoring pregnancy progression and identifying aberrations that may require medical attention. Furthermore, our study has highlighted the intricate interplay between maternal and fetal metabolisms within the AF environment. This intergenerational metabolic dialogue can inform our understanding of fetal development and its susceptibility to external factors.

Supplementary Materials: The following supporting information can be downloaded at: https://www.mdpi.com/article/10.3390/metabo13111147/s1, Table S1. Table representing the characteristic chemical shifts of the identified metabolites, Table S2. Table representing the annotated buckets based on the identification procedure. The term "BX_XXXX" corresponds to ppm. Table S3. Illustration of Biomarker Analysis. In total 50 annotated buckets corresponding to unique metabolites, passed the statistical significance analysis ($p < 0.05$). In bold are presented the 25 annotated buckets with AUROC > 0.75 and p value < 0.05. Table S4. Buckets corresponding to the higher AUROCs and 12 unique metabolites. Figure S1: Graphical illustration of Pathway Analysis.

Author Contributions: Conceptualization, A.A., I.K., P.Z., C.K. (Charalampos Kolvatzis) and A.-M.M.; methodology, P.C., K.T., A.C., N.S.T., P.Z., A.A. and C.K. (Charalampos Kolvatzis); software P.C., K.T. and A.C.; investigation, C.K. (Charalampos Kolvatzis) and P.C.; data curation, C.K. (Charalampos Kolvatzis), P.C., K.T. and A.C.; resources, P.Z., N.S.T., A.A. and C.K. (Charalampos Kolvatzis); visualization, C.K. (Charikleia Kyrkou) and P.C.; writing—original draft preparation, C.K. (Charalampos Kolvatzis), P.C., K.T., A.C., I.T., A.-M.M. and C.K. (Charikleia Kyrkou); writing—review and editing, C.K. (Charalampos Kolvatzis), I.T., P.C., K.T., N.S.T., C.K. (Charikleia Kyrkou), A.A., I.K. and A.-M.M.; supervision, A.A., I.K., P.Z. and A.-M.M.; project administration, P.Z., A.A. and A.-M.M. All authors have read and agreed to the published version of the manuscript.

Funding: This research received no external funding.

Institutional Review Board Statement: The study was conducted in accordance with the Declaration of Helsinki and approved by the Aristotle University of Thessaloniki Research Ethics Committee (Prot. No. 1.662/21 November 2018) for studies involving humans.

Informed Consent Statement: Informed consent was obtained from all subjects involved in the study.

Data Availability Statement: The data presented in the manuscript are available on reasonable request from the corresponding authors. The data are not publicly available due to their containing information that could compromise the privacy of research participants.

Conflicts of Interest: The authors declare no conflict of interest.

References

1. Goldenberg, R.L.; Culhane, J.F.; Iams, J.D.; Romero, R. Epidemiology and causes of preterm birth. *Lancet* **2008**, *371*, 75–84. [CrossRef] [PubMed]
2. Vu, T.N.; Laukens, K. Getting Your Peaks in Line: A Review of Alignment Methods for NMR Spectral Data. *Metabolites* **2013**, *3*, 259–276. [CrossRef] [PubMed]
3. Wojtowicz, W.; Zabek, A.; Deja, S.; Dawiskiba, T.; Pawelka, D.; Glod, M.; Balcerzak, W.; Mlynarz, P. Serum and urine 1H NMR-based metabolomics in the diagnosis of selected thyroid diseases. *Sci. Rep.* **2017**, *7*, 9108. [CrossRef] [PubMed]
4. Souza, R.T.; Mayrink, J.; Leite, D.F.; Costa, M.L.; Calderon, I.M.; Rocha, E.A.; Vettorazzi, J.; Feitosa, F.E.; Cecatti, J.G. Metabolomics applied to maternal and perinatal health: A review of new frontiers with a translation potential. *Clinics* **2019**, *74*, e894. [CrossRef] [PubMed]
5. Pang, Z.; Chong, J.; Zhou, G.; de Lima Morais, D.A.; Chang, L.; Barrette, M.; Gauthier, C.; Jacques, P.-É.; Li, S.; Xia, J. MetaboAnalyst 5.0: Narrowing the gap between raw spectra and functional insights. *Nucleic Acids Res.* **2021**, *49*, W388–W396. [CrossRef] [PubMed]

6. Gil, A.M.; Duarte, D. Biofluid metabolomics in preterm birth research. *Reprod. Sci.* **2018**, *25*, 967–977. [CrossRef] [PubMed]
7. Ansari, A.; Bose, S.; You, Y.; Park, S.; Kim, Y. Molecular mechanism of microbiota metabolites in preterm birth: Pathological and therapeutic insights. *Int. J. Mol. Sci.* **2021**, *22*, 8145. [CrossRef]
8. Li, X.; Huang, S.; Jiao, A.; Yang, X.; Yun, J.; Wang, Y.; Xue, X.; Chu, Y.; Liu, F.; Liu, Y. Association between ambient fine particulate matter and preterm birth or term low birth weight: An updated systematic review and meta-analysis. *Environ. Pollut.* **2017**, *227*, 596–605. [CrossRef]
9. Michaelidou, A.-M.; Tsakoumaki, F.; Fotiou, M.; Kyrkou, C.; Athanasiadis, A.P. Metabolomics in amniotic fluid. In *New Technologies and Perinatal Medicine*; CRC Press: Boca Raton, FL, USA, 2019; pp. 139–148.
10. Kolvatzis, C.; Tsakiridis, I.; Kalogiannidis, I.A.; Tsakoumaki, F.; Kyrkou, C.; Dagklis, T.; Daniilidis, A.; Michaelidou, A.-M.; Athanasiadis, A. Utilizing Amniotic Fluid Metabolomics to Monitor Fetal Well-Being: A Narrative Review of the Literature. *Cureus* **2023**, *15*, e36986. [CrossRef]
11. Graça, G.; Diaz, S.O.; Pinto, J.; Barros, A.S.; Duarte, I.F.; Goodfellow, B.J.; Galhano, E.; Pita, C.; Almeida, M.d.C.; Carreira, I.M. Can biofluids metabolic profiling help to improve healthcare during pregnancy? *Spectrosc. Int. J.* **2012**, *27*, 515–523. [CrossRef]
12. Graca, G.; Moreira, A.S.; Correia, A.J.V.; Goodfellow, B.J.; Barros, A.S.; Duarte, I.F.; Carreira, I.M.; Galhano, E.; Pita, C.; do Céu Almeida, M. Mid-infrared (MIR) metabolic fingerprinting of amniotic fluid: A possible avenue for early diagnosis of prenatal disorders? *Anal. Chim. Acta* **2013**, *764*, 24–31. [CrossRef] [PubMed]
13. Graça, G.; Goodfellow, B.J.; Barros, A.S.; Diaz, S.; Duarte, I.F.; Spagou, K.; Veselkov, K.; Want, E.J.; Lindon, J.C.; Carreira, I.M. UPLC-MS metabolic profiling of second trimester amniotic fluid and maternal urine and comparison with NMR spectral profiling for the identification of pregnancy disorder biomarkers. *Mol. BioSystems* **2012**, *8*, 1243–1254. [CrossRef] [PubMed]
14. Virgiliou, C.; Gika, H.G.; Witting, M.; Bletsou, A.A.; Athanasiadis, A.; Zafrakas, M.; Thomaidis, N.S.; Raikos, N.; Makrydimas, G.; Theodoridis, G.A. Amniotic fluid and maternal serum metabolic signatures in the second trimester associated with preterm delivery. *J. Proteome Res.* **2017**, *16*, 898–910. [CrossRef] [PubMed]
15. Graca, G.; Duarte, I.F.; Barros, A.S.; Goodfellow, B.J.; Diaz, S.O.; Pinto, J.; Carreira, I.M.; Galhano, E.; Pita, C.; Gil, A.M. Impact of prenatal disorders on the metabolic profile of second trimester amniotic fluid: A nuclear magnetic resonance metabonomic study. *J. Proteome Res.* **2010**, *9*, 6016–6024. [CrossRef]
16. Hallingström, M.; Barman, M.; Savolainen, O.; Viklund, F.; Kacerovsky, M.; Brunius, C.; Jacobsson, B. Metabolomic profiles of mid-trimester amniotic fluid are not associated with subsequent spontaneous preterm delivery or gestational duration at delivery. *J. Matern. -Fetal Neonatal Med.* **2022**, *35*, 2054–2062. [CrossRef]
17. Giovannopoulou, E.; Tsakiridis, I.; Mamopoulos, A.; Kalogiannidis, I.; Papoulidis, I.; Athanasiadis, A.; Dagklis, T. Invasive prenatal diagnostic testing for aneuploidies in singleton pregnancies: A comparative review of major guidelines. *Medicina* **2022**, *58*, 1472. [CrossRef]
18. Jacob, D.; Deborde, C.; Lefebvre, M.; Maucourt, M.; Moing, A. NMRProcFlow: A graphical and interactive tool dedicated to 1D spectra processing for NMR-based metabolomics. *Metabolomics* **2017**, *13*, 36. [CrossRef]
19. Xia, J.; Bjorndahl, T.C.; Tang, P.; Wishart, D.S. MetaboMiner–semi-automated identification of metabolites from 2D NMR spectra of complex biofluids. *BMC Bioinform.* **2008**, *9*, 507. [CrossRef]
20. Murgia, F.; Monni, G.; Corda, V.; Hendren, A.J.; Paci, G.; Piras, A.; Ibba, R.M.; Atzori, L. Metabolomics analysis of amniotic fluid in euploid foetuses with thickened nuchal translucency by gas chromatography-mass spectrometry. *Life* **2021**, *11*, 913. [CrossRef]
21. Gauthier, D.W.; Meyer, W.J.; Bieniarz, A. Correlation of amniotic fluid glucose concentration and intraamniotic infection in patients with preterm labor or premature rupture of membranes. *Am. J. Obstet. Gynecol.* **1991**, *165*, 1105–1110. [CrossRef]
22. Romero, R.; Quintero, R.; Nores, J.; Avila, C.; Hanaoka, S.; Hagay, Z.; Merchant, L.; Hobbins, J.C. Amniotic fluid white blood cell count: A rapid and simple test to diagnose microbial invasion of the amniotic cavity and predict preterm delivery. *Am. J. Obstet. Gynecol.* **1991**, *165*, 821–830. [CrossRef] [PubMed]
23. Kirshon, B.; Rosenfeld, B.; Mari, G.; Beifort, M. Amniotic fluid glucose and intraamniotic infection. *Am. J. Obstet. Gynecol.* **1991**, *164*, 818–820. [CrossRef] [PubMed]
24. Parthasarathy, S.; Soundararajan, P.; Sakthivelu, M.; Karuppiah, K.M.; Velusamy, P.; Gopinath, S.C.; Pachaiappan, R. The role of prognostic biomarkers and their implications in early detection of preeclampsia: A systematic review. *Process Biochem.* **2023**, *126*, 238–251. [CrossRef]
25. Wang, M.; Wang, H.; Zheng, H.; Uhrin, D.; Dewhurst, R.J.; Roehe, R. Comparison of HPLC and NMR for quantification of the main volatile fatty acids in rumen digesta. *Sci. Rep.* **2021**, *11*, 24337. [CrossRef]
26. Shyer, J.A.; Flavell, R.A.; Bailis, W. Metabolic signaling in T cells. *Cell Res.* **2020**, *30*, 649–659. [CrossRef]
27. Wan, J.; Jiang, F.; Zhang, J.; Xu, Q.; Chen, D.; Yu, B.; Mao, X.; Yu, J.; Luo, Y.; He, J. Amniotic fluid metabolomics and biochemistry analysis provides novel insights into the diet-regulated foetal growth in a pig model. *Sci. Rep.* **2017**, *7*, 1–10. [CrossRef]
28. Romero, R.; Mazaki-Tovi, S.; Vaisbuch, E.; Kusanovic, J.P.; Chaiworapongsa, T.; Gomez, R.; Nien, J.K.; Yoon, B.H.; Mazor, M.; Luo, J. Metabolomics in premature labor: A novel approach to identify patients at risk for preterm delivery. *J. Matern. -Fetal Neonatal Med.* **2010**, *23*, 1344–1359. [CrossRef]
29. Harman, C.R. Amniotic fluid abnormalities. *Semin. Perinatol.* **2008**, *32*, 288–294. [CrossRef]

30. Dessì, A.; Fanos, V. Myoinositol: A new marker of intrauterine growth restriction? *J. Obstet. Gynaecol.* **2013**, *33*, 776–780. [CrossRef]
31. Orczyk-Pawilowicz, M.; Jawien, E.; Deja, S.; Hirnle, L.; Zabek, A.; Mlynarz, P. Metabolomics of human amniotic fluid and maternal plasma during normal pregnancy. *PLoS ONE* **2016**, *11*, e0152740. [CrossRef]
32. Menon, R. Oxidative stress damage as a detrimental factor in preterm birth pathology. *Front. Immunol.* **2014**, *5*, 567. [CrossRef] [PubMed]